Università degli Studi di Milano

PhD Course in
Experimental Medicine

Cycle XXXIV

PhD thesis

"Endothelium in Petri dish (2D) or on-a-chip (3D): studies on endothelial function / dysfunction"

Candidate: **Dr. Roberta Scrimieri**

Matricola: R12363

Tutor: **Prof. Jeanette A.M. Maier**

Director: **Prof. Nicoletta Landsberger**

Academic Year 2020-2021

"I am among those who think that science has great beauty.
A scientist in his laboratory is not only a technician:
he is also a child placed before natural phenomena
which impress him like a fairy tale."

"Io sono tra quelli che pensano che la scienza abbia una grande bellezza.
Uno scienziato nel suo laboratorio non è solo un tecnico:
è anche un bambino posto di fronte a fenomeni naturali
che lo impressionano come un racconto di fiabe."

– Marie Curie (1867 – 1934)

TABLE OF CONTENT

1. ABSTRACT

Endothelial cells (ECs) form the inner layer of all the blood vessels and, due to this strategic localization, they constantly face oscillating blood glucose concentrations in relation to the pre- and post- prandial cycles. They do not represent a passive barrier between blood and tissues, but they play a wide variety of pivotal roles to control vascular homeostasis. Uncontrolled hyperglycaemia elicits ECs to become dysfunctional, leading to the onset of endothelial dysfunction, defined as a shift of properties of the endothelium toward a proinflammatory and prothrombotic phenotype characterised by altered release of Nitric Oxide (NO) and overproduction of pro-inflammatory cytokines and Reactive Oxygen Species (ROS). Endothelial dysfunction is classically described in patients affected by diabetes and has a role in the pathogenesis of many cardiovascular complications associated with this pathology. In particular, diabetes is a group of life-long chronic metabolic disorders characterized by high levels of glucose in the blood and by a predisposition to premature atherosclerosis, the main reason for high morbidity and impaired life expectancy in patients.

To investigate the effects of high glucose on ECs, Human Umbilical Vein Endothelial Cells (HUVEC) were cultured in the presence of either high glucose-containing medium or of blood sera collected from diabetic patients. Cells were seeded both in 2D cell culture systems on flat dishes, a method which has yielded major advances in our knowledge about endothelial pathophysiology, and in 3D microfluidic chips, which show a higher degree of structural complexity allowing perfusion, thus generating shear stress fundamental for endothelial homeostasis. In 2- and 3- D, the cells were cultured until they reach confluence to reproduce the physiological inner layer of a blood vessel as closely as possible.

High glucose rapidly alters the cellular redox balance resulting in a higher production of ROS associated with a lower content of the antioxidant glutathione (GSH). ROS induce iNOS, which overproduces NO leading to endothelial hyperpermeability. In parallel, mitochondrial dysfunction occurs as a result of the imbalance in mitochondrial dynamics in favour of mitochondrial fission. This evidence is connected to the higher storage of triglycerides caused by both enhanced lipogenesis and reduced β-oxidation.

The next step was to individuate a countermeasure that might prevent the detrimental effects of high glucose on HUVEC. Numerous observational studies demonstrated that the circulating levels of Vitamin D_3 (VitD) are low in patients affected by diabetes. In these

experimental models, VitD is capable of blocking the increase of ROS production, thus preventing all the harmful effects caused by high glucose on HUVEC.

In summary, the results reveal that it is fundamental to keep glycaemia within the physiological range in diabetic patients, preventing hyperglycaemic peaks, and that VitD could represents a serviceable tool to control the redox equilibrium, thus re-establishing NO levels and permeability and mitochondrial fitness, to limit or at least delay the insurgence of endothelial dysfunction caused by high fasting glucose concentrations.

DISCLOSURE FOR RESEARCH INTEGRITY

This research was conducted following the European Code of Conduct for Research Integrity, which includes the values of reliability, rigor, honesty, respect and transparency.

ABBREVIATIONS

α-ketoglutarate, α-KG; Arachidonic acid, AA; Asymmetric dimethylarginine, ADMA; Angiopoietins, Ang; Carnitine Palmitoyl-Transferase 1A, CPT1A; Cellular Adhesion Molecules, CAM; Circulating NO metabolites, NOx; Coronary heart disease, CHD; cyclic Guanosin Monophosphate, cGMP; Cyclophilin D, CYP D; Cryo Soft X-ray Transmission Tomography, Cryo-SXT; Deoxynucleotides, dNTPs; Dynamin-Related Protein 1, DRP1; Endothelial cells, ECs; Endothelial Differentiation-related Factor 1, EDF1; endothelial Nitric Oxide Synthases, eNOS; Endothelin-1, ET-1; Extracellular matrix, ECM; Fatty Acid Oxidation, FAO; Fetal Bovine Serum, FBS; Fibroblast Growth Factor, FGF; Fluorescein isothiocyanate labelled-albumin, FITC-BSA; Forkhead box O1, FOXO1; Fractional Anisotropy, FA; Free fatty acids, FFA; Fructose-2,6-bisphosphate, F2,6P2; Full-width-at-half-maximum, FWHM; Gestational Diabetes Mellitus, GDM; Glycated haemoglobin, HbA1c; Glucokinase, GCK; Glucose Transporter 1, GLUT1; Glutamic acid decarboxylase 6, GAD65; Glutaminase-1, GLS1; Hepatocyte nuclear factor-1A, HNF1A; Hexokinase 2, HK2; Hydrogen peroxide, H2O2; Human Umbilical Vein Endothelial Cells, HUVEC; Krüppel-like Factor 2, KLF2; inducible NOS, iNOS; insulin autoantibodies, IAA; Islet-Associated protein -2/-2β, IA-2/IA-2β; Islet cell autoantibodies, ICA; Lipoprotein lipase, LPL; Low-density proteins, LDL; L-Nω–Nitroarginine-Methyl-Ester, L-NAME; N6–(1-Iminoethyl)-L-Lysine, L-NIL; Matrix Metalloproteinases, MMPs; Maturity Onset Diabetes of the Young, MODY; MHC, Major Complex of Histocompatibility; mitochondrial DNA, mtDNA; mitochondrial ROS, mtROS; N-acetylcysteine, NAC; neuronal NOS, nNOS; Nitric Oxide, NO; Nitric Oxide Synthases, NOS; Nonessential amino acid, NEAA; Nuclear Factor Kappa Beta, NFkB; Nuclear respiratory factor, NRF; Optic Atrophy 1, OPA-1; Oxaloacetate, OAA; Oxidized glutathione, GSSG; Oxidative phosphorylation, OXPHOS; Oxygen Consumption Rate, OCR; Paraoxonase 2, PON2; Pentose phosphate pathway, oxPPP; Peroxisome Proliferator-Activated Receptor γ, PPARγ; Perilipin 2, PLIN2; Phosphate buffered saline, PBS; Phosphofructokinase-1, PFK1; Plasminogen activators, PAIs; Platelet activating factor, PAF; Platelet-Derived Growth Factor, PDGF; Platelet-endothelial cell adhesion molecule 1, PECAM-1; Proliferator-activated receptor gamma coactivator-1α, PGC-1α; Reactive Oxygen Species, ROS; Reduced glutathione, GSH; Retinoid X Receptors, RXRs; ribulose-5-phosphate, Ru5P; Sirtuin 1, SIRT1; Sirtuin 2, SIRT2; small interfering RNA, siRNA; Smooth muscle cells, SMCs; Sodium nitrite standard, NaNO2; Superoxide-dismutase 2, SOD2; Tissue Factor Pathway Inhibitor, TFPI; Thioredoxin Interacting Protein, TXNIP; t-PA, Plasminogen Tissue Activator; Transcription factor A/B, TFAM/TFBM; Transforming Growth Factor β, TGFβ; Tricarboxylic acid cycle, TCA; Trombin-Activatable Fibrinolysis Inhibitor, TAFI; Type 1 Diabetes Mellitus, T1D ; Type 2 Diabetes Mellitus, T2D; Type 3 Diabetes, T3D; u-PA, Plasminogen Urokinase Activator; Vascular endothelial-cadherin, Ve-Cadherin; Vascular Endothelial Growth Factor, VEGF; Vascular endothelial growth factor-1, VEGF-1; VEGF receptor type 2, VEGFR-2; Vitamin D_3, VitD; Vitamin D_3 Receptor, VDR; Vitamin D Response Elements, VDRE; Von Willebrand Factor, vWF; Wheat Germ Agglutinin, WGA; Zonula Occludens 1, ZO-1; 1,25-dihydroxivitamin D_3, 1,25-(OH)2-D_3; 2'-7'-dichlorofluorescein diacetate, DCFH; 6-phosphofructo-2-kinase/fructose-2,6-bisphosphatase 3, PFKFB3; 25-hydroxyvitamin D_3, 25-(OH)-D_3.

2. INTRODUCTION

2.1 BLOOD VESSELS

The human vascular tree is characterized by arteries, veins and capillaries, three different types of blood vessels, whose differences in the function and in the pressure to which they are subjected are reflected on their structure (Figure 1) [Aird 2012]. However, it is possible to identify a common structural organization. Indeed, the wall of the vessels is constituted by three layers, named *tunicae*, which, from the inside to the outside, are identified respectively as *tunica intima*, *tunica media* and *tunica adventitia* [Tabrizchi 2005].

The *tunica intima*, the innermost one, is composed by a covering layer of ECs held up by a connective tissue (called *lamina propria*) and, in the large arteries, an internal elastic lamina, a network of elastic longitudinally oriented fibers that present perforations named *fenestrae*.

The *tunica media* corresponds to the muscular layer. Depending on the type of vessel, it consists mainly of smooth muscle cells (SMCs) for medium and small caliber arteries, of elastic fibers arranged in spiral layers to resist to the high pressure of the blood coming from the heart for large arteries or of fibrous component for veins. This layer is totally absent in the capillaries.

The *tunica adventitia*, the outermost layer, connects the vessels with the surrounding environments. Collagen and elastic fibers are the major components of the adventitia that provides an additional protective layer to the vessels. In the veins and in the arteries its thickness is proportional to the size of the vessels while in the capillaries it exists only in the form of a network of mesenchymal cells called pericytes. Because of its thickness, this layer is nourished by *vasa vasorum*, a network of small blood vessels necessary to provide additional supply of blood. In contrast, the tunica intima and tunica media are fed by diffusion directly from the blood.

Shear stress, i.e. the frictional force generated by blood flow, and different blood pressure diversify the endothelium in arteries, arterioles, post-capillaries venules and capillaries [Van Hinsberg 2012].

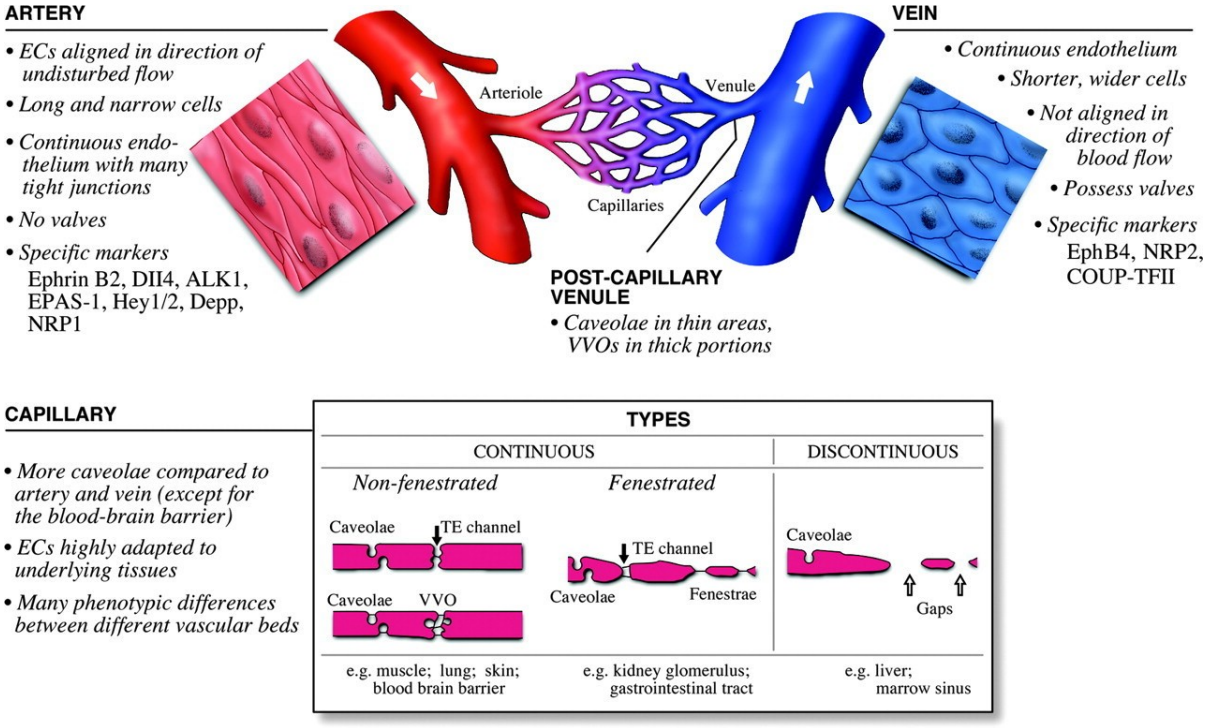

***Figure 1**: Schematic representation of blood vessels' structure and list of parameters differently exhibited, i.e. the number and types of junctions, the alignment or not to the flow and the expression of specific markers [Aird 2012].*

2.2 ENDOTHELIUM

ECs form the inner lining of all the vessels, playing a wide variety of critical roles in the control of vascular integrity and functions [Sena 2013]. It has been estimated that endothelium surface covers about 3000-6000 m^2 for approximately 720 g in an adult [Gimbrone 1986]. Most of it is represented by microvascular ECs that line the capillaries [Van Hinsberg 2012].

Endothelial and haematopoietic cells derive from haemangioblasts [Choi 1998], bipotent blasts which can differentiate either in pre-endothelial cell or in hematopoietic cell (Figure 2) [Psaltis 2011].

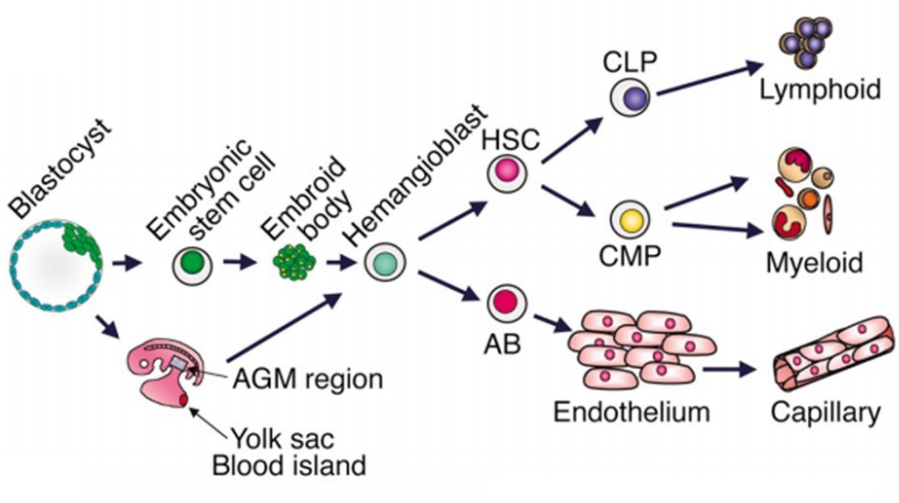

***Figure 2**: Generation of heamangioblast either from blastocyst-derived Embryonic Stem cell, or from the Yolk sac, the Aorta-Gonad-Mesonephros (AGM) region of the early embryo [Aird 2012]. Heamangioblast can differentiate in Hematopoietic Stem Cells (HSCs), giving rise to both Lymphoid and Myeloid lineages, or in Angioblast (AB), the precursor of ECs [Psaltis 2011].*

Von Willebrand Factor (vWF), platelet-endothelial cell adhesion molecule 1 (PECAM-1), endothelial Nitric Oxide Synthases (eNOS) and vascular endothelial-cadherin (Ve-Cadherin) are specific markers of mature endothelial cells [Huang 2008, Bai 2010].

ECs are normally quiescent *in vivo* with a turnover rate of approximately once every three years [Foreman 2003]. Most of ECs in the adult have a cell cycle variable from months to years, unless injury to the vessel wall or angiogenesis occurs, with the exception of the endothelia of endometrium and corpus luteum, which have a turnover rate of weeks. ECs differentiation relies on different stimuli, including Vascular Endothelial Growth Factor (VEGF), highly specific for the endothelium, and Fibroblast Growth Factor (FGF).

2.3 ENDOTHELIAL CELL HETEROGENEITY

The endothelium is highly heterogeneous between different tissues, segments and even in the same organ [Regan 2012]. This heterogeneity can be detected at different levels (morphology and structure, function, gene expression and antigen composition) and it is mediated by two mechanisms: the effect of the surrounding environment and epigenetics (Figure 3) [Regan 2012].

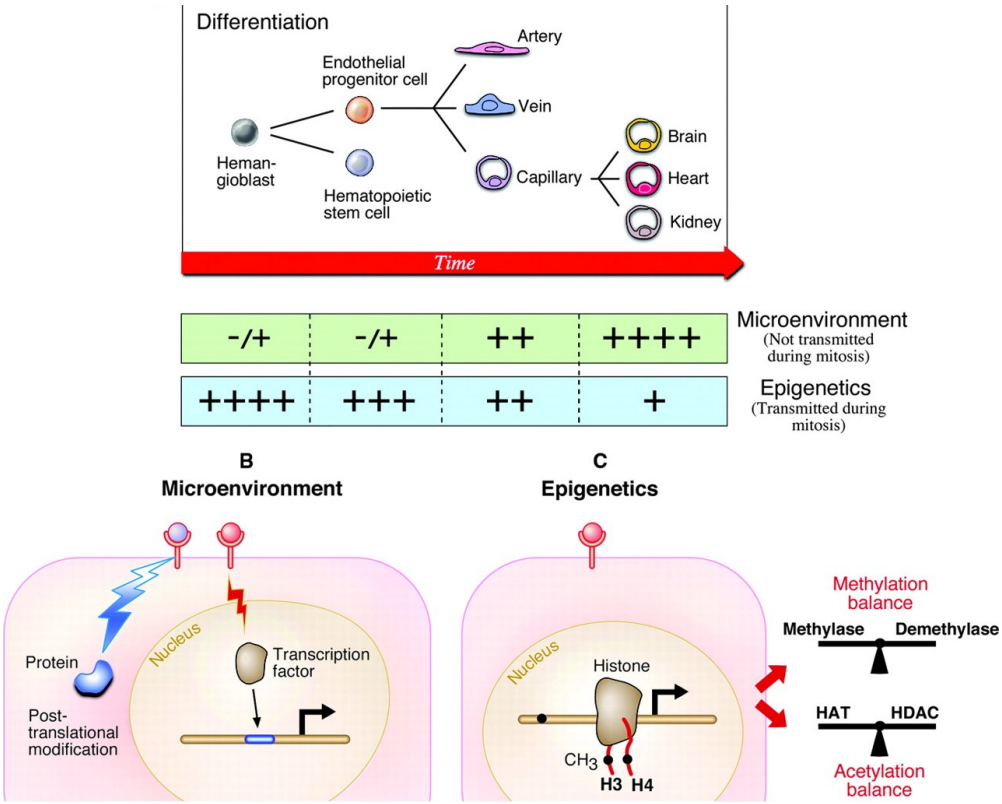

***Figure 3**: Mechanisms of endothelial cell heterogeneity. Starting from the haemangioblast precursor to the terminally differentiated cells, the effects of microenvironment and epigenetic are different. The effect of the microenvironment is predominant in differentiated cells while epigenetics is fundamental in defining the genotypic and phenotypic features of the precursor cells and it is then transmitted to the progeny through mitosis [Aird 2012].*

Concerning the microenvironment, ECs located in different districts of the body are subjected to a variety of stimuli that orchestrate specific reactions and functions on ECs. This type of mechanism is dynamically regulated.

On the other hand, epigenetics modifications define ECs gene expression through inheritable changes of their phenotype determined by DNA and histone methylation, histone acetylation or deacetylation. Even if these epigenetic modifications are triggered by signals from the surrounding environment, as the first mechanism of heterogeneity, they can also persist after the removal of the signals and they are transmitted during mitosis [Aird 2012].

These two mechanisms are responsible for the huge variety of roles and specific functions of ECs at the different levels of the vascular tree.

2.3.1 STRUCTURAL HETEROGENEITY

The shape of ECs can vary very deeply across the vascular tree. They can display a flat morphology or they can appear plump and cuboidal as in venules. Even the thickness can differ, from 0.1 μm in capillaries and veins to 1 μm in big arteries, e.g. aorta [Regan 2012]. In addition, shear stress and different blood pressure along the vascular tree direct the alignment of ECs in straight segments of arteries but not at the level of the ramifications. The vessels length is an important characteristic in determining the effect alignment to the blood flow.

ECs express different types of intercellular junctions: the tight junction (also called *zonula occludens*) and the adherens junction (also named *zonula adherens*). The former type is fundamental for the function of endothelial barrier and allows the cell to maintain a polarity of luminal and apical side [Aird 2012]. For example, the microvasculature of the blood brain barrier is particularly rich in tight junctions, absent in post-capillary venules, to allow the extravasation of leukocytes during inflammation.

Moreover, the endothelium could be continuous, fenestrated or discontinuous (sinusoid), depending on the needs of the surrounding tissue (Figure 4) [Van Hinsberg 2012]. Continuous endothelium is abundant in vessels of brain, heart, lung and skin; fenestrated endothelium is mostly located where filtration or trans-endothelial transport are fundamental (e.g. capillaries of glands and kidney) and discontinuous endothelium is typical of sinusoidal beds [Van Hinsberg 2012].

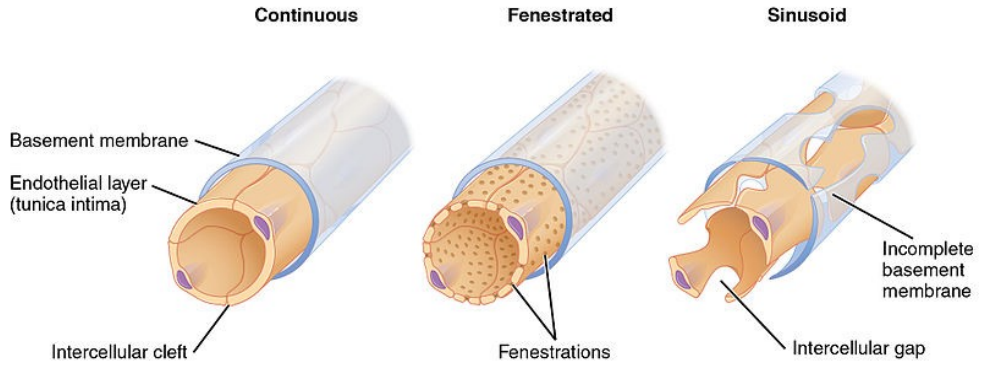

***Figure 4**: Types of endothelium. In continuous capillaries, small solutes and fluids pass constitutively between ECs, while larger solutes are carried through trans-endothelial channels or transcytosis. Fenestrated endothelium is highly permeable to water and small solutes but not to larger macromolecules. Discontinuous endothelium is characterized by fenestrae and it is rich of clathrin-coated pits, which play an important role in receptor-mediated endocytosis [Van Hinsberg 2012].*

2.3.2 FUNCTIONAL HETEROGENEITY

ECs are able to perform different functions to control vascular homeostasis, such as regulation of vascular tone, coagulation and fibrinolysis, leukocytes' trafficking and immune response, most of which are performed by specific subset of blood vessel or vascular beds (Figure 5) [Sena 2013].

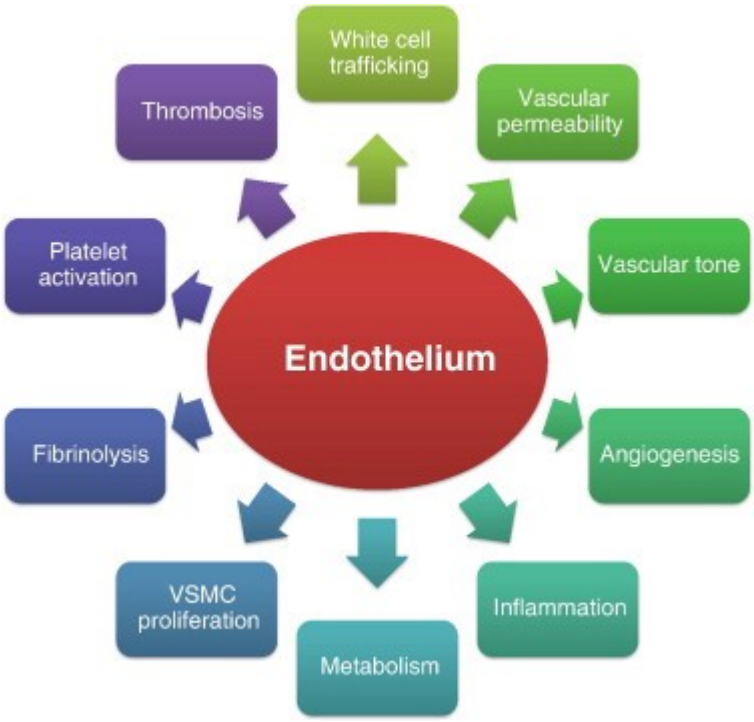

***Figure 5**: Functions of endothelium. ECs are able to perform different functions in order to maintain tissue homeostasis, among which the regulation of coagulation, immune response, permeability, angiogenesis and metabolism [Sena 2013].*

Indeed, since the early 1980s, the concept of endothelium as an inert barrier lining the inner side of blood vessels has been overcome by the finding that ECs are involved in a variety of biological responses and physiological functions. Indeed, nowadays is clear that it is a dynamic and heterogeneous system fundamental in maintaining the integrity of vessels and tissues homeostasis [Galley 2004]. ECs have synthetic, metabolic, secretory and immunologic roles [Cines 1998] that allow the interaction of ECs with the environment and their response after stimuli [Galley 2004]. These functions include fluid filtration, regulation of blood vessel tone and blood vessel formation, neutrophil recruitment, coagulation and fibrinolysis. By virtue of its structural properties, the endothelium is a semipermeable barrier that controls fluids and solutes exchanges between blood and the surrounding tissues

through the regulation of permeability. Fluids and small solutes can cross passively the endothelium through the paracellular pathway. It is mediated by the homophilic adhesion of Ve-Cadherin which can be either stably associated to the membrane or translocated to the cytosol in response of extracellular stimuli, through the remodelling of actin cytoskeleton, mediating the increase of permeability. Particularly, three types of stimuli can induce Ve-Cadherin translocation: c-Src and RhoA activation and/or increased calcium concentration (Figure 6) [Komarova 2010].

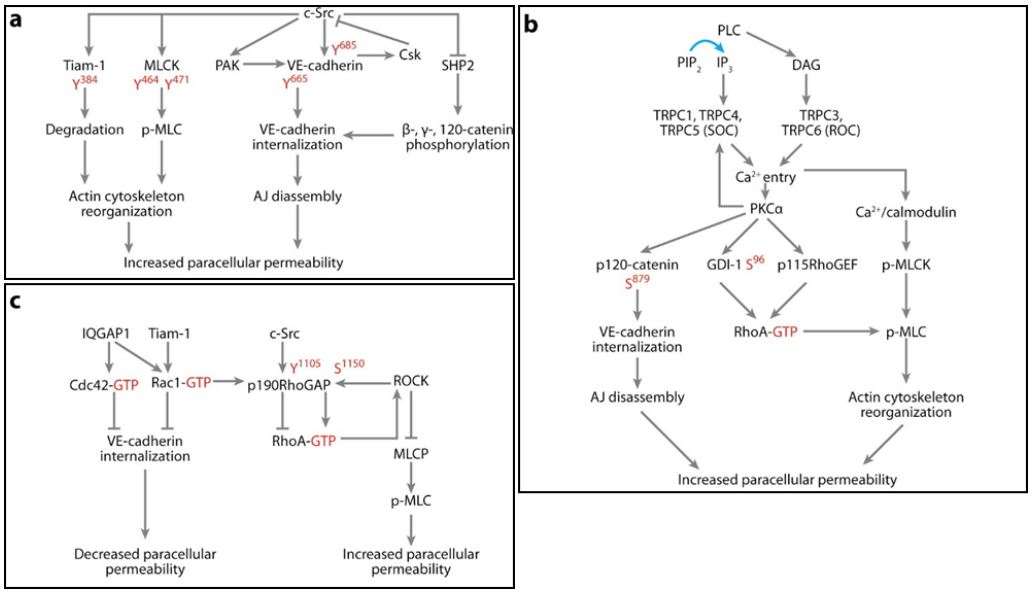

***Figure 6**: Pathways regulating Ve-Cadherin translocation, thus mediating the variation of permeability [Komarova 2010].*

On the other hand, macromolecules are shuttled through the trans-cellular pathway, which can involve receptors (receptor-mediated transcytosis) or can be receptor-independent (fluid-phase transcytosis). This last mechanism is arbitrated by the presence of Caveolae, carrier vesicles composed by Caveolin-1, a scaffold protein on the cytosolic side of the membrane that mediates the internalization of the cargo through the fusion with the plasma membrane. This pathway is well known to be involved in the activation / inactivation process of eNOS in ECs. The binding and the translocation of eNOS from the membrane to the cytosol through Caveolae internalization is associated with enzyme inhibition, while on the contrary SRC-mediated phosphorylation of Caveolin-1 stimulates Caveolae scission, eNOS release and activation, and NO synthesis (Figure 7) [Frank 2006].

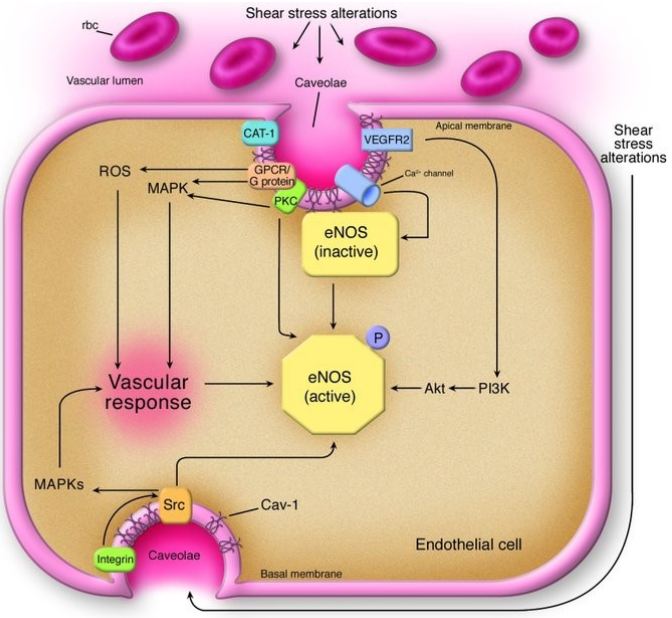

***Figure 7**: Effect of shear stress on Caveolae translocation. Upon stimulation (e.g. shear stress), Caveolae may induce the proper organization of various signal transduction pathways or organize different regulatory proteins essential for rapid eNOS activation [Frank 2006].*

In this context, the junctional and structural heterogeneity and the presence of various types of transcytosis in ECs at different vascular beds define variations in basal permeability. For instance, permeability is inversely proportional to the amount of tight junctions and directly proportional to the presence of fenestrae. Additionally, when acute or chronic inflammation occurs, ECs are capable to mediate inducible leakage mostly in post-capillary venules.

2.4 ANGIOGENESIS

Angiogenesis is a complex multistep process of vascular growth derived by sprouting of pre-existing vessels. Physiologically, it is a highly regulated process driving quiescent ECs into a series of events that culminate with the organization of a vascular network in response to the demands of growing or healing tissues.

Metabolic stress has an impact on angiogenesis since environmental stimuli, including low oxygen tension, low extracellular pH and low glucose concentration, trigger neovascularization. Angiogenesis occurs physiologically not only during fetal development

but also during development and growth, in menstrual cycle and in wound healing / repair or pathologically, particularly in neoplastic and inflammatory diseases.

The steps leading to angiogenesis require cell proliferation, production of molecules to degrade the extracellular matrix (ECM), modulation of adhesion and migration and, finally, differentiation into new functional vessels [Galley 2004].

A balance between pro- and anti- angiogenic factors tightly controls all the steps of angiogenesis. Indeed, components of ECM and soluble molecules can activate or inhibit it. Some angiogenic factors are endothelial-specific, e.g. the members of VEGF, angiopoietin families, Ephrin B2 and 4B. Other growth factors modulate the functions of ECs, including members of the FGF, Platelet-Derived Growth Factor (PDGF) or Transforming Growth Factor (TGF)β families. Additionally, many other gene products – from Notch to transcription factors – have been shown to be crucial for vessel development. In this context, VEGF plays a crucial role as driver of vascular formation being necessary in both vasculogenesis, i.e. the formation of primitive vascular structures during embryogenesis via the differentiation of ECs precursors, and angiogenesis, during early development as well as in the adult. Basically, VEGF binds to its receptor type 2 (VEGFR-2) and generates a tyrosine kinase signalling cascade that stimulates the production of factors regulating vessel permeability (eNOS, producing NO), proliferation/survival, migration (Matrix Metalloproteinases, MMPs) and finally differentiation into mature blood vessels. Therefore, VEGF is a protagonist in all phases of angiogenesis since it increases vascular permeability, stimulates ECM remodelling, induces endothelial proliferation and migration, inhibits apoptosis, enhances branching of the neo-formed vessels and regulates lumen diameter (Figure 8). Indeed, disruption of even a single VEGF allele in mice leads to embryonic death. However, VEGF alone is unable to direct blood vessel organization and maturation and it works in concert with other factors, such as Angiopoietins (Ang) that bind the Ties, a family of receptor tyrosine kinases selectively expressed on the vascular endothelium. Specifically, Ang1 stabilizes the vessel, maximizes interactions between endothelial cells and the surrounding cells and matrix and maintains endothelial quiescence [Fan 2006].

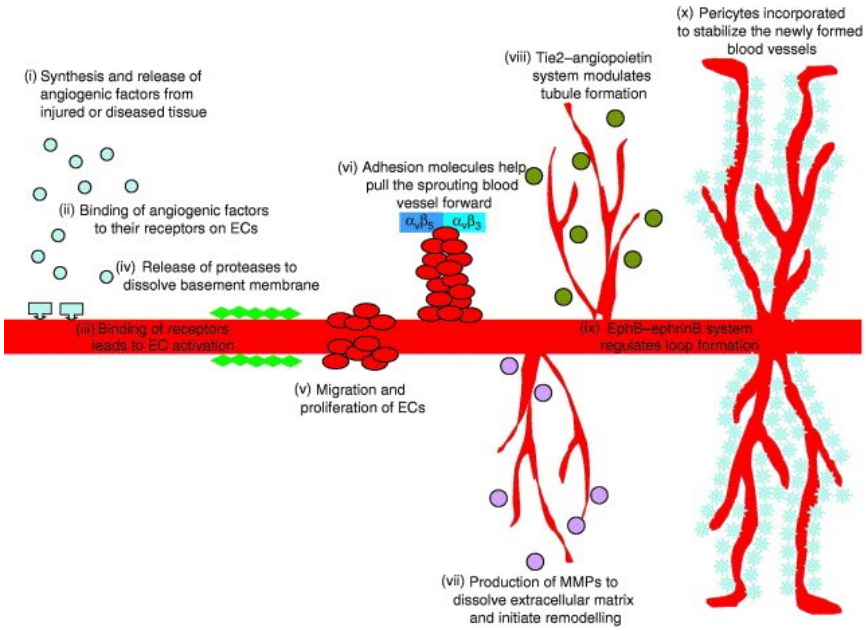

***Figure 8**: Steps of angiogenic pathway [Fan 2006].*

2.5 VASCULAR TONE

The regulation of the vascular tone is another fundamental function of the endothelium, exerted by the production of vasoactive molecules acting on SMCs of the *tunica media*, mediating either relaxation or contraction. Particularly, ECs produce both vasodilator molecules (e.g. NO and prostacyclin) and vasoconstrictor molecules (e.g. endothelin-1, ET-1, and platelet activating factor, PAF).

NO is a soluble gas with a half-life of about 30 seconds, synthetized from L-arginine by Nitric Oxide Synthases (NOS) enzymes. In mammals, three different isoforms of NOS have been identified: neuronal NOS (nNOS), inducible NOS (iNOS) and endothelial NOS (eNOS). eNOS and nNOS are Ca^{2+}-dependent constitutively active enzymes, whereas the inducible isoform is a Ca^{2+}-independent enzyme involved in inflammation and immune response [Shulz 2008]. In particular, NO, spreading rapidly from ECs to SMCs, determines relaxation and vasodilation through the modulation of the activity of soluble Guanylyl Cyclase, producing increased concentrations of cyclic Guanosin Monophosphate (cGMP). cGMP interacts with three types of intracellular receptors: i) cGMP-dependent protein kinases; ii) cGMP-regulated ion channels and iii) cGMP-regulated cyclic nucleotide phosphodiesterases [Moncada 1991] (Figure 9).

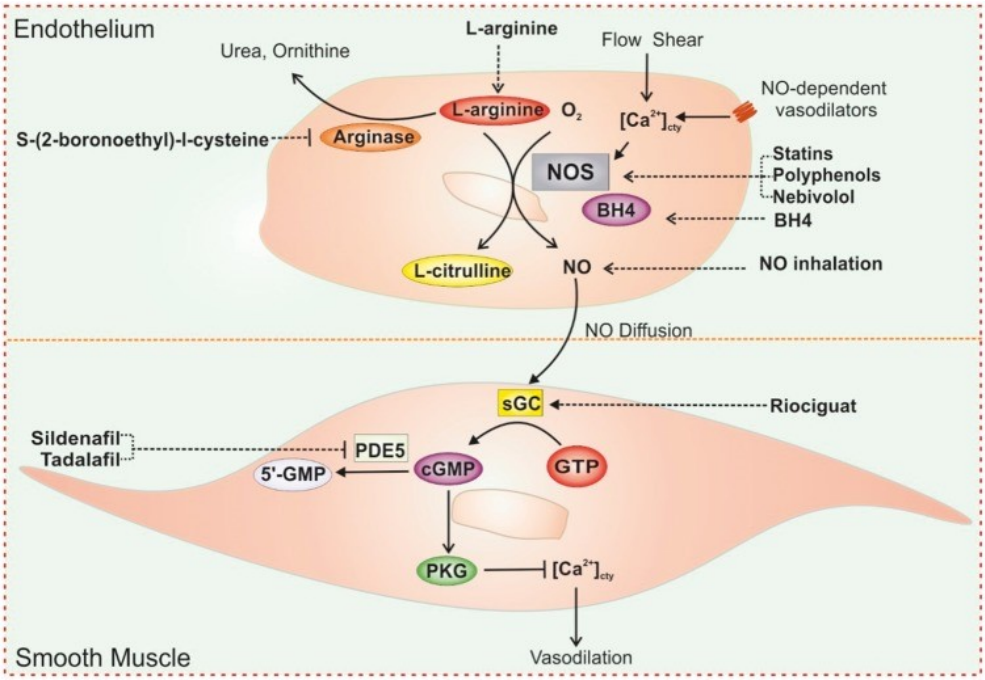

***Figure 9**: NO production from eNOS in EC and its effect on SMCs [Tang 2017].*

The vascular protective action of endothelium-derived NO has expanded beyond its capability to regulate vascular tone. Indeed, NO inhibits endothelial-leukocyte interaction, platelet reactivity, smooth muscle proliferation and the expression of pro-inflammatory and pro-atherogenic cytokines [Tousoulis 2012]. Interestingly, laminar flow and pharmacological agents, such as estrogens, statins and angiotensin-converting enzyme inhibitors, are vascular protective because they enhance endothelium-derived NO synthesis. Consequently, an adequate production of NO through eNOS is a marker of endothelial function to the point that in clinical practise the examination of vasodilation in response to stimuli that release NO is routinely employed to assess endothelial function [Tousoulis 2012]. The continuous basal synthesis of NO from vascular endothelium is crucial to maintain resting vascular tone. On the other hand, in case of endothelial dysfunction, reduced synthesis of NO can be ascribed either to the deficiency of NOS co-factors, such as BH4, or to the overproduction of endogenous inhibitors of NOS, such as asymmetric dimethylarginine (ADMA), while reduced NO availability is mainly due to oxidative stress because ROS oxidize NO and transform it into peroxynitrite [Virdis 2009]. Diminished NO release because of the inhibition of eNOS is associated with many pathological conditions such as atherosclerosis, hypertension, hypercholesterolemia, smoking, diabetes mellitus and heart failure. Under physiological conditions, iNOS is not activated in ECs. Its overexpression determines a high output NO synthesis, with detrimental effects on

endothelial function. As an example, iNOS is expressed in atherosclerotic plaques where it seems to contribute to plaque development [Zhang 2021].

Another vasodilator molecule produced by ECs is the prostacyclin PGI_2, produced from arachidonic acid (AA), which, once secreted, acts both on SMCs, inducing vasodilatation, and on platelets, delaying their aggregation. AA is also the precursor of the vasoconstrictor PAF, a phospholipid located in the membrane where it mediates the adhesion of leukocytes to the endothelium.

Another vasoconstrictor molecule is endothelin, which exists in three isoforms but vascular ECs produce only ET-1, whose biological actions are mediated by two types of receptors: ETA, expressed on SMCs mediating vasoconstriction and cell proliferation, and ETB, expressed predominantly at the endothelial level regulating vasodilation through production of NO and prostacyclin [Galley 2004]. ETB receptors are also present on the surface of SMCs where they exert the same vasoconstrictive role as ETA. ET-1 stimulates cell proliferation and increases the expression of some genes such as collagenase and PDGF [Barst 2007] (Figure10).

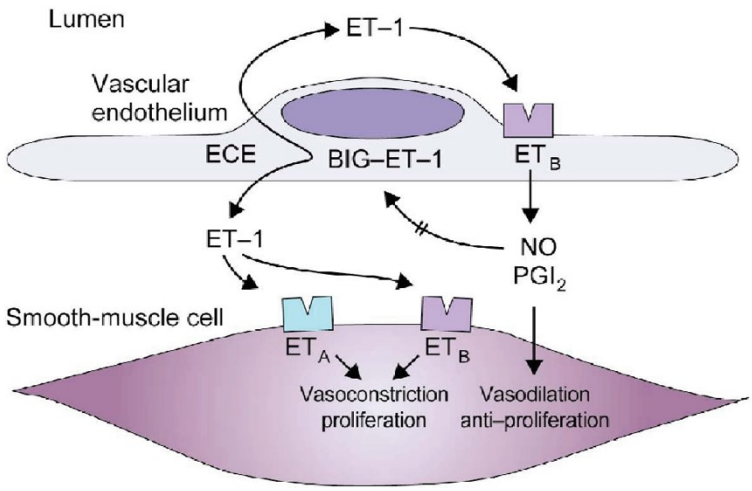

***Figure 10**: Schematic mechanism of action on endothelin on ECs and SMCs [Barst 2007].*

2.6 COAGULATION

The endothelium is also important for the control of the coagulation. In the absence of tissue damage, ECs express antithrombotic and fibrinolytic proteins to avoid the erroneous

triggering of the coagulation process. In the presence of a vessel injury, the endothelium triggers a cascade of events leading to the arrest of blood loss through clot formation and wall repair [Cines 1998; Levi 2002]. In basal conditions, ECs express Tissue Factor Pathway Inhibitor (TFPI), a molecule able to bind the Xa factor forming the TF – FVIIa – FXa complex, hence preventing the conversion of prothrombin into thrombin and inhibiting the conversion of fibrinogen in fibrin. ECs also express Trombomodulin, a membrane glycoprotein that directly binds thrombin and addresses it to degradation, thus preventing its proteolytic activity on fibrinogen and the activation of platelets, factor V and XIII. Furthermore, the endothelium is able to produce Protein S, a cofactor that increases the activity of the C protein implicated in the blocking of factor VII and V of coagulation (Figure 11) [Badimon 2012].

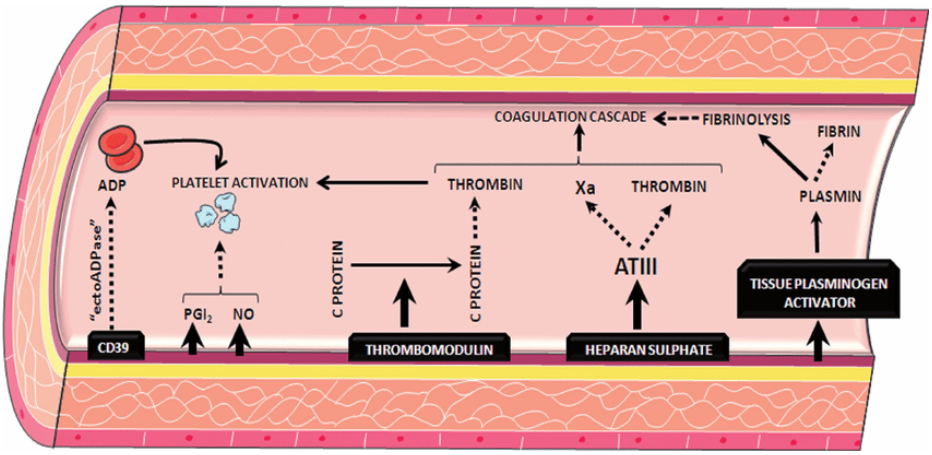

***Figure 11**: Antithrombotic properties of healthy vascular endothelium. Abbreviations: PGI2, prostacyclin; NO, nitric oxide; ATIII, antithrombin III; ADP, adenosine diphosphate [Badimon 2012].*

However, thereupon a vascular damage, ECs express a pro-coagulant phenotype by exposing TF on the surface to initiate the coagulation cascade. Consequently, a cap of platelets adheres to the sub-endothelial surface. Moreover, in this phase, the binding of thrombin to thrombomodulin expressed by ECs leads to the activation of the Trombin-Activatable Fibrinolysis Inhibitor (TAFI), a molecule responsible for slowing down of fibrinolysis speed, in order to allow the complete resolution of the lesion.

Once repaired the lesion, the clot removal is triggered by the activated plasmin, a serin protease produced from the plasminogen by proteolytic cut to mediate the degradation of the fibrin. ECs participate to this process exposing receptors for t-PA (Plasminogen Tissue

Activator) and u-PA (Plasminogen Urokinase Activator) and blocking plasmin degradation mediated by the α2-Plasmin Inhibitor [Cines 1998].

The fibrinolysis is also regulated by the levels of inhibitors of plasminogen activators (PAIs). Physiologically, the liver is the major producer of PAIs but chemicals, among which thrombin, can increase their production by ECs, inhibiting fibrinolysis (Figure 12) [Fitzgerald 2000].

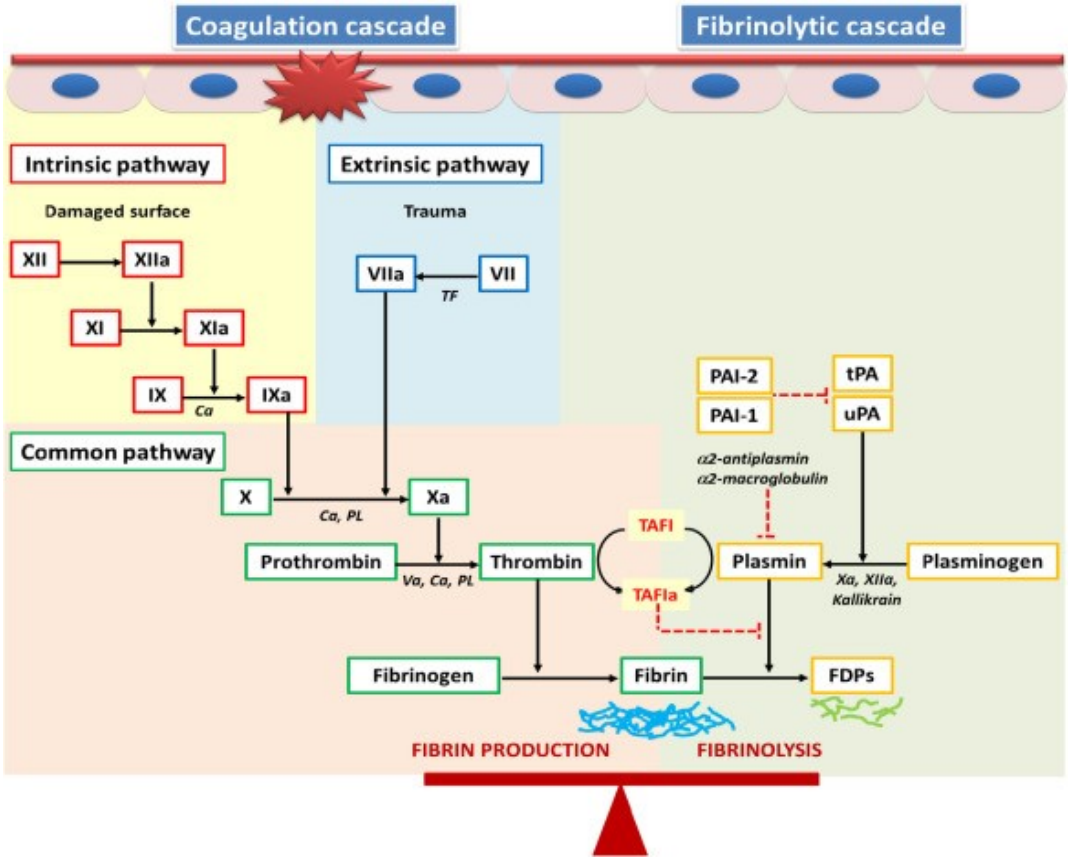

***Figure 12**: Coagulation and fibrinolytic cascades [Fawzy 2015].*

2.7 IMMUNE RESPONSE

ECs are also important mediators of immune response since they actively participate in leukocyte extravasation at the site of infection acting as antigen-presenting cells. Thanks to their ability to express different adhesion molecules, ECs mediate the four phases of leukocyte extravasation: rolling, integrin activation, stable adhesion and trans-endothelial migration (Figure 13) [Lagarrigue 2016].

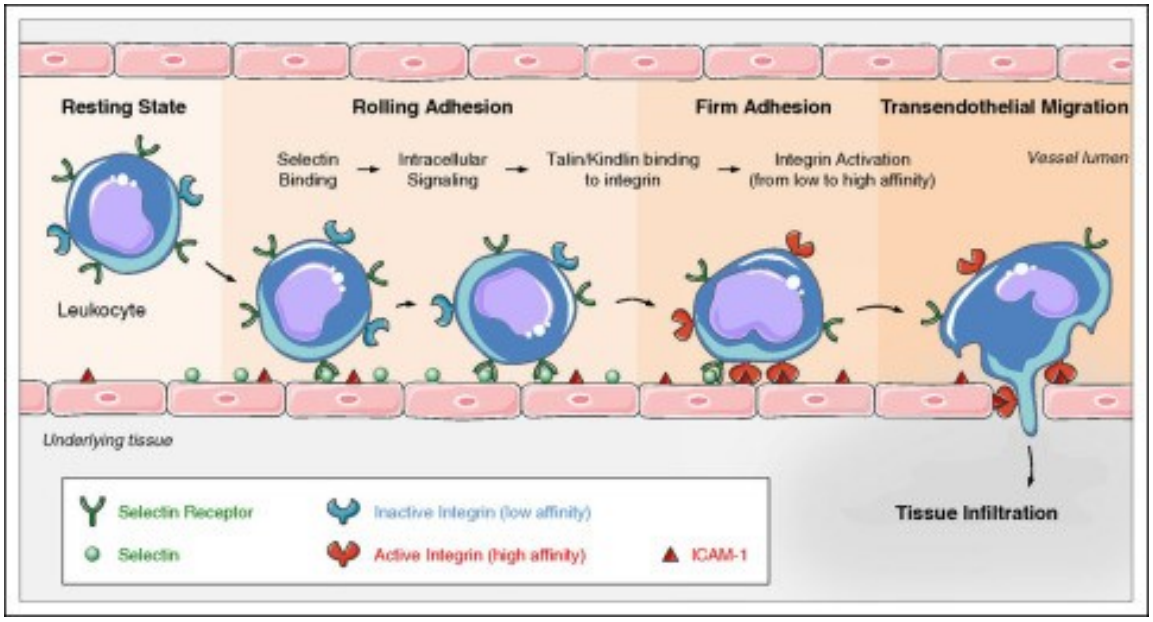

***Figure 13**: Leukocyte trafficking during immune response [Lagarrigue 2016].*

Initially, the ECs express cell adhesion molecules called selectins, belonging to the Cellular Adhesion Molecules (CAM) family. During the rolling phase, weak bonds are established between the selectins of the ECs and the leukocyte membrane's carbohydrates. Since the strength of the blood flow is greater than the bond strength between the adhesion molecules, leukocyte rolls on the endothelial surface. Moreover, other membrane molecules of the ECs, the integrins, change their conformation from the inactive to the active form exposing the binding sites to which leukocytes link with high affinity during the stable adhesion phase. This event generates a stable adhesion that allows the leukocyte to cross the vessel wall reaching the tissue where they are recruited (transendothelial migration). ECs can also act as antigen-presenting cells because they express the MHC (Major Complex of Histocompatibility) class I on their surface, thereby operating as antigen-presenting cells to effector lymphocytes $CD8^+$. Furthermore, in the presence of an intense inflammatory response, ECs also express class II MHC, necessary for the activation of the $CD4^+$ lymphocytes [Mai 2013, Goldsby 2000].

2.8 ENDOTHELIAL METABOLISM

The 85% of the energy produced by ECs derives from glycolysis, since most of ATP is produced by converting glucose to lactate [De Bock 2013]. ECs do not continue generating ATP through oxidative phosphorylation (OXPHOS), i) to protect themselves from oxidative stress, keeping ROS under control and ii) to preserve oxygen for the diffusion in perivascular tissue that need oxygenation [De Bock 2013; Helmlinger 2000]. Moreover, glycolysis is fundamental in hypoxic tissue, where ECs need to rapidly produce ATP to avoid tissue damage and necrosis. The enzyme 6-phosphofructo-2-kinase/fructose-2,6-bisphosphatase 3 (PFKFB3) is the key stimulator of glycolysis in ECs. It produces fructose-2,6-bisphosphate (F2,6P2), a strong allosteric activator of phosphofructokinase-1 (PFK1), a rate-limiting enzyme of glycolysis. Another glycolytic regulator in ECs is Hexokinase 2 (HK2) that phosphorylates glucose to glucose-6-phosphate (Figure 14) [Rohlenova 2018].

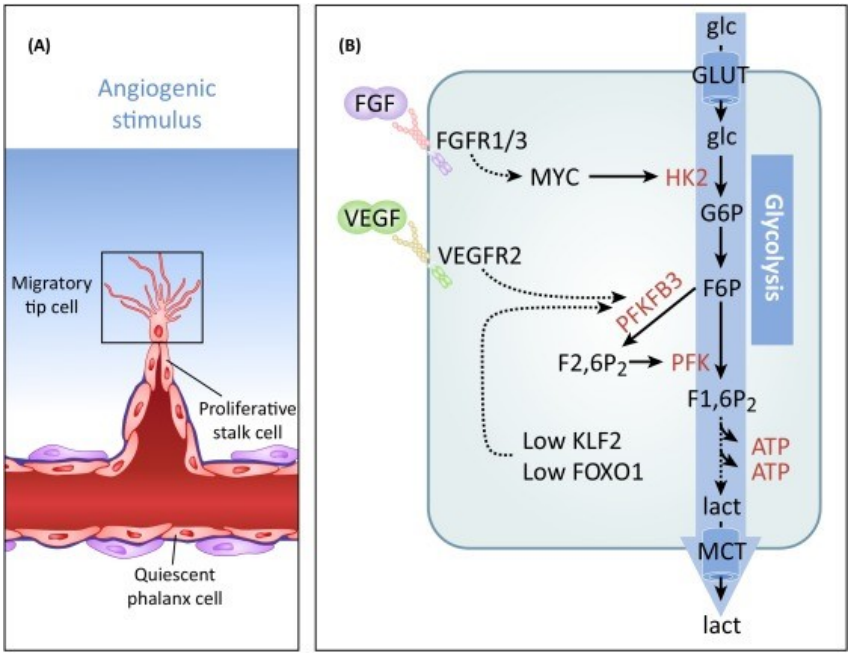

***Figure 14**: Glycolysis is the main energy source in sprouting endothelium. Abbreviations: F1,6P2, fructose-1,6-bisphosphate; F2,6P2, fructose-2,6-bisphosphate; F6P, fructose-6-phosphate; FGF, fibroblast growth factor; FGFR1/3, fibroblast growth factor receptor 1/3; FOXO1, forkhead box O1; G6P, glucose-6-phosphate; glc, glucose; GLUT, glucose transporter; HK2, hexokinase 2; KLF2, Krüppel-like factor; lact, lactate; MCT, monocarboxylate transporter; MYC, c-MYC; PFKFB3, phosphofructokinase-2/fructose-2,6-bisphosphatase; VEGF, vascular endothelial growth factor; VEGFR2, vascular endothelial growth factor receptor 2 [Rohlenova 2018].*

When subjected to laminar shear stress, ECs are kept in a resting state through the activation of Krüppel-like Factor 2 (KLF2), a transcription factor responsible for the inhibition

of the above-mentioned key genes and others [Doddaballapur 2015]. Another transcription factor that keeps ECs in resting state is Forkhead box O1 (FOXO1), since indirectly reduces glycolysis by inhibiting the transcription factor MYC. It is well known that ECs metabolism is a driving and controlling force of angiogenesis. For instance, VEGF stimulates PFKFB3 levels and FGF signalling promotes MYC expression, thereby stimulating HK2 levels and glycolysis. Moreover, PFKFB3 and other glycolytic enzymes are compartmentalized in filopodia and lamellipodia in the so-called “ATP hot-spots”, co-localizing with F-actin in membrane ruffles [Rohlenova 2018].

In this context, mitochondria in ECs are more used as a biosynthetic centre than energy generators. Proliferating ECs metabolize fatty acids to sustain the tricarboxylic acid cycle (TCA), producing the precursors aspartate and glutamate from its intermediates oxaloacetate (OAA) and α-ketoglutarate (α-KG), fundamental for deoxynucleotides (dNTPs) synthesis (Figure 15) [Falkenberg 2019].

In addition, ECs use amino acids for their metabolism. Particularly, they can metabolize glutamine, the most abundant non-essential amino acid (NEAA) in blood [Mayers 2015]. Indeed, the presence of the enzyme glutaminase-1 (GLS1) in ECs allows using glutamine as a source of carbons to sustain TCA cycle for protein and nucleotide synthesis. Furthermore, glutamine is essential for the production of GSH, a key regulator of redox homeostasis.

However, glucose, once converted in glucose-6-phosphate by the hexokinase, can also be destined to the glycogen synthesis or can enter in pentose phosphate pathway (oxPPP) to generate ribulose-5-phosphate (Ru5P), used for nucleotide synthesis and NADPH, fundamental to convert glutathione from its oxidized form, GSSG, to its reduced form, GSH, a key antioxidant [Riganti 2012].

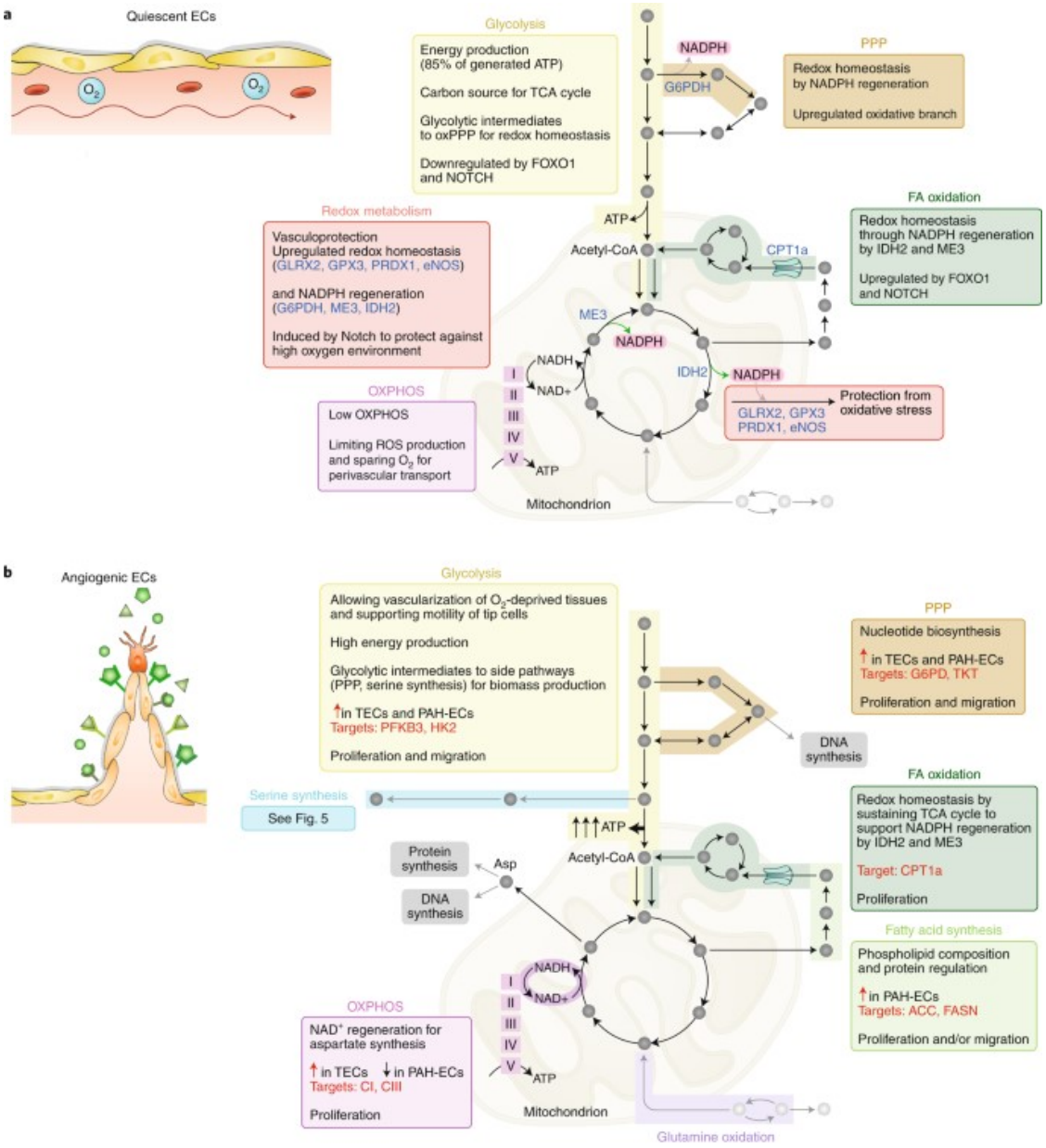

***Figure 15**: Role of mitochondria in ECs metabolism. **A**) Quiescent ECs adapt their metabolism to maintain redox homeostasis to cope with the oxidative-stress-prone high-oxygen environment. **B**) Angiogenic ECs rewire their metabolic pathways for energy and biomass production essential for cell proliferation and migration. Abbreviations: CI, mitochondrial complex I; CIII, mitochondrial complex III; GLRX2, glutaredoxin 2; GPX3, glutathione peroxidase 3; PRDX1, peroxiredoxin 1 [Falkenberg 2019].*

2.9 MITOCHONDRIA IN ECs

Notwithstanding their secondary role in the energy production process, mitochondria in ECs are considered signalling integrators from the environment, thus orchestrating cell response (Figure 16) [Caja 2017].

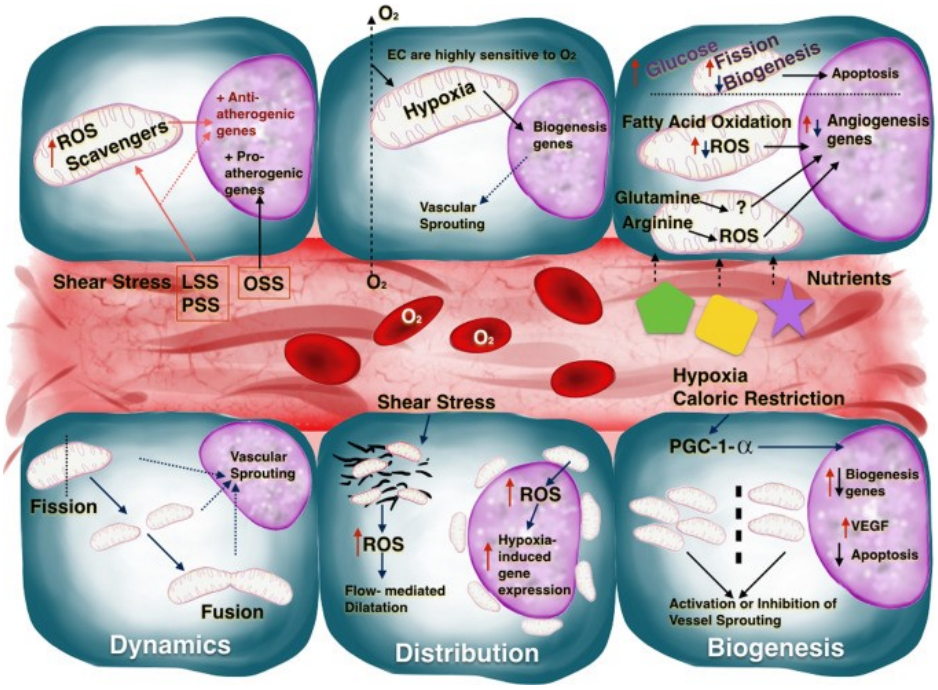

***Figure 16**: ECs mitochondria as signalling organelles for environmental cues. In response to different kind of stimuli such as oxygen, haemodynamic and nutrients mitochondria in ECs modify their biogenesis, dynamics and programmed degradation. Here the effects of LSS and PSS on EC mitochondria are shown as examples. Abbreviations: LSS, laminar shear stress; PSS, pulsatile shear stress; OSS, oscillatory shear stress [Caja 2017].*

Mitochondrial dynamics is determined by the balance between mitochondrial biogenesis and degradation (through the so-called process of mitophagy). Biogenesis requires replication of mitochondrial DNA (mtDNA) and expression of mitochondrial and nuclear genes. The master regulator of this process is the peroxisome proliferator-activated receptor gamma coactivator-1α (PGC-1α), a transcription factor responsible for the activation of nuclear respiratory factor (NRF) -1 and -2, and transcription factor A (mitochondrial TFAM) and transcription factor B (mitochondrial TFBM) that coordinate the expression of genes necessary for the process of biogenesis (the former activate genes encoded by nuclear genes, the latter by mitochondrial genes).

PGC-1α expression is affected by several factors (such as hypoxia and caloric restriction), while it is activated in case of energy demand to increase ATP production by ECs, modulating several genes related to lipid and glucose metabolism [Leone 2011; Patten 2012]. PGC-1α also modulates the expression of vascular endothelial growth factor-1 (VEGF-1) and stimulates angiogenesis [Widlansky 2012]. Additionally, PGC-1α coordinates cellular defences against oxidative stress, protects against apoptosis, limits inflammation and improves NO bioavailability [Valle 2005, Shulz 2008].

Moreover, mitochondrial organization is dynamic because they constantly undergo cycles of fusion and fission. Mitochondrial fusion allows the distribution of metabolites, proteins and mtDNA within the cell and contributes to maintain electrical and biochemical connectivity, while mitochondrial fission is fundamental for typical cell functions like cell division, movement and elimination of damaged or senescent mitochondria (Figure 17). Cytoskeletal organization is fundamental in orchestrating cycles of fusion and fission and determines mitochondrial network spatial organization [Moore 2018].

In particular, mitophagy is the process of degradation of mitochondria and it represents a form of autophagy specific for mitochondria. Autophagy is a well-controlled process that provides energy to the cell through degradation of damaged organelles. The process involves the formation of the double-membrane autophagosome where the cellular components targeted for degradation are engulfed, and the fusion with a lysosome, where the contents and inner membrane are degraded by acid hydrolases and recycled. The stimuli that activate mitophagy also activate PGC-1α and biogenesis to supply new mitochondria as a replacement of the degraded ones.

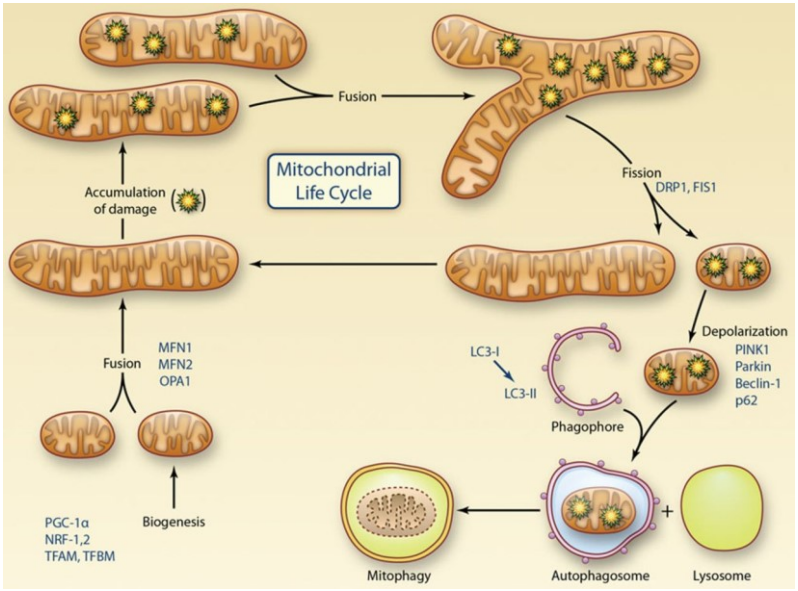

***Figure 17**: Mitochondrial life cycle [Kluge 2018].*

2.10 ENDOTHELIAL DYSFUNCTION

Endothelial dysfunction is defined as a shift of properties of the endothelium toward a proinflammatory and prothrombotic phenotype, characterized by altered release of NO and

overproduction of inflammatory cytokines and ROS. These alterations are associated with most forms of cardiovascular diseases, such as atherosclerosis, hypertension, coronary artery disease, chronic heart failure, peripheral vascular disease, diabetes, chronic kidney failure and severe viral infections (Figure 18).

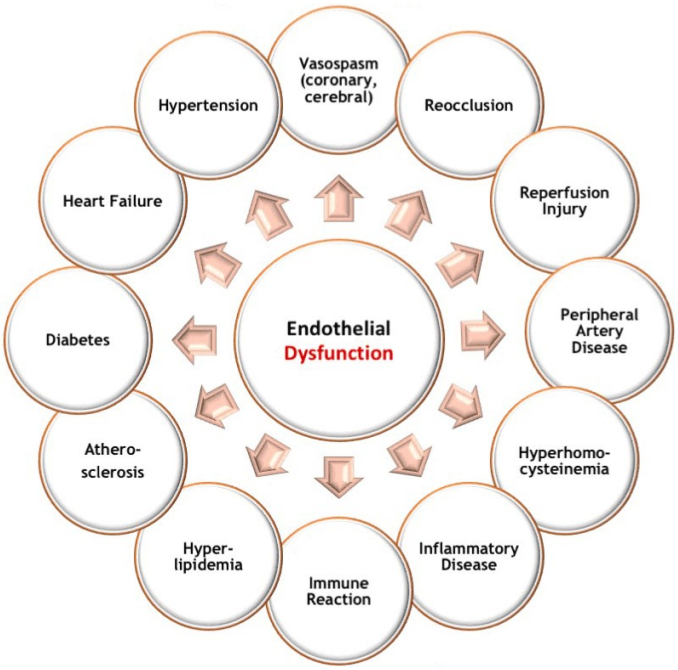

***Figure 18**: Schematic representation of consequences of endothelial dysfunction.*

Oxidative stress is an important factor contributing to endothelial dysfunction, often observed in cardiovascular diseases and linked with increased ROS production and decreased availability of antioxidants such as GSH [Shrestha 2018]. ROS production results from the reduction of molecular oxygen (O_2) to water in a reaction catalysed by Cytochrome C oxidase, a process that leads to the formation of partially reduced oxygen species. Indeed, 2% of total oxygen consumption is converted to superoxide anion radical ($\bullet O_2^-$) [Grishnam 1992]. Excessive production of ROS damages the endothelium and leaves it overly permeable, allowing toxins, various other molecules and, eventually, cells to cross-endothelial barrier and penetrate into the surrounding tissues [Rubanyi 1986, Raiendran 2013]. Physiologically the human body has an adequate supply of antioxidants, in part obtained from the diet, to neutralize these free radicals. However, in case of depletion of the antioxidant defences or of exposure to high amount of pro-oxidants, the endothelium acquires a dysfunctional phenotype, with severe pathophysiological consequences. Moreover, several factors can contribute to the accumulation of free radicals, including

obesity, smoking, sleep deprivation, acute microbial infections, high glucose intake and exposure to metals and air pollutants [O'Donnell 2008].

2.11 ATHEROSCLEROSIS

Endothelial dysfunction is a primary event that forerun the process of atherosclerosis, which is a progressive multifactorial disease characterized by the deposition of fatty material in the wall of arteries. This process entails different stages in response to a damage in the vascular wall, including the formation of fatty streak within the intima, the migration of leukocytes into the vessel wall, the maturation of the macrophages into foam cell and the degradation of extracellular matrix. The formation of atherosclerotic lesions is accelerated in diabetes and metabolic syndromes.

In greater detail, the initial stage of atherosclerosis is characterized by the adhesion of monocytes to the inner layer of the vessels, followed by their transmigration into the sub-endothelial space. Particularly, high glucose levels enhance atherogenesis through the activation of Nuclear Factor Kappa Beta (NFkB), leading to the expression of several inflammatory genes, such as genes encoding for adhesion molecules [Piga 2007]. Subsequently, monocytes differentiate into macrophages able to take up modified low-density proteins (LDL) maturating into foam cells, which accumulate in the wall of the vessel leading to the generation of a fibrous plaque (Figure 19) [Steinl 2015]. Foam cells are capable to release cytokines, which stimulate SMCs migration in the intima where they proliferate and deposit fibrin driving the formation of a fibrous cap [Johansson 2008]. Interestingly, glucose alone can affect monocyte/macrophage activation *in vitro*. Indeed, monocytes cultured in high glucose show an increased expression of proinflammatory cytokines, such as Interleukin-1β and Interleukin-6 [Shanmugam 2003]. These changes can lead to the induction of protein kinase C, to the activation of NFkB and to an increased release of superoxide, which may play a role in glucose-mediated oxidative stress [Venugopal 2002]. Moreover, the endothelium itself is sensitive to high glucose. For instance, diabetes determines an abnormal endothelium response that precedes the development of atherosclerosis. It is known that hyperglycaemia augments the production of proteins modified by advanced-glycation-end-products (among which LDL) and induces oxidative stress and inflammation, leading to the development of endothelial dysfunction [Domingueti 2016].

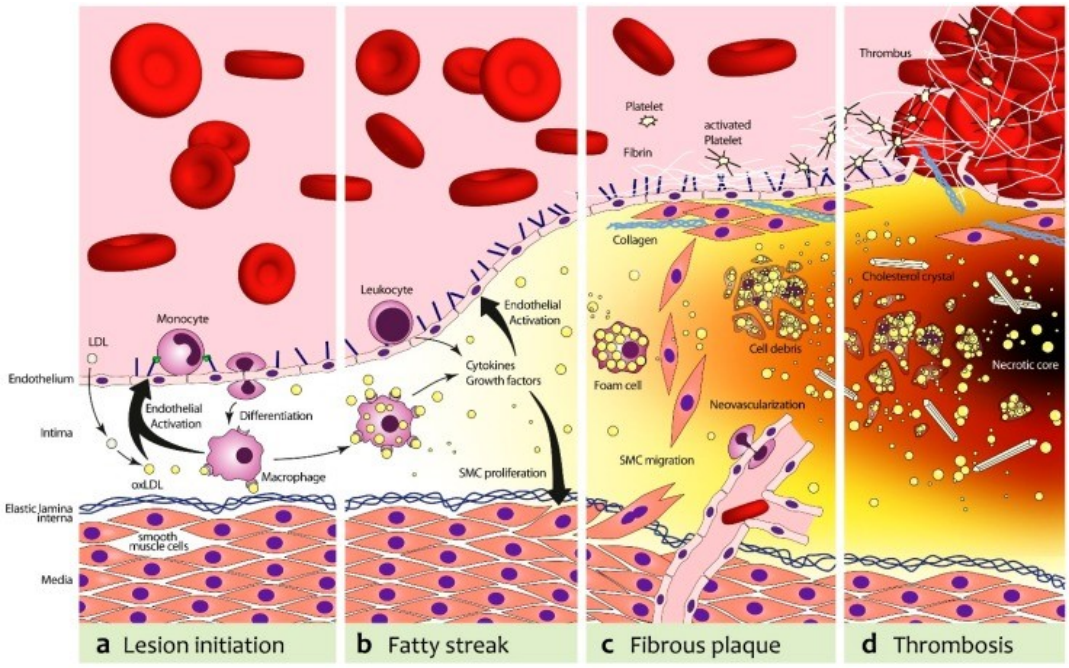

***Figure 19**: Pathogenesis of atherosclerosis. (**A**) Low density lipoprotein-cholesterol (LDL) is deposited in the endothelium and undergoes oxidative modification, resulting in oxidized LDL (oxLDL), which stimulates ECs to express adhesion molecules, i.e. VCAM-1 and P-Selectin, and several chemokines that recruit monocytes, which transmigrate into the intima and differentiate to pro-atherogenic macrophages. (**B**) Macrophages harvest residual oxLDL via their scavenger receptors and induce leukocyte recruitment with the secretion of Tumor Necrosis Factor α (TNF-α) and IL-6. (**C**) The increasing plaque volume promotes neovascularization. Proliferating SMCs stabilize the nascent fibrous plaque, depositing fibrin and activating platelets on the endothelium that expresses tissue factor (TF) and von Willebrand factor (vWF). (**D**) Foam cells can undergo apoptosis and release cell-debris and lipids, resulting in the formation of a necrotic core. In addition, proteases secreted from foam cells can destabilize the plaque. This can lead to plaque rupture, catalysing thrombosis [Steinl 2015].*

2.12 DIABETES

Diabetes Mellitus comprehends a group of life-long chronic metabolic disorders characterized by hyperglycaemia in the blood stream over a prolonged period. In the light of the fact that the endothelium is the gatekeeper of vascular health, it is not astounding that endothelial dysfunction is the crucial event leading to the development of atherosclerotic lesions, associated with a huge number of complications affecting different organs, such as eyes, kidneys, brain and heart [Stepan 2014]. Diabetes is currently a major public health problem since the number of patients rose from 108 million in the late ’80s to 422 million in 2014, according to the World Health Organization epidemiological investigations. Several pathogenic processes are involved in the development of diabetes, ranging from

autoimmune destruction of pancreatic β-cells with consequent insulin deficiency to a series of defects, i.e. inadequate insulin secretion and/or diminished tissue responses to insulin, eventually resulting in insulin resistance. On these bases, diabetes is classified mainly in three types: Type 1 Diabetes Mellitus (T1D), Type 2 Diabetes Mellitus (T2D) and Gestational Diabetes Mellitus (GDM).

T1D, also called “insulin-dependent diabetes mellitus” or “juvenile diabetes”, accounts for 5-10% of the cases of diabetes and it arises from a T cell-mediated autoimmune attack of the pancreatic β-cells, which culminates with the suppression of insulin production [Thomas 2015]. Markers of T1D include islet cell autoantibodies (ICA), autoantibodies against the tyrosine phosphatases of Islet-Associated protein -2 (IA-2) and -2β (IA-2β), insulin autoantibodies (IAA), autoantibodies against glutamic acid decarboxylase 65 (GAD65). Usually more than one of these autoantibodies are present in 85–90% of individuals when fasting hyperglycaemia is initially detected. Additionally, T1D has strong HLA associations, with linkage to the DQA and DQB genes, and it is influenced by the DRB genes [Chen 2021]. In this form of diabetes, the rate of β-cell destruction is quite variable, being rapid in some individuals (mainly infants and children) and slow in others (mainly adults). Some patients, particularly the youngest, may present ketoacidosis as first manifestation of the disease. Others have modest fasting hyperglycaemia that can rapidly evolve to severe hyperglycaemia and/or ketoacidosis in the presence of infection or other stress. Adult patients, on the other hand, may retain residual β-cell function sufficient to prevent ketoacidosis for many years.
Besides the multiple genetic predispositions, the autoimmune destruction of β-cells is also related to environmental factors that are still poorly defined. Moreover, these patients are prone to other autoimmune disorders, including Graves' disease, Hashimoto's thyroiditis, Addison's disease, vitiligo, celiac sprue, autoimmune hepatitis, myasthenia gravis and pernicious anaemia [Lanzinger 2021].

T2D, also called “non-insulin dependent diabetes mellitus”, is the more prevalent form accounting for almost the 90% of all cases of diabetes worldwide. It is a chronic disease characterized by insulin resistance associated with obesity due to the release of free fatty acids and proinflammatory cytokines from the adipose tissue [Thomas 2015]. There are probably many different causes of this form of diabetes. Although the specific etiologies are not known, in this case the autoimmune destruction of β-cells does not occurs and patients

do not show any of the genetic causes above-mentioned. Most T2D patients suffer for obesity, which causes some degree of insulin resistance. Patients not classified as obese by traditional weight criteria may have an increased percentage of body fat predominantly distributed in the abdominal region [Patel 2013]. Moreover, ketoacidosis seldom occurs spontaneously but it usually arises in association with another illness, such as infection. T2D frequently remains undiagnosed for many years because, since hyperglycaemia develops gradually, the disease is often not severe enough at earlier stages to be noticed. Nevertheless, such patients are at increased risk of developing macrovascular and microvascular complications [Nazimek-Siewniak 2002]. In this situation, insulin secretion is defective and therefore insulin levels are insufficient to compensate insulin resistance that may improve with weight reduction and/or pharmacological treatment of hyperglycaemia but is seldom restored to normal.

The risk of developing T2D increases with age, obesity and lack of physical activity. It occurs more frequently in women with prior GDM and in individuals with hypertension or dyslipidaemia and its frequency varies in different racial/ethnic subgroups. The genetics architecture T2D has not been precisely defined yet. The current hypothesis is that T2D is the result of multifactorial aetiology where both genetic and environmental factors are the underlying basis for the pathology of the disease [Hansen 2002].

However, recently some subgroups of T2D have been identified. For example, a relatively small percentage (less than 5%) of non-autoimmune diabetes, referred as Maturity Onset Diabetes of the Young (MODY), is due to monogenic high penetrance mutations in the Hepatocyte nuclear factor-1A (HNF1A) or the glucokinase (GCK) gene [American Diabetes Association 2013]. Another form of diabetes recently identified, known as Type 3 Diabetes (T3D) may lead to abnormalities linked to progressive brain insulin resistance with consequent impairment of central insulin signalling processes, accumulation of neurotoxins, neuronal stress, finally resulting in a course of neurodegeneration [Nguyen 2020]. These forms of diabetes are sometimes misdiagnosed as T2D but clinically they are distinct diseases.

GDM is defined as glucose intolerance that appears during pregnancy and may persist after delivery. It may have previously undiagnosed diabetes or may have developed diabetes coincidentally with pregnancy. It occurs in approximately 7% of pregnancies and women with a history of GDM have a significantly increased risk to develop T2D and cardiovascular disease after childbirth [Gilmartin 2008].

It is widely accepted that diabetes significantly increases the risk of cardiovascular disease [Nazimek-Siewniak 2002]. Indeed, macro- and micro- vascular complications are very common in patients affected by diabetes. Macrovascular complications, the leading cause of mortality associated with diabetes, include coronary heart disease (CHD), cerebrovascular disease and peripheral vascular disease [Abougalambou 2011]. Microvascular complications affect small vessels (arterioles, capillaries and venules) and play an important role in retinopathy and impairment of wound healing [El Asrar 2012].

2.13 VITAMIN D_3

VitD is a vital regulator of several biological processes, such as proliferation and differentiation of various cell types [Pittarella 2015, Gil 2018, Khammissa 2018]. Beyond its canonical role in controlling of calcium and phosphate homeostasis and hormonal secretions, VitD tunes endothelial function and subsequently exerts beneficial effects on the vascular system [Cuenca 2018]. Accordingly, VitD deficiency (circulating 25-hydroxyvitamin D_3, or 25-(OH)-D_3, levels < 20 ng/ml) is considered a risk factor for the development of hypertension, atherosclerosis, metabolic disorders and low grade inflammation, all disorders that share a common feature, i.e. endothelial dysfunction [Mousa 2018; Saheb 2020; Dalan 2014]. Indeed, numerous observational studies have shown associations of low 25-(OH)-D_3 concentrations and high risks of cardiovascular diseases [Swart 2018]. Moreover, there is a strong correlation between insufficient serum levels of VitD and heart failure, myocardial infarction and increased arterial blood pressure [Giovannucci 2008]. In addition, mouse models knockout for Vitamin D_3 Receptor (VDR) or deficient for 1α-hydroxylase (the enzyme responsible for the hydroxylation of VitD into its active form) show elevated arterial blood pressure [Zhou 2008, Li 2002]. Furthermore, VitD has a direct effect on ECs, decreasing coagulation and increasing fibrinolysis [Wu-Wong 2009].

VitD necessitates two steps of maturation before being converted in the active form. Firstly, cholecalciferol is produced in the skin starting from its biological precursor, 7-dehydrocholesterol (7-DHC), after the exposure to UV light, but it is biologically inert (Figure 20). A first hydroxylation in the liver is necessary to form 25-hydroxyvitamin D_3 [25-(OH)-D_3], also known as Calcidiol. Then, a second hydroxylation in the kidneys leads to the formation of the biologically active form 1,25-dihydroxivitamin D_3 [1,25-$(OH)_2$-D_3], also named Calcitriol [Jassil 2017]. Both 25-(OH)-D_3 and 1,25-$(OH)_2$-D_3 are catabolized by CYP24A1, a member

of cytochrome P450 family. 1,25-(OH)2-D_3 is the ligand for VDR, present in different tissues and cells in the human body [De Boer 2008]. VDR is a member of the nuclear hormone receptors superfamily of ligand-inducible transcription factors, which includes also the receptors of glucocorticoids, mineralocorticoids, sex hormones, thyroid hormones and Vitamin A metabolites (retinoids). Upon binding of 1,25-$(OH)_2$-D_3, VDR heterodimerizes with other nuclear hormones receptors (especially Retinoid X Receptors, RXRs), resulting in the dissociation of co-repressor proteins (such as NCoR1, SMRT, Hairless and Alien) and in the interaction with co-activators (such as SRC1, TIF2 and RAC3). The complex VDR-RXR binds to specific DNA sequences, called Vitamin D Response Elements (VDRE), located in the promoter region of VitD-regulated genes, controlling their expression [Carlberg 2009].

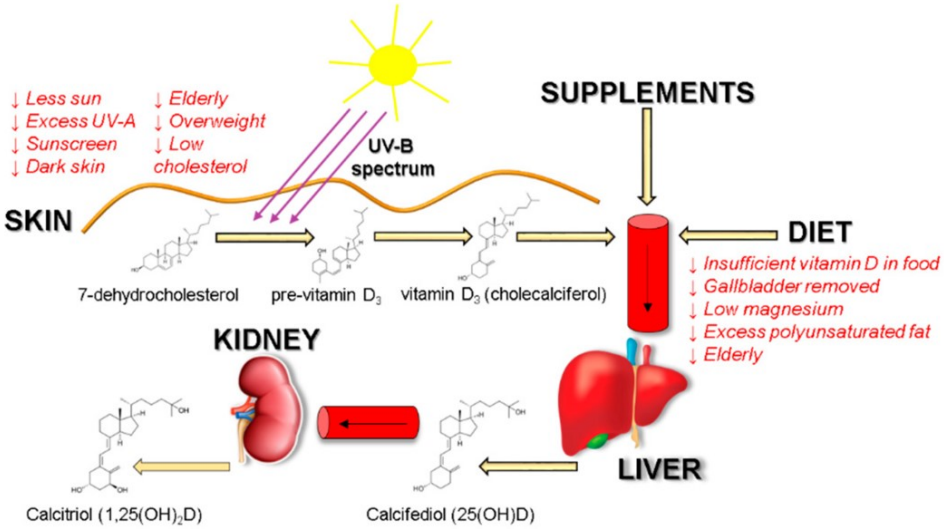

***Figure 20**: Vitamin D_3 sources, biosynthesis and possible factors affecting absorption [Šimoliūnas 2019].*

VitD exerts skeletal and extra-skeletal effects, as summarized in Table 1 [Bover 2015].

SKELETAL EFFECTS OF VITAMIN D		
Skeletal mineral protection	**Osteoclast activation**	**Calcium channel opening**
Skeletal mineral development and maintenance, by adequate osteoblast formation and osteoclast resorption Prevention and treatment of SHP and high turnover bone disease	Maturing and activation of osteoclasts mediated by osteoblasts	Increases its intracellular levels, favouring the mobility and conformational changes essential to adequate osteoblastic function

EXTRASKELETAL EFFECTS OF VITAMIN D			
Renal protection	**Cardiovascular protection**	**Control of systemic inflammation**	**Regulation of apoptosis**
Antiproteinuric effects	RAAS inhibition	Th1 inhibition	Modulation of gene expression Increased intracellular Ca
Increased nephrin expression	ANP regulation	Th2 activation	Apoptosis of cancer cells.
NFkB inactivation (anti-inflammatory action)	Inhibition of smooth muscle cell proliferation	Induction of CD4+CD25+	
Inhibition of TACE (Tumour Necrosis Converting Enzyme)	Decrease in atherosclerosis and vascular calcification	TNFα, ICAM-1 and VCAM 1 inhibition	

SHP: secondary hyperparathyroidism; RAAS: renin-angiotestin-aldosterone system;ANP: atrial natriuretic peptide; NFkB: nuclear factor kappa-light-chain-enhancer of activated B cells; TNF: tumour necrosis factor; ICAM1: Intercellular Adhesion Molecule 1; VCAM1: Vascular Cell Adhesion Molecule 1.

***Table 1**: Skeletal and extraskeletal effects of VitD [Bover 2015].*

Experimental studies indicate that 1,25-$(OH)_2$-D_3 protects against atherosclerosis by inhibiting the conversion of macrophages into foam cells and by enhancing cholesterol efflux [Yin 2015]. 1,25-$(OH)_2$-D_3 also induces the synthesis of VEGF by vascular smooth muscle cells and VEGF promotes endothelial repair. Other anti-atherosclerotic properties of VDR activation include anti-inflammatory actions such as reduction of NFkB and IL-6 expression in ECs, reduction of thrombogenicity – through the downregulation of tissue factor and the upregulation of thrombomodulin expression in ECs and macrophages – and increased endothelial NO production (Figure 21). Interestingly, in mice with endothelial-specific knockout of the *Vdr* gene, vascular function is significantly impaired [Pilz 2016].

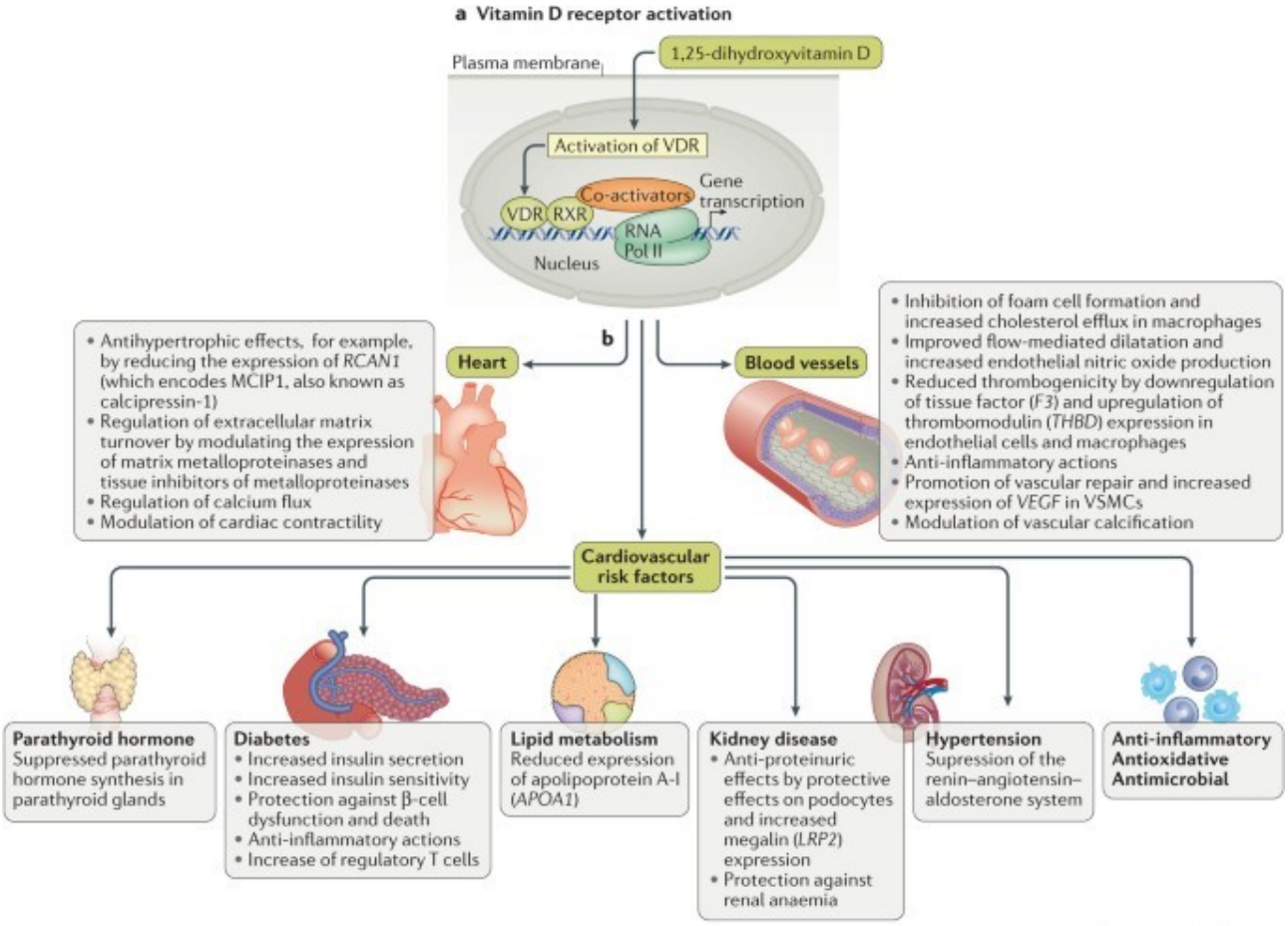

***Figure 21**: Cardiovascular effects of Vitamin D receptor activation [Pilz 2016].*

3. AIM OF THE THESIS

Understanding endothelial dysfunction is a major focus to generate new tools to prevent and treat vascular diseases. The aim of the thesis was to investigate the effects of high glucose levels and of blood serum collected from paediatric T1D patients on endothelial cells monolayers. Human Umbilical Vein Endothelial Cells (HUVEC), a widely used type of macrovascular cells, were cultured either in 2D cell culture systems on flat dishes, a system which has yielded major advances in our knowledge about endothelial pathophysiology, or in 3D microfluidic chips to closely reflect what happens *in vivo*, since they show a higher degree of structural complexity allowing perfusion, thus generating shear stress fundamental for endothelial homeostasis. In 2- and 3- D the cells were cultured until they reach the confluence to reproduce the physiological inner layer of a blood vessel as closely as possible and were exposed to different concentrations of extracellular glucose or to 10% of blood serum from 36 paediatric T1D patients or 14 healthy controls.

4. MATERIALS AND METHODS

4.1 CELL CULTURE

HUVEC, a widely used model of macrovascular ECs, were purchased from Lonza (Basel, Switzerland) and cultured in EGM-2 medium (Euroclone, Milano, Italy) containing 10% of Fetal Bovine Serum (FBS) on collagen-coated dishes (50 µg/ml). The cells were routinely tested for the expression of endothelial markers and used for 6–7 passages.

To perform the experiments, the cells were trypsinized, stained with 0.4% Trypan blue solution and counted using a Luna Automated Cell Counter (Logos Biosystems, Anyang–si, Gyeonggi–do, South Korea). Cells were cultured both in 2D cell culture systems on flat dishes, a methodology which has yielded major advances in our knowledge about endothelial pathophysiology, and in 3D microfluidic chips [Tsvirkun 2017]. In both 2D and 3D systems, the cells were cultured until they reached confluence to reproduce the physiological inner layer of a blood vessel as closely as possible.

4.2 CELL TREATMENTS

D-glucose (Sigma Aldrich, St. Louis, Missouri, USA) was added to the culture medium, which normally contains 1 mg/ml of glucose (5.5 mM, CTR), to obtain the final concentrations of 2 mg/ml (11.1 mM) and 5.4 mg/ml (30 mM) for 24h. L-glucose (Sigma Aldrich) at a concentration of 30 mM was utilized as control for osmolarity. In 3D-microfluidic cell culture experiments, after 7 days in culture with normal medium, D-glucose and L-glucose were added for 24h to the normal medium.
In some experiments, hydrogen peroxide (H_2O_2, 100 mM) and N-acetylcysteine (NAC, 5 mM) (Sigma Aldrich) were used, in combination with D- and L-glucose.
1,25-$(OH)_2$-D_3 (VitD) was used at a concentration of 20 nM. Initially the behavior of HUVEC cultured in the presence of various concentration of VitD for 24h was tested to choose the proper dose to be used. Figure 22 shows that the maximal dose tolerated by the cells is 20 nM, since the higher doses (30, 40 and 50 nM) impair cell proliferation.

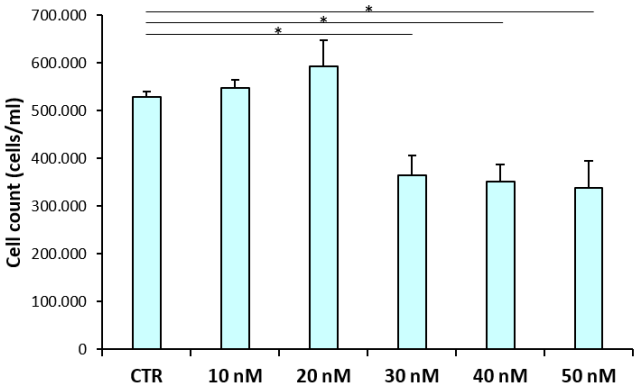

***Figure 22**: HUVEC were cultured in the presence of various concentrations of VitD for 24h and counted. The results are the mean of 3 experiments performed in triplicates ± SD. * p < 0.05.*

In some experiments, FBS in the medium was replaced with 10% of serum collected from 36 paediatric T1D patients (T1D) and 14 age-matched non-diabetic healthy donors (CTR). In this study population cohort, each participant who fulfilled the inclusion criteria was consecutively enrolled. Clinical characteristics of T1D patients and healthy donors are summarized in Table 2. None of the T1D patients was affected by other pathologies, such as retinopathy (evaluated by stereoscopic fundus photography) or neuropathy (evaluated by nervous conduction velocity and autonomic tests) or was under treatment with other drugs except insulin. All patients included in the study were non-smokers; none was taking antioxidant supplements or drugs with known antioxidant activity. The physiological range of glycated haemoglobin (HbA1c) is between 4% and 7.5%. In addition, the expected value of glycaemia ranges between 60 and 100 mg/dl, while, in non-adult patients, fasting hyperglycaemia is defined for values higher than 100 mg/dl. Informed consent was obtained from all subjects included in the study. Sera were collected at the University of Milan–V. Buzzi Children's Hospital. The study was approved by the Buzzi Children's Hospital (ASST Fatebenefratelli–Sacco, Milan, Italy) Ethical Committee (2018/ST/143, 9th October 2018, Milano Area 1). All the procedures followed were in accordance with the ethical standards of the responsible committee on human experimentation (institutional and national) and with the Declaration of Helsinki 1975, as revised in 2008.

	Healthy Subjects (n = 14)	Patients (n = 36)
Sex		
Male	n = 5	n = 12
Female	n = 9	n = 24
Age (years)		
Mean	12.5	13.8
Range	3.1–23.7	4.0–24.0
Hb1Ac (%)		
Mean	5.7	7.15
Range	5.30–6.80	5.10–8.80
PCR (mg/dL)		
Mean	0.53	0.71
Range	0.43–0.61	0.20–2.60
Glycaemia (mg/dL)		
Mean	102	168.26
Range	89.0–117.0	40.0–350.0
Therapy	None	MDI (n = 22) CSII (n = 14)

***Table 2**: Clinical characteristics of paediatric T1D patients and healthy controls. Regarding the T1D patients, 10 were normo-glycaemic, 26 hyper-glycaemic, 11 had high levels of HbA1c (>7.5 %) and 25 had levels of HbA1c within the physiological range.*

4.3 3D-MICROFLUIDIC CELL CULTURE

In 3D experiments, HUVEC were seeded in a microfluidic devices fabricated using a standard soft-lithography technique [Tsvirkun 2017] and subjected to a constant flow of supplemented medium at 1 µl/min, corresponding to a wall shear stress of about 0.2 Pa (representative of physiological conditions for venous endothelial cells) in channels of nominal section 30 × 30 µm. Cells were cultured in the microfluidic device for 7 days and, after the treatments with physiological (5.5 mM, CTR) or high D-glucose (30 mM) and 30 mM of L-glucose, were fixed for immunofluorescence.

4.4 CRYO SOFT X-RAY TOMOGRAPHY

In Cryo Soft X-ray Transmission Tomography (Cryo-SXT) experiments, HUVEC were seeded onto gold Quantifoil R 2/2 holey carbon-film microscopy grids (EMME 3, Rho, Italy) at a concentration of $2x10^4$ cell/cm^2. Cells were incubated at 37 °C in 5% CO_2 for 24h with medium containing different concentrations of D-glucose (5.5 mM, 11.1 mM and 30 mM). L-

glucose (30 mM) was used as control of osmolarity. The samples were then gently rinsed with phosphate buffered saline (PBS) for two times and soon thereafter HUVEC were frozen-hydrated by a rapid plunge freezing in liquid ethane bath cooled with liquid nitrogen using a Leica EM GP robot (Leica Microsystems, L'Hospitalet de Llobregat, Spain). Excess water was removed before plunge freezing via blotting to obtain a total ice thickness below 5 μm, avoiding the formation of vitreous ice upon the samples that causes X-ray absorption. Frozen specimens were transferred into the full field Soft X-ray Transmission microscope of the Mistral beamline at the ALBA-Light Source [Sorrentino 2015], where Cryo-SXT measurements of whole frozen hydrated cells were performed. The cryogenic conditions were maintained during all the experiment.

Cryo-SXT images were recorded at the MISTRAL beamline where photons extracted from a bending magnet source are directed on the sample by a capillary condenser located facing the monochromator exit slit. Behind the sample, a zone plate with an outermost zone width of 40 nm acts as an objective lens of the microscope, generating a magnified image on a direct illumination CCD detector located nearby the specimen [Sorrentino 2015]. Cryo-SXT was carried out at 520 eV to optimize the contrast between the carbon-rich organelles membranes and the water-rich cytoplasmic solutions. For each cell, a tilt series was acquired using an angular step of 1° on a 140° angular range. The effective pixel size in the images was 13 nm. No radiation damage was detected at our spatial resolution. Each transmission projection image of the tilt series was normalized using flat-field images of 1-second acquisition time. The tilt series were manually aligned using eTomo in the IMOD tomography software suite [Kremer 1996]. With the aim to decrease as much as possible the deviations from an ideal rotation that creates artefacts in the reconstructed tomograms, the rotation of Au fiducials of 150 nm (BBI Solutions – Freiburg, Germany) was followed. According with the Beer – Lambert law, the transmission T(x,y) is given by:

$$T(x,y) = \frac{I(x,y)}{I_0(x,y)} = e^{(-\int \mu(x,y,E_0)tdt)} = e^{(-\int \mu_m(x,y,E_0)\rho t dt_m)}$$

Where: I is the transmitted intensity by the sample; I_0 is the incident beam intensity; E_0 is the X-ray LAC at incident energy E_0, $\mu m(E_0) = (E_0)/\rho$ is the mass absorption coefficient at the same energy; ρ is the matrix density; x and y are the coordinates in the transversal plane at the sample position and the integral is extended through all the sample thickness. All the

transmission tilt series have been converted in absorbance using ImageJ by applying the following expression:

$$\mu(E_0)t = -ln(T)$$

The absorbance tilt series were finally reconstructed with TomoJ [Messaoudii 2007], a plugin of ImageJ [Rueden 2017], using the ART iterative-algorithms with 15 iterations and a relaxation coefficient of 0.01. Finally, the images were semi-automatically segmented by Amira software (Thermo Fisher Scientific) and the "Volren" module enabled to render all the segmented regions at the same time with different colour maps. The Volume3D value of each object segmented was calculated by Amira and normalized performing a calibration on the gold nano-beads.

The Fractional Anisotropy (FA) was calculated for all segmented mitochondria and lipid droplets in every cell culture condition. The eigenvalues λ_1, λ_2 and λ_3 were automatically extracted by Amira software and the FA has been calculated by applying the following formula [Basser 2011]:

$$FA = \sqrt{\frac{3}{2}} \frac{\sqrt{(\lambda_1 - \lambda) + (\lambda_2 - \lambda) + (\lambda_3 - \lambda)}}{\sqrt{\lambda_1^2 + \lambda_2^2 + \lambda_3^2}}$$

4.5 siRNA SILENCING AND PHARMACOLOGICAL INHIBITION

NOS was inhibited using either small interfering RNA (siRNA) or pharmacological inhibitors. Sub-confluent cells were transfected with siRNA targeting *eNOS* (NOS3) [20 nmol, 50-TTCGAGGGACACCACGTCATACTCA-30 (Invitrogen Corporation, Carlsbad, CA, USA)] or *iNOS* (NOS2A) [20 nmol, 50-ATCGAATTTGTCAACCAATAT-30 (Invitrogen)]. Lipofectamine RNAiMAX was used as transfection reagent (Invitrogen), according to the manufacturer's recommendations. After 6h, the siRNA transfection medium was replaced with the treatments for 24h. The same experimental approach was used with 10% serum collected from CTR or T1D patients. We tested *eNOS*- and *iNOS*-silencing using Real Time

PCR (Figure 28). Alternatively, sub-confluent cells were pre-treated with 100 μM of pharmacological inhibitors of eNOS [L-N_{ω}–Nitroarginine-Methyl-Ester (L-NAME)] and iNOS [N6–(1-Iminoethyl)-L-Lysine (L-NIL)] (Sigma Aldrich) for 1h. Then, 10% of serum from the cohort or D-glucose were added. The experiments lasted 24h. All the experiments were performed in triplicate three times.

The same protocol was used to inhibit Thioredoxin Interacting Protein (TXNIP) with siRNA targeting *TXNIP* [20 nmol, 5'- AAGCCGTTAGGATCCTGGCT-3' (Quiagen, Hilden, Germany)] and after 6h the siRNA transfection medium was replaced with the culture medium containing D-glucose in the presence or not of 20 nM of VitD. All the experiments were performed in triplicate three times.

4.6 WESTERN BLOT

After the 24h treatments, HUVEC were lysed in 50 mM Tris-HCl (pH 7.4) containing 150 mM NaCl, 1% Nonidet P40 (NP40), 0.25% sodium deoxycholate, protease inhibitors (10 μg/mL Leupeptin, 10 μg/mL Aprotinin, 1 mM PMSF) and phosphatase inhibitors (1 mM sodium fluoride, 1 mM sodium vanadate, 5 mM sodium phosphate). Cell lysates (40 μg/lane) were separated by SDS-PAGE on Mini-PROTEAN TGX Stain-free Gels (Bio-Rad Laboratories, Hercules, California, USA) and transferred to nitrocellulose sheets using Trans-Blot Turbo Transfer System (Bio-Rad).

To study the stress adaptive response of HUVEC upon the treatments, Western Blot analysis was performed using antibodies against: TXNIP (Invitrogen), Paraoxonase (PON) 2 (Invitrogen, Carlsbad, California, USA), Sirtuin 1 (SIRT1) (Thermo Fisher Scientific), Sirtuin 2 (SIRT2) (Millipore, Vimodrone, Italy), Superoxide-dismutase 2 (SOD2) (BD Transduction Laboratories, Milano, Italy), Glucose Transporter 1 (GLUT1) (Invitrogen), Heat Shock Protein 70 kilodaltons (HSP70) (Santa Cruz Biotechnology, Dallas, TX, USA).

To analyze the modulation of NOS enzymes, iNOS (BD Transduction Laboratories), P-eNOS Ser^{1177} (Cell Signaling Technology, Danvers, Massachusetts, USA), eNOS (BD Biosciences) antibodies were utilized.

To study mitochondrial content, antibodies against Cyclophilin D (CYPD) (Invitrogen), Optic Atrophy 1 (OPA1) (Invitrogen) and Dynamin-Related Protein 1 (DRP1) (Invitrogen) were used.

To get insight into the mechanisms underlying endothelial permeability, Western Blot analysis was performed using antibodies against Zonula Occludens 1 (ZO-1) (Invitrogen) and Ve-Cadherin (Cell Signaling Technology).
As markers of lipid metabolism were used antibodies against: endothelial differentiation-related factor-1 (EDF-1) (Aviva, London, UK), peroxisome proliferator-activated receptor ɣ (PPARɣ) (Santa Cruz Biotechnology) and Carnitine Palmitoyl-transferase 1A (CPT1A) (Thermo Fisher Scientific).
Actin antibody (Santa Cruz Biotechnology) was used as a marker of equal loading.

After extensive washing, secondary antibodies labelled with horseradish peroxidase (GE Healthcare, Waukesha, WI, USA) were used. Immunoreactive proteins were detected with Clarity™ Western ECL substrate (Bio-Rad) and images were captured with a ChemiDoc MP Imaging System (Bio-Rad). Densitometry of the bands was performed with Image J Lab software (National Institute of Health, Bethesda, MD, USA). The Western Blots shown are representative and the densitometric analysis was performed on three independent experiments ± SD.

4.7 TRANSWELLL PERMEABILITY ASSAY

Transwelll Permeability Assay was performed in a 24-well receiver plate with individual hanging cell culture inserts (Transwelll Permeable Supports, Euroclone). The transwelll are characterized by two compartments: i) the upper and ii) the lower, divided by a microporous membrane (0.4 μm). The cells were seeded on the microporous membrane in the upper compartment and were incubated for 24h with different cell culture conditions. After the treatment, 1 mg/ml Fluorescein isothiocyanate labelled-albumin (FITC-BSA) (Sigma Aldrich), a fluorescent probe capable to cross the monolayer of ECs at a rate proportional to the monolayer's permeability, was added [Romeo 2019]. The extent of permeability was determined by measuring the fluorescence in the lower chamber. Fluorescence was detected by the Varioskan LUX Multimode Microplate Reader (Thermo Fisher Scientific) at $\lambda_{ex/em}$ = 495/519 nm. The results are the mean of three independent experiments performed in triplicate ± SD.

4.8 NOS ACTIVITY

NOS activity was measured in the conditioned media by using the Griess assay. Conditioned media were mixed with an equal volume of freshly prepared Griess reagent. Griess reagent consists of two solutions, mixed with a 1:1 ratio: solution A is composed by 1% sulphanilamide resuspended in 5% orthophosphoric acid, while solution B is composed by 0,1% N-α-naphtylethylenediamine dichloride in distilled water. The culture media from the samples were de-proteinized with acetone (ratio 1:1) and centrifuged at 14.000 rpm for 10 minutes: the surnatant, representing the de-proteinized medium, was collected and quantified. The concentration of nitrites in the samples was determined using a calibration curve generated with known concentrations of sodium nitrite standard ($NaNO_2$) solutions. The absorbance was measured at 550 nm. The results are the mean of three independent experiments performed in triplicate ± SD.

4.9 ROS PRODUCTION

For the detection of overall cellular ROS, HUVEC were cultured in a 96-well black plate (Greiner Bio-One, Kremsmunster, Austria) and, upon the treatments, incubated for 30 minutes with 20 μM 2'-7'-dichlorofluorescein diacetate (DCFH) solution (Sigma Aldrich). The DCFH fluorescence ($\lambda_{ex/em}$ = 484/535 nm) was monitored using the Varioskan LUX Multimode Microplate Reader (Thermo Fisher Scientific). ROS production was normalized on the cell number. The results are the mean of three independent experiments performed in triplicate ± SD.

4.10 MITOCHONDRIAL ROS

Mitochondrial ROS (mtROS) production was measured by MitoSOX™ Red mitochondrial superoxide indicator (Invitrogen), a fluorogenic dye for highly selective detection of superoxide in the mitochondria of live cells. Once in the mitochondria, the reagent is oxidized by superoxide and it exhibits red fluorescence. Upon the 24h treatments in a 96-well black plate, the cells were incubated for 10 minutes at 37°C with MitoSOX reagent, protected from

light. The fluorescence ($\lambda_{ex/em}$ = 510/580 nm) was measured using the Varioskan LUX Multimode Microplate Reader (Thermo Fisher Scientific). The results are the mean of three independent experiments performed in triplicate ± SD.

4.11 REDUCED *vs* OXIDIZED GLUTHATIONE QUANTIFICATION

Reduced glutathione (GSH) / oxidized glutathione (GSSG) ratio was calculated using the luminescence-based GSH/GSSG-Glo™ Assay (Promega, Madison, Wisconsin, USA), according to the manufacturers' instructions. The assay is based on the lysis of the cells in the presence of a luciferin derivative, Luciferin-NT, which is converted into luciferin in the presence of glutathione. The reaction is catalysed by glutathione-S-transferase enzyme. The luminescent signal, generated in a coupled reaction with firefly luciferase, is proportional to the amount of GSH present in the sample. GSH/GSSG ratios were calculated directly from luminescence measurements. Luminescence was monitored using the Varioskan LUX Multimode Microplate Reader (Thermo Fisher Scientific). The results are the mean of three independent experiments performed in triplicate ± SD.

4.12 LUMINESCENT CELL VIABILITY ASSAY

The CellTiter-Glo Luminescent Cell Viability Assay (Promega) was used to determine the number of viable cells relying on the quantification of the ATP present, according to the manufacturer's instructions. This assay relies on the properties of a thermostable luciferase that, in presence of Mg^{2+}, catalyzes an oxidative reaction thus producing bioluminescence. Starting from luciferin and the co-factors molecular oxygen and ATP, it is produced oxyluciferin and emitted light. After the treatments, the cells were incubated with CellTiter-Glo Reagent, diluted in culture medium with a 1:1 ratio, for 10 minutes at room temperature. The luciferase activity was monitored using the Varioskan LUX Multimode Microplate Reader (Thermo Fisher Scientific). The results are the mean of three independent experiments performed in triplicate ± SD.

4.13 EXTRACELLULAR O_2 CONSUMPTION

The Oxygen Consumption Rate (OCR) was measured by the Extracellular O_2 Consumption Reagent (Abcam), according to the manufacturer's instructions. In particular, the assay is based on the ability of oxygen to quench the excited state of the reagent. During the cell respiration, the oxygen is depleted in the surrounding environment increasing the fluorescent signal. Upon the treatments with conditioned media, the cells were incubated with the Extracellular O_2 Consumption Reagent and sealed by the pre-warmed High Sensitivity mineral oil. H_2O_2 was used as positive control. Subsequently, the 96-well black plate was located into the Varioskan LUX Multimode Microplate Reader (Thermo Fisher Scientific), pre-set to 37°C. The fluorescent signal ($\lambda_{ex/em}$ = 380/650 nm) was measured every 2 minutes for 180 minutes. The results are the mean of three independent experiments performed in triplicate ± SD.

4.14 FATTY ACID OXIDATION

Fatty Acid Oxidation (FAO), the primary metabolic pathway for degradation of fatty acids, was monitored by Fatty Acid Oxidation Assay (Abcam) in living cells. The cells were seeded in a 96-well black plate and, upon the treatment for 24h, were rinsed twice with pre-warmed Fatty Acids-Free medium followed by the addition of pre-warmed Fatty Acids Measurement Medium. In all wells, except the blank control, Extracellular O_2 Consumption Reagent was added. The FAO activator Trifluoromethoxy carbonylcyanide phenylhydrazone (FCCP, 0,625 µM) was used as positive control. Finally, the wells were sealed with pre-warmed High Sensitivity mineral oil and the FAO was measured using the same protocol described for Extracellular O_2 Consumption. The results are the mean of three independent experiments performed in triplicate ± SD.

4.15 LACTATE QUANTIFICATION

L-Lactate was quantified using the luminescence-based Lactate-Glo™ Assay (Promega), according to the manufacturer's recommendations. The assay couples lactate oxidation and

NADH production. Indeed, the enzyme lactate dehydrogenase produces pyruvate and NADH from lactate and NAD+. In the presence of NADH, a pro-luciferin reductase substrate is converted to luciferin by the enzyme reductase, emitting light. The luminescent signal is proportional to the amount of lactate in the sample. Luminescence was monitored using the Varioskan LUX Multimode Microplate Reader (Thermo Fisher Scientific). The results are the mean of three independent experiments performed in triplicate ± SD.

4.16 STAINING OF NEUTRAL LIPIDS

BODIPY^{TM} 493/503 (Invitrogen) is a lipophilic dye used to label cellular neutral lipids, particularly those localized to lipid droplets, both in live and fixed cells. Upon the treatments, the culture medium was replaced with 2 µM BODIPY staining solution in PBS, incubated for 30 minutes at 37°C, protected from light. After intensive washing with PBS to remove the excess of staining solution, images were taken using FLoid Cell Imaging Station (Thermo Fisher Scientific). Alternatively, fluorescence ($\lambda_{ex/em}$ = 493/503 nm) was measured using the Varioskan LUX Multimode Microplate Reader (Thermo Fisher Scientific). In parallel, Oil Red O Staining was used to detect neutral lipids. After the 24h treatments, cells were washed three times with PBS, fixed in PFA 10% for 30 min at room temperature, washed once again with PBS and then stained with 60%-filtered Oil Red O stock solution (Sigma Aldrich) for 20 min. After extensive washing, Oil Red O was solubilized in 100% isopropanol, quantified by measuring the absorbance at 500 nm and normalized to the cell number, after images acquisition using FLoid Cell Imaging Station (Thermo Fisher Scientific). The results are the mean of three independent experiments performed in triplicate ± SD.

4.17 TRIGLYCERIDE QUANTIFICATION

Triglycerides were quantified using Triglyceride Quantification Kit (Sigma Aldrich), according to the manufacturer's recommendations. Briefly, triglycerides are broken down into free fatty acids (FFA) and glycerol, which is then oxidized to generate a fluorescent product ($\lambda_{ex/em}$ = 535/587 nm). Fluorescence was monitored using the Varioskan LUX Multimode Microplate

Reader (Thermo Fisher Scientific). The results are the mean of three independent experiments performed in triplicate ± SD.

4.18 CONFOCAL IMAGING

After the treatments, cells seeded on coverslips or in 3D-microfluidic device, were fixed in PBS containing 4% paraformaldehyde and 2% sucrose pH 7.6 for 30 minutes at 37°C and then were permeabilized with Triton 0.3%.

To analyse cell morphology, the fixed-cells were incubated for 45 minutes with phalloidin-TRITC (1:300) and DAPI (1:10000) to respectively stain F-actin and nuclei.
To analyse the localisation of the junctional proteins ZO-1 and Ve-Cadherin (Cell Signalling Technology), the cells were incubated overnight at 4°C with the specific antibodies. After extensive washing, the samples were incubated with secondary Alexa Fluor 647 antibody (Invitrogen) and DAPI (Sigma-Aldrich) for 1h.

Finally, the cells were mounted with ProLong™ Gold Antifade Mountant (Invitrogen) and images were acquired using a 40X and 63X objective in oil by a SP8 Leica confocal microscope (Leica Microsystems). Images were analysed using ImageJ.

4.19 ACTIN ALIGNMENT QUANTIFICATION

Images derived from immunofluorescence for F-actin performed on HUVEC grown in 3D-flow condition were analysed using the OrientationJ plugin of ImageJ to obtain orientation maps in which an angle theta is attributed to every pixels involved in oriented actin structures. For 2D images, an ideal horizontal axis was assumed as theta = 0, whereas in 3D images, the direction of flow within the 30 × 30 µm channel was assumed as theta = 0. The angular distributions of actin fibers was calculated as the deviation of fibre orientation compared to theta = 0. Angular distributions of actin fibers were calculated over 30 angular bins of width 3°, spanning the range from 0 to 90°. Pixels displaying an angle +theta or -theta were counted in the same angular bin centred on theta. Distributions were plotted as

the fraction of image pixels (called "frequency" in the figures) whose angle falls within a given bin.

4.20 STATISTICAL ANALYSIS

Data are reported as means ± SD. The data were normally distributed and they were analysed using one-way or two-way repeated measures ANOVA. The *p*-values deriving from multiple pairwise comparisons were corrected by the Bonferroni method. Statistical significance was defined for *p*-value < 0.05. Concerning the Figures, * $p < 0.05$; ** $p < 0.01$; *** $p < 0.001$; **** $p < 0.0001$.

5. RESULTS (1)

HIGH GLUCOSE AND OXIDATIVE STRESS

5.1.1 HIGH GLUCOSE CAUSES REDOX IMBALANCE

Oxidative stress is manifested as an imbalance between the excessive production of ROS and the insufficient or defective antioxidant defense systems. It is well documented in literature that high extracellular D-glucose is responsible for the induction of ROS. Accordingly, HUVEC cultured for 24h in a high glucose-containing medium (11.1 mM and 30 mM) showed an increased production of ROS (Figure 23A) and in parallel a significant decrease in the oxidized/reduced (GSH/GSSG) glutathione ratio was measured (Figure 23B).

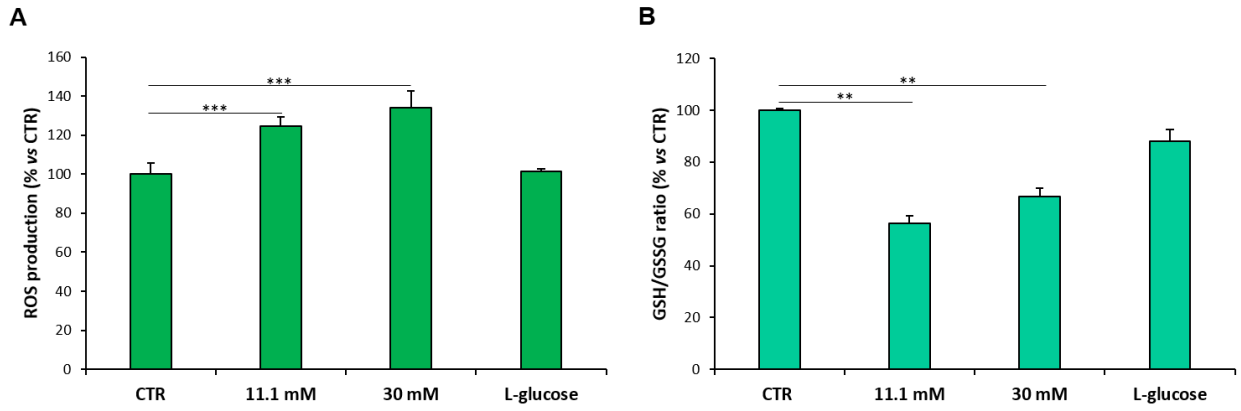

***Figure 23**: (**A**) ROS were measured by DCFH as described in the methods. Data are shown as percentages versus CTR. L-glucose was used as a control of osmolarity. (**B**) GSH/GSSG ratios in cell lysates were measured using GSH/GSSG-Glo™ Assay as described in the methods. Data are shown as percentages versus CTR. The results are the mean of 3 experiments in performed in triplicates ± SD. ** p < 0.01; *** p < 0.001.*

To understand the mechanisms underlying the insurgence of oxidative stress, the total amounts of some pro- and anti- oxidant proteins were investigated by Western blot. In particular, the total amount of TXNIP, a member of the α-arrestin family that acts as an oxidative stress mediator by inhibiting the antioxidant activity of Thioredoxin, was significantly increased in high glucose-cultured cells (Figure 24). Another protein whose expression was modulated by high glucose was SIRT1. It is involved in the cellular response to inflammatory, metabolic and oxidative stimuli, acting as anti-oxidant. Western blot revealed that the total amount of SIRT1 was significantly decreased upon high glucose treatment. On the contrary, no modulation in the total amount of HSP70, PON2, SIRT2 and

SOD2, all of them crucial in buffering ROS thus protecting cells from oxidative stress damage, was detected (Figure 24).

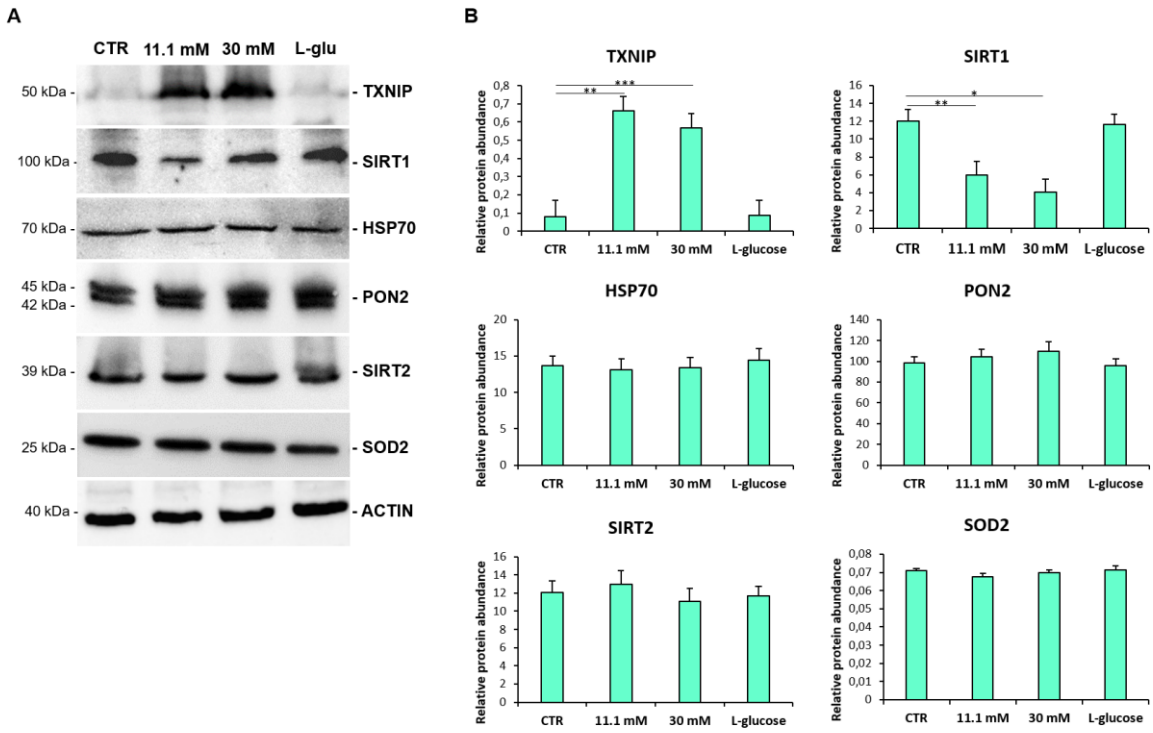

***Figure 24**: (**A**) Western blot was performed on cell lysates using specific antibodies against TXNIP, SIRT1, HSP70, PON2, SIRT2 and SOD2. Actin was used as a marker of loading. (**B**) Densitometric analysis was performed using Image J Lab software. The results are the mean of 3 experiments performed in triplicates ± SD.* p < 0.05; ** p < 0.01; *** p < 0.001.*

5.1.2 *TXNIP* SILENCING, NAC AND VITD PREVENT HIGH GLUCOSE-INDUCED ROS

HUVEC were then transiently silenced with siRNA targeting *TXNIP* and cultured in medium containing physiological or high extracellular D-glucose concentrations for 24h. The genetic inhibition of *TXNIP* restored normal levels of ROS (Figure 25A and 25B). Moreover, since VitD exerts vasculo-protective effects on endothelium but its mechanisms of action are still unclear, it is worth noticing that the supplementation of VitD (20 nM) to the culture media restored normal ROS production, similarly to the administration of the known antioxidant NAC (5 mM), through the inhibition of the overexpression of TXNIP (Figure 25C and 25D).

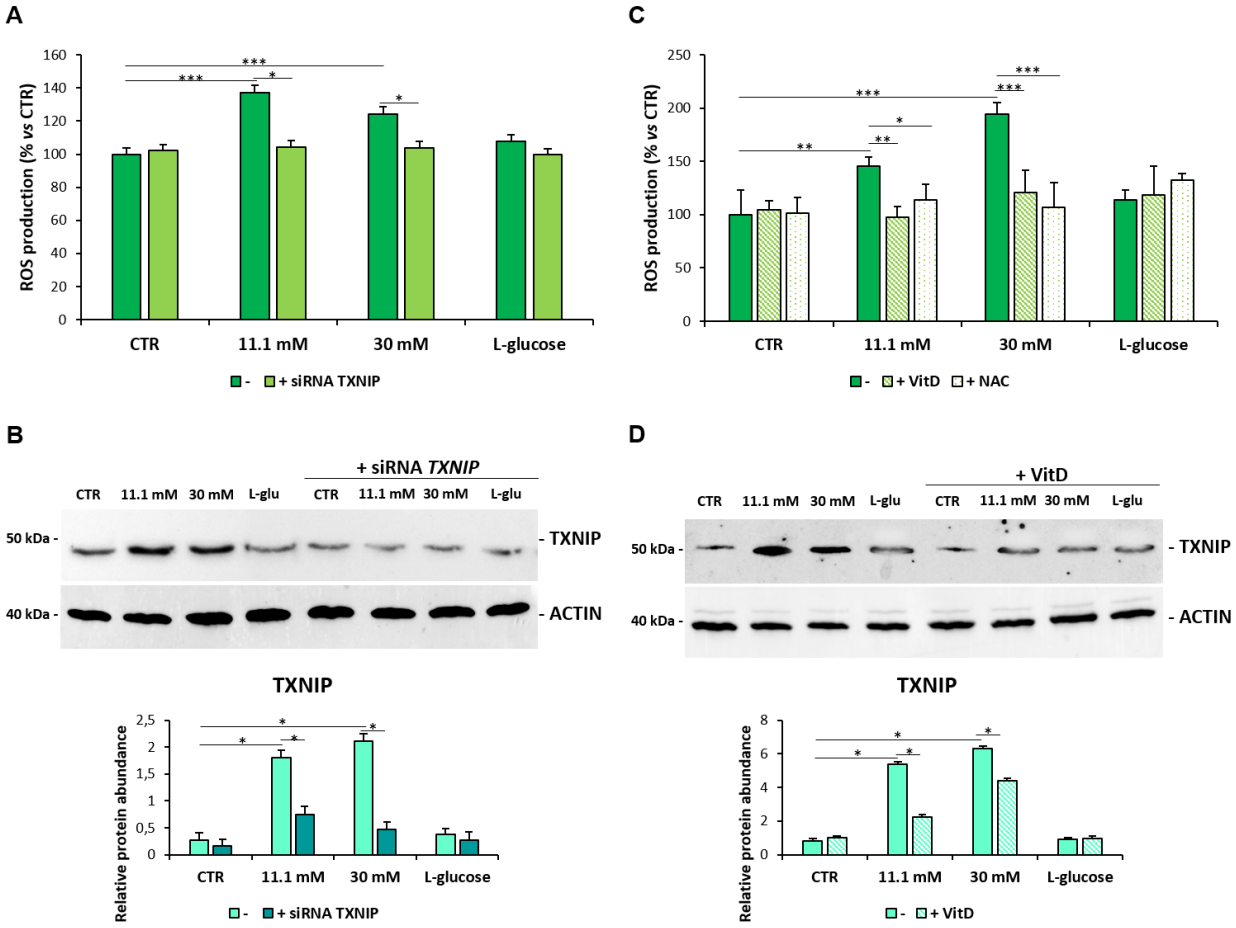

***Figure 25**: (**A**, **C**) ROS were measured by DCFH as described in the methods. L-glucose was used as a control of osmolarity. Data are shown as percentages versus CTR. (**B**, **D**) Western blot was performed on cell lysates using specific antibodies against TXNIP. Actin was used as a marker of loading. Densitometric analysis was performed using Image J Lab software. The results are the mean of 3 experiments performed in triplicates ± SD. * $p < 0.05$; ** $p < 0.01$; *** $p < 0.001$.*

5. RESULTS (2)

HIGH GLUCOSE MODULATES ENDOTHELIAL PERMEABILITY

5.2.1 HIGH GLUCOSE-INDUCED ROS PROMOTE ABNORMAL ENDOTHELIAL PERMEABILITY

Dysregulated endothelial permeability is linked to many pathological conditions, among which atherosclerosis. Therefore, the integrity of endothelial barrier was tested using the Transwelll Permeability assay. Interestingly, high D-glucose increased permeability in comparison to control or L-glucose treated cells (Figure 26A). In addition, to investigate if this alteration is an effect of the enhancement of ROS, HUVEC were either transiently silenced with siRNA *TXNIP* or supplemented with VitD. In both cases, the level of permeability returned comparable to physiological condition (Figure 26A and 26B).

Subsequently, HUVEC were cultured for 24h in medium in which FBS was replaced with 10% of blood sera collected from healthy donors or from paediatric diabetic patients (T1D). Initially, sera were grouped according to fasting glycaemia and the measurement of permeability was increased in hyperglycaemicT1D patients (T1D h.g.) in comparison to healthy (CTR) and normo-glycaemic subjects (T1D n.g.) (Figure 26C). Interestingly, diabetic sera induced hyper-permeability independently from the levels of glycated haemoglobin (HbA1c), a long-term glucose monitoring value very used in clinics (Figure 26D).

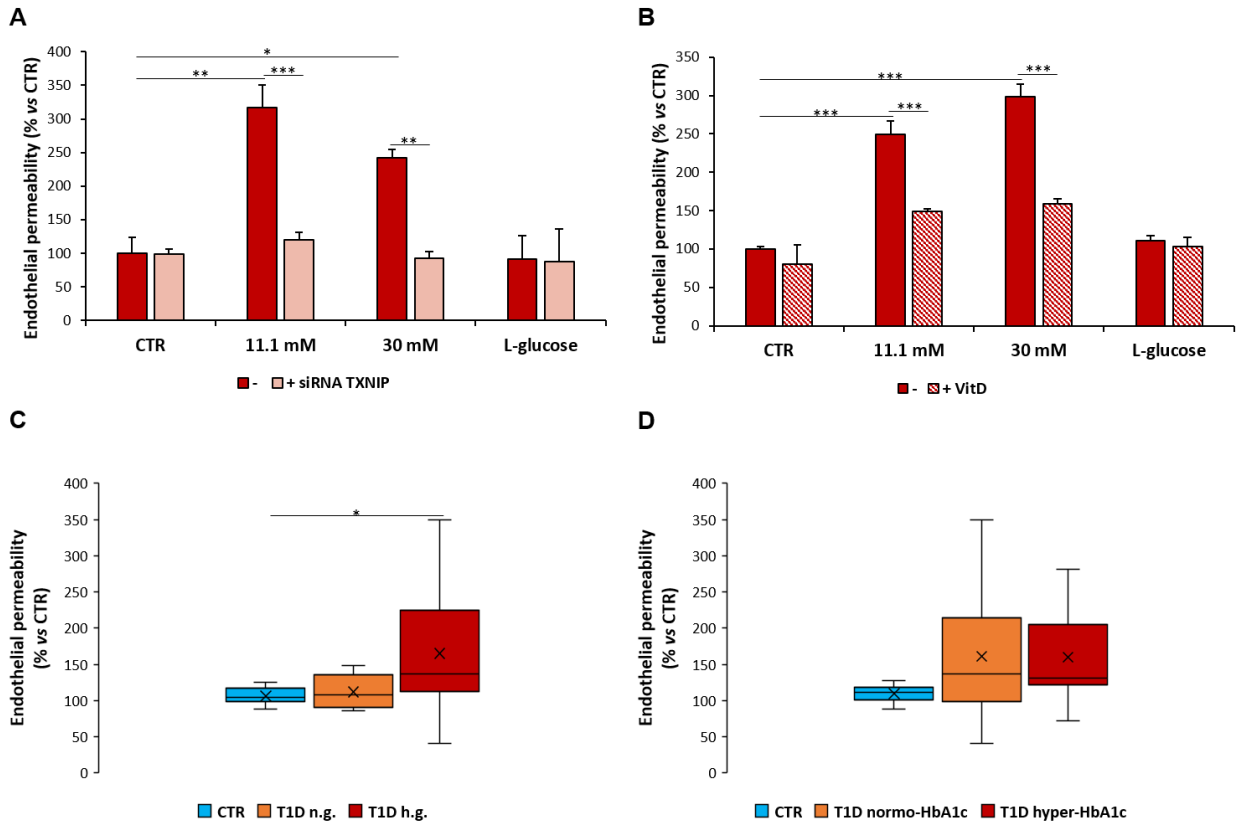

***Figure 26**: Endothelial permeability was measured as described in the methods. Permeability was studied in HUVEC upon TXNIP transient silencing (**A**) or upon the supplementation of VitD (**B**). (**C**, **D**) Endothelial permeability was measured in HUVEC exposed to 10% of sera collected from diabetic patients or from healthy donors. Data are shown as percentages versus CTR. The results are the mean of 3 experiments performed in triplicates ± SD. * p < 0.05; ** p < 0.01; *** p < 0.001.*

5.2.2 VITD PREVENTS HYPER-PERMEABILITY

Remarkably, the supplementation of VitD to high glucose-containing culture media totally prevents high glucose-induced alteration of endothelial permeability (Figure 27A). Moreover, HUVEC cultured in the presence of hyperglycaemic sera but with low levels of VitD in blood showed enhanced endothelial permeability (Figure 27B, red boxplot), that was recovered upon the supplementation of VitD (Figure 27B, yellow boxplot).

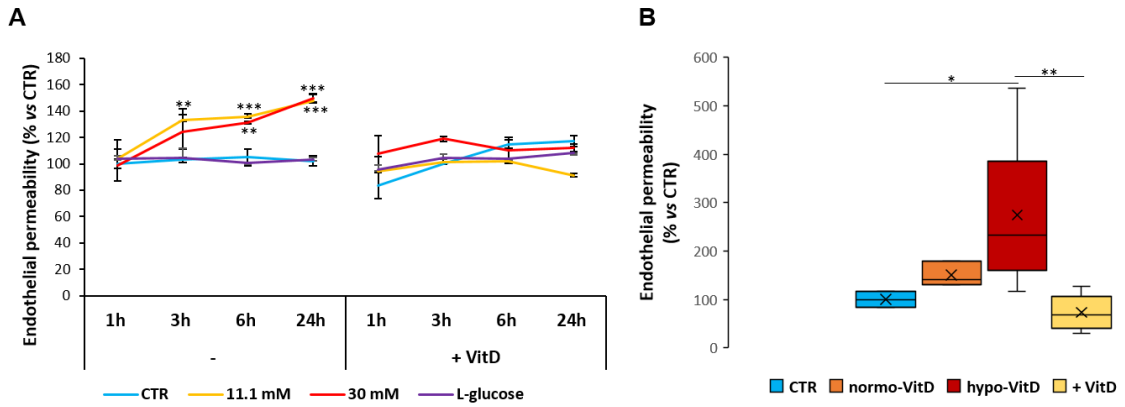

***Figure 27**: (**A**) Endothelial permeability in HUVEC cultured in the presence or not of VitD was measured as described in the methods and monitored for different time points. The statistical analysis (treated cells vs CTR) was calculated using ANOVA. (**B**) Endothelial permeability was measured in HUVEC exposed to 10% of sera collected from diabetic patients or from healthy donors. In this experiments, HUVEC were cultured in the presence of hyperglycaemic sera but with low levels of VitD in blood (red boxplot, "hypo-VitD"), subsequently supplemented with VitD (yellow boxplot, "+ VitD") in comparison with healthy donors (CTR) and sera with normal levels of VitD (normo-VitD). Data are shown as percentages versus CTR. The results are the mean of 3 experiments performed in triplicates ± SD. * p < 0.05; ** p < 0.01; *** p < 0.001.*

5.2.3 HIGH GLUCOSE INDUCES MODIFICATIONS OF INTERCELLULAR JUNCTIONS

To get insight into the pathway underlying hyper-permeability, the total amount of the tight junction ZO-1 and the adhesion protein Ve-Cadherin, two membrane proteins involved in the maintenance of the integrity of intercellular junctions and whose role is determinant in the regulation of the permeability of the endothelium, was assessed. Therefore, HUVEC were cultured for 24h in a high glucose-containing medium (11.1 mM and 30 mM) in the presence or not of VitD. Western Blot analysis revealed that ZO-1 expression was reduced when the cells were exposed to high glucose, but the administration of VitD led to its upregulation (Figure 28A). On the contrary, the total amount of Ve-Cadherin remained unchanged (Figure 28A). These results were confirmed also by confocal microscopy (Figure 28B and 28C).

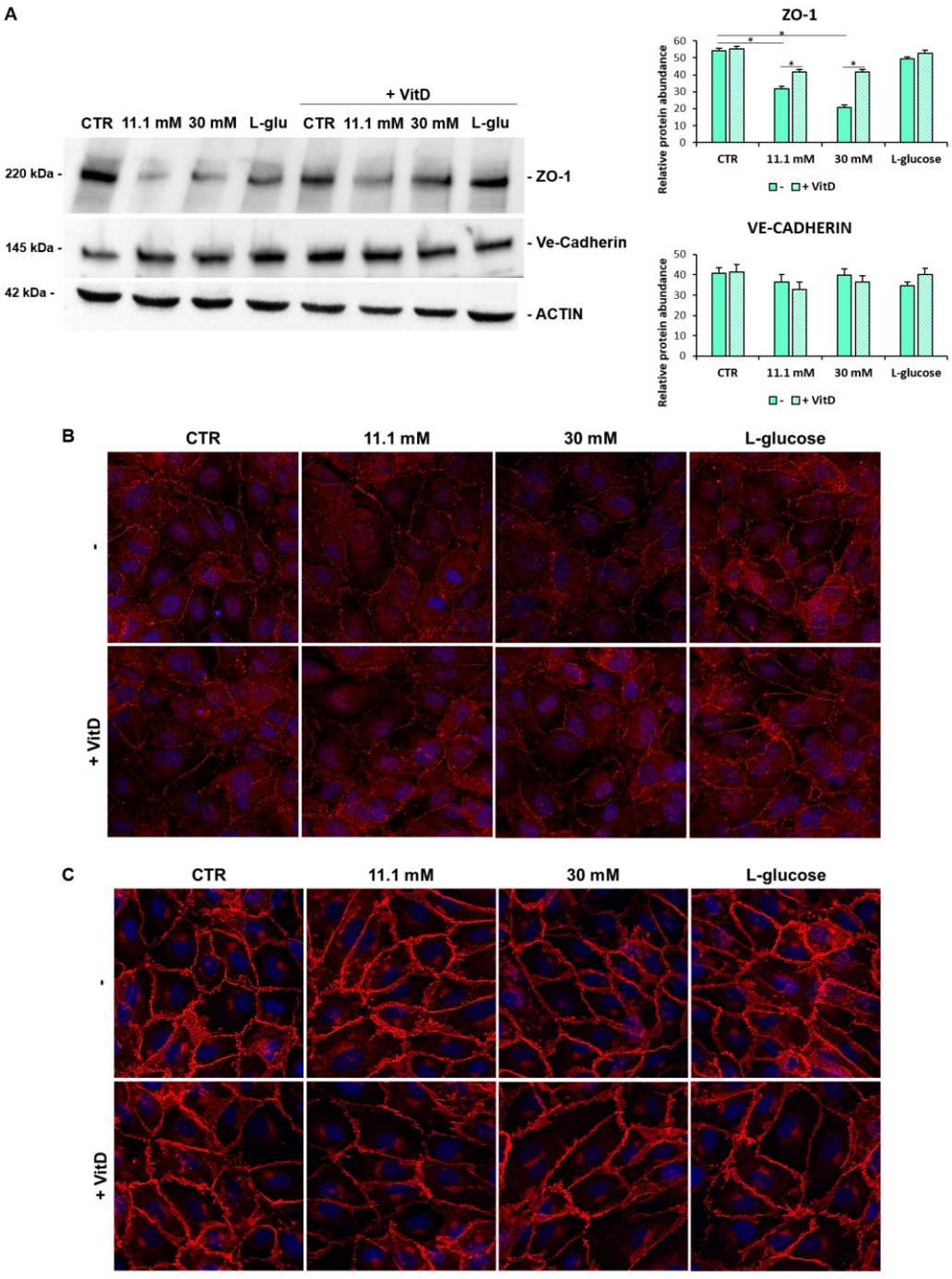

***Figure 28**: (**A**) Western blot was performed on cell lysates using specific antibodies against ZO-1 and VE-Cadherin. The relative control loading is shown in the lower panel. Densitometric analysis was performed using Image J Lab software. The results are the mean of 3 experiments performed in triplicates ± SD. * $p < 0.05$. (**B**) Confocal microscopy was performed on HUVEC stained with ZO-1 and DAPI. (**C**) Confocal microscopy was performed on HUVEC stained with Ve-Cadherin and DAPI. Images were acquired using a 63X objective in oil by a SP8 Leica confocal microscope. The images were processed and analyzed using ImageJ software. Scale bar = 30 µm.*

5. RESULTS (3)

HIGH GLUCOSE AND NITRIC OXIDE

5.3.1 HIGH GLUCOSE INDUCES A TRANSIENT INCREASE OF NITRIC OXIDE

To get insights into the mechanisms underlying high glucose-induced endothelial permeability, NO, a mediator of vascular permeability, was measured in cell culture medium after the treatments. Since the half-life of NO in the circulation is shorter than 0.1 seconds, circulating NO metabolites (NOx) were assessed as indicators of NO production through Griess assay, as reported in the methods. LPS (10 μg/mL) was used as positive control. High D-glucose augmented the release of NOx after 24h of treatments (Figure 29A). Interestingly, higher levels of NOx were detected in hyperglycaemic diabetic sera than sera from healthy donors and to normo-glycaemic patients (Figure 29B). Moreover, enhanced levels of NOx are independent from HbA1c levels in blood sera (Figure 29C).

To understand which isoform of NOS was involved in the overproduction of NO upon treatment with high glucose, the total amounts of iNOS and eNOS, the two enzymes that catalyze the production of NO in ECs, were assessed by Western blot. Also the modulation of the activated form of eNOS, phosphorylated on Ser1177 (P-eNOS^{Ser1177}) was investigated. The total amount of iNOS resulted increased by high D-glucose, while on both eNOS and P-eNOS^{Ser1177} were not significantly modulated by D-glucose (Figure 29D).

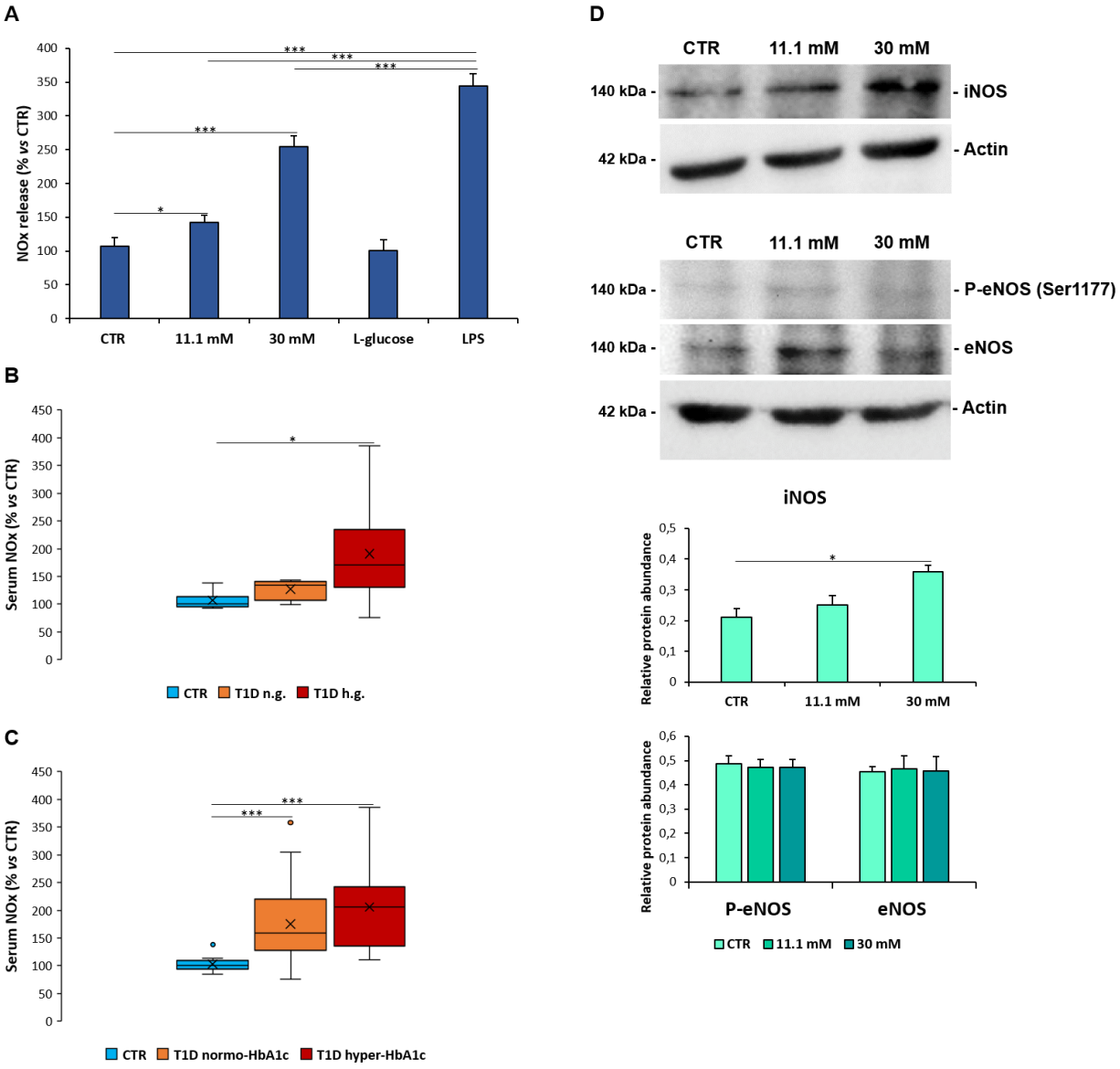

Figure 29: (***A***) *NOx release was measured by Griess assay in media of HUVEC cultured in different concentrations of glucose for 24h. LPS was used as positive control. (**B**) NOx release was measured by Griess assay in sera from healthy donors or T1D patients. Sera were grouped according to fasting glycaemia in healthy donors (CTR), normo-glycaemic (T1D n.g.) and hyperglycaemicsera (T1D h.g.). (**C**) NOx release was measured by Griess assay in sera from healthy donors or T1D patients. Sera were grouped according to HbA1c levels in healthy donors (CTR), T1D normo-HbA1c and hyper-HbA1c. Data are shown as percentages versus CTR. (**D**) Western blot was performed on cell lysates using specific antibodies against iNOS, eNOS and P-eNOS^{Ser1177}. Actin was used as a marker of loading. Densitometric analysis was performed using Image J Lab software. The results are the mean of 3 experiments performed in triplicates ± SD. * $p < 0.05$; *** $p < 0.001$.*

5.3.2 iNOS IS RESPONSIBLE FOR HIGH GLUCOSE-INDUCED HYPER-PERMEABILITY

The role of iNOS and eNOS in modulating endothelial permeability was assessed by either the genetic or the pharmacological inhibition of these enzymes. HUVEC were transiently silenced with specific siRNA against *iNOS* and *eNOS* and then cultured in high glucose-containing medium for 24h. Real Time PCR showed that the siRNA targeting *iNOS* downregulated iNOS in HUVEC cultured in normal and high glucose concentrations (Figure 30A), while siRNA against *eNOS* slightly downregulated eNOS but with no modulation (Figure 30B).

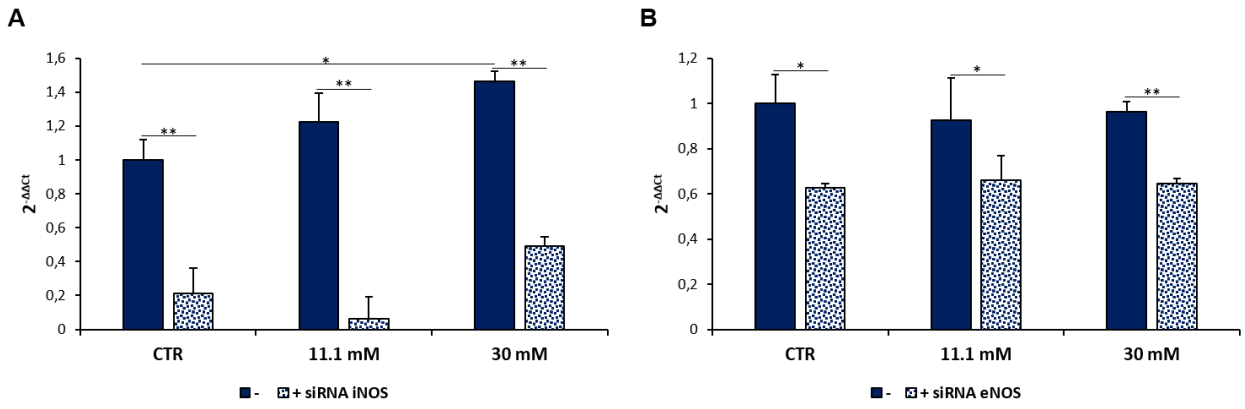

***Figure 30**: Real Time PCR was performed on HUVEC transiently silenced with specific siRNA against iNOS (**A**) or eNOS (**B**). Real Time PCR was performed on RNA samples from 3 different experiments. The results are the mean of 3 experiments performed in triplicates ± SD. * p < 0.05; ** p < 0.01.*

Subsequently, the role of iNOS and eNOS in modulating endothelial permeability was assessed. HUVEC were transiently transfected for 6h with specific siRNAs targeting *eNOS* or i*NOS*, or a scrambled sequence as a control, and then exposed to high glucose for the following 24h. In parallel, HUVEC were pre-treated for 1h with L-NAME (100 μM) and L-NIL (100 μM), pharmacological inhibitors of eNOS and iNOS, respectively, and then exposed to a medium containing high concentrations of glucose for 24h. *iNOS* silencing as well as L-NIL administration prevented glucose-induced NOx accumulation (Figure 31A and 31B) and hyper-permeability (Figure 31C and 31D), whereas L-NAME slightly reduced NOx release and permeability induced by high glucose (Figure 31), as expected since eNOS is constitutively active in endothelial cells.

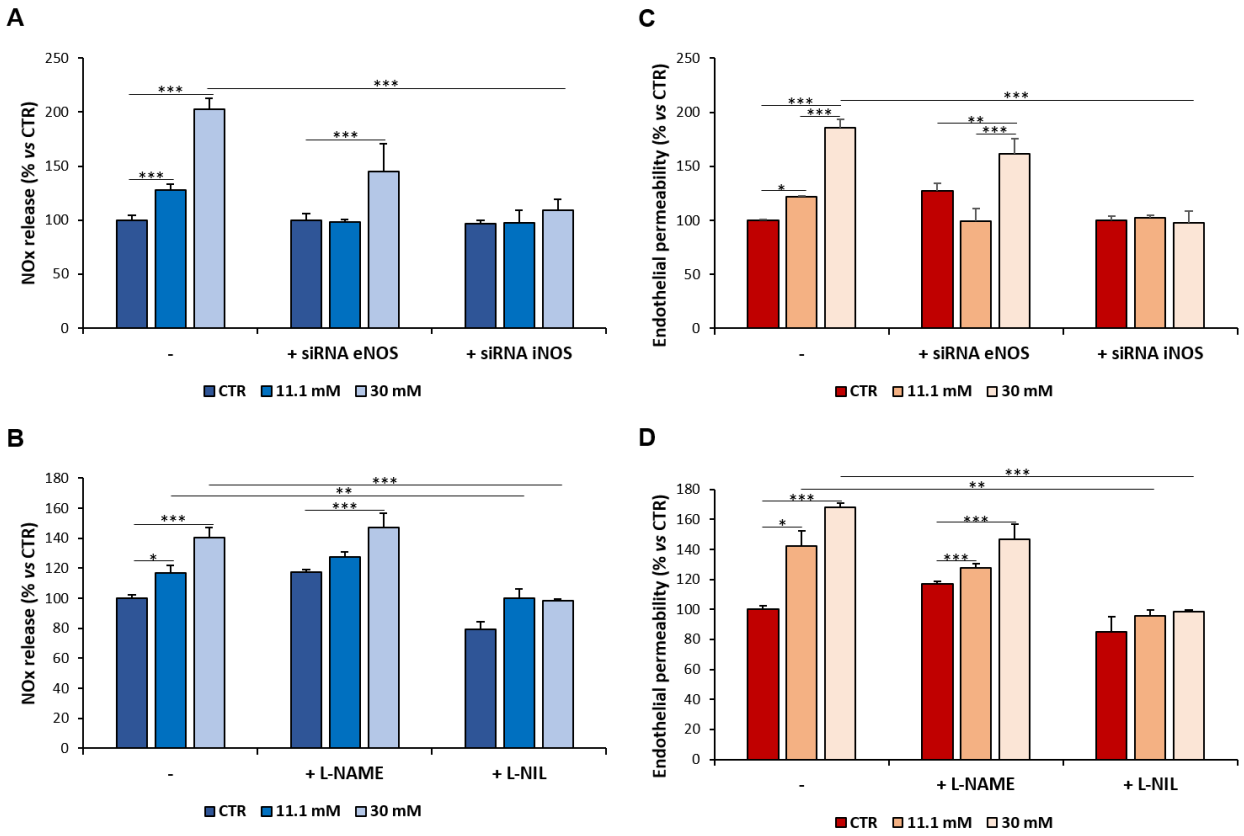

***Figure 31**: NOx release and endothelial permeability were measured respectively by Griess assay and Transwell permeability assay in media of HUVEC cultured in different concentrations of glucose after the inhibition of eNOS or iNOS. NOx was measured after gene silencing with siRNA eNOS or siRNA iNOS (**A**) or after the administration of the pharmacological inhibitors L-NAME or L-NIL, specific respectively for eNOS or iNOS (**B**). Permeability was evaluated after gene silencing with siRNA eNOS or siRNA iNOS (**C**) or after the administration of the pharmacological inhibitors L-NAME or L-NIL (**D**). A scrambled non silencing sequence was used as a control (–) for silencing. Data are shown as percentages versus CTR. The results are the mean of 3 experiments performed in triplicates ± SD. * $p < 0.05$; ** $p < 0.01$; *** $p < 0.001$.*

These results were confirmed when iNOS was inhibited in HUVEC cultured in medium containing hyperglycaemicdiabetic sera. The cells were transiently silenced for *eNOS* and *iNOS* with specific siRNA, while the controls cells were exposed to a scrambled sequence. The silencing of *iNOS* totally prevented hyper-permeability in cells cultured with hyperglycaemicsera (Figure 32A). In parallel, HUVEC were pre-treated for 1h with L-NAME (100 µM) or L-NIL (100 µM) before adding to the culture media 10% of T1D serum from hyperglycaemicor healthy subjects. As shown in Figure 32B, L-NIL reduced endothelial permeability to approximately the same level as the controls.

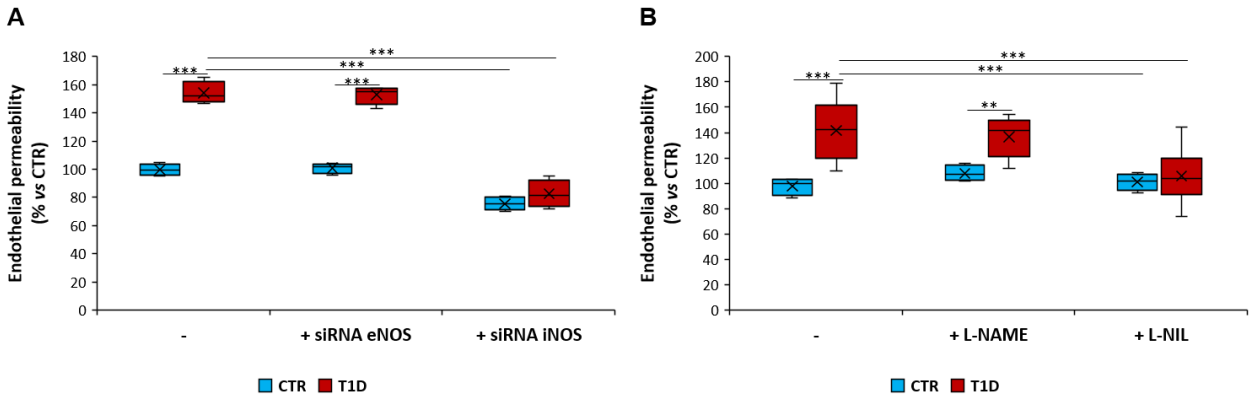

***Figure 32**: Permeability in HUVEC cultured in medium containing 10% hyperglycaemic T1D or CTR sera after genetic or pharmacological inhibition of iNOS or eNOS. HUVEC were cultured in the presence of sera from healthy donors and T1D patients for 24h after gene silencing (**A**) or in the presence of L-NAME or L-NIL (**B**). A scrambled non-silencing sequence was used as a control (–) for silencing. Data are shown as percentages versus CTR. The results are the mean of 3 experiments performed in triplicates ± SD. ** p < 0.01; *** p < 0.001.*

To confirm the direct role of iNOS in inducing hyperpermeability, some kinetics experiments were performed. As reported in Figure 33A, the peak of NO production occurred after 24h of treatment with high glucose. This last evidence is simultaneous to the peak of permeability measured after 24h of exposure to high glucose (Figure 33B). Therefore, the hypothesis is that the higher release of NO is a transitory effect connected to the hyperglycaemic peak.

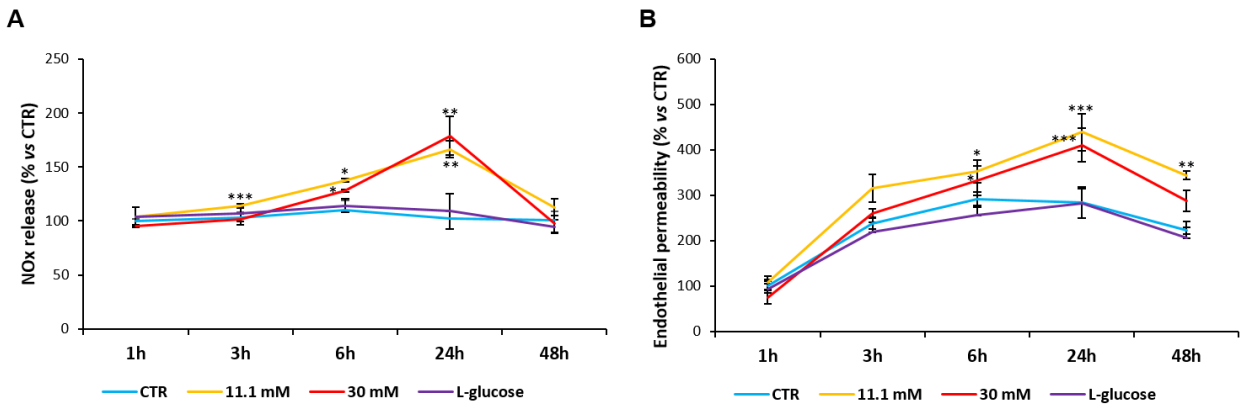

***Figure 33**: (**A**) NOx release was measured by Griess assay in culture media at different time points. Data are shown as percentages versus CTR. (**B**) Endothelial permeability was measured as described in the methods and monitored for different time points. Data are shown as percentages versus CTR. The statistical analysis (treated cells vs CTR) was calculated using ANOVA. The results are the mean of 3 experiments performed in triplicates ± SD. * p < 0.05; ** p < 0.01; *** p < 0.001.*

5. RESULTS (4)

HIGH GLUCOSE-DRIVEN MITOCHONDRIAL DYSFUNCTION AND LIPID DROPLETS ACCUMULATION

5.4.1 3D ULTRASTRUCTURAL QUANTITATIVE ANALYSIS BY SYNCHROTRON-BASED CRYO-SXT

The Cryo-SXT is an imaging technique capable to generate 3D maps of vitrified whole-cell samples at nanometer resolution, allowing the analysis of the cells as closely as possible to their native state, without the necessity of staining, sectioning or the use of enhancing agents [Schneider 2010].

Therefore, HUVEC were treated for 24h with physiological or high concentrations of D-glucose. L-glucose was used as control of osmolarity. Synchrotron-based Cryo-SXT was exploited to perform 3D ultrastructural quantitative analysis of mitochondria at nanoscale. The Cryo-SXT reconstructions allowed obtaining 3D nano-rendering images of the whole cells, with a deep focus on the inside of the cells. This technique endorsed to extract quantitative information about the cell compartments analyzed, i.e. volume, shape and number of mitochondria and lipid droplets.
Figure 34A reports in the upper panel the 2D ultrastructure analysis of HUVEC by Cryo-SXT and in the lower panel the corresponding color-coded manual segmentation of the selected areas of interest. The 3D rendering of representative volume regions shows a lower amount of elongated mitochondria in HUVEC cultured in high D-glucose and, in parallel, a higher number of almost round-shaped mitochondria in comparison to CTR and L-glucose.

To explore in depth the morphological differences between physiological and high glucose-treated mitochondria in HUVEC, the Fractional Anisotropy (FA) value was calculated on each mitochondrion segmented. FA is a scalar value, ranging between 0 and 1, describing the degree of anisotropy of a diffusion process. When the FA verges on 0 the diffusion is isotropic and therefore equally restricted along the three axes (λ_1, λ_2, λ_3), whereas when FA tends to 1 the diffusion has a preferential direction along one axis. Specifically, the eigenvalues of the diffusion tensor allow calculating the FA as described in Materials and Methods. In Figure 34B, the FA of all the mitochondria segmented for each cell culture condition was reported. The FA median value of HUVEC cultured in high glucose confirmed a statistically significant more isotropic shape in comparison to the physiological state. This data is in accordance with the differences observed for the volume of the total mitochondria between high glucose-cultured cells and control cells (Figure 34C). Moreover, no relevant variances were detected concerning the total number of mitochondria. However, the number

of elongated mitochondria (fusion) and the number of fragmented mitochondria (fission) are respectively lower and higher in cells cultured in high D-glucose in comparison to controls (Figure 34D).

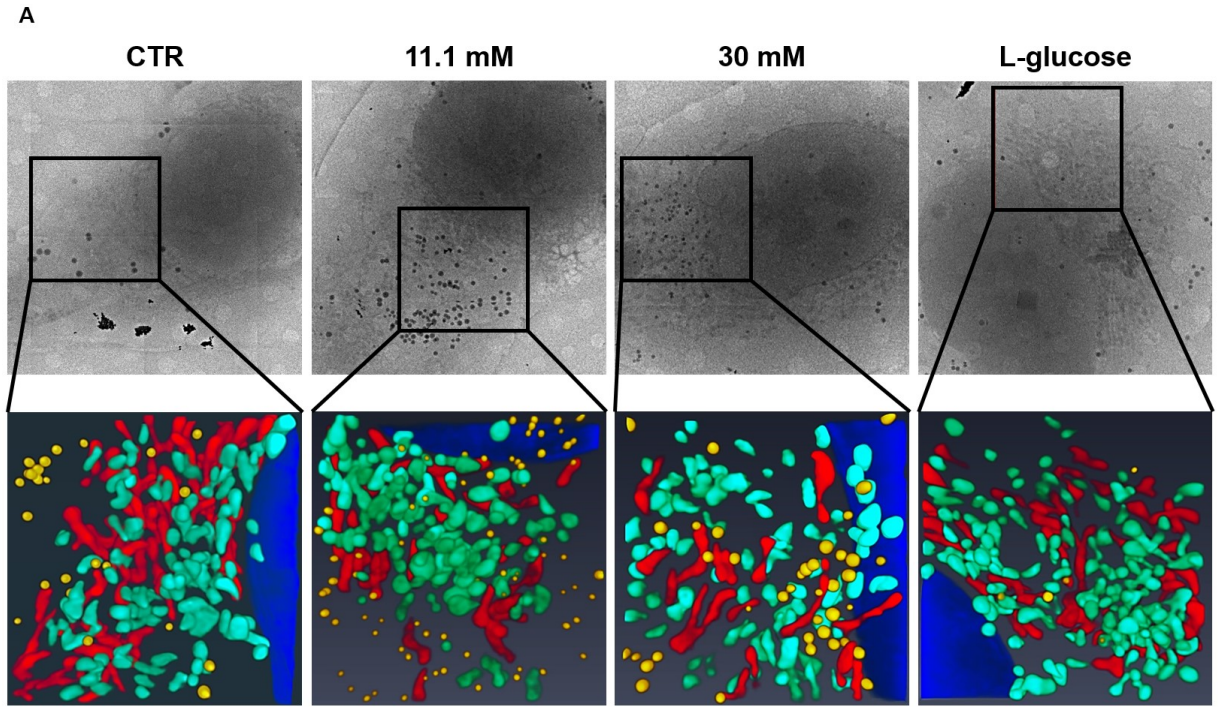

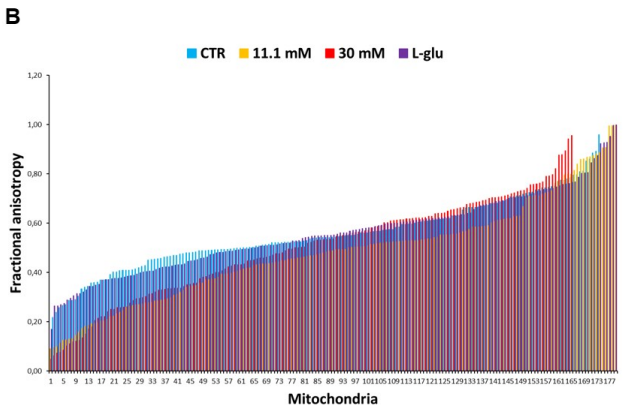

	CTR	11.1 mM	30 mM	L-glucose
n° mitocondria	174	179	165	179
FA (median)	0,54	0,49	0,52	0,55
ANOVA n° mitochondria		*ns*	*ns*	
ANOVA FA		$p < 0,01$	$p < 0,05$	

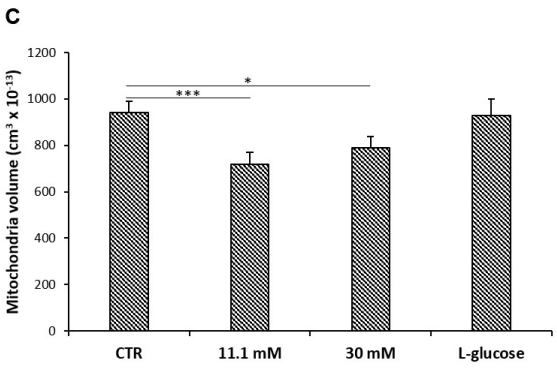

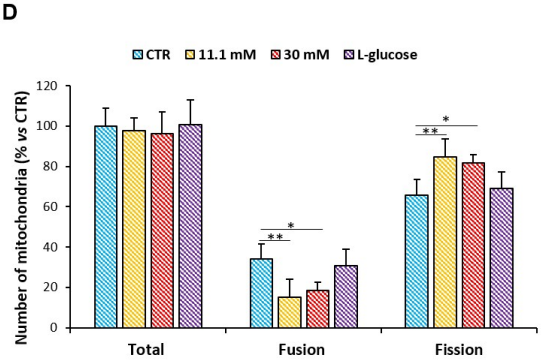

***Figure 34**: (**A**) 3D ultrastructural analysis of HUVEC by synchrotron-based Cryo-SXT. Cells were cultured in medium containing different concentrations of D-glucose for 24h. L-glucose (30 mM) was used as control of osmolarity. In the upper panel, the 2D ultrastructure analysis of HUVEC by Cryo-SXT was reported, while the lower panel represents the corresponding color-coded manual segmentation of the selected areas of interest identifying a portion of the nucleus (blue), mitochondrial fusion (red), mitochondrial fission (green) and lipid droplets (yellow) of 3D reconstruction of whole-cell volumes, obtained by Cryo-SXT (pixel size 13 nm). (**B**) Average differences in Fractional Anisotropy (FA) of 3D reconstructed mitochondria in HUVEC. In the table, the FA median values and the total number of mitochondria were reported. The statistical analysis (11.1 mM / 30 mM vs CTR) was calculated using ANOVA. (**C**) The histogram reports the variances in the volume of all mitochondria segmented in every cell culture condition. (**D**) In the histogram, the total number of mitochondria and the number of mitochondria in fusion / fission were reported, according to the different cell culture conditions. Values are expressed as mean ± SD and compared using one-way repeated measures ANOVA. The p-values deriving from multiple pairwise comparisons were corrected by the Bonferroni method. In the figures, * $p < 0.05$, ** $p < 0.01$, *** $p < 0.001$.*

5.4.2 UNBALANCED MITOCHONDRIAL DYNAMICS IN HIGH GLUCOSE-CULTURED CELLS

To confirm the previous results, attention was focused on the molecular pathways regulating mitochondrial remodeling. The mitochondria dynamics involves a complex signaling regulated by members of dynamin family, among which OPA1, enrolled in controlling mitochondrial fusion, and DRP1, mediating mitochondrial fission. Figure 35A shows a subtle but significant modulation of the total amount of OPA1 and DRP1 in response to high glucose. Indeed, OPA1 and DRP1 are respectively downregulated and upregulated when HUVEC were cultured in high glucose-containing medium. CYPD amount, used as indicator of total mitochondrial content, is not modulated. Moreover, the oxygen consumption rate (OCR) is an important indicator of healthy cellular function and it has been used as one of the most informative marker of mitochondrial fitness. Therefore, it is noteworthy that high levels of glucose triggered a decrease in OCR comparable to the effect of H_2O_2, used in these experiments as positive control (Figure 35B). Additionally, mtROS are overproduced in HUVEC cultured under hyperglycaemic condition (Figure 35C). Hence, the unbalanced rate of fusion/fission, the impairment of oxygen consumption and the production of mtROS disturb the mitochondrial dynamics, resulting in a disequilibrium toward dysfunctional mitochondria.

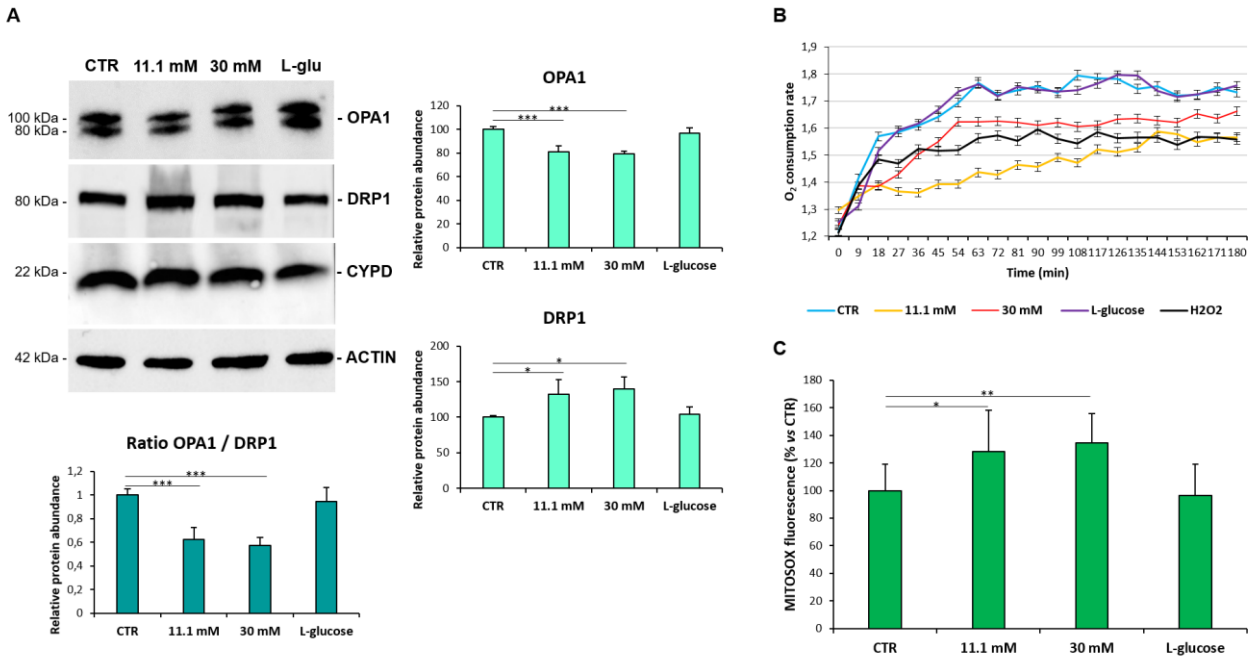

Figure 35: (**A**) *Western blot was performed on cell lysates using specific antibodies against OPA1, DRP1 and CYPD. Actin was used as a marker of loading. The experiments were repeated 3 times and a representative blot is shown. Densitometric analysis (right panel) was performed using Image J Lab software.* (**B**) *The OCR was measured by Extracellular O2 Consumption kit as described in the Methods. Values represent the means ± SD of triplicate experiments. Statistical analysis: 11.1 mM vs CTR *** p < 0.001; 30 mM vs CTR * p < 0.05; H_2O_2 vs CTR *** p < 0.001.* (**C**) *mtROS production was evaluated by MitoSOX Red reagent. Values represent the means ± SD of triplicate experiments and data are shown as percentage versus CTR. In the figures, * p < 0.05, ** p < 0.01, *** p < 0.001.*

5.4.3 3D ULTRASTRUCTURAL QUANTITATIVE ANALYSIS OF HUVEC LIPID DROPLETS BY SYNCHROTRON-BASED CRYO-SXT

Another intriguing result that is worth considering is that the 3D ultrastructure analysis of HUVEC by Cryo-SXT allowed the visualization of an accumulation of lipid droplets in high glucose-treated cells in comparison to CTR and L-glucose (Figure 34A). No morphological differences were detected concerning the volume of the lipid droplets (Figure 36A). Accordingly, the FA median values are similar in all the culture conditions. However, the number of lipid droplets is statistically higher in the presence of high D-glucose than in physiological medium (Figure 36B). In the table, the FA and the number of all the lipid droplets segmented for each cell culture condition are reported (Figure 36C).

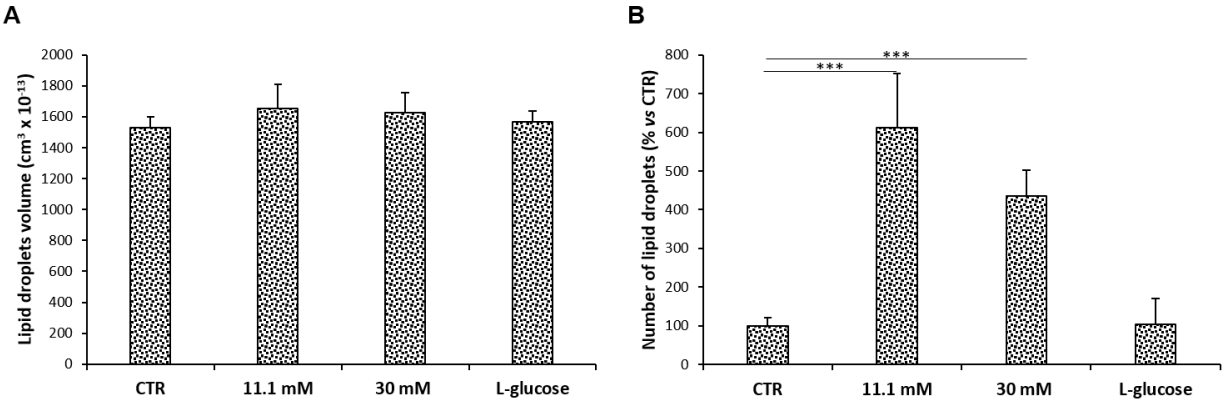

C

	CTR	11.1 mM	30 mM	L-glucose
N° lipid droplets	26	159	113	27
FA (median)	0,16	0,18	0,19	0,14
ANOVA n° lipid droplets		$p < 0,001$	$p < 0,001$	
ANOVA FA		*ns*	*ns*	

***Figure 36**: (**A**) The histogram reports no statistical variances in the total volume of lipid droplets among the different treatments. (**B**) In the histogram, the total number of lipid droplets was reported, according to the different cell culture conditions and the results were reported as % versus CTR. (**C**) In the table, the four FA median values and the total number of lipid droplets segmented were reported. The statistical analysis (11.1 mM / 30 mM vs CTR) was calculated using ANOVA. *** p < 0.001.*

5.4.4 UNDERLYING MECHANISMS OF LIPID DEPOSITION

Since GLUT1, the glucose transporter located on the membrane of endothelial and epithelial cells, was overexpressed after just 8h of treatment with high glucose (Figure 37A), the hypothesis was that the higher amount of glucose in the cells is converted in lactate. Indeed, as reported in Figure 37B, high glucose-cultured cells showed an increased production of lactate. Moreover, it is avowed that, if in excess, lactate can be reversely converted to pyruvate, which, once in the mitochondria, can be transformed in the precursors of fatty acids that in the cytoplasm will be used to form triglycerides [Sun 2016]. Accordingly, a significant accumulation of triglycerides was measured when cells were cultured in high glucose-containing medium (Figure 37C).

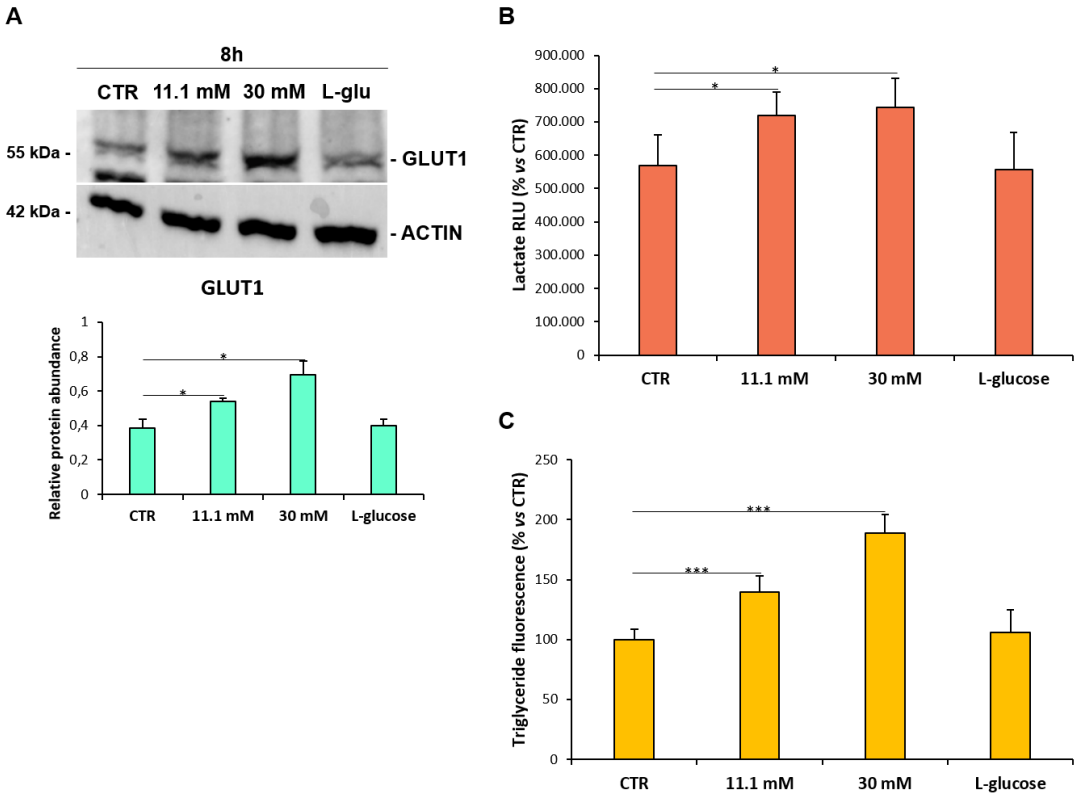

Figure 37: (***A***) *Western blot was performed on cell lysates using specific antibodies against GLUT1. Actin was used as a marker of loading. The experiments were repeated 3 times and a representative blot is shown. Densitometric analysis (right panel) was performed using Image J Lab software. (**B**) Lactate production was measured by Lactate-Glo™ Assay according to manufacturer instructions and luminescence was recorded. (**C**) Triglycerides amount was detected by Triglycerides Assay Kit according to manufacturer instructions and the fluorescence was detected at $\lambda_{ex/em}$ = 535/587 nm. Values are expressed as mean ± SD and compared using one-way repeated measures ANOVA. The p-values deriving from multiple pairwise comparisons were corrected by the Bonferroni method. In the figures, * p < 0.05, *** p < 0.001.*

5.4.5 HIGH GLUCOSE INDUCES ALTERATIONS IN LIPOGENESIS AND FATTY ACIDS β-OXIDATION

Western blot analysis was then performed to investigate if high glucose could alter the expression of some proteins involved in lipid metabolism. In particular, EDF1 is ubiquitously expressed and it exerts its functions both in the cytosol, binding the Ca^{2+}-binding protein calmodulin to modulate several calcium-regulated enzymes, and in the nucleus, acting as a transcriptional coactivator for non-steroid nuclear receptors involved in lipogenesis, such as PPARγ, a nuclear receptor regulating transcription of several genes implicated mainly in fatty acid and energy metabolism. Interestingly, both PPARγ and EDF1 were overexpressed upon high glucose treatment (Figure 38A and 38B). In addition, Carnitine Palmitoyl-

Transferase 1A (CPT1A), a member of carnitine palmitate hydrazine transferase family located on the outer mitochondrial membrane, plays a vital role in the intake of fatty acids into the mitochondria where they undergo fatty acid β-oxidation, the major pathway for the catabolism of fatty acids. After high glucose treatment, the total amount of CPT1A was diminished, suggesting a reduced intake of fatty acids into the mitochondria (Figure 38A and 38B). In accordance with this last result, the β-oxidation rate in high glucose-cultured cells was decreased (Figure 38D). Interestingly, both the addition of VitD to high glucose-containing media and the silencing of *TXNIP* rescued the β-oxidation rate (Figure 38D), as well as restored the total amounts of CPT1A, PPARγ and EDF1 (Figure 38A and 38B).

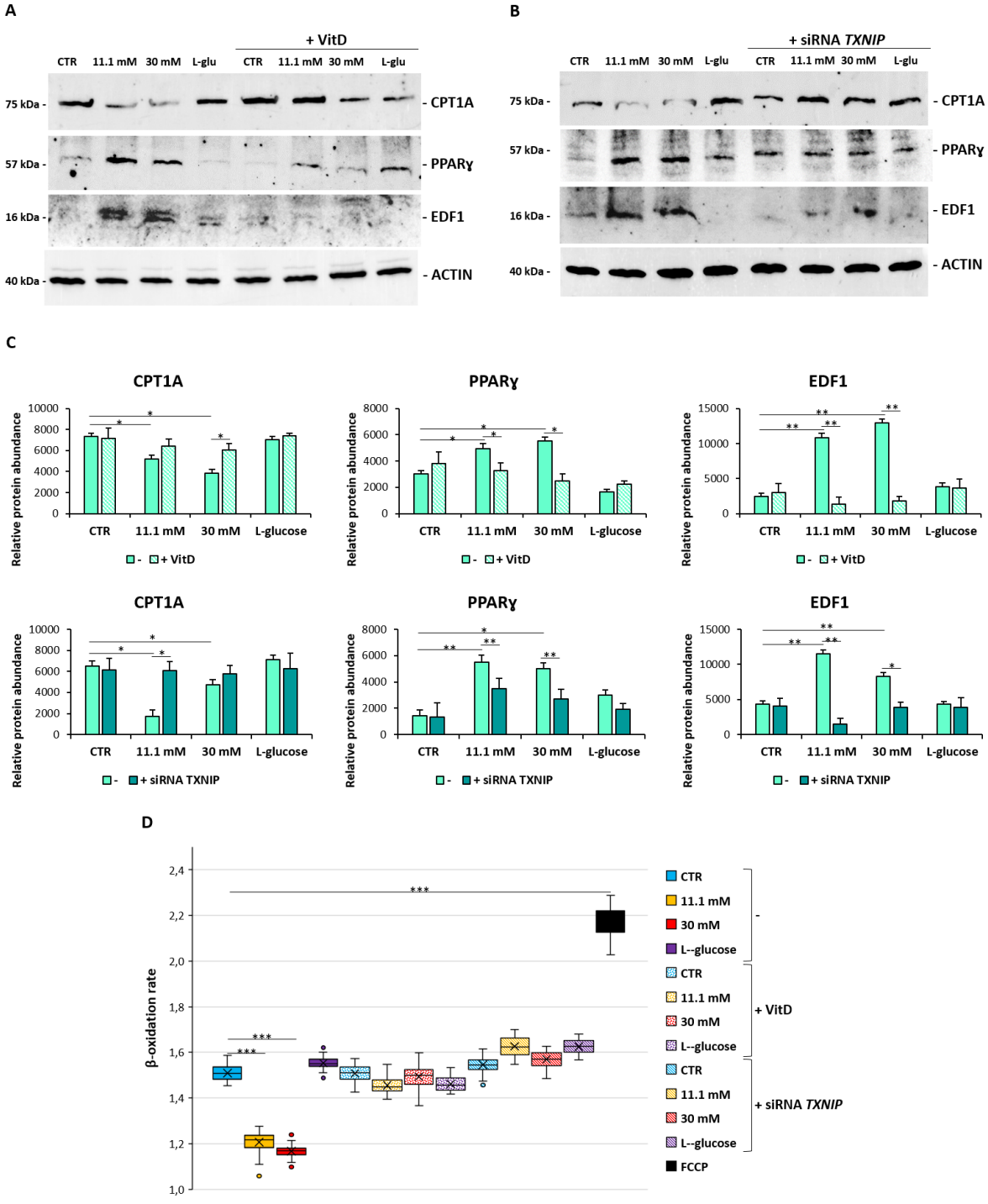

***Figure 38**: (**A**, **B**) Western blot was performed on cell lysates using specific antibodies against CPT1A, PPARγ and EDF1. Actin was used as a marker of loading. The experiments were repeated 3 times and a representative blot is shown. (**C**) Densitometric analysis was performed using Image J Lab software. (**D**) The β-oxidation rate was measured by Fatty Acid Oxidation Assay in living cells as described in the Methods, after the supplementation of VitD or after TXNIP silencing. The FAO activator FCCP (0,625 μM) was used as the positive control. Values represent the means ± SD of triplicate experiments. The significance was calculated vs CTR. The results are the mean of 3 experiments performed in triplicates ± SD. * p < 0.05, ** p < 0.01; *** p < 0.001.*

5.4.6 RESCUE OF NORMAL LIPID CONTENT BY SILENCING *TXNIP* OR EXPOSING TO VITD

In several cell types, the accumulation of lipid droplets storing triglycerides is interpreted as an adaptive response to stress [Jarc 2019]. To test if HUVEC behave in a similar manner, we initially evaluated the amounts of triglycerides in HUVEC cultured in high glucose containing media. CTR and L-glucose-cultured cells contain a certain amount of triglycerides which is dose dependently increased upon exposure to 11.1 mM and 30 mM for 24h. Moreover, the silencing of *TXNIP* reduced triglycerides amounts to physiological levels and VitD mimics the effect of the silencing (Figure 39A).

Subsequently, BODIPY 493/503 (Invitrogen), a lipophilic dye that labels cellular neutral lipids with a particular focus to those localised into lipid droplets, was utilized to quantify triglycerides after different treatments. In particular, cells were either transiently inhibited with siRNA *TXNIP* or supplemented with VitD. In both cases high glucose-induced deposition of lipids was dampened by both *TXNIP* silencing and the administration of VitD (Figure 39B). The results were further confirmed by the staining with Oil Red O to detect neutral lipids (Figure 39C).

Therefore, it is feasible to think that the high glucose is responsible for alterations in lipid metabolism leading to triglycerides accumulation. In this context, the supplementation of VitD is capable to prevent lipogenesis and to stimulate β-oxidation, through the inhibition of ROS production.

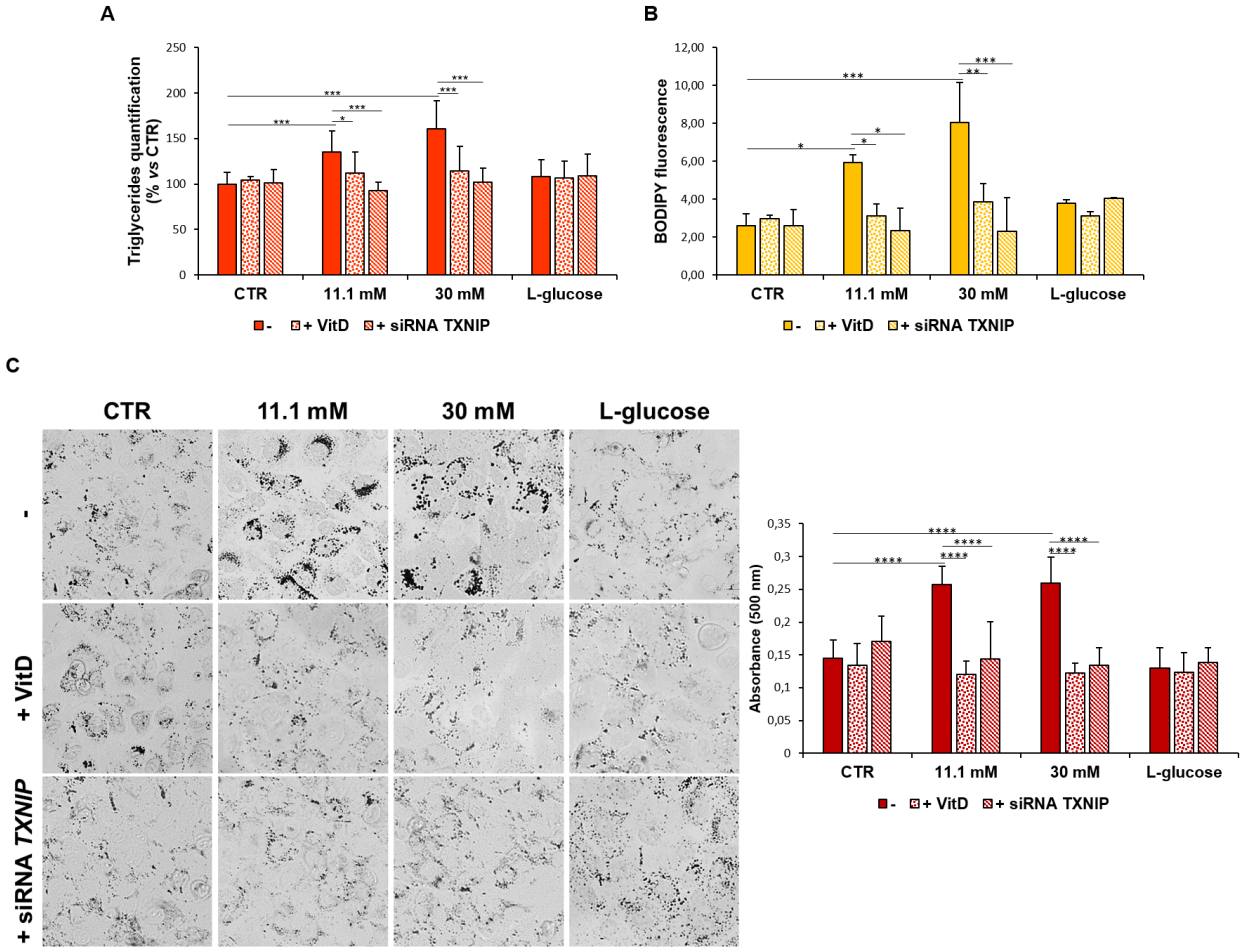

Figure 39: (***A***) *Triglyceride accumulation was calculated by Triglyceride Quantification Kit as described in the methods.* (***B***) *Lipid accumulation was detected using fluorescent BODIPY fluorophore and the relative fluorescence was measured using the Varioskan LUX Multimode Microplate Reader (Thermo Fisher Scientific) and normalized on DAPI staining.* (***C***) *The cells were stained with Oil Red O and, after the images acquisition using FLoid Cell Imaging Station (Thermo Fisher Scientific) (left panel), were solubilized and lipids were quantified by measuring the absorbance at 500 nm using the Varioskan LUX Multimode Microplate Reader (Thermo Fisher Scientific). Absorbance was measured at 500 nm and normalized to the cell number. The results are the mean of 3 experiments performed in triplicates ± SD. * $p < 0.05$; ** $p < 0.01$; *** $p < 0.001$; **** $p < 0.0001$.*

5. RESULTS (5)

FROM 2D TO 3D MICROFLUIDIC CHIP

5.5 WHY MOVING TOWARD 3D CELL CULTURE?

The more physiological culture condition of ECs is represented by 3D structural organization in vessels in the presence of steady flow. In this way, ECs are constantly subjected to the shear stress generated by blood and tangential to ECs surface [Song 2011]. Mechanical stimuli, in combination with biochemical ones coming from extracellular matrix or other cells, are able to modulate ECs functions. Very recently, to face the limitation of typical 2D cell culture, innovative 3D systems have been designed, with a huge range of applications, such as basic or clinical research, screening of new drugs, regenerative medicine and so on [Rimann 2012]. These 3D systems resemble as closely as possible the physiological settings, allowing a deeper investigation of ECs behavior both in healthy and in pathological situation.

The purpose of the last part of the project was to optimize the 3D culture model and to expose macrovascular ECs to high extracellular glucose, able to induce endothelial dysfunction. Therefore, the effects of high glucose were tested on HUVEC cultured both in classical 2D systems and in 3D microfluidic devices, which resemble the physiological spatial organization of ECs in ramification of vessels of different calibers and apply shear stress generated by fluid flow. Two parameters were analyzed: firstly the cytoskeleton, a vital mediator of both mechanical and biochemical signals arising from the microenvironment, and secondly the glycocalyx, a flow sensor located on the apical membrane of ECs.

5.5.1 EFFECT OF HIGH GLUCOSE ON THE ACTIN CYTOSKELETON IN 2D AND IN 3D

HUVEC were cultured either in 2D static petri dish or in 3D microfluidic device and the effect of high glucose on actin cytoskeleton was investigated. Initially, HUVEC were seeded in 2D static petri dish and were treated for 24h with physiological (CTR) or high glucose concentration (30 mM, HG). L-glucose (30 mM) was used as control of osmolarity. Then the amounts of actin and its organization were analysed. In particular, high glucose exerted no significant effect in 2D both on total actin content, as shown in western blot (Figure 40A),

and on its organization in fibers, evaluated using confocal microscopy after staining with phalloidin-TRITC (Figure 40B).). As expected in a static cell culture system, no differences in the total orientation of the fibers was detected (Figure 40C).

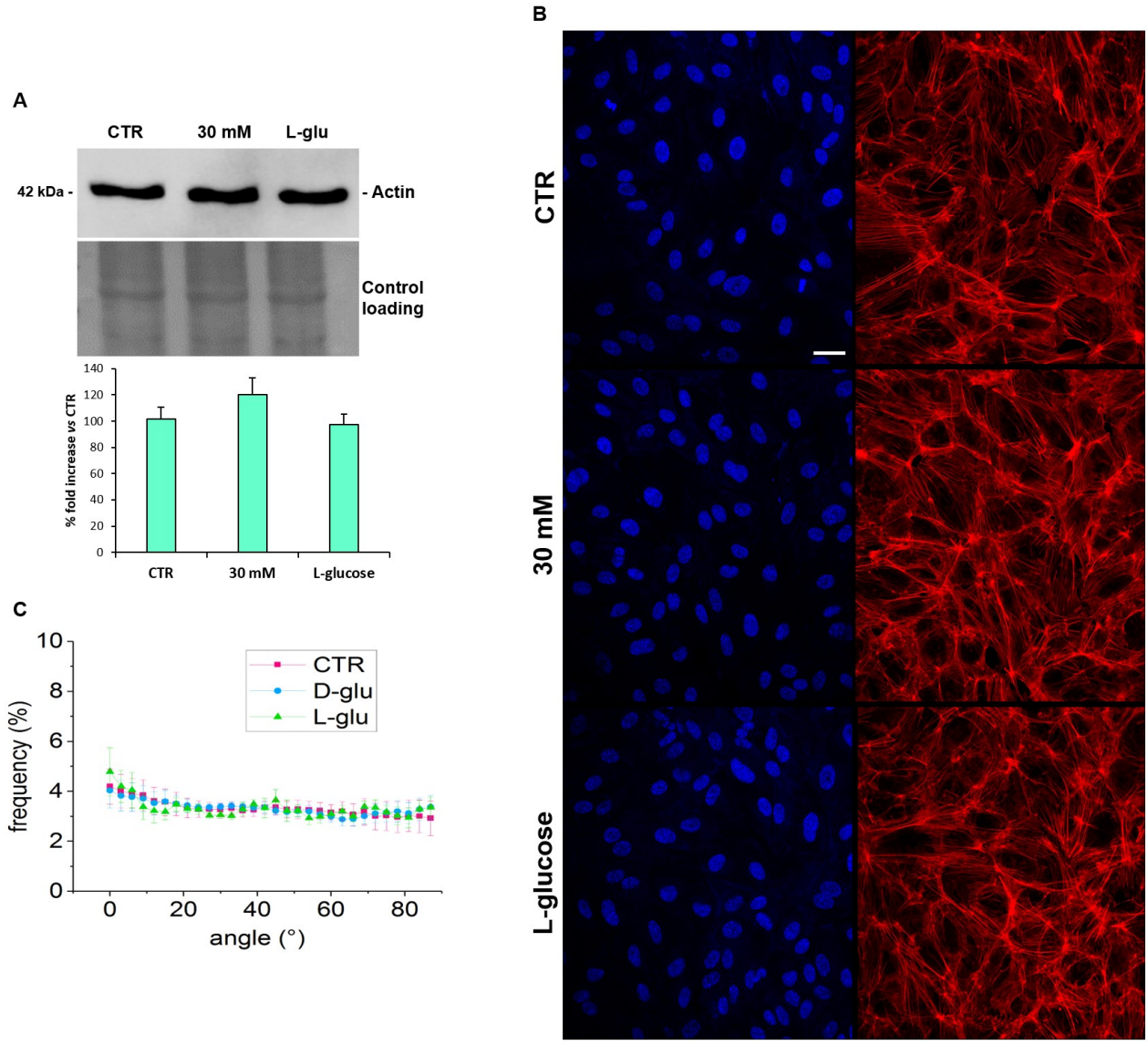

***Figure 40**: (A) Western blot was performed on cell lysates using specific antibodies against Actin. The relative control loading is shown in the lower panel. The experiments were repeated 3 times and a representative blot is shown. Densitometric analysis (lower panel) was performed using Image J Lab software. (B) Confocal microscopy was performed on HUVEC stained with phalloidin-TRITC and Hoechst 33342. The images of actin staining were processed and analyzed using ImageJ software. Scale bar = 30μm. (C) The plot was obtained by the quantification of the angle assumed by fibers in comparison to an ideal horizontal axis (named theta = 0) during the orientation analysis. For each condition and for each angular bin of the distribution, the mean ± 1 standard error computed over n = 6 images was plotted.*

Moving toward the 3D system, the cells were seeded in channels of different calibres and were cultured until they reached the confluence in the presence of a steady flow of culture medium. Channels of nominal section 30×30 μm were chosen as the ideal channels where cells were subjected to a wall shear stress of 0.2 Pa that is representative of physiological conditions for venous ECs. The process of fabrication of the microfluidic device comprehends the following steps: mold fabrication, chip preparation, coating and seeding, cell culture for 1 week and, after the treatment for 24h, the analysis by confocal microscopy (Figure 41). Firstly, a mold recapitulating 8 networks of vessels was produced through soft lithography (phase 1). The networks are composed by ramifications of vessels of different calibres, from 2 channels of 200 μm in the inlet and outlet of the chip to 16 channels of 30 μm in the middle of the chip. Subsequently, a solution of polydimethylsiloxane (PDMS) was mixed with a cross-linking agent, was deprived of air bubbles with a vacuum pump, was poured into the microstructured mold and heated for 3h at 56°C to obtain an elastomeric replica of the mold. Thereafter, the replica was carved out the mold and was sealed to a glass slide to form closed-circuit channels at 56°C for 1 hour (phase 2). Then the chip was connected to a pump system through 2 thin tubes: the inlet tube provided culture medium influx, while the outlet tube discarded the medium coming from the chip into a syringe attached to a pump to guarantee the fluid flow. Next, after the overnight coating with fibronectin (20 μg/ml) (phase 3), the cells were introduced into the chip with a three-step injection and their attachment was facilitated by the permanence in the incubator for 30 minutes after each injection (phase 4). Finally, the chip was connected to the pump to maintain the culture (phase 5) and after 7 days they reached the confluence and therefore they were used for the experiments (phase 6).

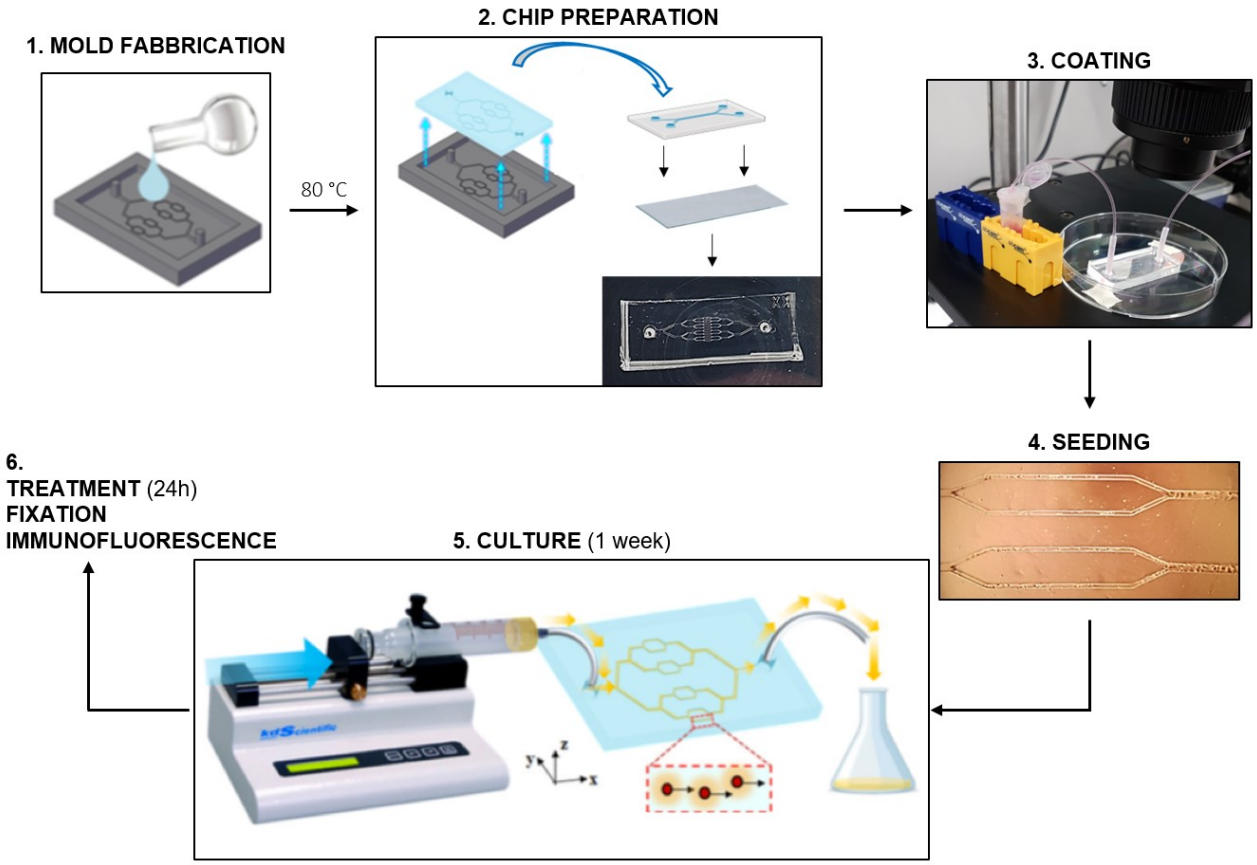

***Figure 41**: Schematic representation of the fabrication of the microfluidic device and the cell culture.*

In this 3D-flow model, the effect of high glucose on actin cytoskeleton was studied. In particular, HUVEC were perfused with medium containing physiological or high concentrations of glucose for 24h. Figure 42 shows in the left panel the images obtained by confocal microscopy of phalloidin-labelled F-actin in the cells after the treatments (a, c, e). The orientation of actin was analyzed using ImageJ software (b, d, e) and the angle assumed by actin fibers subjected to flow direction was plotted on the graphs in the right panel. HUVEC in control and L-glucose showed spindle-like morphology in response to flow, whereas HUVEC in D-glucose were less elongated. Stress fibers were clearly visible in both conditions, but they tended to be shorter and less flow-aligned in high glucose-cultured cells.

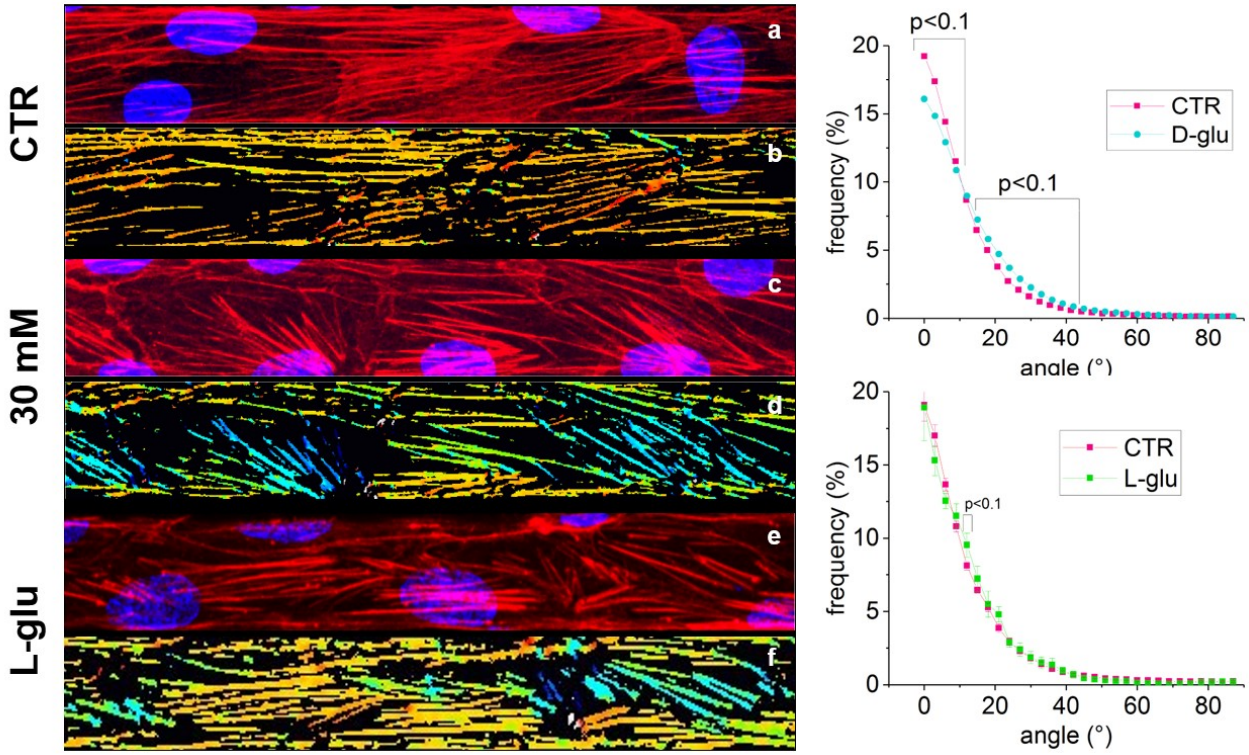

***Figure 42**: Actin organization and orientation analysis in HUVEC cultured in 3D microfluidic chips in the presence of physiological or high glucose. Confocal microscopy (left panel, a, c, d) was performed on HUVEC stained with phalloidin-TRITC and Hoechst 33342. The respective orientation analyses performed using ImageJ software are shown below each treatment (b, d, f). Considering the flow direction as theta=0, the angular distributions of actin fibers shown in the right panels were built by counting in the same (positive) angular bin the data having +theta or -theta orientation.*

5.5.2 EVALUATION OF VE-CADHERIN AND LIPID ACCUMULATION IN 3D MICROFLUIDIC DEVICE

After the optimization of the 3D culture model, the analysis of Ve-Cadherin and the evaluation of lipid content in HUVEC subjected to shear stress in the presence or not of high glucose was performed. Just as in 2D-cultured cells, also in 3D no modulations in the total amount nor in the localization of Ve-Cadherin were detected upon high glucose treatment, as reported in Figure 43. Moreover, the accumulation of lipid droplets in high glucose-cultured cells was confirmed also in 3D (Figure 43, yellow).

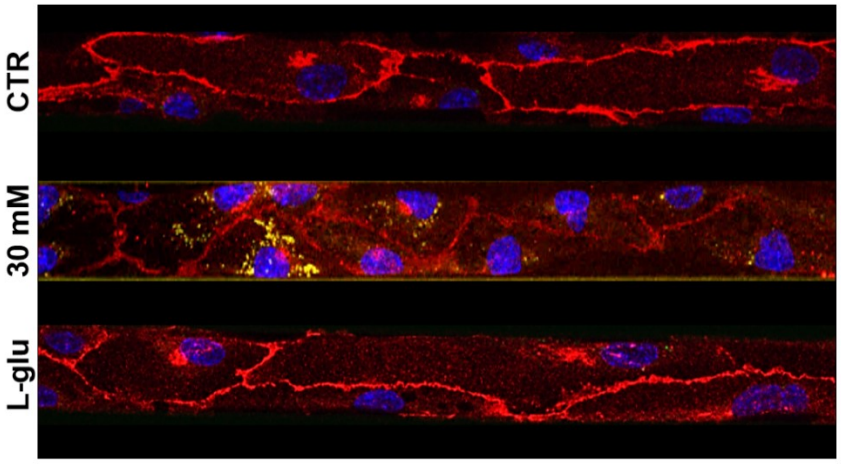

***Figure 43**: Confocal microscopy was performed on HUVEC stained with VE-Cadherin (red), BODIPY (yellow) and DAPI (blue). Images were acquired using a 63X objective in oil by a SP8 Leica confocal microscope. The images were processed and analyzed using ImageJ software. Scale bar = 30 µm.*

5.5.3 EVALUATION OF GLYCOCALYX

Since shedding of the glycocalyx, a flow sensor located on the apical membrane of ECs, contributes to diabetes-induced vascular dysfunction [Yilmaz O 2019], it is feasible to hypothesize that cytoskeletal alterations can be a consequence of modifications of the glycocalyx. Therefore, staining with Wheat Germ Agglutinin (WGA) conjugated with Alexa Fluor 488 (5 µg/ml, Molecular Probes) on living cells was utilized to study the thickness of glycocalyx in HUVEC cultured in the microchannels by confocal microscopy. Images in horizontal planes were acquired to determine the thickness of the glycocalyx (Figure 44A). Intensity profiles across the fluorescent layer were plotted and the full-width-at-half-maximum (FWHM) was determined (Figure 44B, left panel) as a measure of the glycocalyx thickness, plotted in Figure 44B, right panel. No significant differences concerning the thickness of the glycocalyx were detected between CTR cells and high glucose-cultured cells. This result could be explained by the fact that the culture media is a very simplified example of a diabetic-like environment, lacking of many pro-inflammatory stimuli typically involved in this pathology. Therefore, the future perspectives include also 3D experiments in which HUVEC will be cultured in the presence of sera from patients that better reassume the diabetic-like environment.

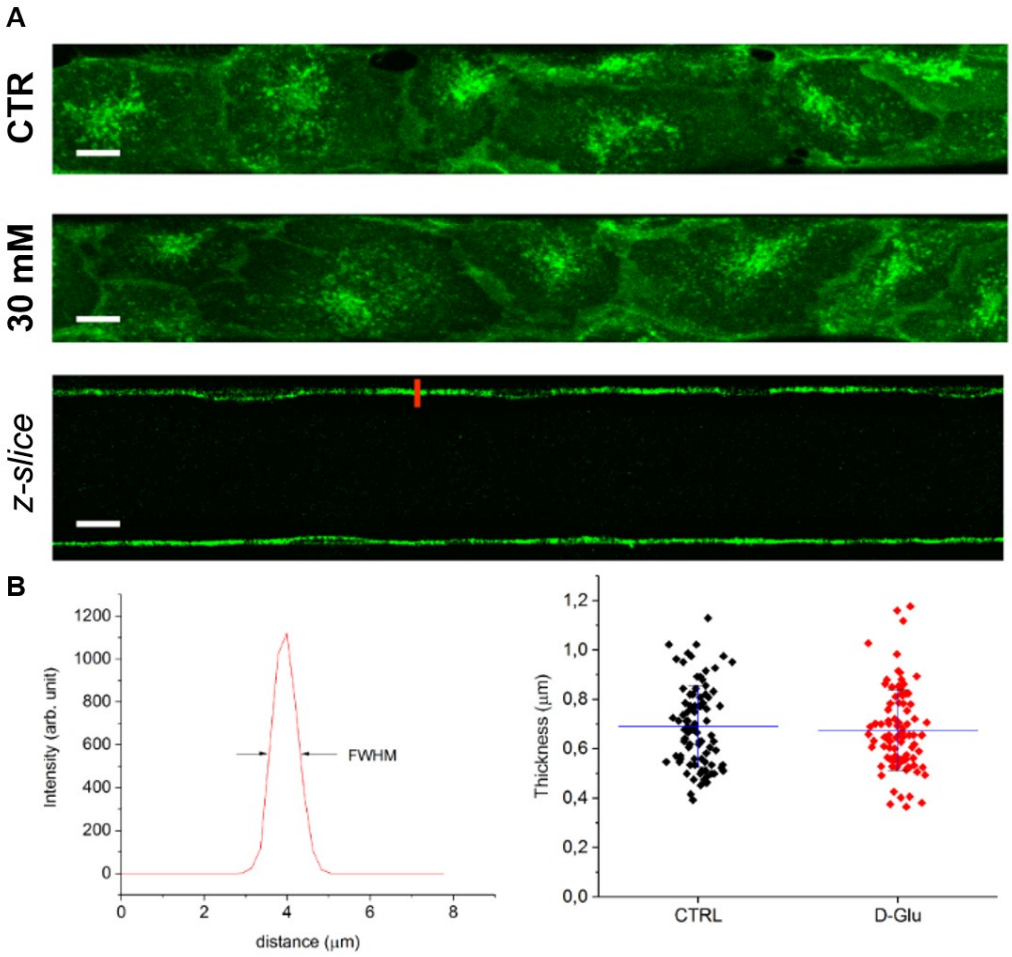

***Figure 44**: (**A**) Confocal microscopy was performed on HUVEC stained with WGA-Alexa Fluor 488. Images were acquired using a 63X objective in oil by a SP8 Leica confocal microscope. The images were processed and analyzed using ImageJ software. Scale bar = 30 μm. (**B**) Intensity profile (left panel) measured along the red line drawn on Figure 31A, from which the glycocalyx thickness was measured as the full width at half maximum. The thickness (right panel) was measured at 29 different locations along the 100 μm-long image section shown, illustrating the spatial homogeneity of glycocalyx.*

6. DISCUSSION

Hyperglycaemia is a term derived from the combination of the Greek words ὑπέρ- (hyper-), γλυκός (sweet/sugar) and αἷμα (blood). Indeed, hyperglycaemia is defined for fasting blood glucose higher than 125 mg/dl and greater than 180 mg/dl 2 hours postprandial. ECs form the inner layer of all the blood vessels and, due to this strategic localization, they constantly face oscillating blood glucose concentrations in relation to the pre- and post- prandial cycles [Meza 2019]. ECs do not represent a passive barrier between blood and tissues, but they play a wide variety of pivotal roles to control vascular homeostasis, among which the regulation of permeability and vascular tone through the secretion of vasoactive substances, the activation of immune cells through either antigen presentation or the release of cytokines and the secretion of pro- / anti- coagulant molecules, therefore maintaining the integrity of vascular wall and the circulatory functions [Sena 2013, Michiels 2003]. However, uncontrolled hyperglycaemia elicits ECs to become dysfunctional, leading to the onset of the so-called endothelial dysfunction, defined as a shift of properties of the endothelium toward a proinflammatory and prothrombotic phenotype characterised by altered release of NO and overproduction of pro-inflammatory cytokines and ROS [Mittal 2014]. These alterations have been highlighted in most forms of cardiovascular diseases, including atherosclerosis, diabetes, hypertension, coronary artery disease and severe viral infections [Tabit 2010, Sena 2013]. Endothelial dysfunction is a primary event that forerun the process of atherosclerosis, a progressive multifactorial disease characterized by the deposition of fatty material in the wall of vessels [Eckel 2021]. This process is highly accelerated in diabetes and metabolic syndromes. In particular, diabetes, a group of life-long chronic metabolic disorders characterized by high levels of glucose in the blood, predisposes to premature atherosclerosis, the main reason for high morbidity and impaired life expectancy in patients [Domingueti 2016, Rask-Madsen 2013].

Several mechanisms have been described to mediate hyperglycaemia-dependent endothelial dysfunction, among which the accumulation of ROS thus leading to oxidative stress, an important factor linked either to the increased production of oxidizing species or to a significant decreased availability of antioxidant defences such as glutathione [Shrestha 2018, Asmat 2016]. In accordance with the literature, high-glucose cultured HUVEC showed an overproduction of ROS and in parallel a reduced supply of the antioxidant glutathione. In particular, this imbalance in the redox system was pinpointed in the high glucose-induced overexpression of TXNIP, able to bind to Thioredoxin via disulphide bonds thus inhibiting its antioxidant capacity, and in the simultaneous downregulation of SIRT1, a NAD^+-dependent

deacetylase protein involved both in stress responses and in cellular metabolism improving insulin sensitivity.

One of the issues of this thesis to deal with was to identify a potential countermeasure that might prevent or at least delay the detrimental effects of high glucose on HUVEC. It is well documented that VitD deficiency (circulating levels < 20 ng/mL) is considered a risk factor for the development of endothelial dysfunction associated to diabetes [Mason 2015, Giovannucci 2008], just as its beneficial effects on the cardiovascular system [Drechsler 2010]. Indeed, beyond its canonical role in controlling calcium and phosphate homeostasis in bones, VitD protects against atherosclerosis by inhibiting the conversion of macrophages into foam cells and by enhancing cholesterol efflux [Pilz 2016]. Therefore, since the underlying mechanisms by which VitD exerts its vasculo-protective roles still need to be characterized, the effects of VitD on high glucose-treated cells were tested. Interestingly, VitD restored normal levels of ROS by inhibiting the overexpression of TXNIP, thus mimicking the effects of *TXNIP* silencing, highlighting TXNIP as one of the targets of VitD in HUVEC cultured in high glucose-containing media. Despite it was originally isolated as a VitD-upregulated protein [Chung 2006], TXNIP is differently regulated by VitD according to the cell type considered [Abu 2018]. Indeed, cell specificity in the modulation of the response to VitD is possible, and the downregulation of TXNIP after exposure to VitD seems to occur in cells harbouring wild type p53 [Abu 2018], including HUVEC.

Moreover, one of the earliest events in atherogenesis is the alteration of endothelial permeability that favours the accumulation of lipoproteins into the intima where they are oxidized worsening endothelial dysfunction [Gimbrone 2016]. Indeed, it is well known that high glucose is responsible for the impairment of endothelial permeability in diabetes [Hempel 1997] through the alteration of intercellular junctions, fundamental in the maintenance of the integrity of vascular barrier. Many data are available concerning the effect of high glucose on the gap junctions, i.e. Cx43 whose expression is decreased in diabetic patients [Yang 2020, Fernandes 2004]. Moreover, along with the adherens junctions, i.e. Ve-Cadherin, the tight junctions, i.e. ZO-1, form apical junctional complexes both in epithelial and endothelial cells, playing a central role in controlling the paracellular permeability and in maintaining cell polarity [Bazzoni 2001, Stevenson 1999]. In accordance with the literature, hyperpermeability occurs in response to exaggerated high glucose-induced oxidative stress. These results were phenocopied when the cells were cultured in

the presence of diabetic hyperglycaemic sera, independently from the levels of HbA1c, meaning that it is sufficient to expose HUVEC to high glucose to induce hyperpermeability. Moreover, the total amount of ZO-1 was decreased by high glucose, whereas the Ve-Cadherin levels and subcellular localization remained unchanged. This last evidence could be explained by a previous work demonstrating that high glucose is accountable for the Tyrosine phosphorylation of Ve-Cadherin causing the disruption of the adherens junctions associated with the activation of the Wnt/β-catenin signalling pathway and with the increase of the leukocytes transendothelial migration [Haidari 2014]. Interestingly, the supplementation of VitD to high glucose-containing media completely mended endothelial permeability preventing the downregulation of ZO-1.

A fundamental mediator of vascular permeability is NO. Indeed, NO modulates endothelial permeability, regulating the cell cytoskeletal architecture through Rho signalling pathway [Di Lorenzo 2013]. Therefore, the levels of NOx were measured in culture media and the results pointed to a direct effect of high glucose in enhancing NOx release. Indeed, HUVEC cultured in high glucose-containing media released more NOx than controls through the upregulation of iNOS, the inducible isoform of NOS active during inflammation and immune response. In addition, a very strong association between elevated amounts of NOx in diabetic sera and fasting glucose concentrations was found. In agreement with these findings, the overexpression of iNOS was found to be responsible for the increase of NOx levels in alloxan-induced T1D rats [Sartoretto 2019]. Moreover, a quite recent study confirmed that circulating inflammatory markers have been detected in young diabetic patients, a result consistent with the inflammation-induced vascular pathology typical of diabetes [Aulich 2019]. Indeed, diabetes is associated with a pro-inflammatory environment since elevated plasma concentrations of pro-inflammatory cytokines, i.e. IL-1β and IL-17A, as well as IFNɣ, TNF-α and IL-23 were measured in patients [Fatima 2016]. These cytokines activate iNOS leading to exaggerated NO synthesis in many cell types, including ECs [Fatima 2016]. Accordingly, either the genetic or the pharmacological inhibition of iNOS totally forestalled the overproduction of NO thus preventing the increase of endothelial permeability caused by high glucose. Therefore, it is feasible to hypothesize that transient peaks of hyperglycaemia can be harmful for endothelial integrity because they are liable for the enhanced permeability by stimulating NO production.

It has been proven that in response to oxidative stress TXNIP relocates from the nucleus into the mitochondria [Saxena 2010], eliciting mitochondrial dysfunction. Mitochondrial content in ECs is relatively low in comparison to cells with high-energy demand. Indeed, the higher energy source of ECs comes from anaerobic glycolysis [Dumas 2020], a metabolic pathway that entails lower ATP production than oxidative phosphorylation, protecting the cells from oxidative stress and preserving oxygen diffusion into perivascular tissues [Li 2019]. Therefore, mitochondria in ECs are not bioenergetics supplier but rather biosynthetic factories since they regulate cellular homeostasis, integrating signals coming from the microenvironment and sensing cellular stress. However, the presence of some risk factors, such as redox imbalance typical of a hyperglycaemic microenvironment, leads to mitochondria damage. Therefore, since in the last years many evidences revealed that mitochondrial dysfunction is implicated in the pathophysiology of diabetes [Kwak 2010], it is not astounding that in high glucose-cultured HUVEC an alteration in mitochondrial dynamics occurs, due to the overexpression of DRP1, a mediator of mitochondrial fission, and to the downregulation of OPA1, enrolled in mitochondrial fusion. In addition, no variation in mitochondrial content where detected. Indeed, in hyperglycaemic environment, ROCK1, a key regulator of mitochondrial dynamics, is able to phosphorylate DRP1 leading to mitochondrial fission and mtROS overproduction with the subsequent release of cytochrome c [Wang 2012]. Furthermore, the selective upregulation of OPA1 stimulated the fusion process thus improving mitochondrial fitness in high-glucose cultured cardiomyocytes [Ding 2020]. Moreover, high glucose-induced imbalance in favour of mitochondrial fission occurs simultaneously with reduced oxygen consumption and overproduction of mtROS, all of which entail mitochondrial damage [Yu 2008].

Mitochondria are also the headquarters of fatty acid catabolism. Indeed, ECs metabolize fatty acids to form Acetyl-CoA, used as a fuel to sustain TCA cycle [Hülsmann 1988]. CPT1A, a member of carnitine palmitate hydrazine transferase family located on the outer mitochondrial membrane, is a rate-controlling enzyme involved in the intake of fatty acids into mitochondria where they are subjected to fatty acid β-oxidation, the major pathway for the catabolism of fatty acids [Kerner 2000]. After high glucose treatment, the total amount of CPT1A was diminished and consequently the β-oxidation rate in high glucose-cultured cells was decreased. In accordance with these results, the reduced intake of fatty acids into the mitochondria explains the accumulation of triglycerides observed in HUVEC cultured in high glucose-containing media. Besides the lower β-oxidation rate, another explanation for

the high glucose-induced lipid accumulation is the higher synthesis of fatty acids. Two proteins involved lipogenesis are EDF1 and PPARɣ. In particular, EDF1 is a small protein ubiquitously expressed [Dragoni 1998]. It exerts its function both in the cytosol, where upon the binding with calmodulin it modulates several calcium-regulated enzymes [López-Victorio 2013], and in the nucleus, where it interacts with several transcription factors and acts as a transcriptional coactivator for non-steroid nuclear receptors involved in lipid metabolism, among which PPARγ [Brendel 2002]. In ECs PPARγ exerts a wide range of fundamental functions, including lipid metabolism, since it regulates the expression of some genes involved in release, transport and storage of fatty acids, such as lipoprotein lipase (LPL) and the fatty acid transporter CD36 [Lehrke 2005]. High glucose-cultured HUVEC showed an upregulation of both EDF1 and PPARγ. The activation of the EDF-1/PPARγ axis might fuel fatty acid synthesis in HUVEC. A similar conclusion was reached in HUVEC cultured in low magnesium-containing medium [Locatelli 2021], thus suggesting that lipid accumulation is a common feature in ECs exposed to metabolic stress. Notably, lipid droplets are promptly formed in murine intact aortic EC *in vivo* and *ex vivo* after a load of fatty acid, suggesting that, beyond being an energy resource, endothelial lipid droplets could represent a defense mechanism against lipotoxicity [Kuo 2017]. Therefore, whether lipid droplet-derived fatty acids are used as substrates for energy metabolism or for protection against lipoperoxidation in this experimental model remains to be elucidated. Moreover, the overexpression of GLUT1 transporter after few hours of treatment with high glucose is an indicator of an excessive intake of glucose into the cells. Considering the decreased oxygen consumption at mitochondrial level, the hypothesis is that the overload of glucose in the cells is converted through anaerobic glycolysis in lactate that can be used as a substrate for triglycerides synthesis. Indeed, lactate can be reversibly converted to pyruvate in a reaction catalysed by the enzyme lactate dehydrogenase, therefore supporting the synthesis of fatty acids [Sun 2016]. Interestingly, the inhibition of the overproduction of ROS with the supplementation of VitD restored normal lipid content by both decreasing EDF1 and PPARγ and increasing CPT1A expression.

The results explained hereinbefore were obtained on monolayers of ECs in two-dimensional culture systems in the absence of flow. Albeit this typical 2D experimental approach has been yielding major advances in our knowledge about endothelial pathophysiology, it presents some limitations due to the fact that 2D culture does not replicate the complex structural organization of the endothelium. Therefore, recently alternative experimental

models have been developed to better mimic the complexity of the vascular system allowing perfusion, thus generating shear stress fundamental for endothelial homeostasis [Rimann 2012]. In particular, the response to high glucose was tested on HUVEC cultured in biomimetic microchannels fabricated through soft lithography and perfused to generate shear stress. These devices have sequential bifurcations and channels of different caliber thus mimicking geometrical features of the vasculature [Tsvirkun 2017]. Firstly, the attention was focused on the cytoskeleton, a target of both mechanical and biochemical signals coming from the microenvironment [Ingber 2006, Locatelli 2020]. As expected, in 3D condition control cells showed spindle-like morphology in response to the flow. On the contrary, high glucose-cultured HUVEC were less elongated. In both treatments, stress fibers were clearly observable, but they tended to be shorter and less flow-aligned in high glucose-cultured cells. Moreover, in 3D no modulations in the total amount nor in the localization of Ve-Cadherin were detected upon high glucose treatment and the accumulation of lipid droplets in high glucose-cultured cells was confirmed. Therefore, even if these results are in a preliminary phase, they are confirmed both in 2D and in 3D. In addition, since shedding of the glycocalyx, a flow sensor located on the apical membrane of ECs, contributes to diabetes-induced vascular dysfunction [Yilmaz 2019], it is feasible to hypothesize that cytoskeletal alterations can be a consequence of changes of the glycocalyx. Indeed, in *db/db* transgenic diabetic mice the observed alterations in glycocalyx composition and/or structure render the cells less sensitive to flow and, consequently, impair the shear stress response [Targosz-Korecka 2017]. However, in this experimental model no significant differences concerning the thickness of the glycocalyx were detected upon high glucose treatment. This result could be explained by the fact that the culture media is a very simplified example of a diabetic-like environment, lacking of many pro-inflammatory stimuli typical of the pathology. Therefore, the future perspectives include also 3D experiments in which HUVEC will be cultured in the presence of sera from patients that better reassume the diabetic-like environment.

In summary (Figure 45), these results demonstrated that i) the detrimental effects of high glucose are firstly manifested with alterations in the cellular redox system; ii) the second transitory effect is the overproduction of NO leading to hyperpermeability; iii) mitochondrial dysfunction occurs as a result of the imbalance in mitochondrial dynamics iv) which is tied to the higher storage of triglycerides caused both by enhanced lipogenesis and reduced β-oxidation. In this context, VitD blocks the increased ROS production, thus preventing all the

detrimental effects of high glucose on HUVEC. Therefore, the results reveal that it is fundamental to keep glycaemia within the physiological range in diabetic patients, preventing hyperglycaemic peaks. Moreover, considering its vasculo-protective effects, it could be feasible to establish a nutritional/dietetic regimen that includes the tailored supplementation of VitD in hyperglycaemic patients. Indeed, it could represents a serviceable tool to control the redox equilibrium, thus re-establishing NOx levels and permeability and mitochondrial function, to limit or, at least, delay the insurgence of endothelial dysfunction caused by high fasting glucose concentrations.

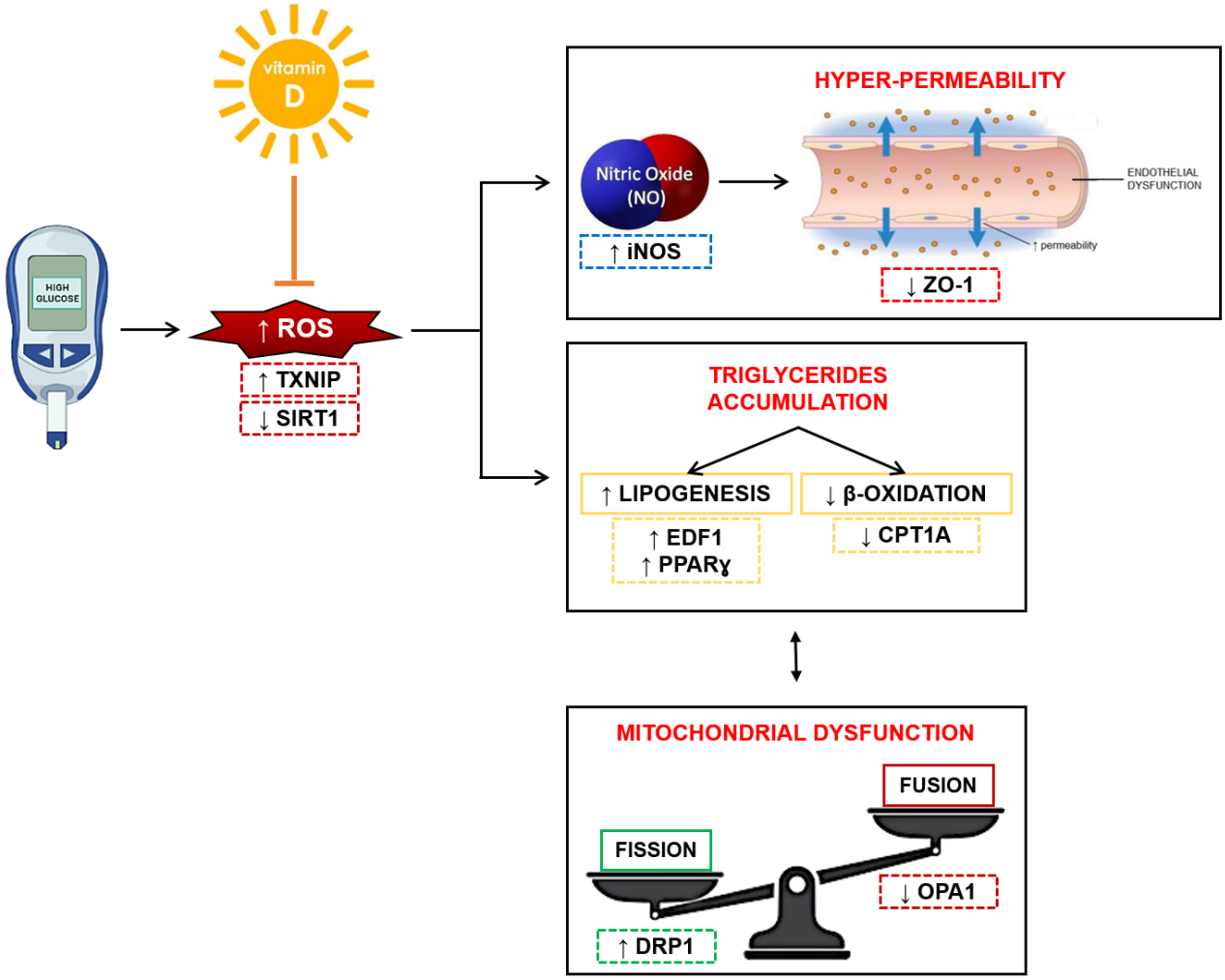

***Figure 45**: Schematic representation of the results.*

7. ACKNOWLEDGMENT

I acknowledge Università degli Studi di Milano for granting my 3-years PhD course in Experimental Medicine and especially Professor Maier for giving me the opportunity to join her laboratory allowing my professional growth. A special thank goes to Alessandra for sharing this journey with me, started four years ago by now, and facing the ups and downs of this job together. Thanks also to my colleagues Monica, Laura and Giorgia that, despite my mood swings, have always been supportive. It is the best “loser group” I have ever been in.

I sincerely thank my mum Antonella, who has never gave me time to give up, and Chetto, who never wants to be thanked. I also acknowledge my dad Roberto who, despite the distance, is always here next to me. Finally yet importantly, a special thanks to my sister Chiara e my brother Emanuele, who never leave me alone for a second, physically as well as mentally. If I had the courage to experiment with new ideas, to put myself in the game and to understand that, after all, obstacles exist to be overcome, the credit is above all of you.

Thanks also to Chiara, my glowing wife who has always kept the "seaweed promise" with a bit of patience and many glasses of wine, and to Federica, who is always well disposed to listen and to give me valuable advices.

Lastly, this thesis is dedicated to those who have always doubted my potentiality because of envy and fear of being left behind, you have been the fuel for my determination, and to myself and my tenacity that have allowed me to get there.

7. RINGRAZIAMENTI

Ringrazio l'Università degli Studi di Milano per avermi selezionata per questi tre anni di Dottorato in Medicina Sperimentale e soprattutto la Professoressa Maier per avermi dato l'opportunità di entrare a far parte del suo laboratorio permettendo la mia crescita professionale. Un ringraziamento particolare va ad Alessandra per aver condiviso con me questo percorso, iniziato ormai quattro anni fa, e per aver affrontato insieme gli alti e bassi di questo lavoro. Grazie anche alle mie colleghe Monica, Laura e Giorgia che, nonostante i miei sbalzi d'umore, mi sono sempre state di supporto. È il miglior "gruppo sfigate" di cui abbia mai fatto parte.

Ringrazio di cuore mia mamma Antonella, che non mi ha mai dato tempo per arrendermi, e Chetto, che non vuole mai essere ringraziato. Ringrazio anche mio papà Roberto che, nonostante la distanza, è sempre al mio fianco. Infine, ma non meno importante, un ringraziamento speciale a mia sorella Chiara e mio fratello Emanuele, che non mi lasciano mai sola un secondo, fisicamente oltre che mentalmente. Se ho avuto il coraggio di sperimentare nuove idee, di mettermi in gioco e di capire che, in fondo, gli ostacoli esistono per essere superati, il merito è soprattutto vostro.

Grazie anche a Chiara, la mia luccicante moglie che da sempre mantiene la “promessa dell’alga” con un po’ di pazienza e molti bicchieri di vino, e a Federica, sempre pronta ad ascoltarmi e darmi consigli preziosi.

Questa tesi, infine, è dedicata a chi ha sempre dubitato delle mie potenzialità per invidia e paura di rimanere indietro, siete stati carburante per la mia determinazione, e a me stessa e alla mia tenacia che mi hanno permesso di arrivare fin qui.

8. REFERENCES

- Abougalambou SS, Abougalambou AS, Sulaiman SA, Hassali MA. *Prevalence of hypertension, control of blood pressure and treatment in hypertensive with type 2 diabetes in Hospital University Sains Malaysia*. Diabetes Metab Syndr. 2011; 5(3): 115-9.
- Abu El Maaty MA, Almouhanna F, Wölfl S. *Expression of TXNIP in Cancer Cells and Regulation by 1,25(OH)$_2$D$_3$: Is It Really the Vitamin D$_3$ Upregulated Protein?* Int J Mol Sci. 2018 Mar 10;19(3):796.
- Aird WC. *Endothelial cell heterogeneity*. Cold Spring Harb Perspect Med. 2012 Jan;2(1):a006429.
- American Diabetes Association. *Diagnosis and classification of diabetes mellitus. Diabetes Care*. 2013 Jan;36 Suppl 1(Suppl 1):S67-74.
- Asmat U, Abad K, Ismail K. *Diabetes mellitus and oxidative stress-A concise review*. Saudi Pharm J. 2016 Sep;24(5):547-553.
- Aulich J, Cho YH, Januszewski AS, Craig ME, Selvadurai H, Wiegand S, Jenkins AJ, Donaghue KC. *Associations between circulating inflammatory markers, diabetes type and complications in youth*. Pediatr Diabetes. 2019 Dec;20(8):1118-1127.
- Bai K, Huang Y, Jia X, Fan Y, Wang W. *Endothelium oriented differentiation of bone marrow mesenchymal stem cells under chemical and mechanical stimulations*. J Biomech. 2010 Apr 19;43(6):1176-81.
- Badimon L, Padró T, Vilahur G. *Atherosclerosis, platelets and thrombosis in acute ischaemic heart disease*. Eur Heart J Acute Cardiovasc Care. 2012 Apr;1(1):60-74.
- Barst RJ. *A review of pulmonary arterial hypertension: role of ambrisentan*. Vasc Health Risk Manag. 2007;3(1):11-22.
- Basser PJ, Pierpaoli C. *Microstructural and physiological features of tissues elucidated by quantitative-diffusion-tensor MRI*. 1996. J Magn Reson. 2011 Dec;213(2):560-70.
- Bazzoni G, Dejana E. *Pores in the sieve and channels in the wall: control of paracellular permeability by junctional proteins in endothelial cells*. Microcirculation. 2001 Jun;8(3):143-52.

- Bover J, Egido J, Fernández-Giráldez E, Praga M, Solozábal-Campos C, Torregrosa JV, Martínez-Castelao A. *Vitamin D, vitamin D receptor and the importance of its activation in patients with chronic kidney disease*. Nefrologia. 2015;35(1):28-41. English, Spanish.
- Brendel C, Gelman L, Auwerx J. *Multiprotein bridging factor-1 (MBF-1) is a cofactor for nuclear receptors that regulate lipid metabolism*. Mol Endocrinol. 2002 Jun;16(6):1367-77.
- Caja S, Enríquez JA. *Mitochondria in endothelial cells: Sensors and integrators of environmental cues*. Redox Biol. 2017 Aug;12:821-827.
- Carlberg C, Seuter S. *A genomic perspective on vitamin D signalling*. Anticancer Res. 2009;29(9): 3485-93.
- Chen W, Chen X, Zhang M, Huang Z. *The association of human leukocyte antigen class II (HLA II) haplotypes with the risk of Latent autoimmune diabetes of adults (LADA): Evidence based on available data*. Gene. 2021 Jan 30;767:145177.
- Choi K. *Hemangioblast development and regulation*. Biochem Cell Biol. 1998;76(6):947-56.
- Chung JW, Jeon JH, Yoon SR, Choi I. *Vitamin D_3 upregulated protein 1 (VDUP1) is a regulator for redox signaling and stress-mediated diseases*. J Dermatol. 2006 Oct;33(10):662-9.
- Cines DB, Pollak ES, Buck CA, Loscalzo J, Zimmerman GA, McEver RP, Pober JS, Wick TM, Konkle BA, Schwartz BS, Barnathan ES, McCrae KR, Hug BA, Schmidt AM, Stern DM. *Endothelial cells in physiology and in the pathophysiology of vascular disorders*. Blood. 1998 May 15;91(10):3527-61.
- De Bock K, Georgiadou M, Carmeliet P. *Role of endothelial cell metabolism in vessel sprouting*. Cell Metab. 2013 Nov 5;18(5):634-47.
- De Bock K, Georgiadou M, Schoors S, Kuchnio A, Wong BW, Cantelmo AR, Quaegebeur A, Ghesquière B, Cauwenberghs S, Eelen G, Phng LK, Betz I, Tembuyser B, Brepoels K, Welti J, Geudens I, Segura I, Cruys B, Bifari F, Decimo I, Blanco R, Wyns S, Vangindertael J, Rocha S, Collins RT, Munck S, Daelemans D, Imamura H, Devlieger R, Rider M, Van Veldhoven PP, Schuit F, Bartrons R, Hofkens J, Fraisl P, Telang S, Deberardinis RJ, Schoonjans L, Vinckier S, Chesney J, Gerhardt H, Dewerchin M, Carmeliet P. R*ole of PFKFB3-driven glycolysis in vessel sprouting*. Cell. 2013 Aug 1;154(3):651-63.

- De Boer IH, Tinker LF, Connelly S, Curb JD, Howard BV, Kestenbaum B, Larson JC, Manson JE, Margolis KL, Siscovick DS, Weiss NS. *Calcium plus vitamin D supplementation and the risk of incident diabetes in the Women's Health Initiative*. Diabetes Care. 2008; 31(4): 701-7.
- Di Lorenzo A, Lin MI, Murata T, Landskroner-Eiger S, Schleicher M, Kothiya M, Iwakiri Y, Yu J, Huang PL, Sessa WC. *eNOS-derived nitric oxide regulates endothelial barrier function through VE-cadherin and Rho GTPases*. J Cell Sci. 2013 Dec 15;126(Pt 24):5541-52.
- Ding M, Liu C, Shi R, Yu M, Zeng K, Kang J, Fu F, Mi M. *Mitochondrial fusion promoter restores mitochondrial dynamics balance and ameliorates diabetic cardiomyopathy in an optic atrophy 1-dependent way*. Acta Physiol (Oxf). 2020 May;229(1):e13428.
- Doddaballapur A, Michalik KM, Manavski Y, Lucas T, Houtkooper RH, You X, Chen W, Zeiher AM, Potente M, Dimmeler S, Boon RA. *Laminar shear stress inhibits endothelial cell metabolism via KLF2-mediated repression of PFKFB3*. Arterioscler Thromb Vasc Biol. 2015 Jan;35(1):137-45.
- Domingueti CP, Sant'Ana Dusse LM, Das Graças Carvalho M, Pires de Sousa L, Gomes KB, Fernandes AP. *Diabetes mellitus: the linkage between oxidative stress, inflammation, hypercoagulability and vascular complications*. Journ of Diabetes and its Compl. 2016; 30(4):738-745.
- Dragoni I, Mariotti M, Consalez GG, Soria MR, Maier JA. *EDF-1, a novel gene product down-regulated in human endothelial cell differentiation*. J Biol Chem. 1998 Nov 20;273(47):31119-24.
- Drechsler C, Pilz S, Obermayer-Pietsch B, et al. *Vitamin D deficiency is associated with sudden cardiac death, combined cardiovascular events and mortality in haemodialysis patients*. Eur Heart J. 2010; 31(18): 2253–2261.
- Dumas SJ, García-Caballero M, Carmeliet P. *Metabolic Signatures of Distinct Endothelial Phenotypes*. Trends Endocrinol Metab. 2020 Aug;31(8):580-595.
- Eckel RH, Bornfeldt KE, Goldberg IJ. C*ardiovascular disease in diabetes, beyond glucose*. Cell Metab. 2021 Aug 3;33(8):1519-1545.
- El Asrar MA, Adly AA, Ismail EA. *Soluble CD40L in children and adolescents with type 1 diabetes: relation to microvascular complications and glycaemic control*. Pediatr Diabetes. 2011; 13(8): 616-24.

- Falkenberg KD, Rohlenova K, Luo Y, Carmeliet P. *The metabolic engine of endothelial cells*. Nat Metab. 2019 Oct;1(10):937-946.
- Fan TP, Yeh JC, Leung KW, Yue PY, Wong RN. *Angiogenesis: from plants to blood vessels*. Trends Pharmacol Sci. 2006 Jun;27(6):297-309.
- Fatima N, Faisal SM, Zubair S, Ajmal M, Siddiqui SS, Moin S, Owais M. *Role of Pro-Inflammatory Cytokines and Biochemical Markers in the Pathogenesis of Type 1 Diabetes: Correlation with Age and Glycemic Condition in Diabetic Human Subjects*. PLoS One. 2016 Aug 30;11(8):e0161548.
- Fawzy MS, Toraih EA. *Data supporting the structural and functional characterization of Thrombin-Activatable Fibrinolysis Inhibitor in breast cancer*. Data Brief. 2015 Nov 14;5:981-9.
- Fernandes R, Girão H, Pereira P. *High glucose down-regulates intercellular communication in retinal endothelial cells by enhancing degradation of connexin 43 by a proteasome-dependent mechanism*. J Biol Chem. 2004 Jun 25;279(26):27219-24.
- Fitzgerald U, Hettle S, MacDonald C, McLean JS. U*mbilical cord endothelial cells expressing large T antigen: comparison with primary cultures and effect of cell age*. In Vitro Cell Dev Biol Anim. 2000 Apr;36(4):222-7.
- Foreman KE, Tang J. M*olecular mechanisms of replicative senescence in endothelial cells*. Exp Gerontol. 2003 Nov-Dec;38(11-12):1251-7.
- Frank PG, Lisanti MP. R*ole of caveolin-1 in the regulation of the vascular shear stress response*. J Clin Invest. 2006 May;116(5):1222-5.
- Galley HF, Webster NR. *Physiology of the endothelium*. Br J Anaesth. 2004 Jul;93(1):105-13.
- Gil Á, Plaza-Diaz J, Mesa MD. *Vitamin D: Classic and Novel Actions*. Ann Nutr Metab. 2018;72(2):87-95.
- Gilmartin AB, Ural SH, Repke JT. *Gestational diabetes mellitus*. Rev Obstet Gynecol. 2008;1(3): 129-34.
- Gimbrone MA Jr. *Vascular endothelium: nature's blood-compatible container*. Ann N Y Acad Sci. 1987;516:5-11.
- Goldsby R.A., Kindt T.J., Osborne B.A. (2000). Kuby *Immunologia*. Seconda Edizione UTET.

- Giovannucci E, Liu Y, Hollis BW, Rimm EB. *25-hydroxyvitamin D and risk of myocardial infarction in men: a prospective study*. Arch Intern Med. 2008; 168(11): 1174–1180.
- Grisham MB, Ware K, Gilleland HE Jr, Gilleland LB, Abell CL, Yamada T. *Neutrophil-mediated nitrosamine formation: role of nitric oxide in rats*. Gastroenterology. 1992 Oct;103(4):1260-6.
- Haidari M, Zhang W, Willerson JT, Dixon RA. *Disruption of endothelial adherens junctions by high glucose is mediated by protein kinase C-β-dependent vascular endothelial cadherin tyrosine phosphorylation*. Cardiovasc Diabetol. 2014 Jul 15;13:105.
- Hansen T. *Type 2 diabetes mellitus--a multifactorial disease*. Ann Univ Mariae Curie Sklodowska Med. 2002;57(1):544-9.
- Helmlinger G, Endo M, Ferrara N, Hlatky L, Jain RK. *Formation of endothelial cell networks*. Nature. 2000 May 11;405(6783):139-41.
- Hempel A, Maasch C, Heintze U, Lindschau C, Dietz R, Luft FC, Haller H. *High glucose concentrations increase endothelial cell permeability via activation of protein kinase C alpha*. Circ Res. 1997 Sep;81(3):363-71.
- Huang NF, Li S. *Mesenchymal stem cells for vascular regeneration*. Regen Med. 2008 Nov;3(6):877-92.
- Hülsmann WC, Dubelaar ML*. Aspects of fatty acid metabolism in vascular endothelial cells*. Biochimie. 1988 May;70(5):681-6.
- Ingber DE. *Cellular mechanotransduction: putting all the pieces together again*. FASEB J. 2006 May;20(7):811-27.
- Jarc E, Petan T. Lipid Droplets and the Management of Cellular Stress. Yale J Biol Med. 2019 Sep 20;92(3):435-452.
- Jassil NK, Sharma A, Bikle D, Wang X. *Vitamin D binding protein and 25-hydroxyvitamin D levels: emerging clinical applications*. Endocr Pract. 2017; 23(5): 605-613.
- Johansson F, Kramer F, Barnhart S, Kanter JE, Vaisar T, Merrill RD, Geng L, Oka K, Chan L, Chait A, Heinecke JW, Bornfeldt KE. *Type 1 diabetes promotes disruption of advanced atherosclerotic lesions in LDL receptor-deficient mice*. Proc Natl Acad Sci USA. 2008; 105(6):2082-7.
- Kerner J, Hoppel C. *Fatty acid import into mitochondria*. Biochim Biophys Acta. 2000 Jun 26;1486(1):1-17.

- Kluge MA, Fetterman JL, Vita JA. *Mitochondria and endothelial function*. Circ Res. 2013 Apr 12;112(8):1171-88.
- Khammissa RAG, Fourie J, Motswaledi MH, Ballyram R, Lemmer J, Feller L. *The Biological Activities of Vitamin D and Its Receptor in Relation to Calcium and Bone Homeostasis, Cancer, Immune and Cardiovascular Systems, Skin Biology, and Oral Health*. Biomed Res Int. 2018 May 22;2018:9276380.
- Komarova Y, Malik AB. *Regulation of endothelial permeability via paracellular and transcellular transport pathways*. Annu Rev Physiol. 2010;72:463-93.
- Kremer JR, Mastronarde DN, McIntosh JR. Computer visualization of three-dimensional image data using IMOD. J Struct Biol. 1996 Jan-Feb;116(1):71-6.
- Kuo A, Lee MY, Sessa WC*. Lipid Droplet Biogenesis and Function in the Endothelium*. Circ Res. 2017 Apr 14;120(8):1289-1297.
- Kwak SH, Park KS, Lee KU, Lee HK. *Mitochondrial metabolism and diabetes*. J Diabetes Investig. 2010 Oct 19;1(5):161-9.
- Lagarrigue F, Kim C, Ginsberg MH. *The Rap1-RIAM-talin axis of integrin activation and blood cell function*. Blood. 2016 Jul 28;128(4):479-87.
- Lanzinger S, Altug H, Schikowski T, Khodaverdi S, Rosenbauer J, Rathmann W, Praedicow K, Schönau E, Holl RW; DPV initiative. *Longitudinal relationship of particulate matter and metabolic control and severe hypoglycaemia in children and adolescents with type 1 diabetes*. Environ Res. 2021 Aug 10;203:111859.
- Lehrke M, Lazar MA. *The many faces of PPARgamma*. Cell. 2005 Dec 16;123(6):993-9.
- Leone TC, Kelly DP. *Transcriptional control of cardiac fuel metabolism and mitochondrial function*. Cold Spring Harb Symp Quant Biol. 2011;76:175-82.
- Levi M, ten Cate H, van der Poll T. *Endothelium: interface between coagulation and inflammation*. Crit Care Med. 2002 May;30(5 Suppl):S220-4.
- Li YC, Kong J, Wei M, Chen ZF, Liu SQ, Cao LP. *1,25-Dihydroxyvitamin D(3) is a negative endocrine regulator of the renin-angiotensin system*. J Clin Invest. 2002; 110(2): 229-38.
- Li X, Kumar A, Carmeliet P. Meta*bolic Pathways Fueling the Endothelial Cell Drive*. Annu Rev Physiol. 2019 Feb 10;81:483-503.

- Locatelli L, Fedele G, Castiglioni S, Maier JA. *Magnesium Deficiency Induces Lipid Accumulation in Vascular Endothelial Cells via Oxidative Stress-The Potential Contribution of EDF-1 and PPARγ*. Int J Mol Sci. 2021 Jan 21;22(3):1050.
- Locatelli L, Cazzaniga A, De Palma C, Castiglioni S, Maier JAM. *Mitophagy contributes to endothelial adaptation to simulated microgravity*. FASEB J. 2020 Jan;34(1):1833-1845.
- López-Victorio CJ, Velez-delValle C, Beltrán-Langarica A, Kuri-Harcuch W. *EDF-1 downregulates the CaM/Cn/NFAT signaling pathway during adipogenesis*. Biochem Biophys Res Commun. 2013 Mar 1;432(1):146-51.
- Mai J, Virtue A, Shen J, Wang H, Yang XF. A*n evolving new paradigm: endothelial cells--conditional innate immune cells*. J Hematol Oncol. 2013 Aug 22;6:61.
- Mason D, Donabella PJ, Nnani D, Musteata FM. *Normalized vitamin D metabolite concentrations are better correlated to pharmacological effects than measured concentrations*. Future Sci OA. 2015; 1(4):FSO83.
- Mayers JR, Vander Heiden MG. *Famine versus feast: understanding the metabolism of tumors in vivo*. Trends Biochem Sci. 2015 Mar;40(3):130-40.
- Messaoudii C, Boudier T, Sanchez Sorzano CO, Marco S. *TomoJ: tomography software for three-dimensional reconstruction in transmission electron microscopy*. BMC Bioinformatics. 2007 Aug 6;8:288.
- Meza CA, La Favor JD, Kim DH, Hickner RC. Endothelial Dysfunction: Is There a Hyperglycemia-Induced Imbalance of NOX and NOS? Int J Mol Sci. 2019 Aug 2;20(15):3775.
- Michiels C. *Endothelial cell functions*. J Cell Physiol. 2003 Sep;196(3):430-43.
- Mittal M, Siddiqui MR, Tran K, Reddy SP, Malik AB. Reactive oxygen species in inflammation and tissue injury. Antioxid Redox Signal. 2014 Mar 1;20(7):1126-67.
- Moncada S, Palmer RM, Higgs EA. *Nitric oxide: physiology, pathophysiology, and pharmacology*. Pharmacol Rev. 1991 Jun;43(2):109-42.
- Moore AS, Holzbaur ELF. *Mitochondrial-cytoskeletal interactions: dynamic associations that facilitate network function and remodelling*. Curr Opin Physiol. 2018 Jun;3:94-100.
- Mousa A, Naderpoor N, Teede H, Scragg R, de Courten B. *Vitamin D supplementation for improvement of chronic low-grade inflammation in patients with type 2 diabetes: a systematic review and meta-analysis of randomized controlled trials*. Nutr Rev. 2018 May 1;76(5):380-394.

- Nazimek-Siewniak B, Moczulski D, Grzeszczak W. *Risk of macrovascular and microvascular complications in Type 2 diabetes: results of longitudinal study design*. J Diabetes Complications. 2002 Jul-Aug;16(4):271-6.
- Nguyen TT, Ta QTH, Nguyen TKO, Nguyen TTD, Giau VV. *Type 3 Diabetes and Its Role Implications in Alzheimer's Disease*. Int J Mol Sci. 2020 Apr 30;21(9):3165.
- O'Donnell S, Cranney A, Horsley T, Weiler HA, Atkinson SA, Hanley DA, Ooi DS, Ward L, Barrowman N, Fang M, Sampson M, Tsertsvadze A, Yazdi F. *Efficacy of food fortification on serum 25-hydroxyvitamin D concentrations: systematic review*. Am J Clin Nutr. 2008 Dec;88(6):1528-34.
- Patel P, Abate N. *Body fat distribution and insulin resistance*. Nutrients. 2013 Jun 5;5(6):2019-27.
- Patten IS, Arany Z. *PGC-1 coactivators in the cardiovascular system*. Trends Endocrinol Metab. 2012 Feb;23(2):90-7.
- Piga R, Naito Y, Kokura S, Handa O, Yoshikawa T. *Short-term high glucose exposure induces monocytes-endothelial cells adhesion and transmigration by increasing VCAM-1 and MCP-1 expression in human aortic endothelial cells*. Atherosclerosis. 2007; 193(3): 328-34.
- Pilz S, Verheyen N, Grübler MR, Tomaschitz A, März W. *Vitamin D and cardiovascular disease prevention*. Nat Rev Cardiol. 2016; 13(7): 404-17.
- Pittarella P, Squarzanti DF, Molinari C, Invernizzi M, Uberti F, Renò F. *NO-dependent proliferation and migration induced by Vitamin D in HUVEC*. J Steroid Biochem Mol Biol. 2015 May;149:35-42.
- Psaltis PJ, Harbuzariu A, Delacroix S, Holroyd EW, Simari RD. *Resident vascular progenitor cells--diverse origins, phenotype, and function*. J Cardiovasc Transl Res. 2011 Apr;4(2):161-76.
- Rajendran P, Rengarajan T, Thangavel J, Sakthisekaran D, Sethi G and Nishigaky Y. *The vascular endothelium and human disease*. International Journal of Biological Sciences. 2013.9(10): 1057-1069.
- Rask-Madsen C, King GL. *Vascular complications of diabetes: mechanisms of injury and protective factors*. Cell Metab. 2013 Jan 8;17(1):20-33.
- Regan ER, Aird WC. *Dynamical systems approach to endothelial heterogeneity*. Circ Res. 2012 Jun 22;111(1):110-30.

- Riganti C, Gazzano E, Polimeni M, Aldieri E, Ghigo D. *The pentose phosphate pathway: an antioxidant defense and a crossroad in tumor cell fate*. Free Radic Biol Med. 2012 Aug 1;53(3):421-36.
- Rimann M, Graf-Hausner U. *Synthetic 3D multicellular systems for drug development*. Curr Opin Biotechnol. 2012 Oct;23(5):803-9.
- Rinkoo Dalan, Huiling Liew, Wai Kit Alvin Tan, Daniel E.K. Chew, Melvin Khee-Shing Leow, *Vitamin D and the endothelium: basic, translational and clinical research updates*. IJC Metabolic & Endocrine. 2014(4):4-17.
- Rohlenova K, Veys K, Miranda-Santos I, De Bock K, Carmeliet P. *Endothelial Cell Metabolism in Health and Disease*. Trends Cell Biol. 2018 Mar;28(3):224-236.
- Rubanyi GM, Vanhoutte PM. *Superoxide anions and hyperoxia inactivate endothelium-derived relaxing factor(s)*. American Journal of Physiology. 1986; 250:H822-H827.
- Rueden CT, Schindelin J, Hiner MC, DeZonia BE, Walter AE, Arena ET, Eliceiri KW. *ImageJ2: ImageJ for the next generation of scientific image data*. BMC Bioinformatics. 2017 Nov 29;18(1):529.
- Saheb Sharif-Askari F, Saheb Sharif-Askari N, Halwani R, Abusnana S, Hamoudi R, Sulaiman N. *Low Vitamin D Serum Level Is Associated with HDL-C Dyslipidemia and Increased Serum Thrombomodulin Levels of Insulin-Resistant Individuals*. Diabetes Metab Syndr Obes. 2020 May 12;13:1599-1607.
- Sartoretto SM, Santos FF, Costa BP, Ceravolo GS, Santos-Eichler R, Carvalho MHC, Fortes ZB, Akamine EH. *Involvement of inducible nitric oxide synthase and estrogen receptor ESR2 (ERβ) in the vascular dysfunction in female type 1 diabetic rats*. Life Sci. 2019 Jan 1;216:279-286.
- Saxena G, Chen J, Shalev A. *Intracellular shuttling and mitochondrial function of thioredoxin-interacting protein*. J Biol Chem. 2010 Feb 5;285(6):3997-4005.
- Schneider G, Guttmann P, Heim S, Rehbein S, Mueller F, Nagashima K, Heymann JB, Müller WG, McNally JG. *Three-dimensional cellular ultrastructure resolved by X-ray microscopy*. Nat Methods. 2010 Dec;7(12):985-7.
- Schulz E, Dopheide J, Schuhmacher S, Thomas SR, Chen K, Daiber A, Wenzel P, Münzel T, Keaney JF Jr. *Suppression of the JNK pathway by induction of a metabolic stress response prevents vascular injury and dysfunction*. Circulation. 2008 Sep 23;118(13):1347-57.

- Sena CM, Pereira AM, Seiça R. *Endothelial dysfunction - a major mediator of diabetic vascular disease*. Biochim Biophys Acta. 2013 Dec;1832(12):2216-31.
- Shanmugan N, Reddy MA, Guha M, Natarajan R. *High-glucose-induced expression of proinflammatory cytokine and chemokine genes in monocytic cells*. Diabetes. 2003; 52(5):1256-64.
- Shrestha B, Prasai PK, Kaskas AM, Khanna A, Letchuman V, Letchuman S, Alexander JS, Orr AW, Woolard MD, Pattillo CB. *Differential arterial and venous endothelial redox responses to oxidative stress*. Microcirculation. 2018 Oct;25(7):e12486.
- Šimoliūnas E, Rinkūnaitė I, Bukelskienė Ž, Bukelskienė V. *Bioavailability of Different Vitamin D Oral Supplements in Laboratory Animal Model*. Medicina (Kaunas). 2019 Jun 10;55(6):265.
- Song JW, Munn L.L. *Fluid forces control endothelial sprouting*. Proc. Natl. Acad. Sci. USA. 2011;108:15342–15347.
- Sorrentino A, Nicolás J, Valcárcel R, Chichón FJ, Rosanes M, Avila J, Tkachuk A, Irwin J, Ferrer S, Pereiro E. *MISTRAL: a transmission soft X-ray microscopy beamline for cryo nano-tomography of biological samples and magnetic domains imaging*. J Synchrotron Radiat. 2015 Jul;22(4):1112-7.
- Steinl DC, Kaufmann BA. *Ultrasound imaging for risk assessment in atherosclerosis*. Int J Mol Sci. 2015 Apr 29;16(5):9749-69.
- Stepan JG, London DA, Boyer MI, Calfee RP. *Blood glucose levels in diabetic patients following corticosteroid injections into the hand and wrist*. J Hand Surg Am. 2014; 39(4):706-12.
- Stevenson BR. *Understanding tight junction clinical physiology at the molecular level*. J Clin Invest. 1999 Jul;104(1):3-4.
- Sun J, Ye X, Xie M, Ye J. *Induction of triglyceride accumulation and mitochondrial maintenance in muscle cells by lactate*. Sci Rep. 2016 Sep 20;6:33732.
- Swart KM, Lips P, Brouwer IA, Jorde R, Heymans MW et al. *Effects of vitamin D supplementation on markers for cardiovascular disease and type 2 diabetes: an individual participant data meta-analysis of randomized controlled trials*. Am J Clin Nutr. 2018; 107(6):1043-1053.
- Tabit CE, Chung WB, Hamburg NM, Vita JA. *Endothelial dysfunction in diabetes mellitus: molecular mechanisms and clinical implications*. Rev Endocr Metab Disord. 2010 Mar;11(1):61-74.

- Tabrizchi R. *Ecosinoids and blood vessel structure*. Vasc Health Risk Manag. 2005;1(2):91-2.
- Tang H, Vanderpool RR, Wang J, Yuan JX. *Targeting L-arginine-nitric oxide-cGMP pathway in pulmonary arterial hypertension*. Pulm Circ. 2017 Jul-Sep;7(3):569-571.
- Targosz-Korecka M, Jaglarz M, Malek-Zietek KE, Gregorius A, Zakrzewska A, Sitek B, Rajfur Z, Chlopicki S, Szymonski M. *AFM-based detection of glycocalyx degradation and endothelial stiffening in the db/db mouse model of diabetes*. Sci Rep. 2017 Nov 21;7(1):15951.
- Thomas CC, Philipson LH. *Update on diabetes classification*. Med Clin North Am. 2015; 99(1):1-16.
- Tousoulis D, Kampoli AM, Tentolouris C, Papageorgiou N, Stefanadis C. *The role of nitric oxide on endothelial function*. Curr Vasc Pharmacol. 2012 Jan;10(1):4-18.
- Tsvirkun D, Grichine A, Duperray A, Misbah C, Bureau L. *Microvasculature on a chip: study of the Endothelial Surface Layer and the flow structure of Red Blood Cells*. Sci Rep. 2017 Mar 24;7:45036.
- Valle I, Alvarez-Barrientos A, Arza E, Lamas S, Monsalve M. *PGC-1alpha regulates the mitochondrial antioxidant defense system in vascular endothelial cells*. Cardiovasc Res. 2005 Jun 1;66(3):562-73.
- Van Hinsbergh VW. *Endothelium--role in regulation of coagulation and inflammation*. Semin Immunopathol. 2012 Jan;34(1):93-106.
- Venugopal SK, Devaraj S, Yang T, Jialal I. *Alpha-tocopherol decreases superoxide anion release in human monocytes under hyperglycaemic conditions via inhibition of protein kinase C-alpha*. Diabetes. 2002; 51(10): 3049-54.
- Vila Cuenca M, Ferrantelli E, Meinster E, Pouw SM, Kovačević I, de Menezes RX, Niessen HW, Beelen RHJ, Hordijk PL, Vervloet MG. *Vitamin D Attenuates Endothelial Dysfunction in Uremic Rats and Maintains Human Endothelial Stability*. J Am Heart Assoc. 2018 Sep 4;7(17):e008776.
- Virdis A, Colucci R, Fornai M, Polini A, Daghini E, Duranti E, Ghisu N, Versari D, Dardano A, Blandizzi C, Taddei S, Del Tacca M, Monzani F. *Inducible nitric oxide synthase is involved in endothelial dysfunction of mesenteric small arteries from hypothyroid rats*. Endocrinology. 2009 Feb;150(2):1033-42.
- Wang W, Wang Y, Long J, Wang J, Haudek SB, Overbeek P, Chang BH, Schumacker PT, Danesh FR. *Mitochondrial fission triggered by hyperglycemia is*

mediated by ROCK1 activation in podocytes and endothelial cells. Cell Metab. 2012 Feb 8;15(2):186-200.

- Widlansky ME, Gutterman DD. *Regulation of endothelial function by mitochondrial reactive oxygen species*. Antioxid Redox Signal. 2011 Sep 15;15(6):1517-30.
- Wu-Wong JR. *Potential for vitamin D receptor agonists in the treatment of cardiovascular disease*. Br J Pharmacol. 2009; 158(2): 395-412.
- Yang L, Zhou G, Li M, Li Y, Yang L, Fu Q, Tian Y. *High Glucose Downregulates Connexin 43 Expression and Its Gap Junction and Hemichannel Function in Osteocyte-like MLO-Y4 Cells Through Activation of the p38MAPK/ERK Signal Pathway*. Diabetes Metab Syndr Obes. 2020 Feb 26;13:545-557.
- Yilmaz O, Afsar B, Ortiz A, Kanbay M. *The role of endothelial glycocalyx in health and disease*. Clin Kidney J. 2019 Apr 23;12(5):611-619.
- Yin K, You Y, Swier V, Tang L, Radwan MM, Pandya AN, Agrawal DK. *Vitamin D Protects Against Atherosclerosis via Regulation of Cholesterol Efflux and Macrophage Polarization in Hypercholesterolemic Swine.* Arterioscler Thromb Vasc Biol. 2015 Nov;35(11):2432-42.
- Yu T, Sheu SS, Robotham JL, Yoon Y. Mitochondrial fission mediates high glucose-induced cell death through elevated production of reactive oxygen species. Cardiovasc Res. 2008 Jul 15;79(2):341-51.
- Zhang X, Qin Y, Wan X, Liu H, Lv C, Ruan W, He L, Lu L, Guo X. *Rosuvastatin exerts anti-atherosclerotic effects by improving macrophage-related foam cell formation and polarization conversion via mediating autophagic activities*. J Transl Med. 2021 Feb 10;19(1):62.
- Zhou Y, Zhou X, Wang X. *1,25-Dihydroxyvitamin D_3 prevented allergic asthma in a rat model by suppressing the expression of inducible nitric oxide synthase*. Allergy Asthma Proc. 2008; 29(3): 258-67.

9. LIST OF FIGURES AND TABLES

***Figure 27**: (**A**) Endothelial permeability in HUVEC cultured in the presence or not of VitD was measured as described in the methods and monitored for different time points. The statistical analysis (treated cells vs CTR) was calculated using ANOVA. (**B**) Endothelial permeability was measured in HUVEC exposed to 10% of sera collected from diabetic patients or from healthy donors. In this experiments, HUVEC were cultured in the presence of hyperglycaemicsera but with low levels of VitD in blood (red boxplot, "hypo-VitD"), subsequently supplemented with VitD (yellow boxplot, "+ VitD") in comparison with healthy donors (CTR) and sera with normal levels of VitD (normo-VitD). Data are shown as percentages versus CTR. The results are the mean of 3 experiments performed in triplicates ± SD. * p < 0.05; ** p < 0.01; *** p < 0.001. pp. 61*

***Figure 28**: (**A**) Western blot was performed on cell lysates using specific antibodies against ZO-1 and VE-Cadherin. The relative control loading is shown in the lower panel. Densitometric analysis was performed using Image J Lab software. The results are the mean of 3 experiments performed in triplicates ± SD. * p < 0.05. (**B**) Confocal microscopy was performed on HUVEC stained with ZO-1 and DAPI. (**C**) Confocal microscopy was performed on HUVEC stained with Ve-Cadherin and DAPI. Images were acquired using a 63X objective in oil by a SP8 Leica confocal microscope. The images were processed and analyzed using ImageJ software. Scale bar = 30 µm. pp. 63*

***Figure 29**: (**A**) NOx release was measured by Griess assay in media of HUVEC cultured in different concentrations of glucose for 24h. LPS was used as positive control. (**B**) NOx release was measured by Griess assay in sera from healthy donors or T1D patients. Sera were grouped according to fasting glycaemia in healthy donors (CTR), normo-glycaemic (T1D n.g.) and hyperglycaemicsera (T1D h.g.). (**C**) NOx release was measured by Griess assay in sera from healthy donors or T1D patients. Sera were grouped according to HbA1c levels in healthy donors (CTR), T1D normo-HbA1c and hyper-HbA1c. Data are shown as percentages versus CTR. (**D**) Western blot was performed on cell lysates using specific antibodies against iNOS, eNOS and P-eNOS^{Ser1177}. Actin was used as a marker of loading. Densitometric analysis was performed using Image J Lab software. The results are the mean of 3 experiments performed in triplicates ± SD. * p < 0.05; *** p < 0.001. pp. 66*

***Figure 30**: Real Time PCR was performed on HUVEC transiently silenced with specific siRNA against iNOS (**A**) or eNOS (**B**). Real Time PCR was performed on RNA samples from 3 different experiments. The results are the mean of 3 experiments performed in triplicates ± SD. * p < 0.05; ** p < 0.01. pp. 67*

***Figure 31**: NOx release and endothelial permeability were measured respectively by Griess assay and Transwell permeability assay in media of HUVEC cultured in different concentrations of glucose after the inhibition of eNOS or iNOS. NOx was measured after gene silencing with siRNA eNOS or siRNA iNOS (**A**) or after the administration of the pharmacological inhibitors L-NAME or L-NIL, specific respectively for eNOS or iNOS (**B**). Permeability was evaluated after gene silencing with siRNA eNOS or siRNA iNOS (**C**) or after the administration of the pharmacological inhibitors L-NAME or L-NIL (**D**). A scrambled non silencing sequence was used as a control (–) for silencing. Data are shown as percentages versus CTR. The results are the mean of 3 experiments performed in triplicates ± SD. * p < 0.05; ** p < 0.01; *** p < 0.001. pp. 68*

***Figure 32**: Permeability in HUVEC cultured in medium containing 10% hyperglycaemic T1D or CTR sera after genetic or pharmacological inhibition of iNOS or eNOS. HUVEC were cultured in the presence of sera from healthy donors and T1D patients for 24h after gene silencing (**A**) or in the presence of L-NAME or L-NIL (**B**). A scrambled non-silencing sequence was used as a control (–) for silencing. Data are shown as percentages versus CTR. The results are the mean of 3 experiments performed in triplicates ± SD. ** p < 0.01; *** p < 0.001. pp. 69*

***Figure 33**: (**A**) NOx release was measured by Griess assay in culture media at different time points. Data are shown as percentages versus CTR. (**B**) Endothelial permeability was measured as described in the methods and monitored for different time points. Data are shown as percentages versus CTR. The statistical analysis (treated cells vs CTR) was calculated using ANOVA. The results are the mean of 3 experiments performed in triplicates ± SD. * p < 0.05; ** p < 0.01; *** p < 0.001. pp. 69*

***Figure 34**: (**A**) 3D ultrastructural analysis of HUVEC by synchrotron-based Cryo-SXT. Cells were cultured in medium containing different concentrations of D-glucose for 24h. L-glucose (30 mM) was used as control of osmolarity. In the upper panel, the 2D ultrastructure analysis*

*a representative blot is shown. Densitometric analysis (right panel) was performed using Image J Lab software. (**B**) Lactate production was measured by Lactate-Glo™ Assay according to manufacturer instructions and luminescence was recorded. (**C**) Triglycerides amount was detected by Triglycerides Assay Kit according to manufacturer instructions and the fluorescence was detected at $\lambda_{ex/em}$ = 535/587 nm. Values are expressed as mean ± SD and compared using one-way repeated measures ANOVA. The p-values deriving from multiple pairwise comparisons were corrected by the Bonferroni method. In the figures, * p < 0.05, *** p < 0.001. pp. 76*

***Figure 38**: (**A**, **B**) Western blot was performed on cell lysates using specific antibodies against CPT1A, PPARɣ and EDF1. Actin was used as a marker of loading. The experiments were repeated 3 times and a representative blot is shown. (**C**) Densitometric analysis was performed using Image J Lab software. (**D**) The β-oxidation rate was measured by Fatty Acid Oxidation Assay in living cells as described in the Methods, after the supplementation of VitD or after TXNIP silencing. The FAO activator FCCP (0,625 μM) was used as the positive control. Values represent the means ± SD of triplicate experiments. The significance was calculated vs CTR. The results are the mean of 3 experiments performed in triplicates ± SD. * p < 0.05, ** p < 0.01; *** p < 0.001. pp. 78*

***Figure 39**: (**A**) Triglyceride accumulation was calculated by Triglyceride Quantification Kit as described in the methods. (**B**) Lipid accumulation was detected using fluorescent BODIPY fluorophore and the relative fluorescence was measured using the Varioskan LUX Multimode Microplate Reader (Thermo Fisher Scientific) and normalized on DAPI staining. (**C**) The cells were stained with Oil Red O and, after the images acquisition using FLoid Cell Imaging Station (Thermo Fisher Scientific) (left panel), were solubilized and lipids were quantified by measuring the absorbance at 500 nm using the Varioskan LUX Multimode Microplate Reader (Thermo Fisher Scientific). Absorbance was measured at 500 nm and normalized to the cell number. The results are the mean of 3 experiments performed in triplicates ± SD. * p < 0.05; ** p < 0.01; *** p < 0.001; **** p < 0.0001. pp. 80*

***Figure 40**: (**A**) Western blot was performed on cell lysates using specific antibodies against Actin. The relative control loading is shown in the lower panel. The experiments were repeated 3 times and a representative blot is shown. Densitometric analysis (lower panel) was performed using Image J Lab software. (**B**) Confocal microscopy was performed on*

10. APPENDIX

biomedicines

an Open Access Journal by MDPI

Indexed in: PubMed | CITESCORE 3.6 SCOPUS | IMPACT FACTOR 6.081

CERTIFICATE OF ACCEPTANCE

Certificate of acceptance for the manuscript (**biomedicines-1423576**) titled:

Vitamin D prevents high glucose-induced lipid droplets accumulation in cultured endothelial cells by downregulating TXNIP

Authored by:

Roberta Scrimieri; Alessandra Cazzaniga; Sara Castiglioni; Jeanette Anne Marie Maier

has been accepted in *Biomedicines* (ISSN 2227-9059) on 06 December 2021

MDPI Academic Open Access Publishing since 1996

Basel, December 2021

biomedicines

MDPI

Article

Vitamin D Prevents High Glucose-Induced Lipid Droplets Accumulation in Cultured Endothelial Cells: The Role of Thioredoxin Interacting Protein

Roberta Scrimieri [1,*], Alessandra Cazzaniga [1], Sara Castiglioni [1] and Jeanette A. M. Maier [1,2]

[1] Department of Biomedical and Clinical Sciences "Luigi Sacco", Università di Milano, 20157 Milano, Italy; roberta.scrimieri@unimi.it (R.S.); alessandra.cazzaniga@unimi.it (A.C.); sara.castiglioni@unimi.it (S.C.); jeanette.maier@unimi.it (J.A.M.)

[2] Interdisciplinary Centre for Nanostructured Materials and Interfaces (CIMaINa), Università di Milano, 20133 Milano, Italy

* Correspondence: roberta.scrimieri@unimi.it

Abstract: Vitamin D (VitD) exerts protective effects on the endothelium, which is fundamental for vascular integrity, partly by inhibiting free radical formation. To obtain insights into high glucose level-induced redox imbalance in the endothelium, we exposed cultured human endothelial cells to high levels of glucose and found the upregulation of the Thioredoxin Interacting Protein (TXNIP). We show that increased amounts of TXNIP are responsible for the accumulation of reactive oxygen species and, as a consequence, of lipid droplets. This is associated with increased amounts of triglycerides as the result of increased lipogenesis and reduced fatty acid oxidation. VitD prevents high glucose level-induced TXNIP upregulation. Consistently, VitD rebalances the redox equilibrium, restores normal lipid content, and prevents the accumulation of lipid droplets. Our results highlight TXNIP as one of the targets of VitD in high glucose-cultured endothelial cells and shed some light on the protective effect of VitD on the endothelium.

Keywords: D-glucose; endothelial cell; vitamin D; oxidative stress; lipid metabolism

Citation: Scrimieri, R.; Cazzaniga, A.; Castiglioni, S.; Maier, J.A.M. Vitamin D Prevents High Glucose-Induced Lipid Droplets Accumulation in Cultured Endothelial Cells: the Role of Thioredoxin Interacting Protein. *Biomedicines* **2021**, *9*, x. https://doi.org/10.3390/xxxxx

Academic Editor(s): Giuseppe Murdaca and Sebastiano Gangemi

Received: 12 November 2021
Accepted: 06 December 2021
Published: date

1. Introduction

Vascular endothelial cells (EC) form a quiescent monolayer that coats the inner lumen of all vessels and retains critical functions that are essential to preserve the integrity of the vasculature and, consequently, health [1]. They act as a metabolic interface between the blood and tissues and ensure optimal nutrient and oxygen delivery to all of the tissues [2]. EC are steadily exposed to glucose, which is taken up from the blood, mainly through the glucose transporter 1 (GLUT1). Glucose is partially utilized for endothelial metabolic needs and is also delivered to the surrounding cells and tissues. Rather than shunting glucose to oxidative phosphorylation to maximize adenosine triphosphate (ATP) production, EC rely on glycolysis, which takes place in the cytosol and does not demand oxygen [3]. As a consequence, oxygen is saved to be delivered to the parenchymal tissues, protecting the EC against the accumulation of Reactive Oxygen Species (ROS), which are typically produced during oxidative phosphorylation [4]. Additionally, the high extent of Fatty Acid β-Oxidation (FAO) in quiescent EC makes important contributions to the maintenance of the redox balance [5]. Therefore, EC sustain different metabolic pathways to protect themselves against oxidative stress, which is the root of endothelial dysfunction [6]. It is avowed that high glucose levels are detrimental for the endothelium both in the large vessels as well as in the microvasculature [2]. When fasting, the EC are exposed to about 5 mmol/L (5 mM) D-glucose, a concentration that increases post-prandially and that

remains below 7.8 mmol/L (7.8 mM) in healthy people. The failure to contain post-prandial glucose spikes as well as the chronic increase of glucose in uncontrolled diabetic patients ultimately generate endothelial dysfunction [2], partly through the increased endothelial production of free radicals [7,8], and partly through conducted through metabolic reprogramming [9]. High extracellular glucose boosts glucose uptake and metabolism through different pathways, i.e., the polyol pathway, which promotes oxidative stress by consuming Nicotinamide Adenine Dinucleotide Phosphate Hydrogen (NADPH), and glycolytic side branches, such as the hexosamine and the pentose phosphate pathways [2,10]. Moreover, it also results in the activation of Protein-kinase C (PKC) because diacyl glycerol accumulates in response to high intracellular glucose concentrations [11]. As a result of endothelial-altered metabolism caused by high glucose, advanced glycation end products (AGE), which activate the inflammatory response, are generated. Both PKC activation and AGE formation are implicated in the promotion of oxidative stress in EC that have been exposed to high glucose levels [12]. Far less is known about fatty acid metabolism in EC. FAO plays an important role in endothelial homeostasis both *in vitro* and *in vivo* [13]. It sustains nucleotide synthesis, fuels the tricarboxylic acid cycle and, as mentioned above, contributes to redox homeostasis via the synthesis of NADPH [14]. A particular light has been shed on Carnitine Palmitoyltransferase 1A (CPT1A), a crucial enzyme that converts long-chain acyl-CoAs into long-chain acyl-carnitines, which then enter the mitochondria where FAO takes place [15]. Silencing *CPT1A* in the EC triggers oxidative stress and the overexpression of genes that are involved in controlling redox balance [14].

Remarkably, EC can generate lipid droplets and dynamic cytosolic fat storage compartments [16]. This means that EC can store neutral lipids, which then provide fatty acids to be metabolized in the mitochondria or to be transported to nearby tissues [16]. It is also emerging that lipid droplets are critical components of the cellular stress response, as they protect against lipotoxicity [16]. Lipid supplementation for 24h to cultured EC results in the reversible accumulation of lipid droplets, and similar results were observed in the aortic endothelium of hypertriglyceridemic mice [17].

Beyond its essential role in bone health, Vitamin D (VitD) exerts protective effects on the endothelium. Indeed, VitD deficiency is related to endothelial dysfunction, partially because of the downregulation of the VitD Receptor (VDR) [18]. Consistently, VitD supplementation in VitD-deficient diabetic patients improved endothelial function [19], and a recent systematic review and metanalysis of randomized clinical trials demonstrated that VitD supplementation decreases circulating inflammatory cytokines in patients with altered glucose tolerance [20]. However, another study reported no significant effects of VitD supplementation on endothelial dysfunction [21]. The results that have been obtained *in vitro* sustain a beneficial effect of VitD in the EC. Indeed, in Human Umbilical Vein Endothelial Cells (HUVEC), 1,25$(OH)_2D_3$ (calcitriol), the most active metabolite of VitD, prevents leptin-induced endothelial dysfunction in a VDR-dependent fashion [22]. Moreover, in HUVEC treated with acetoacetate in order to mimic ketosis, VitD inhibits ROS formation and monocyte adhesion [19]. Our study sought to address some fundamental questions on the response of HUVEC to high D-glucose and on the potential protective role of VitD. Initially, we investigated the levels of some pro- and antioxidant proteins. Then, we studied the contribution of oxidative stress in reprogramming lipid metabolism. Finally, we focused on the effects of VitD in protecting HUVEC from oxidative stress, metabolic derangements, and lipid droplet accumulation.

2. Materials and Methods

2.1. Cell Culture

HUVEC were purchased from the American Type Culture Collection (ATCC, Manassas, WV, USA), cultured in medium M199 (Euroclone, Milano, Italy) containing 10% Fetal Bovine Serum (FBS), 1 mM L-Glutamine, 1 mM Sodium Pyruvate, 1 mM Penicillin-

Streptomycin, 5 U/mL Heparin, and 150 µg/mL Endothelial Cell Growth Supplement on collagen-coated dishes (50 µg/mL). The cells were routinely tested for the expression of endothelial markers and were used for 6–7 passages. D-glucose (Sigma-Aldrich, St. Louis, MO, USA) was used at the concentrations of 11.1 mM and 30 mM, and L-glucose (Sigma-Aldrich) was used as a control of osmolarity at the concentration of 30 mM. After testing 1α,25-Dihydroxyvitamin D_3 (VitD) (Sigma-Aldrich) cytotoxicity in a dose-dependent fashion by 3-(4,5-dimethylthiazol-2-yl)-2,5-diphenyl-2H-tetrazolium bromide (MTT) assay (the data are available at the following link https://dataverse.unimi.it/dataverse/biomedicines/ accessed on 30th September 2021), VitD was used at the concentration of 20 nM. Thioredoxin Interacting Protein (TXNIP) was inhibited using small interfering RNAs (siRNAs). Subconfluent cells were transfected with siRNAs targeting *TXNIP* (20 nmol, 5′-AAGCCGTTAGGATCCTGGCT-3′ (Qiagen, Hilden, Germany)). All the non-silenced samples were transfected with a scrambled non-silencing sequence (NS) (20 nmol, Qiagen, cat. n° 1027310) that was used as a control, which produced the same results as the non-transfected samples (data not shown). Lipofectamine RNAiMAX was used as a transfection reagent (Invitrogen, Carlsbad, CA, USA) and was used according to the manufacturer's recommendations. After 6-h, the siRNA transfection medium was replaced with a culture medium with the addition of either 11.1 mM or 30 mM of D-glucose in the presence or not of 20 nM of VitD. In some experiments, N-acetylcysteine (NAC, 5 mM) (Sigma-Aldrich) was used as antioxidant [23], in combination or not with high glucose. All the experiments were performed in triplicate.

2.2. ROS Production

For ROS detection, confluent HUVEC were cultured in a 96-well black plate (Greiner Bio-One, Kremsmunster, Austria) and, at the end of the experiments, they were incubated for 30 min with 10 mM 2′-7′-dichlorofluorescein diacetate (DCFH) solution (Sigma-Aldrich). The DCFH dye emission was monitored at 535 nm (excitation λ = 484 nm) using the Varioskan LUX Multimode Microplate Reader (Thermo Fisher Scientific, Waltham, MA, USA). Then, the cells were fixed in Phosphate Buffered Saline (PBS) containing 3% paraformaldehyde (PFA) and 2% sucrose (pH 7.6) for 30 min and, after extensive washing, the cells were incubated with 4′,6-diamidino-2-phenylindole (DAPI), which was used to stain the nuclei (1:10,000). DAPI florescence ($\lambda_{ex/em}$ = 350/470 nm) was monitored using the Varioskan LUX Multimode Microplate Reader (Thermo Fisher Scientific) and was used to normalize the DCFH dye emission [7]. The results are the mean of three independent experiments performed in triplicate ± SD.

2.3. Triglyceride Quantification

Triglycerides were quantified using a Triglyceride Quantification Kit (Sigma-Aldrich) according to the manufacturer's recommendations. Briefly, triglycerides are broken down into free fatty acids and glycerol, which is then oxidized to generate a fluorescent product ($\lambda_{ex/em}$ = 535/587 nm). Fluorescence was monitored using the Varioskan LUX Multimode Microplate Reader (Thermo Fisher Scientific). Prior to the extraction of the triglycerides, the cells were trypsinized. An aliquot was stained with 0.4% trypan blue solution and were counted using a Luna Automated Cell Counter (Logos Biosystems, Anyang-si, Gyeonggi-do, Korea). The fluorescent results were normalized on the cell number. The results are the mean of three independent experiments that were performed in triplicate ± SD.

2.4. Staining of Neutral Lipids

HUVEC were seeded to detect lipids as well as to perform the MTT assay under the same experimental conditions. Oil Red O Staining was used to detect neutral lipids. After the 24h treatments, the cells were washed three times with PBS, fixed in PFA 10% for 30 min at room temperature, washed once again with PBS, and then stained with 60% filtered

Oil Red O stock solution (Sigma-Aldrich) for 20 min. After extensive washing, the Oil Red O was solubilized in 100% isopropanol, was quantified by measuring the absorbance at 500 nm, and was normalized to the cell number by MTT assay [24,25] after image acquisition using FLoid Cell Imaging Station (Thermo Fisher Scientific). To further confirm the results, staining with BODIPY 493/503 was performed (see dataverse at the following link https://dataverse.unimi.it/dataverse/biomedicines/ accessed on 30th September 2021). The results are the mean of three independent experiments performed in triplicate ± SD.

2.5. Western Blot Analysis

HUVEC were lysed in 50 mM Tris-HCl (pH 7.4) containing 150 mM NaCl, 1% NP40, 0.25% sodium deoxycholate, protease inhibitors (10 μg/mL Leupeptin, 10 μg/mL Aprotinin and 1 mM Phenylmethylsulfonyl fluoride, PMSF), and phosphatase inhibitors (1 mM sodium fluoride, 1 mM sodium vanadate, 5 mM sodium phosphate). Lysates (40 μg/lane) were separated on SDS–PAGE and were transferred to nitrocellulose sheets using the Trans-Blot Turbo Transfer System (Biorad, Hercules, CA, USA.). Western Blot analysis was performed using antibodies against TXNIP (Thermo Fisher Scientific, cat. n° 40–3700, 1:250), Sirtuin 1 (SIRT1) (Thermo Fisher Scientific, cat. n° PA5–17074, 1:1000), Sirtuin 2 (SIRT2) (Millipore, Vimodrone, Italy, cat. n° 09–843, 1:4000), Superoxide-dismutase 2 (SOD2) (BD Transduction Laboratories, Milano, Italy, cat. n° 611580, 1:1000), Heat Shock Protein 70 kilodaltons (HSP70) (Santa Cruz Biotechnology, Dallas, TX, USA, cat. n° sc-1060, 1:200), EDF1 (Aviva Biosciences, San Diego, CA, USA, cat. n° ARP37729_T100, 1:500), PPARɣ (Santa Cruz, cat. n° sc-7196, 1:200), and CPT1A (Thermo Fisher Scientific, cat. n° 15184-1-AP, 1:1000). Actin (Santa Cruz, cat. n° sc-1616, 1:200) was used as the equal loading control. After extensive washing, secondary antibodies labelled with horseradish peroxidase (GE Healthcare, Waukesha, WI, USA) were used. Immunoreactive proteins were detected by the SuperSignal Chemiluminescence Kit (Thermo Fisher Scientific). A representative blot is shown. The densitometric analysis was performed using Image J Lab software (Biorad). The results are the mean of three independent experiments ± SD.

2.6. Fatty Acid Oxidation

FAO, the primary metabolic pathway for the degradation of fatty acids, was monitored by Fatty Acid Oxidation assay (Abcam) in living cells. The cells were seeded in a 96-well black plate (Greiner Bio-One), and upon treatment with high glucose for 24h, they were rinsed twice with pre-warmed Fatty Acid-Free medium followed by the addition of pre-warmed Fatty Acid Measurement Medium. Extracellular O_2 Consumption Reagent (Abcam) was added into all the wells except for the blank control well. The FAO activator carbonyl cyanide-p-trifluoromethoxyphenylhydrazone (FCCP, 0.625 μM) was used as the positive control. Finally, the wells were sealed with pre-warmed high-sensitivity mineral oil. Subsequently, the 96-well black plate was placed into the Varioskan LUX Multimode Microplate Reader (Thermo Fisher Scientific), which had been pre-set to 37 °C. The fluorescent signal ($\lambda_{ex/em}$ = 380/650 nm) was measured every 2 min for 180 min. To simplify the procedure, the results were expressed in a box plot graph. The results are the mean of three independent experiments performed in triplicate ± SD.

2.7. Statistical Analysis

Data are reported as means ± standard deviation (SD). The data were normally distributed, and they were analyzed using the two-way repeated measures ANOVA. The *p*-values deriving from multiple pairwise comparisons were corrected using the Bonferroni method. Statistical significance was defined for *p*-value < 0.05. Concerning the figures, * $p < 0.05$; ** $p < 0.01$; *** $p < 0.001$; **** $p < 0.0001$.

3. Results

3.1. TXNIP Is Upregulated in HUVEC Exposed to High Glucose

To get insights into the mechanisms that are involved in high glucose-triggered oxidative stress, we analysed the levels of some of the proteins that are implicated in the control of redox balance. HUVEC were cultured in media containing physiological (5.5 mM, CTR) or high glucose (11.1 mM and 30 mM) concentrations for 24h. L-glucose (30 mM) was used as a control for osmolarity. As shown in Figure 1, we found a substantial increase in the total amounts of TXNIP. When the cells were cultured at the highest D-glucose concentration (30 mM), we also observed the significant downregulation of SIRT1, the most evolutionarily conserved member of the sirtuin family, which exerts beneficial effects on the endothelium. HSP70, PON2, SIRT2, and SOD2 were not modulated. L-glucose exerted no effects (Figure 1).

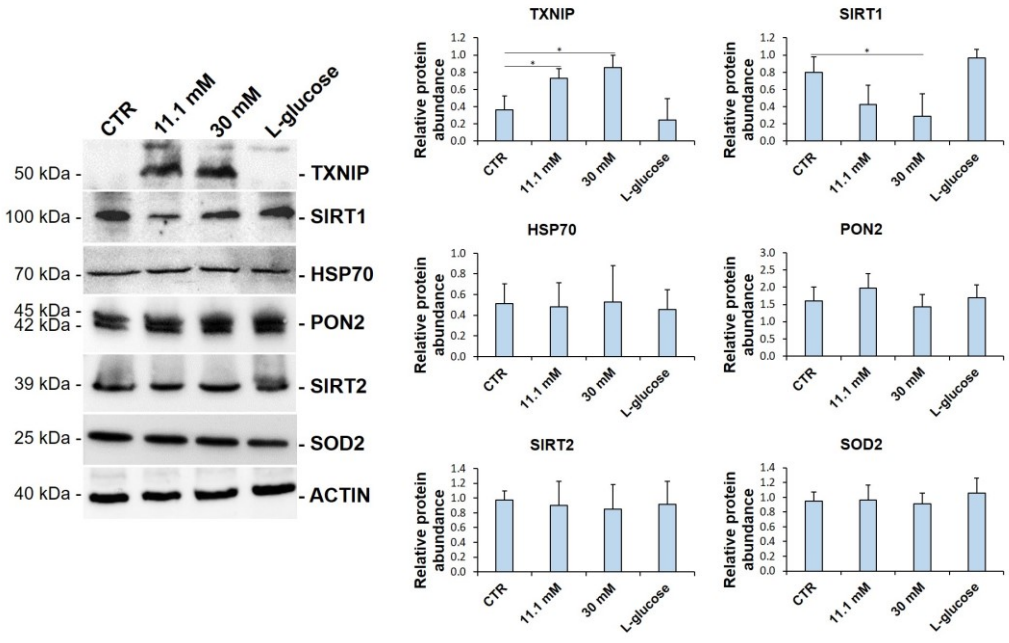

Figure 1. High glucose upregulates TXNIP and downregulates SIRT1 in HUVEC. Western blot (left panel) was performed on cell lysates using specific antibodies against TXNIP, SIRT1, HSP70, PON2, SIRT2, and SOD2. Actin was used as an equal loading control. A representative blot is shown. Densitometric analysis (right panel) was performed using Image J Lab software on three different blots, and the results are the mean of three independent experiments ± SD. * $p < 0.05$.

3.2. TXNIP Upregulation Accounts for ROS Accumulation in HUVEC Cultured in High Glucose

In this paper, we focused on the role of TXNIP upregulation in high glucose-treated HUVEC. For this purpose, we transiently silenced the cells with specific siRNAs targeting *TXNIP*. Then, HUVEC were cultured for 24h in medium containing physiological (5.5 mM, CTR), high-extracellular D-glucose (11.1 mM and 30 mM) or L-glucose (30 mM) as a control. Figure 2A shows that *TXNIP* silencing prevents high glucose-induced TXNIP increases. Moreover, upon *TXNIP* silencing, high glucose-induced ROS production was dampened by the same amount after the administration of the antioxidant NAC (5 mM), the precursor of glutathione that is widely used as an antioxidant (Figure 2B).

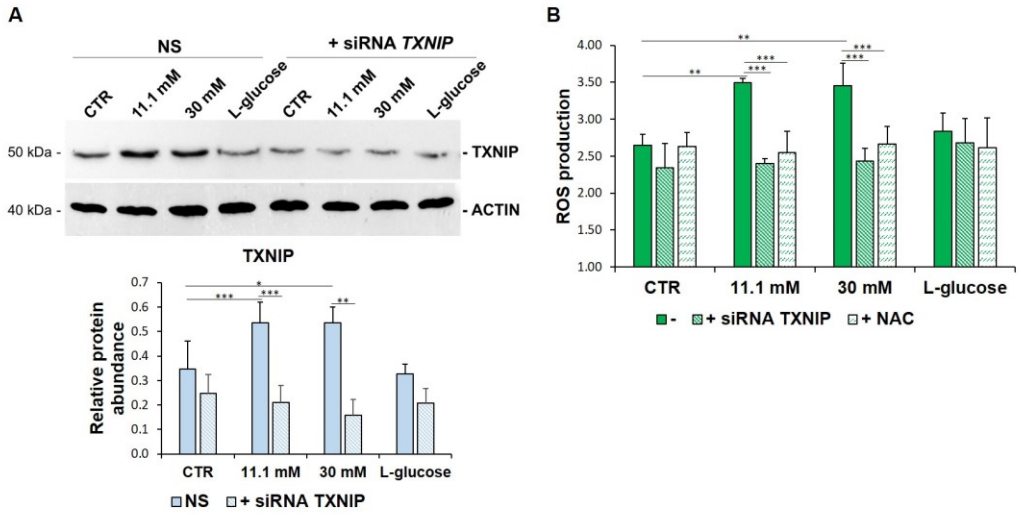

Figure 2. TXNIP upregulation is responsible for ROS accumulation in HUVEC cultured in high glucose levels. (**A**) HUVEC were cultured in medium containing 5 mM (CTR), 11.1 mM or 30 mM of D-glucose after *TXNIP* silencing. A scrambled non-silencing sequence (NS) was used as a control for silencing. Western blot (upper panel) was performed on cell lysates using specific antibodies against TXNIP. Actin was used an equal loading control. A representative blot is shown. Densitometric analysis (lower panel) was performed using Image J Lab software on three different blots, and the results are the mean of three independent experiments ± SD. (**B**) HUVEC were cultured in medium containing 5 mM (CTR), 11.1 mM, or 30 mM of D-glucose (-) and either after *TXNIP* silencing or the addition of NAC 5 mM. L-glucose (30 mM) was used as a control of osmolarity. ROS production was evaluated by DCFH, as described in the methods. The results are the mean of three experiments performed in triplicate ± SD. * $p < 0.05$; ** $p < 0.01$; *** $p < 0.001$.

3.3. VitD Prevents TXNIP Upregulation in HUVEC Cultured in High Glucose

Since (i) TXNIP was initially characterized as a target of VitD and since (ii) VitD exerts a protective effect upon metabolic challenge in HUVEC, we anticipated that VitD might affect the levels of TXNIP found in HUVEC cultured in high glucose conditions. Therefore, we exposed HUVEC to media containing high levels of glucose in the presence or in the absence of VitD (20 nM) for 24h. VitD counters high glucose-induced TXNIP upregulation and ROS accumulation (Figure 3A and 3B).

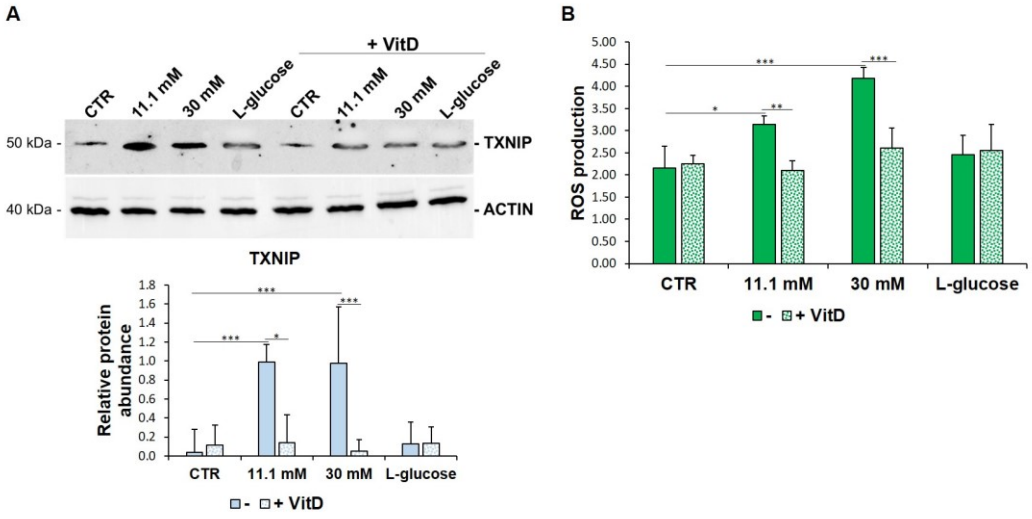

Figure 3. VitD prevents TXNIP upregulation and ROS accumulation in HUVEC cultured in high glucose conditions. (**A**) Western blot (upper panel) was performed on cell lysates using specific antibodies against TXNIP. Actin was used as an equal loading control. A representative blot is shown. Densitometric analysis (lower panel) was performed using Image J Lab software on three different blots, and the results are the mean of three independent experiments ± SD. (**B**) HUVEC were cultured in medium containing 5 mM (CTR), 11.1 mM, or 30 mM of D-glucose in the absence (-) or in the presence of VitD 20 nM. L-glucose (30 mM) was used as a control of osmolarity. ROS production was evaluated by DCFH, as described in the methods. The results are the mean of three experiments performed triplicate ± SD. * $p < 0.05$; ** $p < 0.01$; *** $p < 0.001$.

3.4. VitD Hinders Lipid Droplets Formation in HUVEC Exposed to High Glucose

In several cell types, the accumulation of lipid droplets storing triglycerides is interpreted as an adaptive response to stress. To test whether HUVEC behaves in a similar manner, we initially evaluated the amounts of triglycerides in HUVEC that had been cultured in media containing high levels of glucose. Control and L-glucose-cultured cells contain a certain amount of triglycerides that is dose-dependently increased upon exposure to 11.1 mM and 30 mM of D-glucose for 24h. Moreover, the silencing of *TXNIP* as well as the treatment with VitD reduced the triglyceride amounts to normal physiological levels (Figure 4A).

We then stained HUVEC, exposed to high levels of glucose for 24h, with Oil Red O to detect neutral lipids to analyse the potential role of TXNIP in driving the accumulation of lipids. Moreover, since treatment with VitD downregulates TXNIP, we also treated the cells with VitD. It is noteworthy that, at baseline, HUVEC contain lipid droplets and that high D-glucose levels increase their number. Interestingly, the high glucose-induced deposition of lipids is dampened by *TXNIP* silencing as well as by the addition of VitD (Figure 4B).

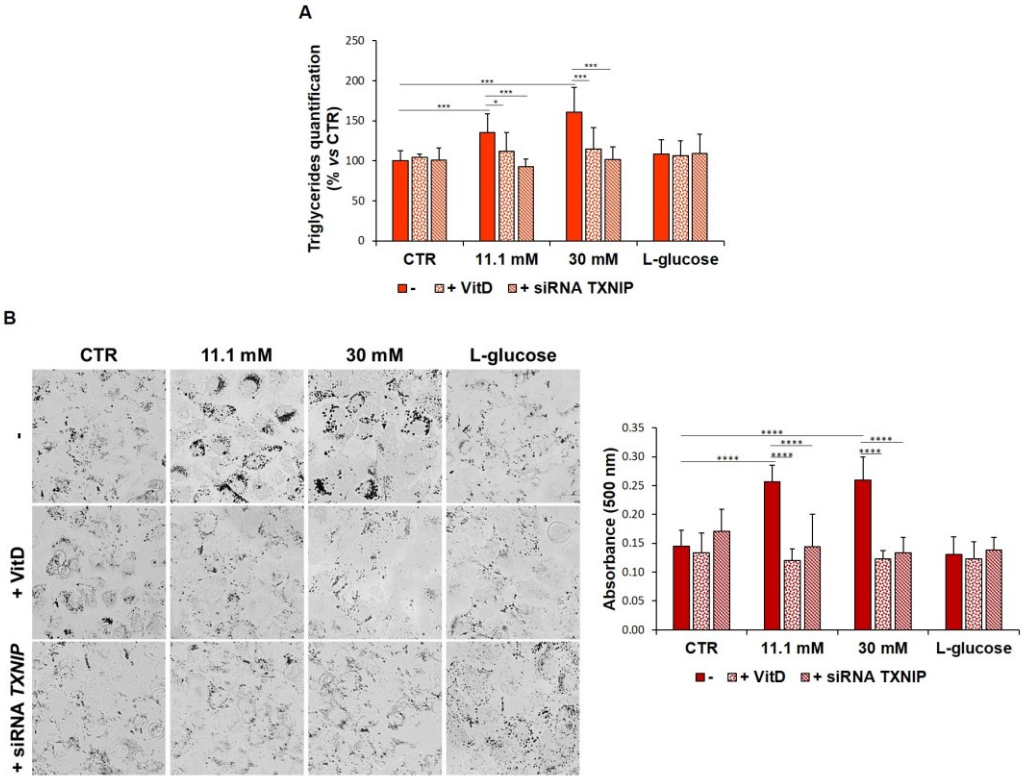

Figure 4. VitD and *TXNIP* silencing prevent high glucose-induced accumulation of triglycerides and lipid droplets. HUVEC were cultured in medium containing 5 mM (CTR), 11.1, or 30 mM of D-glucose (-) and either after *TXNIP* silencing or after the administration of 20 nM VitD. L-glucose (30 mM) was used as a control of osmolarity. (**A**) Triglyceride accumulation was measured by the Triglyceride Quantification Kit, as described in the methods. (**B**) The cells were stained with Oil Red O, and after the image acquisition using the FLoid Cell Imaging Station (Thermo Fisher Scientific) (left panel), the cells were solubilized, and the triglycerides were quantified by measuring the absorbance at 500 nm using the Varioskan LUX Multimode Microplate Reader (Thermo Fisher Scientific) (right panel). The results are the mean of three experiments that were repeated in triplicate ± SD. * $p < 0.05$; *** $p < 0.001$; **** $p < 0.0001$.

3.5. VitD Corrects High Glucose-Induced Imbalance of Lipid Metabolism in HUVEC

To shed some light on the pathways leading to the deposition of triglycerides, we analysed some key markers that have been found to be involved in lipid metabolism. First, we focused our attention on some molecules that are involved in lipogenesis. We analysed the modulation of PPARγ and its transcriptional coactivator EDF1, both of which are required for lipogenesis. In high glucose level-cultured cells, Western blot revealed a significant upregulation of both EDF1 and PPARγ, which was averted by VitD (Figure 5A) and *TXNIP* silencing (Figure 5B). Secondly, we analysed the expression of CPT1A, an enzyme that is located on the mitochondrial membrane and that is involved in the transport of fatty acids into the mitochondria to undergo β-oxidation. The total amount of CPT1A was reduced in the cells that had been cultured in high glucose-containing media, and VitD rescued it to normal levels, as did *TXNIP* silencing (Figure 5A and 5B). This result is in accordance with the decreased β-oxidation rate that was measured in the high glucose–cultured cells, which was recovered in the presence of VitD and after *TXNIP* silencing (Figure 5D).

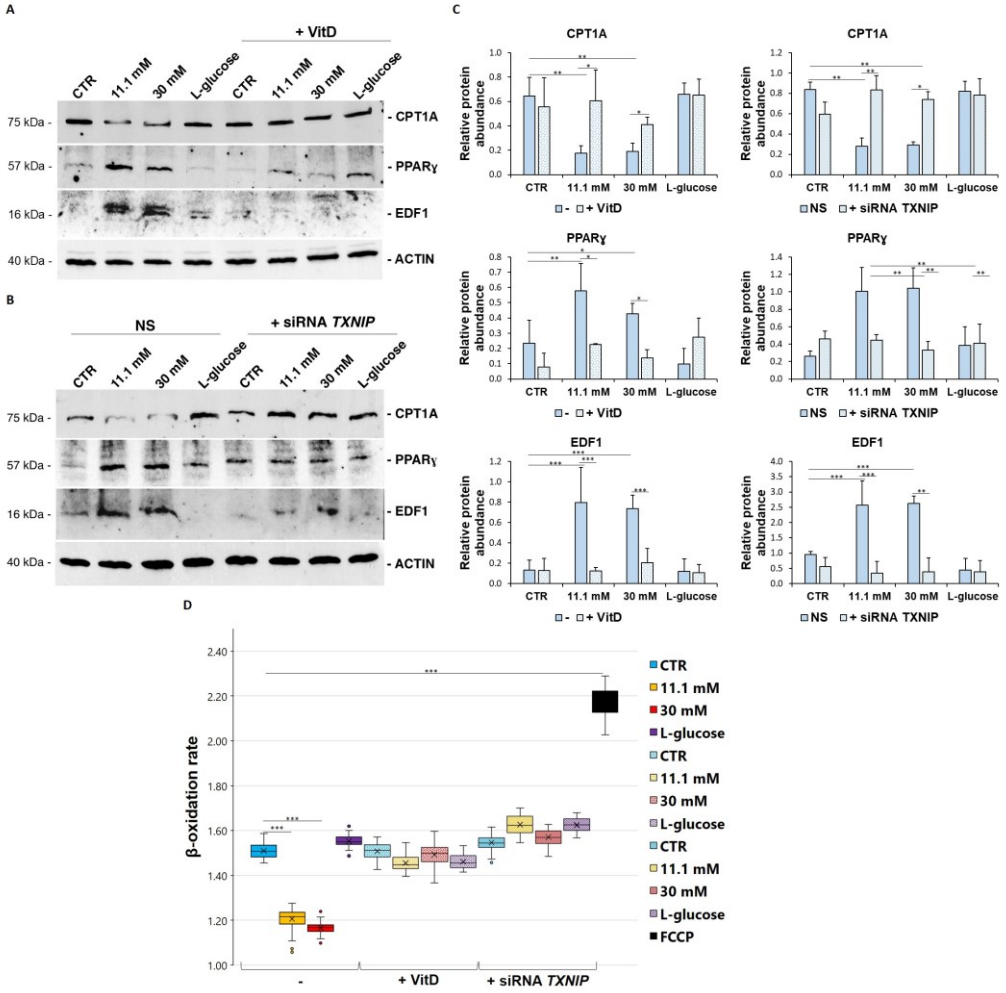

Figure 5. VitD and *TXNIP* silencing restore lipid metabolism in HUVEC cultured in high glucose. HUVEC were cultured in medium containing 5 mM (CTR), 11.1, or 30 mM of D-glucose (-) and either after *TXNIP* silencing or after the administration of 20 nM VitD. L-glucose (30 mM) was used as a control of osmolarity. (**A**,**B**) Western blot was performed on cell lysates using specific antibodies against CPT1A, PPARγ, and EDF1. Actin was used as an equal loading control. A representative blot is shown. (**C**) Densitometric analysis was performed using Image J Lab software on three different blots, and the results are the mean of three independent experiments ± SD. (**D**) The β-oxidation rate was measured using a fatty acid oxidation assay kit, as described in the methods. The results are the mean of three experiments that were conducted in triplicate ± SD. * $p < 0.05$; ** $p < 0.01$; *** $p < 0.001$.

4. Discussion

Observational data have consistently established low serum concentrations of VitD in patients with Type 2 Diabetes Mellitus (T2D). Of note, it seems that the duration of diabetes rather than glycemic control is associated with VitD deficiency [26]. Remarkably, observational studies as well as preclinical data support that low VitD correlates with increased risk of hypertension, atherosclerosis, metabolic disorders, and low-grade inflammation, all of which are conditions that share endothelial dysfunction as a common element [27–29]. Accordingly, through the high-frequency ultrasonographic imaging of the brachial artery to assess endothelium-dependent flow-mediated vasodilation, it was demonstrated that VitD improves endothelial function in VitD-deficient subjects [30] and in patients with T2D and with low serum levels of VitD [31]. These findings prompted us

to investigate the effects of VitD on HUVEC. VitD has been reported to protect HUVEC from hydrogen peroxide-induced oxidative stress by inhibiting superoxide formation as well as to improve antioxidant defenses in HUVEC that have been treated with high concentrations of ketone bodies [19,32]. Here, we show that VitD downregulates TXNIP and, accordingly, mimics the effects of *TXNIP* silencing in HUVEC that have been cultured in high levels of glucose by preventing oxidative stress and by correcting lipid metabolism and storage in lipid droplets.

Despite originally being isolated as a VitD-upregulated protein [33,34], TXNIP is differently regulated by VitD in various cell types [35]. Cell specificity in the modulation of the response to VitD is described, and the downregulation of TXNIP after exposure to VitD seems to occur in cells harboring wild type p53 [35], as HUVEC do. Elevated TXNIP is implicated in the pathogenesis of various complex diseases, including diabetes and neurologic and inflammatory disorders [36]. This is not surprising since TXNIP regulates lipid and glucose metabolism both dependently and independently from the inhibition of thioredoxin (TRX) [36]. Focusing on the endothelium, TXNIP is overexpressed in the vascular EC of many vessels in hypertensive rats and contributes to oxidative stress and endothelial dysfunction in hypertension [7,37,38]. It is upregulated in the aortic endothelium of diabetic rats and in human aortic EC that have been cultured in high levels of glucose, associated with dysfunction in both cases [38]. Interesting results were obtained in endothelial TXNIP knockout mice under metabolic stress since the aorta was protected from damage through anti-oxidant and anti-inflammatory mechanisms [39]. Additionally, long non-coding RNAs (lnc), which disrupt the stability of the target protein, are involved in the regulation of TXNIP. Indeed, a recent report showed that high glucose-treated HUVEC downregulate lnc-SNHG15, which reduces TXNIP expression by enhancing its ubiquitination [40], thus mitigating high glucose-induced endothelial dysfunction. Our results are in keeping with the increasing evidence pointing to upregulated TXNIP as a player in endothelial dysfunction in response to high glucose levels. Indeed, we found that the downregulation of *TXNIP* by specific siRNAs reduces oxidative stress and the accumulation of triglycerides in lipid droplets in HUVEC.

Lipid droplets are intracellular organelles that store neutral lipids and have been detected in many eukaryotic cell types and have been interpreted as an adaptation mechanism under metabolic stress [16,17]. Interestingly, they are very abundant in the EC lining of mammalian atheromas and in cultured EC that have been exposed to hypercholesterolemic serum [41]. A seminal paper showed the prompt formation of lipid droplets in intact murine aortic EC *in vivo* and *ex vivo* after a load of fatty acid [17]. This study suggests that beyond being an energy resource, endothelial lipid droplets represent a defense mechanism against lipotoxicity. Here, we show that 24h culture in media containing high levels of glucose results in lipid droplet accumulation in HUVEC. To get insights into the involved mechanisms, we evaluated the amounts of PPARγ and its transcriptional coactivator EDF1. PPARγ is a ligand-activated transcription factor that is able to exert a broad spectrum of biological functions, including fatty acid handling and storage [42]. EDF1 is a low molecular weight protein that shuttles between the cytosol and the nucleus in response to environmental challenge [43] and is induced in HUVEC that have been exposed to oxidative stress [25]. When nuclear, it functions as a transcriptional coactivator for PPARγ [24,44]. HUVEC cultured in the presence of high glucose upregulate both PPARγ and EDF1. We hypothesize that the activation of the EDF1/PPARγ axis might fuel fatty acid synthesis in HUVEC. A similar conclusion was reached in HUVEC that had been cultured in a medium containing low levels of magnesium [25], thus suggesting that lipid accumulation is a common feature in EC exposed to metabolic stress. Moreover, culture in high glucose downregulates CPT1A, which consequently impairs lipid transport to the mitochondria. Accordingly, FAO is reduced in HUVEC that have been exposed to high amounts of glucose. We propose that the formation of lipid droplets in response to high amounts of glucose results from an imbalance between the synthesis and oxidation of fatty acids.

Whether lipid droplet-derived fatty acids are used as substrates for energy metabolism or for protection against lipoperoxidation in our experimental model remains to be elucidated. Other interesting aspects that we plan to investigate are the dynamics and the fate of these organelles. Moreover, a topic that we only mentioned briefly but that deserves more attention is the reason why SIRT1 appeared to be downregulated in our experimental setting. For this purpose, we recall that SIRT1 exerts beneficial effects on the endothelium, and consistently, antidiabetic drugs, anti-oxidants, and anti-inflammatory agents increase its amounts [45,46].

In conclusion, we identified TXNIP as one of the targets of VitD in HUVEC cultured in media containing high amounts of glucose. Therefore, VitD might represent a serviceable tool that can be used to control redox equilibrium with the aim of limiting or, at least, of delaying the onset of high glucose-induced endothelial dysfunction.

Author Contributions: Conceptualization, R.S. and J.A.M.; methodology, R.S. and A.C.; formal analysis, R.S.; resources, J.A.M.; writing—original draft preparation, R.S. and J.A.M.; writing—review and editing, J.A.M., R.S., and S.C.; supervision, J.A.M. and S.C.; funding acquisition, J.A.M. All authors have read and agreed to the published version of the manuscript.

Funding: This research was funded, in part, by Regione Lombardia, PRINTMED.

Data Availability Statement: Data are available in a publicly accessible repository. The data presented in this study are openly available in Dataverse at the following link: https://dataverse.unimi.it/dataverse/biomedicines/ accessed on 30th September 2021.

Conflicts of Interest: The authors declare no conflicts of interest.

References

1. Cahill, P.A.; Redmond, E.M. Vascular endothelium—Gatekeeper of vessel health. *Atherosclerosis* **2016**, *248*, 97–109. https://doi.org/10.1016/j.atherosclerosis.2016.03.007.
2. Clyne, A.M. Endothelial response to glucose: Dysfunction, metabolism, and transport. *Biochem. Soc. Trans.* **2021**, *49*, 313–325. https://doi.org/10.1042/BST20200611.
3. Dumas, S.J.; García-Caballero, M.; Carmeliet, P. Metabolic Signatures of Distinct Endothelial Phenotypes. *Trends Endocrinol. Metab.* **2020**, *31*, 580–595. https://doi.org/10.1016/j.tem.2020.05.009.
4. Eelen, G.; de Zeeuw, P.; Treps, L.; Harjes, U.; Wong, B.W.; Carmeliet, P. Endothelial Cell Metabolism. *Physiol. Rev.* **2018**, *98*, 3–58. https://doi.org/10.1152/physrev.00001.2017.
5. Kalucka, J.; Bierhansl, L.; Conchinha, N.V.; Missiaen, R.; Elia, I.; Brüning, U.; Scheinok, S.; Treps, L.; Cantelmo, A.R.; Dubois, C.; et al. Quiescent Endothelial Cells Upregulate Fatty Acid β-Oxidation for Vasculoprotection via Redox Homeostasis. *Cell Metab.* **2018**, *28*, 881–894.e13. https://doi.org/10.1016/j.cmet.2018.07.016.
6. Falkenberg, K.D.; Rohlenova, K.; Luo, Y.; Carmeliet, P. The metabolic engine of endothelial cells. *Nat. Metab.* **2019**, *1*, 937–946. https://doi.org/10.1038/s42255-019-0117-9.
7. Scrimieri, R.; Locatelli, L.; Cazzola, R.; Maier, J.A.M.; Cazzaniga, A. Reactive oxygen species are implicated in altering magnesium homeostasis in endothelial cells exposed to high glucose. *Magnes. Res.* **2019**, *32*, 54–62. https://doi.org/10.1684/mrh.2019.0456.
8. Giacco, F.; Brownlee, M. Oxidative stress and diabetic complications. *Circ. Res.* **2010**, *107*, 1058–1070. https://doi.org/10.1161/CIRCRESAHA.110.223545.
9. Theodorou, K.; Boon, R.A. Endothelial Cell Metabolism in Atherosclerosis. *Front. Cell Dev. Biol.* **2018**, *6*, 82. https://doi.org/10.3389/fcell.2018.00082.
10. Eelen, G.; de Zeeuw, P.; Simons, M.; Carmeliet, P. Endothelial cell metabolism in normal and diseased vasculature. *Circ. Res.* **2015**, *116*, 1231–1244. https://doi.org/10.1161/CIRCRESAHA.116.302855.
11. Kolczynska, K.; Loza-Valdes, A.; Hawro, I.; Sumara, G. Diacylglycerol-evoked activation of PKC and PKD isoforms in regulation of glucose and lipid metabolism: A review. *Lipids Health Dis.* **2020**, *19*, 113. https://doi.org/10.1186/s12944-020-01286-8.
12. Tumova, S.; Kerimi, A.; Porter, K.E.; Williamson, G. Transendothelial glucose transport is not restricted by extracellular hyperglycaemia. *Vascul. Pharmacol.* **2016**, *87*, 219–229. https://doi.org/10.1016/j.vph.2016.11.001.
13. Xiong, J.; Kawagishi, H.; Yan, Y.; Liu, J.; Wells, Q.S.; Edmunds, L.R.; Fergusson, M.M.; Yu, Z.-X.; Rovira, I.I.; Brittain, E.L.; et al. A Metabolic Basis for Endothelial-to-Mesenchymal Transition. *Mol. Cell* **2018**, *69*, 689–698.e7. https://doi.org/10.1016/j.molcel.2018.01.010.

14. Schoors, S.; Bruning, U.; Missiaen, R.; Queiroz, K.C.; Borgers, G.; Elia, I.; Zecchin, A.; Cantelmo, A.R.; Christen, S.; Goveia, J.; et al. Fatty acid carbon is essential for dNTP synthesis in endothelial cells. *Nature* **2015**, *520*, 192–197. https://doi.org/10.1038/nature14362.
15. Lai, C.-Q.; Parnell, L.D.; Smith, C.E.; Guo, T.; Sayols-Baixeras, S.; Aslibekyan, S.; Tiwari, H.K.; Irvin, M.R.; Bender, C.; Fei, D.; et al. Carbohydrate and fat intake associated with risk of metabolic diseases through epigenetics of CPT1A. *Am. J. Clin. Nutr.* **2020**, *112*, 1200–1211. https://doi.org/10.1093/ajcn/nqaa233.
16. Jarc, E.; Petan, T. Lipid Droplets and the Management of Cellular Stress. *Yale J. Biol. Med.* **2019**, *92*, 435–452.
17. Kuo, A.; Lee, M.Y.; Sessa, W.C. Lipid Droplet Biogenesis and Function in the Endothelium. *Circ. Res.* **2017**, *120*, 1289–1297. https://doi.org/10.1161/CIRCRESAHA.116.310498.
18. Jablonski, K.L.; Chonchol, M.; Pierce, G.L.; Walker, A.E.; Seals, D.R. 25-Hydroxyvitamin D deficiency is associated with inflammation-linked vascular endothelial dysfunction in middle-aged and older adults. *Hypertens* **2011**, *57*, 63–69. https://doi.org/10.1161/HYPERTENSIONAHA.110.160929.
19. Kanikarla-Marie, P.; Jain, S.K. 1,25(OH)$_2$D$_3$ inhibits oxidative stress and monocyte adhesion by mediating the upregulation of GCLC and GSH in endothelial cells treated with acetoacetate (ketosis). *J. Steroid Biochem. Mol. Biol.* **2016**, *159*, 94–101. https://doi.org/10.1016/j.jsbmb.2016.03.002.
20. Dashti, F.; Mousavi, S.M.; Larijani, B.; Esmaillzadeh, A. The effects of vitamin D supplementation on inflammatory biomarkers in patients with abnormal glucose homeostasis: A systematic review and meta-analysis of randomized controlled trials. *Pharmacol. Res.* **2021**, *170*, 105727. https://doi.org/10.1016/j.phrs.2021.105727.
21. Pincombe, N.L.; Pearson, M.J.; Smart, N.A.; King, N.; Dieberg, G. Effect of vitamin D supplementation on endothelial function—An updated systematic review with meta-analysis and meta-regression. *Nutr. Metab. Cardiovasc. Dis.* **2019**, *29*, 1261–1272. https://doi.org/10.1016/j.numecd.2019.08.005.
22. Teixeira, T.M.; da Costa, D.C.; Resende, A.C.; Soulage, C.O.; Bezerra, F.F.; Daleprane, J.B. Activation of Nrf2-Antioxidant Signaling by 1,25-Dihydroxycholecalciferol Prevents Leptin-Induced Oxidative Stress and Inflammation in Human Endothelial Cells. *J. Nutr.* **2017**, *147*, 506–513. https://doi.org/10.3945/jn.116.239475.
23. Pedre, B.; Barayeu, U.; Ezeriņa, D.; Dick, T.P. The mechanism of action of N-acetylcysteine (NAC): The emerging role of H(2)S and sulfane sulfur species. *Pharmacol. Ther.* **2021**, *228*, 107916. https://doi.org/10.1016/j.pharmthera.2021.107916.
24. Leidi, M.; Mariotti, M.; Maier, J.A.M. Transcriptional coactivator EDF-1 is required for PPARgamma-stimulated adipogenesis. *Cell. Mol. Life Sci.* **2009**, *66*, 2733–2742. https://doi.org/10.1007/s00018-009-0069-4.
25. Locatelli, L.; Fedele, G.; Castiglioni, S.; Maier, J.A. Magnesium Deficiency Induces Lipid Accumulation in Vascular Endothelial Cells via Oxidative Stress-The Potential Contribution of EDF-1 and PPARγ. *Int. J. Mol. Sci.* **2021**, *22*, 1050. https://doi.org/10.3390/ijms22031050.
26. Alaidarous, T.A.; Alkahtani, N.M.; Aljuraiban, G.S.; Abulmeaty, M.M.A. Impact of the Glycemic Control and Duration of Type 2 Diabetes on Vitamin D Level and Cardiovascular Disease Risk. *J. Diabetes Res.* **2020**, *2020*, 8431976. https://doi.org/10.1155/2020/8431976.
27. Mousa, A.; Naderpoor, N.; Teede, H.; Scragg, R.; de Courten, B. Vitamin D supplementation for improvement of chronic low-grade inflammation in patients with type 2 diabetes: A systematic review and meta-analysis of randomized controlled trials. *Nutr. Rev.* **2018**, *76*, 380–394. https://doi.org/10.1093/nutrit/nux077.
28. Bouillon, R.; Manousaki, D.; Rosen, C.; Trajanoska, K.; Rivadeneira, F.; Richards, J.B. The health effects of vitamin D supplementation: Evidence from human studies. *Nat. Rev. Endocrinol.* **2021**, *2021*, 1–15. https://doi.org/10.1038/s41574-021-00593-z.
29. Saheb Sharif-Askari, F.; Saheb Sharif-Askari, N.; Halwani, R.; Abusnana, S.; Hamoudi, R.; Sulaiman, N. Low Vitamin D Serum Level Is Associated with HDL-C Dyslipidemia and Increased Serum Thrombomodulin Levels of Insulin-Resistant Individuals. *Diabetes Metab. Syndr. Obes.* **2020**, *13*, 1599–1607. https://doi.org/10.2147/DMSO.S245742.
30. Tarcin, O.; Yavuz, D.G.; Ozben, B.; Telli, A.; Ogunc, A.V.; Yuksel, M.; Toprak, A.; Yazici, D.; Sancak, S.; Deyneli, O.; et al. Effect of vitamin D deficiency and replacement on endothelial function in asymptomatic subjects. *J. Clin. Endocrinol. Metab.* **2009**, *94*, 4023–4030. https://doi.org/10.1210/jc.2008-1212.
31. Sugden, J.A.; Davies, J.I.; Witham, M.D.; Morris, A.D.; Struthers, A.D. Vitamin D improves endothelial function in patients with Type 2 diabetes mellitus and low vitamin D levels. *Diabet. Med.* **2008**, *25*, 320–325. https://doi.org/10.1111/j.1464-5491.2007.02360.x.
32. Uberti, F.; Lattuada, D.; Morsanuto, V.; Nava, U.; Bolis, G.; Vacca, G.; Squarzanti, D.F.; Cisari, C.; Molinari, C. Vitamin D protects human endothelial cells from oxidative stress through the autophagic and survival pathways. *J. Clin. Endocrinol. Metab.* **2014**, *99*, 1367–1374. https://doi.org/10.1210/jc.2013-2103.
33. Chung, J.W.; Jeon, J.-H.; Yoon, S.-R.; Choi, I. Vitamin D3 upregulated protein 1 (VDUP1) is a regulator for redox signaling and stress-mediated diseases. *J. Dermatol.* **2006**, *33*, 662–669. https://doi.org/10.1111/j.1346-8138.2006.00156.x.
34. Chen, K.S.; DeLuca, H.F. Isolation and characterization of a novel cDNA from HL-60 cells treated with 1,25-dihydroxyvitamin D-3. *Biochim. Biophys. Acta* **1994**, *1219*, 26–32. https://doi.org/10.1016/0167-4781(94)90242-9.
35. Abu El Maaty, M.A.; Almouhanna, F.; Wölfl, S. Expression of TXNIP in Cancer Cells and Regulation by 1,25(OH)$_2$D$_3$: Is It Really the Vitamin D$_3$ Upregulated Protein? *Int. J. Mol. Sci.* **2018**, *19*, 796. https://doi.org/10.3390/ijms19030796.
36. Qayyum, N.; Haseeb, M.; Kim, M.S.; Choi, S. Role of Thioredoxin-Interacting Protein in Diseases and Its Therapeutic Outlook. *Int. J. Mol. Sci.* **2021**, *22*, 2754. https://doi.org/10.3390/ijms22052754.

37. Wang, R.; Guo, Y.; Li, L.; Luo, M.; Peng, L.; Lv, D.; Cheng, Z.; Xue, Q.; Wang, L.; Huang, J. Role of thioredoxin-interacting protein in mediating endothelial dysfunction in hypertension. *Genes Dis.* **2020**, 1–13. https://doi.org/10.1016/j.gendis.2020.08.008.
38. Li, X.; Kover, K.L.; Heruth, D.P.; Watkins, D.J.; Guo, Y.; Moore, W.V.; He, L.G.; Zang, M.; Clements, M.A.; Yan, Y. Thioredoxin-interacting protein promotes high-glucose-induced macrovascular endothelial dysfunction. *Biochem. Biophys. Res. Commun.* **2017**, *493*, 291–297. https://doi.org/10.1016/j.bbrc.2017.09.028.
39. Bedarida, T.; Domingues, A.; Baron, S.; Ferreira, C.; Vibert, F.; Cottart, C.-H.; Paul, J.-L.; Escriou, V.; Bigey, P.; Gaussem, P.; et al. Reduced endothelial thioredoxin-interacting protein protects arteries from damage induced by metabolic stress in vivo. *FASEB J. Off. Publ. Fed. Am. Soc. Exp. Biol.* **2018**, *32*, 3108–3118. https://doi.org/10.1096/fj.201700856RRR.
40. Zhu, Q.-Q.; Lai, M.-C.; Chen, T.-C.; Wang, X.; Tian, L.; Li, D.-L.; Wu, Z.-H.; Wang, X.-H.; He, Y.-Y.; He, Y.-Y.; et al. LncRNA SNHG15 relieves hyperglycemia-induced endothelial dysfunction via increased ubiquitination of thioredoxin-interacting protein. *Lab. Invest.* **2021**, *101*, 1142–1152. https://doi.org/10.1038/s41374-021-00614-5.
41. Simionescu, M. Implications of early structural-functional changes in the endothelium for vascular disease. *Arterioscler. Thromb. Vasc. Biol.* **2007**, *27*, 266–274. https://doi.org/10.1161/01.ATV.0000253884.13901.e4.
42. Plutzky, J. The PPAR-RXR transcriptional complex in the vasculature: Energy in the balance. *Circ. Res.* **2011**, *108*, 1002–1016. https://doi.org/10.1161/CIRCRESAHA.110.226860.
43. Ballabio, E.; Mariotti, M.; De Benedictis, L.; Maier, J.A.M. The dual role of endothelial differentiation-related factor-1 in the cytosol and nucleus: Modulation by protein kinase A. *Cell. Mol. Life Sci.* **2004**, *61*, 1069–1074. https://doi.org/10.1007/s00018-004-4016-0.
44. Brendel, C.; Gelman, L.; Auwerx, J. Multiprotein bridging factor-1 (MBF-1) is a cofactor for nuclear receptors that regulate lipid metabolism. *Mol. Endocrinol.* **2002**, *16*, 1367–1377. https://doi.org/10.1210/mend.16.6.0843.
45. Pal, P.B.; Sonowal, H.; Shukla, K.; Srivastava, S.K.; Ramana, K.V. Aldose reductase regulates hyperglycemia-induced HUVEC death via SIRT1/AMPK-α1/mTOR pathway. *J. Mol. Endocrinol.* **2019**, *63*, 11–25. https://doi.org/10.1530/JME-19-0080.
46. Chen, Y.; Wang, Y.; Jiang, Y.; Zhang, X.; Sheng, M. High-glucose treatment regulates biological functions of human umbilical vein endothelial cells via Sirt1/FOXO3 pathway. *Ann. Transl. Med.* **2019**, *7*, 199. https://doi.org/10.21037/atm.2019.04.29.

International Journal of
Molecular Sciences

MDPI

Article

Endothelial Hyper-Permeability Induced by T1D Sera Can be Reversed by iNOS Inactivation

Alessandra Cazzaniga [1,*,†], Roberta Scrimieri [1,†], Elisa Giani [2], Gian Vincenzo Zuccotti [1,‡] and Jeanette A. M. Maier [1,‡]

[1] Department of Biomedical and Clinical Sciences "Luigi Sacco", Università di Milano, 20157 Milan, Italy; roberta.scrimieri@unimi.it (R.S.); patgen@unimi.it (G.V.Z.); jeanette.maier@unimi.it (J.A.M.M.)
[2] Humanitas Clinical and Research Center, 20089 Rozzano, Italy; generalepatologia@gmail.com
* Correspondence: alessandra.cazzaniga@unimi.it; Tel.: +39-025-031-9660
† These authors contributed equally to this work.
‡ These authors contributed equally to this work.

Received: 12 March 2020; Accepted: 14 April 2020; Published: 17 April 2020

Abstract: Type 1 Diabetes Mellitus (T1D) is associated with accelerated atherosclerosis that is responsible for high morbidity and mortality. Endothelial hyperpermeability, a feature of endothelial dysfunction, is an early step of atherogenesis since it favours intimal lipid uptake. Therefore, we tested endothelial leakage by loading the sera from T1D patients onto cultured human endothelial cells and found it increased by hyperglycaemic sera. These results were phenocopied in endothelial cells cultured in a medium containing high concentrations of glucose, which activates inducible nitric oxide synthase with a consequent increase of nitric oxide. Inhibition of the enzyme prevented high glucose-induced hyperpermeability, thus pointing to nitric oxide as the mediator involved in altering the endothelial barrier function. Since nitric oxide is much higher in sera from hyperglycaemic than normoglycaemic T1D patients, and the inhibition of inducible nitric oxide synthase prevents sera-dependent increased endothelial permeability, this enzyme might represent a promising biochemical marker to be monitored in T1D patients to predict alterations of the vascular wall, eventually promoting intimal lipid accumulation.

Keywords: endothelial cells; permeability; diabetes mellitus type 1; nitric oxide

1. Introduction

Type 1 Diabetes Mellitus (T1D) is a multifactorial disease characterized by chronic hyperglycaemia that arises from a T cell-mediated autoimmune attack of the pancreatic β-cells and culminates with the suppression of insulin production [1]. The worldwide incidence is rising by 3% per year and the major risk of mortality is due to cardiovascular complications caused by accelerated atherosclerosis [2,3]. Since the endothelium is the gate-keeper of vascular health, it is not surprising that endothelial dysfunction is the early event leading to the development of atherosclerotic lesions [4]. Non-laminar flow, metabolic challenge and inflammatory cytokines model endothelial function [5].In particular,, hyperglycaemia contributes to macrovascular endothelial dysfunction in T1D by activating multiple pathways through the accumulation of free radicals and glycolytic intermediates, among others [6]. Accordingly, a high percentage of paediatric patients with T1D shows endothelial dysfunction [7] strictly associated with poor glycaemic control. However, the mechanisms underlying the insurgence of cardiovascular damage in patients with T1D are not entirely known and, more importantly, there are no biomarkers for an early diagnosis. In vivo, endothelial dysfunction is defined by the inability of the artery to sufficiently dilate in response to a transient reduction of flow and is considered an indirect measure of nitric oxide (NO) released by the endothelium [8]. Considering in vivo, endothelial

dysfunction is defined by altered NO synthesis, increased expression of inflammatory molecules, exaggerated generation of reactive oxygen species (ROS) and enhanced permeability of the cell layer [9].

NO is a simple molecule with complex biological activities. It is implicated in the regulation of many physiological pathways and it is a key player of vascular health, contributing to the maintenance of vascular tone and exerting anti-platelet, anti-thrombotic and anti-inflammatory properties [10]. Under physiological conditions, NO generated by endothelial NO Synthase (eNOS) represents the main source of circulating NO [11]. However, NO can be produced in excess in several clinical conditions, such as inflammation, when inducible NOS (iNOS) is activated by inflammatory stimuli. While low levels of NO are beneficial to harmonize coagulation, inflammation and vascular tone, high levels of NO exert detrimental effects, among which is a reversible increase of endothelial permeability [12], a relevant early event in atherogenesis.

In vivo NO is oxidized to the stable NO products nitrate and nitrite (NOx). A causal relationship between NO and plasma levels of NOx exists to the point that NOx plasma measurements reflect NO bioavailability [13]. Circulating high levels of NO have been reported in T1D patients [14,15] as well as in diabetic rats [16]. A recent meta-analysis discloses a significant increase in NOx levels in European T1D patients [17]. Interestingly, the high concentration of NO observed in the serum of paediatric T1D patients is responsible for mediating hyperfiltration and persistent microalbuminuria, thus linking vascular to glomerular dysfunction in hyperglycaemic conditions [14]. The increment of NO could be due to the induction of iNOS in phagocytes in response to the release of pro-inflammatory cytokines [15]. Moreover, an iNOS-induced elevation of circulating NO seems to be strictly correlated with insulin-resistant states [18].

On these bases, we measured NOx levels in the sera from 36 T1D paediatric patients and 14 healthy controls. Next, we evaluated the effects of these sera on endothelial permeability.

2. Results

2.1. Serum NOx Levels and Endothelial Permeability Are Not Associated with Increased Glycated Haemoglobin in T1D Subjects

Since the half-life of NO in the circulation is shorter than 0.1 s, circulating NO metabolites are assessed as indicators of NO production [13]. We utilized the Griess assay, a method widely used in epidemiologic studies [19], to measure NOx in the serum from healthy and T1D subjects. We initially grouped the sera from our T1D patients according to normal or high levels of glycated haemoglobin (HbA1c), the surrogate biochemical marker of the average glycaemia over a preceding period of 2–3 months. We detected statistically significant higher amounts of NOx in the sera from T1D patients, independently from the levels of HbA1c (Figure 1A). We then cultured HUVEC with the same sera (10%) for 24 h to test the endothelial barrier function and found a feeble, albeit not significant, increase of endothelial permeability in cells incubated with sera from T1D patients with normal or high HbA1c (Figure 1B).

2.2. Serum NOx Levels and Endothelial Permeability Are Associated with Hyperglycaemia

We then anticipated that the effects of the sera from T1D patients might depend upon high blood glucose. Therefore, we grouped these sera according to fasting glycaemia and compared the amounts of NOx in healthy, normo- and hyperglycaemic T1D subjects. Figure 2A shows that levels of NOx were significantly increased only in the sera obtained from hyperglycaemic subjects (T1D h.g.). The same result was obtained when we evaluated endothelial permeability in relation to glycaemia. Indeed, Figure 2B shows that permeability is markedly increased in HUVEC exposed for 24 h to sera from hyperglycaemic individuals (T1D h.g.), whereas no significant differences exist between sera from normoglycaemic T1D (T1D n.g.) and healthy subjects (CTR).

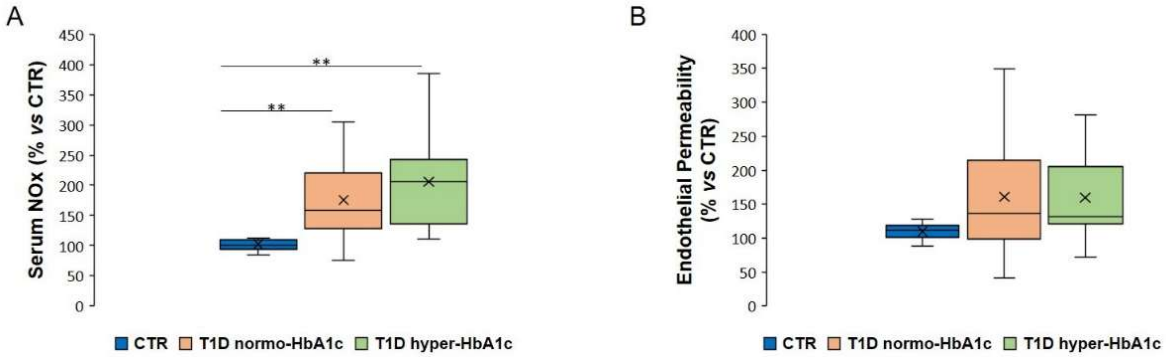

Figure 1. Amounts of NOx in the sera from healthy individuals, T1D patients with normal or high HbA1c and the effects of the same sera on endothelial permeability. The sera of patients were grouped according to the levels of HbA1c and their effects on HUVEC were compared to those of sera from healthy controls. (**A**) The levels of NOx were measured in the sera from healthy donors (CTR) and T1D subjects with normal or high HbA1c (T1D normo-HbA1c or T1D hyper-HbA1c). (**B**) The effect of the above-described sera on endothelial permeability was evaluated using a Transwell Permeability Assay. The results are the mean of three experiments in triplicate. ** $p < 0.01$.

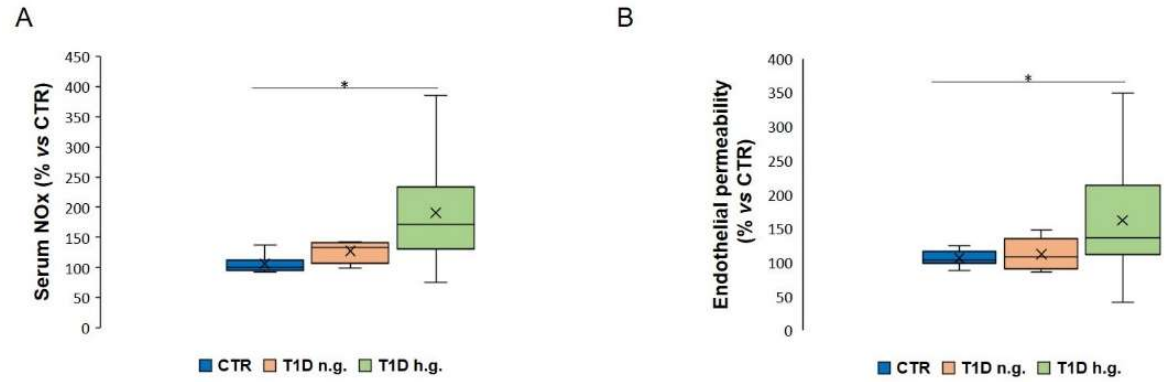

Figure 2. Determination of NOx in the sera from healthy individuals, T1D patients with normal or high glycaemia and effects of these sera on HUVEC permeability. The sera of patients were grouped according to fasting glycaemia. (**A**) The levels of NOx were measured in the sera from healthy subjects (CTR) and T1D individuals with normal (T1D n.g.) or high glycaemia (T1D h.g.) as described in the methods. (**B**) Endothelial permeability was measured in HUVEC exposed to 10% of the sera using a Transwell Permeability Assay. The results are the mean of three experiments in triplicate. * $p < 0.05$.

2.3. High Concentrations of Extracellular Glucose Increase Endothelial NOx Release and Permeability in Endothelial Cells

To get insights into a possible role of high glucose in inducing endothelial permeability, we performed experiments on HUVEC exposed to physiological (5.5 mM, CTR) or high (11.1 and 30 mM) concentrations of extracellular glucose for 24 h. Bradykinin (10 μM) was used as a positive control for endothelial permeability, while lipopolysaccharide (LPS, 10 μg/mL) was the positive control for NOx release. L-Glucose (30 mM) was utilized as a control of osmolarity. D-glucose increased endothelial release of NOx (Figure 3A) as well as permeability (Figure 3B) in a concentration-dependent manner, while L-glucose exerted no effects, thus indicating the pivotal role of high glucose, and not increased osmolarity, in inflecting endothelial performance.

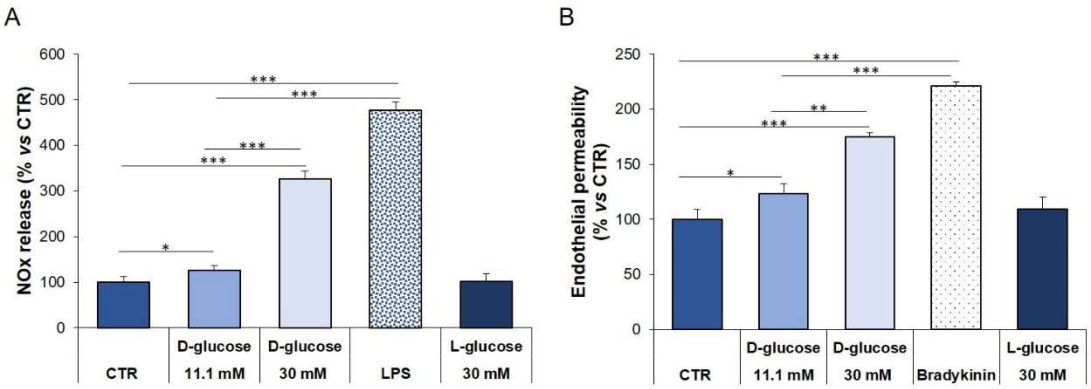

Figure 3. NOx release and permeability in HUVEC exposed to different concentrations of glucose. HUVEC were cultured in a medium containing 5 mM (CTR), 11.1 and 30 mM glucose for 24 h. LPS and Bradykinin were used as positive controls. (**A**) Media were collected and NOx levels were measured as described in the methods. (**B**) Endothelial permeability was studied as described in the methods. The results are the mean of three experiments in triplicates ± standard deviation (SD). * $p < 0.05$; ** $p < 0.01$; *** $p < 0.001$.

2.4. The Upregulation of iNOS is Responsible for the Increase of NOx in HUVEC Exposed to High Glucose

To understand which isoform of NOS is involved in the increase of NO upon treatment with high extracellular glucose, we assessed the total amounts of iNOS and eNOS, the two enzymes that catalyse the production of NO in endothelial cells. We also investigated the activated form eNOS, which is phosphorylated on Ser1177 (P-eNOS^{Ser1177}). The total amount of iNOS were increased by high D-glucose (Figure 4A). Conversely, both the eNOS and P-eNOS^{Ser1177} were not significantly modulated by high glucose (Figure 4B).

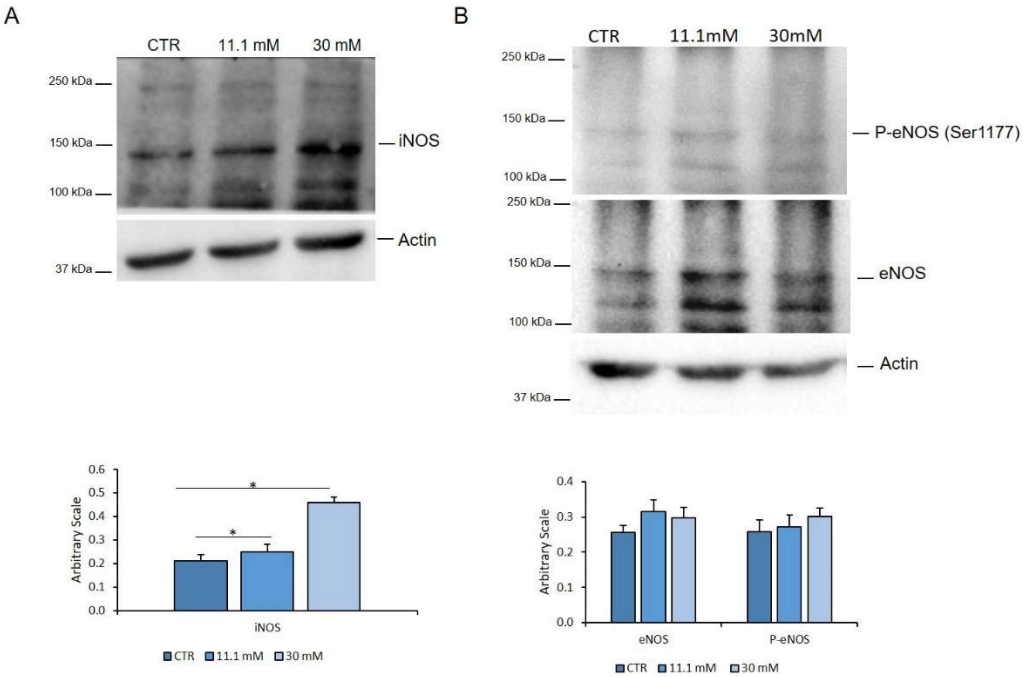

Figure 4. iNOS and eNOS in HUVEC exposed to different concentrations of glucose. HUVEC were cultured in a medium containing 5 mM (CTR), 11.1 and 30 mM glucose for 24 h. Western blot was performed using specific antibodies against iNOS (**A**), P-eNOS^{Ser1177}, and eNOS (**B**). Actin was used as a marker of loading. The experiments were repeated three times and a representative blot is shown. Densitometry was performed by Image J software calculating the ratio between the protein of interest and actin on three separate experiments ± SD. * $p < 0.05$.

We then assessed the role of iNOS and eNOS in modulating endothelial permeability. HUVEC were pre-treated for 1 h with L-NAME (100 μM) and L-NIL (100 μM), pharmacological inhibitors of eNOS and iNOS, respectively, and then exposed to a medium containing high concentrations of glucose for 24 h. In parallel, HUVEC were transiently transfected for 6 h with specific siRNAs targeting *iNOS* and *eNOS*, or a scrambled sequence as a control, and then exposed to high glucose for the following 24 h. Figure 5 shows that iNOS silencing as well as L-NIL prevented glucose-induced NOx accumulation and hyperpermeability, whereas L-NAME slightly reduced NOx release and permeability in HUVEC cultured in high glucose, as expected since eNOS is constitutively active in endothelial cells.

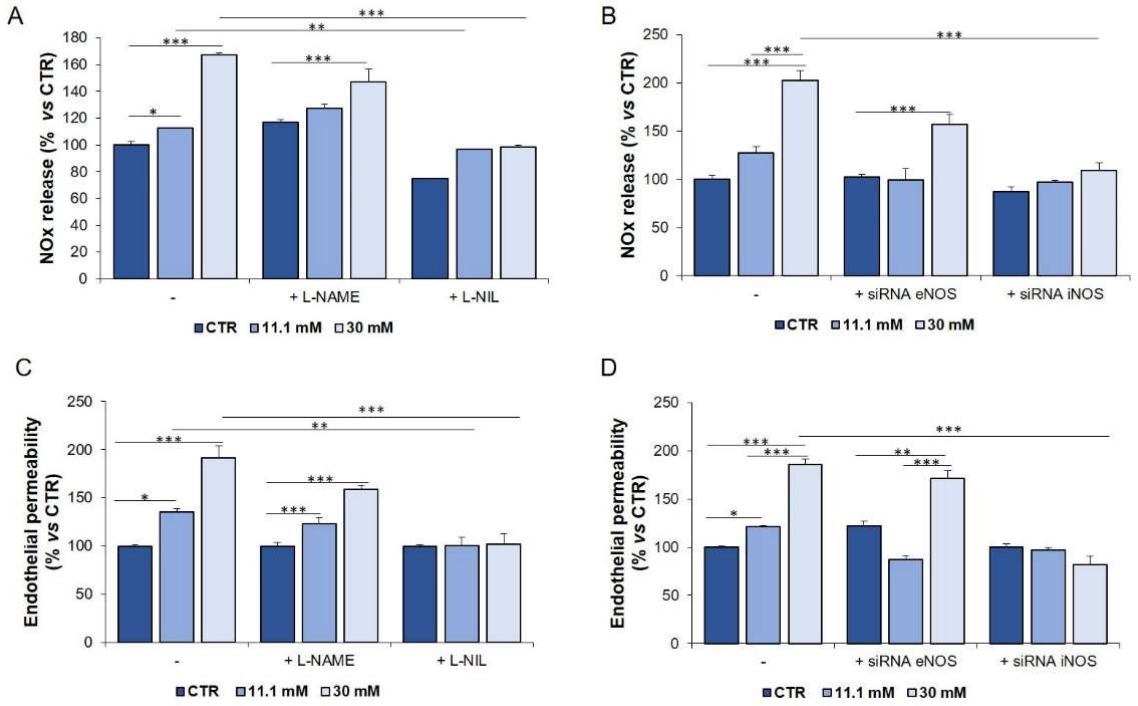

Figure 5. NOx release and permeability in HUVEC cultured in a medium containing different concentrations of glucose after genetic and pharmacological inhibition of iNOS or eNOS. HUVEC were cultured in a medium containing 5 mM (CTR), 11.1 and 30 mM glucose for 24 h in the presence of L-NAME or L-NIL (**A**,**C**) or after gene silencing (**B**,**D**). A scrambled non silencing sequence was used as a control (–) for silencing. The results are the mean of three experiments in triplicate ± SD. * $p < 0.05$; ** $p < 0.01$; *** $p < 0.001$.

2.5. Genetic and Pharmacological Inhibition of iNOS Restores Endothelial Permeability in Cells Exposed to Sera from Hyperglycaemic T1D Patients

We then asked whether the increase of endothelial permeability by sera from hyperglycaemic T1D patients was dependent upon the induction of iNOS. Endothelial cells were pre-treated for 1 h with L-NAME (100 μM) or L-NIL (100 μM) before adding to the culture media 10% of T1D serum from hyperglycaemic or healthy subjects. As shown in Figure 6A, L-NIL reduced endothelial permeability to approximately the same level as the controls. We also transiently silenced *eNOS* and *iNOS* utilizing specific siRNAs (Figure 6B), while the controls were exposed to a scrambled sequence. We found a marked reduction of endothelial permeability when a siRNA was used against *iNOS*.

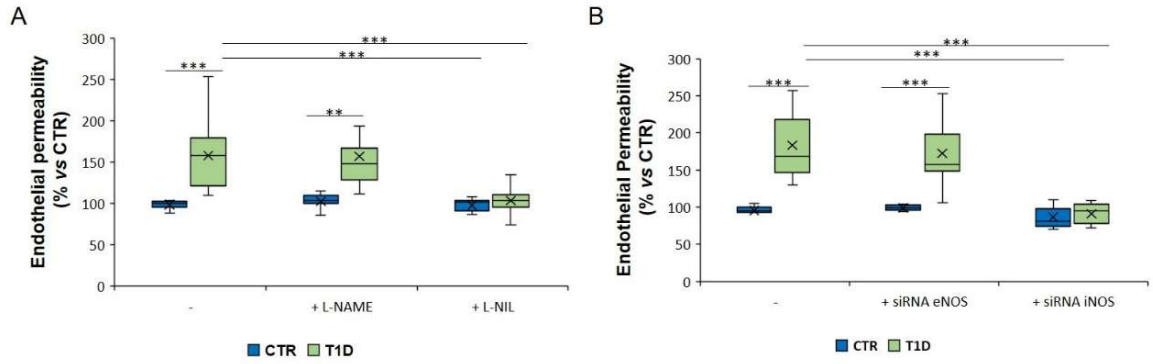

Figure 6. Permeability in HUVEC cultured in medium containing 10% hyperglycaemic T1D or CTR sera after genetic and pharmacological inhibition of iNOS or eNOS. HUVEC were cultured in the presence of sera from healthy and T1D subjects for 24 h with or without L-NAME or L-NIL (**A**) or after gene silencing (**B**). A scrambled non-silencing sequence was used as a control (–) for silencing. The results are the mean of three experiments in triplicate. ** $p < 0.01$; *** $p < 0.001$.

3. Discussion

T1D predisposes to premature atherosclerosis, the main reason for high morbidity and impaired life expectancy in T1D patients [20]. One of the earliest events in atherogenesis is the elevated permeability of the endothelium, which favours the accumulation of lipoproteins into the intima where they are oxidized and propagate endothelial dysfunction [4].

Here we show that sera from hyperglycaemic T1D subjects markedly enhance endothelial leakage, whereas sera from normoglycaemic T1D or healthy individuals do not. Since it suffices to expose HUVEC to high extracellular D-glucose to augment their permeability, we anticipate that hyperglycaemia is responsible for the increase of endothelial permeability observed when we use sera from hyperglycaemic T1D patients. Consistently, high glucose was shown to stimulate endothelial transport of dextran through the activation of the Rho signalling pathway, which leads to the contraction of the cytoskeleton and the consequent loss of endothelial connections [21]. We focused on the identification of the mediators involved in high glucose-induced hyperpermeability with the goal of individuating potential biochemical markers that might be useful for the early recognition of alterations of the endothelial barrier and, eventually, become a target to limit and delay atherogenesis. Among others, NO modulates endothelial cell permeability in vivo and in vitro [22], because it regulates cytoskeletal architecture through Rho [12] and downregulates VE-cadherin [22]. Therefore, we evaluated the levels of NOx in the sera from our T1D patients and found a very strong association between elevated amounts of serum NOx and fasting glucose concentrations. We argue that transient isolated peaks of glycaemia can be detrimental for the integrity of the endothelium because they increase permeability by stimulating NO production. This is particularly true in the light of the so-called "metabolic memory", a theory indicating that glycaemic instability promotes metabolic and epigenetic changes that remain also when glucose levels return normal [23]. Indeed, exposure of HUVEC to oscillating high glucose is more detrimental than constant high glucose and induces a metabolic memory after glucose normalization [24]. It is, therefore, important to establish a therapeutic/dietetic regimen which keeps glycaemia within the physiological range.

While higher amounts of serum NOx in T1D patients versus controls are reported also by other authors [17,25], the source of NOx remains undetermined. T1D is associated with a pro-inflammatory environment [26,27]. Plasma concentrations of pro-inflammatory cytokines IL-1β and IL-17A, as well as T cell synthesized cytokines IFN-γ, TNF-α and IL-23, are increased in T1D subjects [27]. These cytokines activate iNOS and stimulate NO synthesis in various cell types, including the vascular cells. Accordingly, lung microvascular endothelial cells cultured in a high glucose-containing medium and then challenged with LPS upregulate iNOS [28]. However, no evidence is provided that the increased amounts of iNOS is responsible for

hyperpermeability, since no pharmacological or genetic inhibition was performed [28]. Additionally, considering the high heterogeneity of the endothelium and the unique features of lung vasculature, human pulmonary microvascular endothelial cells are likely to behave differently from the macrovascular endothelial cells used in our experiments [29].

Our results point to a direct effect of high glucose in increasing NOx levels. Indeed, HUVEC cultured in media containing high glucose release more NOx than controls in a dose-dependent fashion through the upregulation of iNOS. Accordingly, genetic or pharmacological inhibition of iNOS prevents the increase of endothelial permeability caused by the sera from hyperglycaemic T1D patients. In agreement with our findings, in alloxan-induced T1D rats NOx are increased through the overexpression of iNOS [30]. To this purpose, it is interesting that aerobic exercise significantly decreases iNOS in pre-diabetic rats [31]. Therefore, physical activity might represent a preventive strategy to control iNOS expression in T1D patients, thus tempering endothelial damage. Moreover, it should be recalled that, besides NOS-derived NO, the steady-state systemic NO concentrations are regulated by the dietary intake of nitrates and nitrites that can be metabolized into bioactive NO via stepwise reductions [32]. Currently, no data are available about tailored nutritional approaches as tools to control NOx levels and prevent endothelial hyperpermeability in T1D patients [33].

A last point needs to be considered, i.e., the predictive value of measuring HbA1c as a marker to individuate early alterations of endothelial function. We found increased NOx amounts independently from HbA1c levels. Interestingly, increased levels of NOx were reported also in patients with T2D, the most prevalent form of diabetes. Different from our findings in T1D, NOx levels positively correlate with both HbA1c and fasting glycaemia in T2D individuals [17]. It would be interesting to unveil the effects of the sera from T2D patients on endothelial permeability and the levels of NOS.

To conclude, although limited by the small number of subjects included in the study, our results suggest that sporadic transitory peaks of glycaemia in T1D patients lead to the activation of iNOS. The consequent increase of NOx impairs the endothelial barrier, thus facilitating subendothelial accumulation of macromolecules that alter the microenvironment of the intima and promote vascular disease.

4. Materials and Methods

4.1. Study Population

This is a cohort study in which each participant who fulfilled the inclusion criteria was consecutively enrolled. The study was carried out in 36 paediatric T1D patients (T1D) and in 14 age-matched non-diabetic healthy donors (CTR). Clinical characteristics of T1D patients and healthy controls are summarized in Table 1. None of the diabetic patients was affected by other complications, such as retinopathy (evaluated by stereoscopic fundus photography) or neuropathy (evaluated by nervous conduction velocity and autonomic tests) or was in treatment with other drugs except insulin. All patients included in the study were nonsmokers; none was taking antioxidant supplements or drugs with known antioxidant activity. Normal glycated haemoglobin (HbA1c) is between 4% and 7.5%. Normal glycaemia ranges between 60 and 100 mg/dL, while fasting hyperglycaemia was defined for values higher than 100 mg/dl. Informed consent was obtained from all subjects included in the study. Sera were collected at the University of Milan–V. Buzzi Children's Hospital. The study was approved by the Buzzi Children's Hospital (ASST Fatebenefratelli–Sacco, Milan, Italy) Ethical Committee (2018/ST/143, 9th October 2018, Milano Area 1). All procedures followed were in accordance with the ethical standards of the responsible committee on human experimentation (institutional and national) and with the Declaration of Helsinki 1975, as revised in 2008.

Table 1. Clinical characteristics of paediatric T1D patients and healthy controls. Among the T1D patients, 10 were normoglycaemic, 26 hyper-glycaemic, 11 had high levels of HbA1c (>7.5 %) and 25 had levels of HbA1c within the physiological range.

	Healthy Subjects (n = 14)	Patients (n = 36)
Sex		
Male	n = 5	n = 12
Female	n = 9	n = 24
Age (years)		
Mean	12.5	13.8
Range	3.1–23.7	4.0–24.0
Hb1Ac (%)		
Mean	5.7	7.15
Range	5.30–6.80	5.10–8.80
PCR (mg/dL)		
Mean	0.53	0.71
Range	0.43–0.61	0.20–2.60
Glycaemia (mg/dL)		
Mean	102	168.26
Range	89.0–117.0	40.0–350.0
Therapy	None	MDI (n = 22) CSII (n = 14)

4.2. Cell Culture

Human Umbilical Vein Endothelial Cells (HUVEC) were obtained from the American Type Culture Collection (ATCC, Manassas, WV, USA) and cultured in medium M199 (Euroclone, Milano, Italy) with 10% fetal bovine serum (FBS), 1 mM L–Glutamine, 1 mM Sodium Pyruvate, 1 mM Penicillin–Streptomycin, 5 U/mL Heparin and 150 µg/mL Endothelial Cell Growth Factor on 2% gelatin-coated dishes [34] added. To test the sera of the participants, FBS was substituted by 10% of serum collected from subjects (CTR) or paediatric diabetic patients (T1D). The cells were routinely tested for the expression of endothelial markers and used for 6–7 passages. To perform the experiments, the cells were trypsinized, stained with 0.4% trypan blue solution and counted using a Luna Automated Cell Counter (Logos Biosystems, Anyang–si, Gyeonggi–do, South Korea). D–glucose (Sigma–Aldrich, St. Louis, MO, USA) was used at the concentrations of 11.1 mM and 30 mM and L–glucose (Sigma–Aldrich) was used as a control of osmolarity at the concentration of 30 mM.

Nitric Oxide Synthase (NOS) was inhibited using either small interfering RNA (siRNA) or pharmacological inhibitors. Subconfluent cells were transfected with siRNA targeting *eNOS* (NOS3) [20 nmol, 5′-TTCGAGGGACACCACGTCATACTCA-3′ (Invitrogen Corporation, Carlsbad, CA, USA)] or *iNOS* (NOS2A) [20 nmol, 5′-ATCGAATTTGTCAACCAATAT-3′ (Invitrogen)] [35]. Lipofectamine RNAiMAX was used as a transfection reagent (Invitrogen), according to the manufacturer's recommendations. After 6 h, the siRNA transfection medium was replaced with a culture medium added with 11.1 mM or 30 mM of glucose. The same experimental approach was used with 10% serum collected from CTR or T1D patients. We tested *eNOS*- and *iNOS*-silencing using Real Time PCR (not shown). Alternatively, subconfluent cells were pre-treated with 100 µM of pharmacological inhibitors of eNOS [L-Nω–Nitroarginine-Methyl-Ester (L-NAME) and iNOS [N6–(1-Iminoethyl)-L-Lysine (L-NIL) (Sigma–Aldrich) for 1 h. Then, 10% of serum from the cohort or two different concentrations of glucose were added. The experiment lasted 24 h. All the experiments were performed in triplicate 3 times.

4.3. Transwell Permeability Assay

The Transwell Permeability Assay was performed in a 24-well receiver plate with individual hanging cell culture inserts (Transwell® Permeable Supports, Euroclone, 0.4 μm micropores, (Euroclone, Milano, Italy)). HUVEC were seeded into the inserts and, when confluent, incubated for 24 h with a medium containing 10% of serum collected from CTR or T1D patients or with a culture medium containing 11.1 mM or 30 mM glucose. After the treatment, 1 mg/mL Fluorescein isothiocyanate labelled–albumin (FITC–BSA) (Sigma–Aldrich), a fluorescent probe able to cross the monolayer of endothelial cells at a rate proportional to the monolayer's permeability, was added [36]. The extent of permeability was determined by measuring the fluorescence in the lower compartment. Fluorescence was detected by the Promega Glomax Multi Detection System at excitation and emission spectrum wavelengths of 495/519 nm. The experiment was performed in triplicate 2 times.

4.4. NOS Activity

NOS activity was measured in the culture media and in the serum from the patients using the Griess Assay [19] which measures NO oxidative products (NOx). Briefly, culture media or sera were mixed with freshly prepared Griess reagent and the absorbance was measured at 550 nm. The concentration of nitrites in the samples was determined using a calibration curve generated with a known concentration of sodium nitrite ($NaNO_2$) solutions. The experiment was performed in triplicate 3 times.

4.5. Western Blot Analysis

HUVECs were lysed in 50 mM Tris–HCl (pH 7.4) containing 150 mM NaCl, 1% NP40, 0.25% sodium deoxycholate, protease inhibitors (10 μg/mL Leupeptin, 10 μg/mL Aprotinin, 1 mM PMSF) and phosphatase inhibitors (1 mM sodium fluoride, 1 mM sodium vanadate, 5 mM sodium phosphate). Lysates (40 μg/lane) were separated on SDS–PAGE and transferred to nitrocellulose sheets at 400 mA for 2 h at 4 °C. Western Blot analysis was performed using antibodies against iNOS (BD Biosciences, Milano, Italy), P-eNOS^{Ser1177} (Cell Signaling Technology, Danvers, Massachusetts, USA), eNOS (BD Biosciences) and Actin (Santa Cruz Biotechnology, Dallas, TX, USA) [37]. After extensive washing, secondary antibodies labelled with horseradish peroxidase (GE Healthcare, Waukesha, WI, USA) were used. Immunoreactive proteins were detected by the SuperSignal Chemiluminescence Kit (Thermo Fisher Scientific Waltham, MA, USA) [35]. The experiment was performed 3 times and quantified using Image J software (National Institutes of Health, Bethesda, MD, USA).

4.6. Statistical Analysis

Data are reported as means ± SD. The data were normally distributed and they were analyzed using one-way repeated measures ANOVA. The p-values deriving from multiple pairwise comparisons were corrected by the Bonferroni method. Statistical significance was defined for p-value ≤ 0.05. Regarding the Figures, * $p \leq 0.05$; ** $p \leq 0.01$; *** $p \leq 0.001$.

5. Conclusions

In this study, we show that sera from hyperglycaemic T1D patients significantly increase endothelial permeability through the upregulation of iNOS. Therefore, the identification of iNOS as a possible biomarker that promotes the insurgence of vascular disease in T1D could entail potential planning for the prevention of cardiovascular complications in T1D.

Author Contributions: A.C., E.G., G.V.Z. and J.A.M.M. designed the experiments. A.C. and R.S. set up the experimental plan and performed the experiments. E.G. generated the database and recruited the patients. J.A.M.M. wrote the manuscript. All authors have read and agreed to the published version of the manuscript.

Funding: This research was sustained by intramural funds. Alessandra Cazzaniga is a post-doctoral fellow of Fondazione Invernizzi.

Conflicts of Interest: The authors declare no conflict of interest.

Abbreviations

T1D	Type 1 diabetes
NO	Nitric Oxide
ROS	Reactive Oxygen Species
eNOS	endothelial Nitric Oxide Synthase
eNOSSer1177	eNOS phosphorylated on Ser1177
iNOS	inducible Nitric Oxide Synthase
NOx	nitrate and nitrite
Hb1Ac	glycated haemoglobin
HUVEC	Human Umbilical Vein Endothelial Cells
FBS	Fetal Bovine Serum
L-NAME	L-Nω–Nitroarginine-Methyl-Ester
L-NIL	N6–(1-Iminoethyl)-L-Lysine
LPS	lipopolysaccharide

References

1. Thomas, C.C.; Philipson, L.H. Update on Diabetes Classification. *Med Clin. N. Am.* **2015**, *99*, 1–16. [CrossRef] [PubMed]
2. Giannini, C.; Mohn, A.; Chiarelli, F.; Kelnar, C.J.H. Macrovascular angiopathy in children and adolescents with type 1 diabetes. *Diabetes/Metab. Res. Rev.* **2011**, *27*, 436–460. [CrossRef] [PubMed]
3. Hoffman, R.P. Vascular endothelial dysfunction and nutritional compounds in early type 1 diabetes. *Curr. Diabetes Rev.* **2014**, *10*, 201–207. [CrossRef] [PubMed]
4. Gimbrone, M.A.; García-Cardeña, G. Endothelial Cell Dysfunction and the Pathobiology of Atherosclerosis. *Circ. Res.* **2016**, *118*, 620–636. [CrossRef]
5. Deanfield, J.E.; Halcox, J.; Rabelink, T.J. Endothelial Function and Dysfunction. *Circulation* **2007**, *115*, 1285–1295. [CrossRef]
6. Bakker, W.; Eringa, E.C.; Sipkema, P.; Van Hinsbergh, V.W.M. Endothelial dysfunction and diabetes: Roles of hyperglycemia, impaired insulin signaling and obesity. *Cell Tissue Res.* **2008**, *335*, 165–189. [CrossRef]
7. Scaramuzza, A.E.; Redaelli, F.; Giani, E.; Macedoni, M.; Giudici, V.; Gazzarri, A.; Bosetti, A.; De Angelis, L.; Zuccotti, G. V Adolescents and young adults with type 1 diabetes display a high prevalence of endothelial dysfunction. *Acta Paediatr.* **2015**, *104*, 192–197. [CrossRef]
8. Liao, J.K. Linking endothelial dysfunction with endothelial cell activation. *J. Clin. Investig.* **2013**, *123*, 540–541. [CrossRef]
9. Popov, D. Endothelial cell dysfunction in hyperglycemia: Phenotypic change, intracellular signaling modification, ultrastructural alteration, and potential clinical outcomes. *Int. J. Diabetes Mellit.* **2010**, *2*, 189–195. [CrossRef]
10. Sharma, J.; Al-Omran, A.; Parvathy, S.S. Role of nitric oxide in inflammatory diseases. *Inflammopharmacology* **2007**, *15*, 252–259. [CrossRef]
11. Caimi, G.; Hopps, E.; Montana, M.; Noto, D.; Canino, B.; Presti, R.L.; Averna, M. Evaluation of nitric oxide metabolites in a group of subjects with metabolic syndrome. *Diabetes Metab. Syndr. Clin. Res. Rev.* **2012**, *6*, 132–135. [CrossRef] [PubMed]
12. Di Lorenzo, A.; Lin, M.I.; Murata, T.; Landskroner-Eiger, S.; Schleicher, M.; Kothiya, M.; Iwakiri, Y.; Yu, J.; Huang, P.; Sessa, W.C. eNOS-derived nitric oxide regulates endothelial barrier function through VE-cadherin and Rho GTPases. *J. Cell Sci.* **2013**, *126*, 5541–5552. [CrossRef] [PubMed]
13. Csonka, C.; Páli, T.; Bencsik, P.; Gorbe, A.; Ferdinandy, P.; Csont, T. Measurement of NO in biological samples. *Br. J. Pharmacol.* **2014**, *172*, 1620–1632. [CrossRef] [PubMed]
14. Chiarelli, F.; Cipollone, F.; Romano, F.; Tumini, S.; Costantini, F.; Di Ricco, L.; Pomilio, M.; Pierdomenico, S.D.; Marini, M.; Cuccurullo, F.; et al. Increased circulating nitric oxide in young patients with type 1 diabetes and persistent microalbuminuria: Relation to glomerular hyperfiltration. *Diabetes* **2000**, *49*, 1258–1263. [CrossRef]

15. González, M.; Rojas, S.; Avila, P.; Cabrera, L.; Villalobos, R.; Palma, C.; Aguayo, C.; Peña, E.; Gallardo, V.; Guzmán-Gutiérrez, E.; et al. Insulin Reverses D-Glucose–Increased Nitric Oxide and Reactive Oxygen Species Generation in Human Umbilical Vein Endothelial Cells. *PLoS ONE* **2015**, *10*, e0122398. [CrossRef]
16. Adela, R.; Nethi, S.K.; Bagul, P.K.; Barui, A.K.; Mattapally, S.; Kuncha, M.; Patra, C.R.; Reddy, P.N.C.; Banerjee, S.K. Hyperglycaemia Enhances Nitric Oxide Production in Diabetes: A Study from South Indian Patients. *PLoS ONE* **2015**, *10*, e0125270. [CrossRef]
17. Assmann, T.S.; Brondani, L.A.; Bouças, A.P.; Rheinheimer, J.; De Souza, B.M.; Canani, L.H.; Bauer, A.C.; Crispim, D. Nitric oxide levels in patients with diabetes mellitus: A systematic review and meta-analysis. *Nitric Oxide* **2016**, *61*, 1–9. [CrossRef]
18. Bahadoran, Z.; Mirmiran, P.; Ghasemi, A. Role of Nitric Oxide in Insulin Secretion and Glucose Metabolism. *Trends Endocrinol. Metab.* **2019**, *31*, 118–130. [CrossRef]
19. Miranda, K.M.; Espey, M.G.; Wink, D.A. A Rapid, Simple Spectrophotometric Method for Simultaneous Detection of Nitrate and Nitrite. *Nitric Oxide* **2001**, *5*, 62–71. [CrossRef]
20. Rask-Madsen, C.; King, G.L. Vascular complications of diabetes: Mechanisms of injury and protective factors. *Cell Metab.* **2013**, *17*, 20–33. [CrossRef]
21. Zhao, X.-Y.; Wang, X.-F.; Li, L.; Zhang, L.; Shen, D.-L.; Li, D.-H.; Jin, Q.-S.; Zhang, J.-Y. Effects of high glucose on human umbilical vein endothelial cell permeability and myosin light chain phosphorylation. *Diabetol. Metab. Syndr.* **2015**, *7*, 98. [CrossRef] [PubMed]
22. Yang, B.; Cai, B.; Deng, P.; Wu, X.; Guan, Y.; Zhang, B.; Cai, W.; Schaper, J.; Schaper, W. Nitric Oxide Increases Arterial Endotheial Permeability through Mediating VE-Cadherin Expression during Arteriogenesis. *PLoS ONE* **2015**, *10*, e0127931. [CrossRef] [PubMed]
23. Testa, I.; Bonfigli, A.R.; Prattichizzo, F.; La Sala, L.; De Nigris, V.; Ceriello, A. The "Metabolic Memory" Theory and the Early Treatment of Hyperglycemia in Prevention of Diabetic Complications. *Nutrients* **2017**, *9*, 437. [CrossRef]
24. Schisano, B.; Tripathi, G.; McGee, K.; McTernan, P.G.; Ceriello, A. Glucose oscillations, more than constant high glucose, induce p53 activation and a metabolic memory in human endothelial cells. *Diabetology* **2011**, *54*, 1219–1226. [CrossRef] [PubMed]
25. Ghasemi, A.; Zahediasl, S.; Azizi, F. Reference values for serum nitric oxide metabolites in an adult population. *Clin. Biochem.* **2010**, *43*, 89–94. [CrossRef] [PubMed]
26. Aulich, J.; Cho, Y.H.; Januszewski, A.S.; E Craig, M.; Selvadurai, H.; Wiegand, S.; Jenkins, A.J.; Donaghue, K. Associations between circulating inflammatory markers, diabetes type and complications in youth. *Pediatr. Diabetes* **2019**, *20*, 1118–1127. [CrossRef]
27. Fatima, N.; Faisal, S.M.; Zubair, S.; Ajmal, M.; Siddiqui, S.S.; Moin, S.; Owais, M. Role of Pro-Inflammatory Cytokines and Biochemical Markers in the Pathogenesis of Type 1 Diabetes: Correlation with Age and Glycemic Condition in Diabetic Human Subjects. *PLoS ONE* **2016**, *11*, e0161548. [CrossRef]
28. Liu, X.-J.; Zhang, Z.-D.; Ma, X.-C. High glucose enhances LPS-stimulated human PMVEC hyperpermeability via the NO pathway. *Exp. Ther. Med.* **2013**, *6*, 361–367. [CrossRef]
29. Shelton, J.L.; Wang, L.; Cepinskas, G.; Sandig, M.; Inculet, R.; McCormack, D.G.; Mehta, S. Albumin leak across human pulmonary microvascular vs. umbilical vein endothelial cells under septic conditions. *Microvasc. Res.* **2006**, *71*, 40–47. [CrossRef]
30. Sartoretto, S.M.; Santos, F.F.; Costa, B.P.; Ceravolo, G.S.; Santos-Eichler, R.; Carvalho, M.H.C.; Fortes, Z.B.; Akamine, E.H. Involvement of inducible nitric oxide synthase and estrogen receptor ESR2 (ERbeta) in the vascular dysfunction in female type 1 diabetic rats. *Life Sci.* **2019**, *216*, 279–286. [CrossRef]
31. Wang, S.; Li, J.; Zhang, C.; Xu, G.; Tang, Z.; Zhang, Z.; Liu, Y.; Wang, Z. Effects of aerobic exercise on the expressions and activities of nitric oxide synthases in the blood vessel endothelium in prediabetes mellitus. *Exp. Ther. Med.* **2019**, *17*, 4205–4212. [CrossRef] [PubMed]
32. Bondonno, C.; Croft, K.D.; Hodgson, J.M. Dietary Nitrate, Nitric Oxide, and Cardiovascular Health. *Crit. Rev. Food Sci. Nutr.* **2015**, *56*, 2036–2052. [CrossRef] [PubMed]
33. McCarthy, O.; Moser, O.; Eckstein, M.L.; Bain, S.; Pitt, J.; Bracken, R.M. Supplementary Nitric Oxide Donors and Exercise as Potential Means to Improve Vascular Health in People with Type 1 Diabetes: Yes to NO? *Nutrients* **2019**, *11*, 1571. [CrossRef] [PubMed]
34. Cazzaniga, A.; Locatelli, L.; Castiglioni, S.; Maier, J.A.M. The dynamic adaptation of primary human endothelial cells to simulated microgravity. *FASEB J.* **2019**, *33*, 5957–5966. [CrossRef] [PubMed]

35. Leidi, M.; Dellera, F.; Mariotti, M.; Banfi, G.; Crapanzano, C.; Albisetti, W.; Maier, J.A.M. Nitric oxide mediates low magnesium inhibition of osteoblast-like cell proliferation. *J. Nutr. Biochem.* **2012**, *23*, 1224–1229. [CrossRef] [PubMed]
36. Romeo, V.; Cazzaniga, A.; Maier, J.A.M. Magnesium and the blood-brain barrier in vitro: Effects on permeability and magnesium transport. *Magnes. Res.* **2019**, *32*, 16–24. [PubMed]
37. Leidi, M.; Mariotti, M.; Maier, J.A.M. EDF-1 contributes to the regulation of nitric oxide release in VEGF-treated human endothelial cells. *Eur. J. Cell Boil.* **2010**, *89*, 654–660. [CrossRef] [PubMed]

Reactive oxygen species are implicated in altering magnesium homeostasis in endothelial cells exposed to high glucose

Roberta Scrimieri, Laura Locatelli, Roberta Cazzola, Jeanette A.M. Maier, Alessandra Cazzaniga

Università di Milano, Dipartimento di Scienze Biomediche e Cliniche L. Sacco, Milano 20157, Italy

Correspondence: Jeanette A.M. Maier, Università di Milano, Dipartimento di Scienze Biomediche e Cliniche L. Sacco, Via GB Grassi 74, 20157 Milano, Italy
<jeanette.maier@unimi.it>

Abstract. Transient Receptor Potential Melastatin (TRPM)7 is important in maintaining the intracellular homeostasis of magnesium (Mg), which is instrumental for vital cellular functions. Since the upregulation of TRPM7 has been proposed as a marker of endothelial dysfunction, we evaluated the effects of high glucose, which markedly impacts endothelial performance, on TRPM7 and intracellular Mg homeostasis in human macrovascular endothelial cells. We show that glucose-induced free radicals increase the amounts of TRPM7 as well as total intracellular magnesium. On the contrary, the highly selective Mg transporter MagT1 is not modulated by high glucose, hydrogen peroxide and low extracellular magnesium. We conclude that in endothelial cells high glucose alters Mg homeostasis through the upregulation of TRPM7.

Key words: endothelium, TRPM7, magnesium, reactive oxygen species, glucose

Introduction

Uncontrolled hyperglycemia causes endothelial dysfunction [1, 2], the first step of a cascade of events leading to vascular complications among which stroke, coronary artery and peripheral vascular diseases [3]. Several mechanisms seem to mediate hyperglycemia-dependent endothelial dysfunction such as the accumulation of reactive oxygen species (ROS), the activation of the polyol pathway and the increased amounts of nonenzymatically glycated proteins [4, 5].

In vitro high concentrations of extracellular glucose affect the function of endothelial cells of different types. Both human endothelial cells from the umbilical vein (HUVEC), widely used as a model of macrovascular endothelium, and human dermal microvascular endothelial cells exposed to high extracellular glucose are growth inhibited and show symptoms of premature senescence [6]. These results are explained, in part, by a time and dose-dependent increase of ROS due to high extracellular glucose. In addition, increased levels of calcium (Ca) both in the mitochondria and in the cytoplasm have been reported and linked to the induction of apoptosis [3, 7].

Rather little is known about the homeostasis of magnesium (Mg) in endothelial cells exposed

doi: 10.1684/mrh.2019.0456

To cite this article: Scrimieri R, Locatelli L, Cazzola R, Maier JAM, Cazzaniga A. *Magnes Res* 2019; 32(3): 54-62. doi: 10.1684/mrh.2019.0456

to high glucose. Mg is important in numerous biochemical processes, from energy generation to the synthesis of DNA, RNA and proteins and is a natural Ca antagonist [8]. Consequently, it is involved in many physiological processes, *i.e.* muscle contraction/relaxation, bone formation, brain activity, and others. In the vascular tree, the maintenance of Mg homeostasis is crucial to regulate blood pressure and prevent inflammation and thrombosis [9]. At the endothelial level, Mg is pivotal in governing barrier function [10], release of vasoactive molecules, fibrinolytic and anticoagulation factors, chemokines and cytokines [11]. Accordingly, Mg deficiency promotes a pro-inflammatory pro-atherogenic phenotype in these cells [12]. Vascular endothelial cells express both the Transient Receptor Potential Melastatin (TRPM)7 and the specific Mg transporter MagT1, and both cooperate to ensure Mg entry in these cells [13]. TRPM7 is a ubiquitous bifunctional protein endowed with a channel for divalent cations and an α kinase domain in its C-terminal [14], whereas MagT1 specifically transports Mg and is also involved in N-glycosylation [15]. In HUVEC low extracellular Mg, which impairs their function [11, 16, 17], upregulates TRPM7 through the increase of ROS [18]. Accordingly, hydrogen peroxide increases TRPM7 protein level [18]. On these bases, we proposed that high levels of TRPM7 might be a marker of endothelial dysfunction [13, 18]. This issue is supported by *in vivo* studies showing that elevated TRPM7 in the aortas from Mg-deficient mice correlates with increased amounts of vascular cell adhesion molecule-1 and plasminogen activator inhibitor-1 [19], both implicated in developing a pro-inflammatory and pro-atherogenic environment. At the moment no data are available about MagT1 and endothelial function.

The aim of this study was to evaluate TRPM7 and MagT1 as well as intracellular Mg levels in HUVEC cultured in the presence of high extracellular glucose, known to induce endothelial dysfunction.

Material and methods

Cell culture

HUVEC were obtained from the American Type Culture Collection (ATCC Manassas, Virginia, USA) and cultured in medium M199 (Euroclone, Milano, Italy) added with fetal bovine serum (FBS, 10%) (Euroclone), L-Glutamine (1 mM), Sodium Pyruvate (1 mM), Penicillin-Streptomycin (1 mM), Heparin (5 U/ml) and Endothelial Cell Growth Factor (ECGS, 150 µg/ml) on 2% gelatin-coated dishes. All culture reagents were from Sigma Aldrich (St. Louis, Missouri, USA). The cells were routinely tested for the expression of endothelial markers and used for 9-10 passages. All the experiments were performed on subconfluent cells. D-glucose (Sigma Aldrich) was used at a concentrations of 11.1 mM and 30 mM. The same concentrations of L-glucose (Sigma Aldrich) were utilized as a control for osmolarity. In some experiments hydrogen peroxide (H_2O_2) (100 µM) and N-acetylcysteine (NAC) (5 mM) (Sigma Aldrich) were used. In some experiments HUVEC were cultured in Mg-free medium (Thermo Fisher Scientific Waltham, MA, USA) supplemented with magnesium sulfate ($MgSO_4$) (Sigma Aldrich) to reach a final concentration of 0.1 mM Mg to mimic Mg deficiency or 1.0 mM, which is Mg physiological concentration [20].

Western blot analysis

HUVEC were lysed in 50 mM Tris-HCl (pH 7.4), 150 mM NaCl, 1% NP40, 0.25% NaDeoxy, protease inhibitors (10 µg/ml Leupeptin, 10 µg/ml Aprotinin, PMSF 1 mM) and phosphatase inhibitors (NaF 1 mM, NaV 1 mM, NaP 5 mM). Lysates (40 µg/lane) were separated on SDS-PAGE and transferred to nitrocellulose sheets using Trans-Blot Turbo Transfer System (Biorad, Hercules, USA). Western Blot analysis was performed using antibodies against TRPM7 (Bethyl, Montgomery, USA), MagT1 (Abcam, Cambridge, UK), thioredoxin-interacting protein (TXNIP) (Invitrogen Corporation, Carlsbad, USA) and superoxide dismutase (SOD)2 (BD Biosciences, Milano, Italy). After extensive washing, secondary antibodies labeled with horseradish peroxidase (GE Healthcare, Waukesha, WI, USA) were used. Immunoreactive proteins were detected by the SuperSignal Chemiluminescence Kit (Thermo Fisher Scientific) [21, 22]. The nitrocellulose sheets are used as control loading. A representative blot is shown. The densitometric analysis was performed using Image J Lab software (Biorad). The results are the mean of three independent

experiments performed in triplicate ± standard deviation.

ROS activity

For the detection of ROS, HUVEC were cultured in a 96-well black plate (Greiner Bio-One, Kremsmünster, Austria) and incubated for 30 minutes with 10 mM 2′-7′-dichlorofluorescein diacetate (DCFH) solution. The DCFH dye emission was monitored at 535 nm (excitation $\lambda = 484$ nm) using the VICTOR X5 multilabel plate (Perkin Elmer, Milano, Italy). ROS production was normalized on the basis of cell number as described [22]. The results are the mean of three independent experiments performed in triplicate ± standard deviation.

Quantification of total intracellular Mg

Total intracellular Mg was measured using the fluorescent chemosensor DCHQ5 (kindly donated by Prof. S. Iotti, University of Bologna) as described [23]. Fluorescence intensities were acquired at 510 nm. Mg concentrations were obtained by the interpolation of their fluorescence with the standard curve performed using known concentrations of $MgSO_4$. The results are the mean of three independent experiments performed in triplicate ± standard deviation.

Measurement of total levels of cellular ATP

The Luminescent ATP Detection Assay Kit (Promega Madison, Wisconsin, USA) was used to measure the level of ATP within the cell, according to the manufacturer's instructions.

Statistical analysis

Statistical significance was determined using Student's t test and set as follows: $*P < 0.05$, $**P < 0.01$, $***P < 0.001$.

Results

HUVEC exposed to high extracellular D-glucose accumulate ROS and upregulate TRPM7

HUVEC were cultured for 24 h in a medium containing the physiological (5.5 mM, CTR) or high concentrations of D-glucose (11.1 mM and 30 mM). 11.1 or 30 mM of L-glucose were utilized as controls of osmolarity. As shown in *figure 1A*,

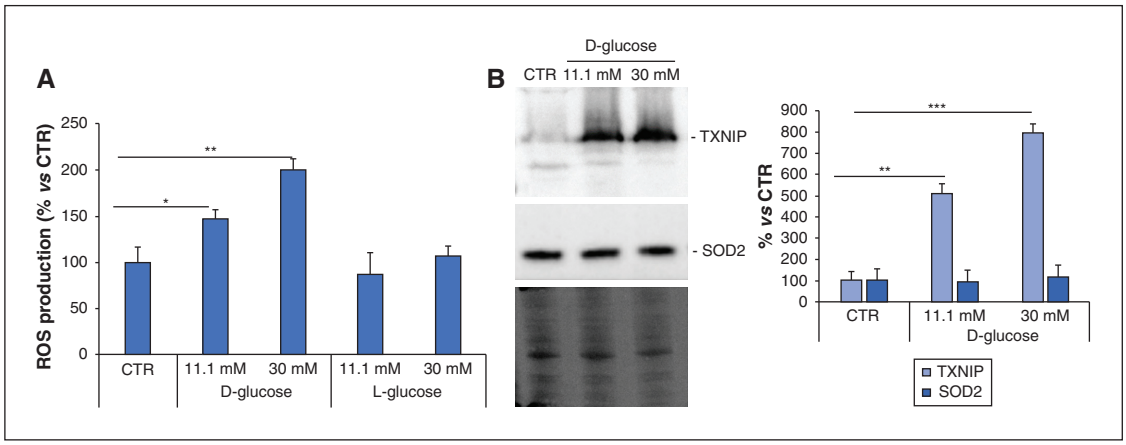

Figure 1. High D-glucose stimulates ROS accumulation. HUVEC were cultured under physiological (5.5 mM) (CTR) or two different high glucose concentrations (11.1 mM and 30 mM). **A)** ROS were measured by DCFH. Data are shown as percentages of ROS levels in HUVEC cultured in high concentrations of glucose *versus* CTR. L-glucose was used as a control of osmolarity. **B)** Western blot was performed on cell lysates using specific antibodies against TXNIP and SOD2. The relative control loading is shown in the lower panel. Densitometric analysis was performed using Image J Lab software.

exposure to high extracellular D-glucose significantly increased ROS in a dose-dependent manner, while L-glucose exerted no effect. To understand the mechanisms involved, we evaluated the total amounts of Superoxide Dismutase (SOD)2, the first line of defence against ROS, and the pro-oxidant protein Thioredoxin-Interacting Protein (TXNIP). The cells were maintained in 5.5, 11.1 or 30 mM D-glucose for 24 h. Western blot revealed a marked upregulation of TXNIP, but no alterations of the levels of SOD2 in high glucose-treated HUVEC (*figure 1B*), thereby suggesting that TXNIP has a role in the accumulation of ROS in these experimental conditions.

The total amounts of TRPM7 were then evaluated after 24 h of exposure to 5.5, 11.1, or 30 mM of glucose. By western blot, we found an increase of TRPM7 levels in response to high extracellular D-glucose, whereas the same concentrations of L-glucose did not exert any effect (*figure 2*).

MagT1 is not modulated by high D-glucose, hydrogen peroxide or low concentrations of extracellular Mg

We then evaluated the total amounts of MagT1 in HUVEC exposed to 5.5, 11.1, or 30 mM of D- or L-glucose for 24 h and found no significant modulation (*figure 3A*). Since very little is known about MagT1 in endothelial cells, we asked whether MagT1 is modulated in response to low extracellular Mg (0.1 mM), which induces oxidative stress and increases cardiovascular risk [11], and hydrogen peroxide (100 μM), from which hydroxyl radicals are produced by the Fenton reaction. *Figure 3B* shows that culture in low Mg or in the presence of hydrogen peroxide (H_2O_2) for 24 h did not exert any effect on MagT1 levels (*figure 3B*).

The antioxidant NAC prevents TRPM7 upregulation by high D-glucose

We then focused on TRPM7. To investigate if its upregulation by high glucose is due to the increase of ROS, HUVEC were treated with the antioxidant NAC (5 mM) in medium containing high or physiological concentrations of D-glucose for 24 h. NAC prevented ROS accumulation (*figure 4A*) and, in parallel, TRPM7 upregulation (*figure 4B*), thereby suggesting that the increased amounts of TRPM7 are due to D-glucose-induced ROS.

High D-glucose increases total intracellular magnesium, but not ATP

The concentration of intracellular total Mg was measured using the fluorescent chemosensor DCHQ5 in HUVEC cultured in a medium containing 5.5, 11.1, or 30 mM D- or L-glucose for 24 h. We found that intracellular Mg

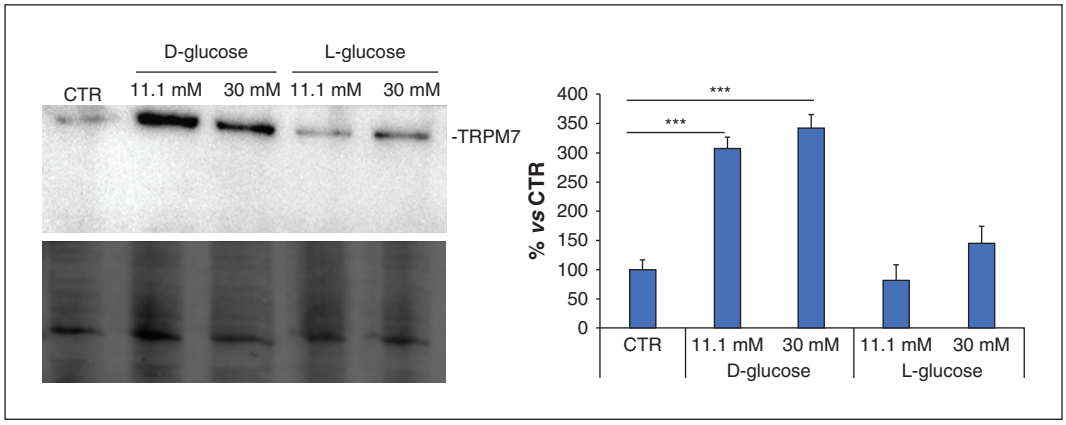

Figure 2. High D-glucose upregulates TRPM7. HUVEC were exposed to different concentrations of glucose for 24 h. Western blot was performed on cell lysates using antibodies against TRPM7. The relative control loading is shown in the lower panel. Densitometric analysis was performed using Image J Lab software.

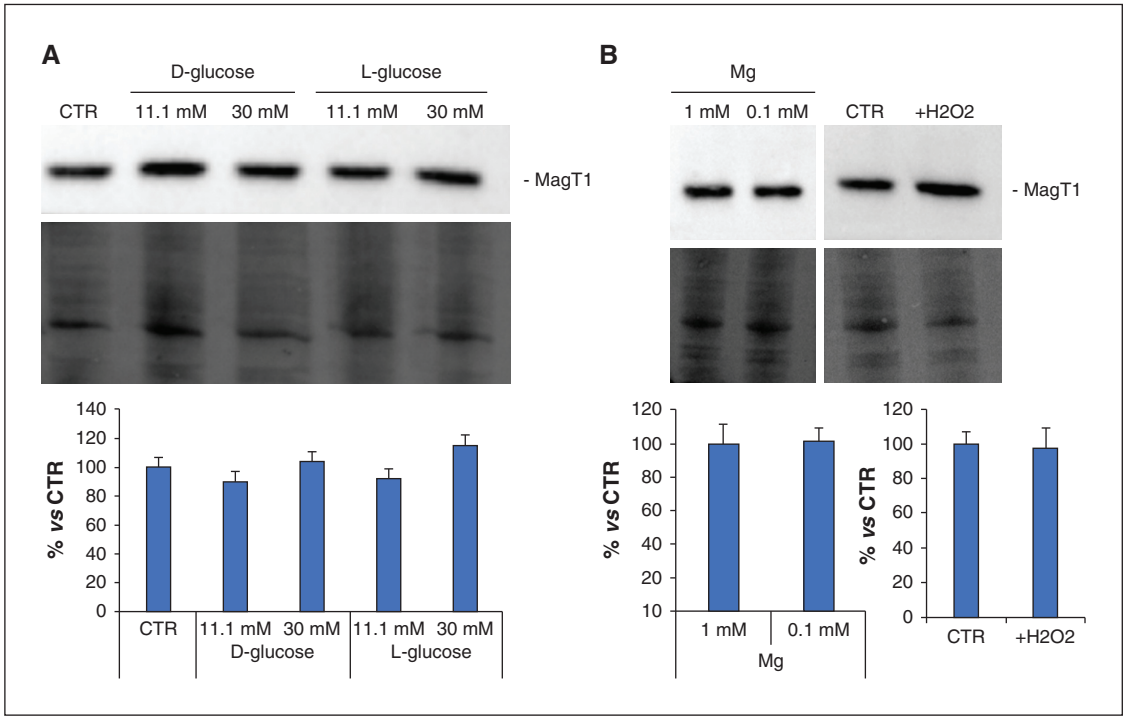

Figure 3. High D-glucose does not modulate MagT1 levels. **A)** HUVEC were exposed to 5.5 (CTR), 11.1 and 30 mM of glucose for 24 h. L-glucose was used as a control of osmolarity. **B)** HUVEC were cultured for 24 h in medium containing physiological (1 mM) and low (0.1 mM) concentrations of Mg (left panel) or in control medium (CTR) in the presence or not of 100 μM of hydrogen peroxide (H_2O_2) (right panel). In A and B western blot was performed on cell lysates using anti MagT1 antibodies. The relative control loading is shown in the lower panel. Densitometric analysis was performed using Image J Lab software.

increased in response to high D-glucose, an effect that is prevented by the addition of NAC (*figure 5A*). L-glucose did not modulate intracellular magnesium.

We also measured ATP content in HUVEC cultured for 24 h in a medium containing 5.5, 11.1, or 30 mM D-glucose in the presence or not of NAC and found no significant differences (*figure 5B*).

Discussion

High extracellular glucose alters Mg homeostasis in human macrovascular endothelial cells. In our experimental model, we found a direct correlation between high-glucose-induced ROS and TXNIP. TXNIP inhibits thioredoxin, a ubiquitous redox protein that reduces thiol and controls levels of ROS to limit damage from oxidative stress. In agreement with our data, the overexpression of TXNIP has been described in a rat model of type 1 diabetes as well as in cultured human aortic endothelial cells exposed to high glucose [24]. We propose that increased TXNIP has a role in generating oxidative stress in response to high glucose, but more experiments are necessary to validate this hypothesis. It is also of interest that no modulation of the antioxidant enzyme SOD2 at the protein level, which is critical in protecting the cardiovascular system [25], occurs. Therefore, we propose that in HUVEC high glucose favors the acquisition of a pro-oxidant phenotype, which is responsible for the upregulation of the Mg channel TRPM7. Our data confirm and broaden a previous study describing the upregulation of TRPM7 in HUVEC exposed for 72 h to high concentrations

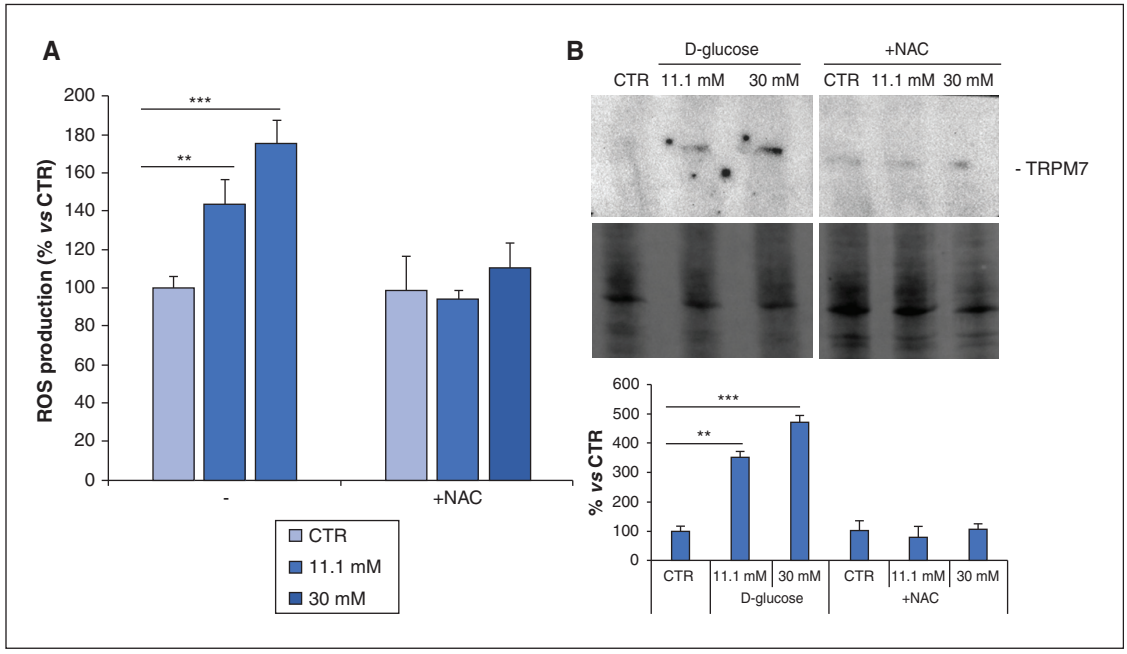

Figure 4. NAC prevents TRPM7 upregulation by high D-glucose. HUVEC were pretreated for 1 h with 5 mM NAC. The cells were then cultured for 24 h in the presence of 5.5, 11.1, and 30 mM glucose with or without NAC. **A)** ROS production was evaluated by DCFH. Data are shown as percentages of ROS levels *versus* CTR. **B)** Western blot was performed on cell lysates using anti TRPM7 antibodies. The relative control loading is shown in the lower panel. Densitometric analysis was performed using Image J Lab software.

of extracellular D-glucose [26]. We also show that an antioxidant, *i.e.*, NAC, prevents high-glucose-induced ROS and TRPM7 accumulation. We have previously shown that TRPM7 is modulated by ROS [18]. Indeed, TRPM7 increased in HUVEC cultured in low Mg [18], which promotes oxidative stress and is a risk factor for coronary artery disease [27], or exposed to hydrogen peroxide to simulate a condition of oxidative stress. On these bases we proposed that high levels of TRPM7 might be considered as a marker of endothelial dysfunction. The results reported in this paper reinforce this view.

On the contrary, MagT1 is not modulated by high glucose, low Mg, or hydrogen peroxide. We only considered the total amounts of the protein. However, it is possible that high glucose alters its function as a component of the N-oligosaccharyl transferase (OST) complex.

We propose that the increase of total intracellular Mg in HUVEC exposed to high concentrations of D-glucose is mainly due to the upregulation of TRPM7. This result is puzzling, since most mammalian cells retain their basal Mg content virtually unchanged [28]. Moreover, no alterations of intracellular Mg concentration were detected in HUVEC stably silencing TRPM7 [29]. We hypothesize that other transporters or channels vicariate TRPM7 knock down, and work is in progress to test this issue. Since ATP exists mainly as a complex with Mg, it is noteworthy that no differences of ATP content were detected in HUVEC exposed to high glucose *versus* controls. This finding is interesting in the light of Inoue's report showing that oxidative stress inhibits TRPM7 current only when intracellular ATP depletion occurs, while the maintenance of adequate ATP content prevents TRPM7 inhibition in HEK293 cells [30]. Since endothelial cells predominantly catabolize glucose via glycolysis [31], we hypothesize that high glucose enhances the glycolytic flux in HUVEC,

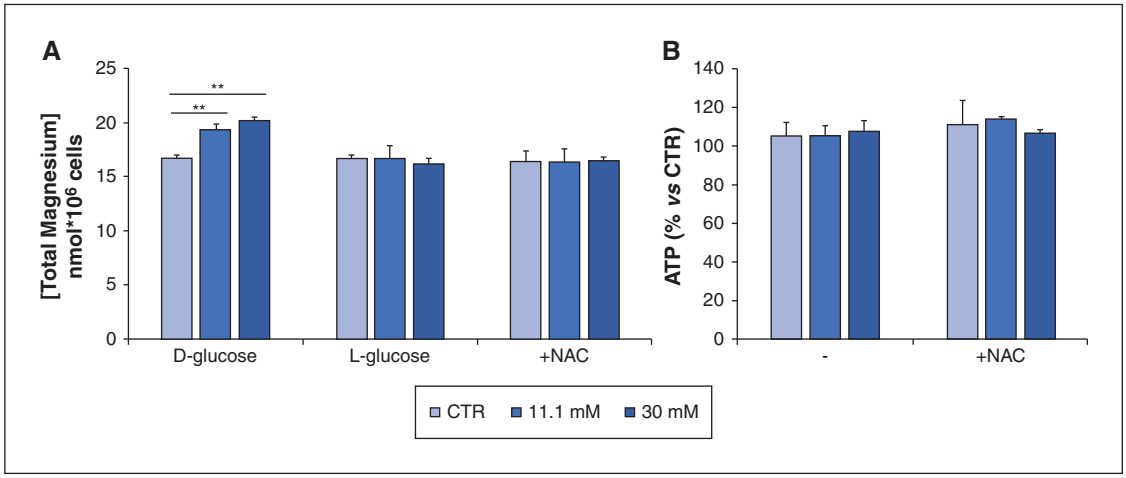

Figure 5. High D-glucose impacts on total intracellular Mg concentration without affecting ATP levels. HUVEC were exposed to high concentrations of extracellular D- and L-glucose in the presence or not of NAC for 24 h. **A)** Total intracellular Mg was measured using the fluorescent chemosensor DCHQ5. **B)** ATP was measured using a luminescent detection kit.

thus increasing the production of glycolytic phosphomonoester intermediates, whose bioactive forms bind to Mg. The consequences of high intracellular Mg on cell function are not clear. Because it is reported that high D-glucose results in increased intracellular Ca [3, 7], it is feasible to propose that the balance Ca/Mg, essential in regulating several cell functions, is maintained through a higher transport of Mg via TRPM7.

It is noteworthy that TRPM7 upregulation in response to elevated concentrations of D-glucose is a common denominator of all the principal cell types implicated in atherogenesis. In rabbit smooth muscle cells, high D-glucose enhances TRPM7 by increasing oxidative stress and this is associated with the development of a proliferative phenotype [32]. In human monocytes, high glucose-induced oxidative stress leads to the overexpression of several transient receptor potential channels, including TRPM7 [33]. These two studies do not offer any insight into intracellular Mg concentrations.

While increased amounts of TRPM7 seem to be involved in endothelial dysfunction and atherogenesis, a potential contribution of MagT1 is hard to envisage since MagT1 is not modulated by high D-glucose, low Mg, or hydrogen peroxide. A recent paper has reported the contribution of both TRPM7 and MagT1 in altering endothelial barrier function [13], a crucial early step in endothelial dysfunction, but more efforts are needed to define MagT1 role in the vasculature.

In conclusion, we propose that 24 h exposure to high D-glucose suffices to edit Mg homeostasis in HUVEC.

Acknowledgements

We thank Prof. S. Iotti and Prof. M. Lombardo from University of Bologna for kindly donating the fluorescent chemosensor DCHQ5.

Disclosure

The authors declare no conflict of interest.

References

1. Tabit CE, Chung WB, Hamburg NM, Vita JA. Endothelial dysfunction in diabetes mellitus: molecular mechanisms and clinical implications. *Rev Endocr Metab Disord* 2010; 11 : 61-74.
2. Sena CM, Pereira AM, Seiça R. Endothelial dysfunction – A major mediator of diabetic vascular disease. *Biochim Biophys Acta* 2013; 1832 : 2216-31.

3. Chen W, Yang J, Chen S, *et al*. Importance of mitochondrial calcium uniporter in high glucose-induced endothelial cell dysfunction. *Diabetes Vasc Dis Res* 2017; 14 : 494-501.
4. De Vriese AS, Verbeuren TJ, Van de Voorde J, Lameire NH, Vanhoutte PM. Endothelial dysfunction in diabetes. *Br J Pharmacol* 2000; 130 : 963-74.
5. Hadi HAR, Al Suwaidi JA. Endothelial dysfunction in diabetes mellitus. *Vasc Health Risk Manage* 2007; 3 : 853-76.
6. Mortuza R, Chen S, Feng B, Sen S, Chakrabarti S. High glucose induced alteration of SIRTs in endothelial cells causes rapid aging in a p300 and FOXO regulated pathway. *PLoS One* 2013; 8 : e54514.
7. Hou Q, Lei M, Hu K, Wang M. The effects of high glucose levels on reactive oxygen species-induced apoptosis and involved signaling in human vascular endothelial cells. *Cardiovasc Toxicol* 2015; 15 : 140-6.
8. de Baaij JHF, Hoenderop JGJ, Bindels RJM. Magnesium in man: implications for health and disease. *Physiol Rev* 2015; 95 : 1-46.
9. Severino P, Netti L, Mariani MV, *et al*. Prevention of cardiovascular disease: screening for magnesium deficiency. *Cardiol Res Pract* 2019; 2019 : 4874921.
10. Romeo V, Cazzaniga A, Maier JAM. Magnesium and the blood-brain barrier *in vitro*: effects on permeability and magnesium transport. *Magnes Res* 2019; 32 : 16-24.
11. Maier JAM. Endothelial cells and magnesium: implications in atherosclerosis. *Clin Sci* 2012; 122 : 397-407.
12. Castiglioni S, Cazzaniga A, Locatelli L, Maier JA. Burning magnesium, a sparkle in acute inflammation: gleams from experimental models. *Magnes Res* 2017; 30 : 8-15.
13. Zhu D, You J, Zhao N, Xu H. Magnesium regulates endothelial barrier functions through TRPM7, MagT1, and S1P1. *Adv Sci* 2019; 6 : 1901166.
14. Park HS, Hong C, Kim BJ, So I. The pathophysiologic roles of TRPM 7 channel. *Korean J Physiol Pharmacol* 2014; 18 : 15-23.
15. Cherepanova NA, Shrimal S, Gilmore R. Oxidoreductase activity is necessary for N-glycosylation of cysteine-proximal acceptor sites in glycoproteins. *J Cell Biol* 2014; 206 : 525-39.
16. Maier JAM, Malpuech-Brugère C, Zimowska W, Rayssiguier Y, Mazur A. Low magnesium promotes endothelial cell dysfunction: implications for atherosclerosis, inflammation and thrombosis. *Biochim Biophys Acta* 2004; 1689 : 13-21.
17. Ferrè S, Baldoli E, Leidi M, Maier JAM. Magnesium deficiency promotes a pro-atherogenic phenotype in cultured human endothelial cells *via* activation of NFkB. *Biochim Biophys Acta* 2010; 1802 : 952-8.
18. Baldoli E, Castiglioni S, Maier JAM. Regulation and function of TRPM7 in human endothelial cells: TRPM7 as a potential novel regulator of endothelial function. *PLoS One* 2013; 8 : 1-7.
19. Paravicini TM, Yogi A, Mazur A, Touyz RM. Dysregulation of vascular TRPM7 and annexin-1 is associated with endothelial dysfunction in inherited hypomagnesemia. *Hypertension* 2009; 53 : 423-9.
20. Castiglioni S, Cazzaniga A, Maier JAM. Potential interplay between NFκB and PPARγ in human dermal microvascular endothelial cells cultured in low magnesium. *Magnes Res* 2014; 27 : 86-93. doi: 10.1684/mrh.2014.0365.
21. Cazzaniga A, Moscheni C, Trapani V, *et al*. The different expression of TRPM7 and MagT1 impacts on the proliferation of colon carcinoma cells sensitive or resistant to doxorubicin. *Sci Rep* 2017; 7 : 40538.
22. Cazzaniga A, Locatelli L, Castiglioni S, Maier JAM. The dynamic adaptation of primary human endothelial cells to simulated microgravity. *FASEB J* 2019; 33 : 5957-66.
23. Sargenti A, Farruggia G, Zaccheroni N, *et al*. Synthesis of a highly Mg 2+-selective fluorescent probe and its application to quantifying and imaging total intracellular magnesium. *Nat Protoc* 2017; 12 : 461-71.
24. Li X, Kover KL, Heruth DP, *et al*. Thioredoxin-interacting protein promotes high-glucose-induced macrovascular endothelial dysfunction. *Biochem Biophys Res Commun* 2017; 493 : 291-7.
25. Li Y, Huang TT, Carlson EJ, *et al*. Dilated cardiomyopathy and neonatal lethality in mutant mice lacking manganese superoxide dismutase. *Nat Genet* 1995; 10 : 196-201.
26. Sun H, Leng T, Zeng Z, *et al*. Role of TRPM7 channels in hyperglycemia-mediated injury of vascular endothelial cells. *PLoS One* 2013; 8 : 1-12.
27. Rooney MR, Misialek JR, Alonso A, *et al*. Serum magnesium and the incidence of coronary heart disease over 20 years of follow-up: the atherosclerosis risk in communities (ARIC) study. *Circulation Conference: American Heart Association's Epidemiology and Prevention/Lifestyle and Cardiometabolic Health* 2018; 137 : 1-9.

28. Romani AMP. Intracellular magnesium homeostasis. *Magnesium in the Central Nervous System* 2011; 512 : 13-58.

29. Malucelli E, Procopio A, Fratini M, *et al*. Single cell *versus* large population analysis: cell variability in elemental intracellular concentration and distribution. *Anal Bioanal Chem* 2018; 410 : 337-48.

30. Inoue H, Murayama T, Tashiro M, Sakurai T, Konishi M. Mg(2+)- and ATP-dependent inhibition of transient receptor potential melastatin 7 by oxidative stress. *Free Radic Biol Med* 2014; 72 : 257-66.

31. Eelen G, de Zeeuw P, Treps L, *et al*. Endothelial cell metabolism. *Physiol Rev* 2018; 98 : 3-58.

32. Yang M, Fang J, Liu Q, Wang Y, Zhang Z. Role of ROS-TRPM7-ERK1/2 axis in high concentration glucose-mediated proliferation and phenotype switching of rat aortic vascular smooth muscle cells. *Biochem Biophys Res Commun* 2017; 494 : 526-33.

33. Wuensch T, Thilo F, Krueger K, *et al*. High glucose-induced oxidative stress increases. *Diabetes* 2010; 59 : 3-8.

11. DISSEMINATION OF RESULTS

11.1 LAY SUMMARY OF THIS RESEARCH

Understanding endothelial dysfunction is a major focus to generate new tools to prevent and treat vascular diseases. This research had the purpose to investigate the effects of high glucose levels and of blood serum collected from paediatric diabetic patients on endothelial cells monolayers. Human Umbilical Vein Endothelial Cells (HUVEC), a widely used type of macrovascular cells, were cultured either in 2D cell culture systems on flat dishes, a system which has yielded major advances in our knowledge about endothelial pathophysiology, or in 3D microfluidic chips to closely reflect what happens *in vivo*, since they show a higher degree of structural complexity allowing perfusion, thus generating shear stress fundamental for endothelial homeostasis. In 2- and 3- D the cells were cultured until they reach the confluence to reproduce the physiological inner layer of a blood vessel as closely as possible and were exposed to different concentrations of extracellular glucose or to 10% of blood serum from 36 paediatric diabetic patients or 14 healthy controls.

Comprendere la disfunzione endoteliale è un obiettivo importante per prevenire e curare le malattie vascolari. Questa ricerca ha lo scopo di indagare l'effetto dell'alto glucosio o del siero sanguigno prelevato da pazienti pediatrici diabetici su cellule endoteliali. Le cellule endoteliali della vena ombelicale umana (HUVEC), un tipo ampiamente utilizzato di cellule macrovascolari, sono state coltivate in classici sistemi di coltura cellulare 2D, sistema che ha permesso il progresso di conoscenze sulla fisiopatologia endoteliale, o in chip microfluidici 3D che da vicino riflettono ciò che accade *in vivo*, poiché sono caratterizzati da un grado più elevato di complessità strutturale consentendo la perfusione, generando così lo shear stress fondamentale per l'omeostasi endoteliale. In 2- e 3-D le cellule sono state coltivate fino a raggiungere la confluenza per riprodurre il più fedelmente possibile lo strato fisiologico interno di un vaso sanguigno e sono state esposte a diverse concentrazioni di glucosio extracellulare o al 10% di siero sanguigno prelevato da 36 diabetici pediatrici pazienti o 14 controlli sani.

11.2 PUBLICATIONS

- Manuscript (biomedicines-1423576) accepted in Biomedicines (ISSN 2227-9059) on 06 December 2021 entitled: "*Vitamin D prevents high glucose-induced lipid droplets*

accumulation in cultured endothelial cells: the role of Thioredoxin Interacting Protein". Authors: **Roberta Scrimieri** *; Alessandra Cazzaniga; Sara Castiglioni; Jeanette Anne Marie Maier.

* corresponding author

- Locatelli, L.; Cazzaniga, A.; Fedele, G.; Zocchi, M.; **Scrimieri, R.**; Moscheni, C.; Castiglioni, S.; Maier, J.A. "*A Comparison of Doxorubicin-Resistant Colon Cancer LoVo and Leukemia HL60 Cells: Common Features, Different Underlying Mechanisms*". Curr. Issues Mol. Biol. 2021, 43, 163–175. DOI:10.3390/cimb43010014.
- Alessandra Cazzaniga, **Roberta Scrimieri**, Massimo Galli, Jeanette Maier and Stefano Rusconi. "*Unveiling the basis of antiretroviral therapy-induced osteopenia: the effects of Dolutegravir, Darunavir and Atazanavir on osteogenesis*". AIDS 2021, 35:213–218. DOI:10.1097/QAD.0000000000002732.
- Zocchi M, **Scrimieri R**, Locatelli L, Cazzaniga A., Fedele G., Maier J.A.M., Castiglioni S. "*TRPM7 and MagT1 regulate the proliferation of osteoblast-like SaOS-2 cells through different mechanisms*". Magnes Res. 2020;33(1):12-20. DOI:10.1684/mrh.2020.0463.
- Cazzaniga A *, **Scrimieri R** *, Giani E, Zuccotti GV, Maier JAM. "*Endothelial hyper-permeability induced by T1D sera can be reversed by iNOS inactivation*". Int J Mol Sci. 2020 Apr 17;21(8). pii: E2798. DOI: 10.3390/ijms21082798.
- **Scrimieri R**, Locatelli L, Cazzola R, Maier JAM, Cazzaniga A. "*Reactive oxygen species are implicated in altering magnesium homeostasis in endothelial cells exposed to high glucose*". Magnes Res. 2019 Aug 1;32(3):54-62. doi:10.1684/mrh.2019.0456.

11.3 COMMUNICATION TO CONGRESSES

- **R. Scrimieri**, L. Locatelli, J. Maier, A. Cazzaniga. "*TRPM7, but not MAGT1, is upregulated in endothelial cells exposed to high concentrations of glucose*" - AMP Europe 2021, Clinical Genomics: beyond the somatic mutation (virtual meeting, June 14th-18th 2021).
- Giorgia Fedele, Sara Castiglioni, Laura Locatelli, **Roberta Scrimieri**, Monica Zocchi, Alessandra Cazzaniga. "*BDNF and GABA-R expression is modulated in human mini-*

brain organoids in response to magnesium" - 2nd Workshop on Magnesium Neuroscience and Nutrition in current Covid-19 Pandemia (virtual meeting, May 28th-29th 2021).

- Laura Locatelli, Valentina Romeo, **Roberta Scrimieri**, Monica Zocchi, Giorgia Fedele, Sara Castiglioni, Alessandra Cazzaniga. "*Comparison of the efficiency of different endothelial cells in a model of BBB*" - 2nd Workshop on Magnesium Neuroscience and Nutrition in current Covid-19 Pandemia (virtual meeting, May 28th-29th 2021).
- **Roberta Scrimieri**, Laura Locatelli, Giorgia Fedele, Monica Zocchi, Alessandra Cazzaniga. "*Vitamin D prevents triglycerides accumulation in endothelial cells exposed to high glucose*" – 93rd National Congress of the Italian Society of Experimental Biology (virtual meeting, Palermo, Italy, April 22nd-25th 2021). Oral communication.
- Monica Zocchi, Laura Locatelli, Giorgia Fedele, Alessandra Cazzaniga, **Roberta Scrimieri**, Sara Castiglioni. "*Magnesium deficiency impacts on skeletal muscle regeneration by influencing membrane fusion*" – 93rd National Congress of the Italian Society of Experimental Biology (virtual meeting, Palermo, Italy, April 22nd-25th 2021).
- Giorgia Fedele, **Roberta Scrimieri**, Monica Zocchi, Alessandra Cazzaniga, Sara Castiglioni, Laura Locatelli. "*Magnesium deficiency induces lipid accumulation by upregulating EDF-1 and Peroxisome Proliferator-Activated Receptor gamma*" – 93rd National Congress of the Italian Society of Experimental Biology (virtual meeting, Palermo, Italy, April 22nd-25th 2021).
- **Roberta Scrimieri**, Laura Locatelli, Giorgia Fedele, Monica Zocchi, and Alessandra Cazzaniga. "V*itamin D_3 as Countermeasure to Prevent Endothelial Dysfunction in Diabetes*" – ASIP Meeting "Pathobiology that drives discovery, diagnosis and treatment of human diseases: present and future" (virtual meeting, Pisa 2020, November 9th-13th 2020).
- **R. Scrimieri**, E. Giani, C. Mameli, G.V. Zuccotti, J. Maier and A. Cazzaniga. "*The role of iNOS in the onset of endothelial dysfunction in Type I Diabetes*" – SIPMeT Young Scientists Meeting "Pathobiology: from molecular disease to clinical application" (University of Florence - September, 13th-14th, 2019). Oral communication.

- Cazzaniga A., Romeo V., Locatelli L., **Scrimieri R.**, Castiglioni S., Maier J.A.M. "*Stressed cerebral organoids: can magnesium help?*" – "XV International Magnesium Symposium - magnesium in health and disease" (Bethesda - NIH, March 20th-22nd, 2019).
- Locatelli L., Cazzaniga A., Romeo V., **Scrimieri R.**, Castiglioni S., Maier J. "*HUVEC in simulated microgravity: interplay between magnesium homeostasis and cytoskeleton*". – "XV International Magnesium Symposium - magnesium in health and disease" (Bethesda - NIH, March 20th-22nd, 2019).
- **R. Scrimieri**, L. Locatelli, V. Romeo, E. Giani, J. Maier, G.V. Zuccotti and A. Cazzaniga. "*Vitamin D prevents high glucose-induced endothelial permeability*" – SIPMeT "Pathology and Laboratory Medicine 4.0" (October, 23rd-25th, 2018).
- A. Cazzaniga, L. Locatelli, V. Romeo, **R. Scrimieri**, S. Castiglioni and J. Maier. "*EDF-1 contributes to pparg transcriptional activation in endothelial cells treated with VEGF*" – SIPMeT "Pathology and Laboratory Medicine 4.0" (October, 23rd-25th, 2018).
- L. Locatelli, A. Cazzaniga, S. Castiglioni, **R. Scrimieri** and J.A.M. Maier. "*The pathophysiology of the endothelium: moving from 2d to 3d culture and beyond*" – SIPMeT "Pathology and Laboratory Medicine 4.0" (October, 23rd-25th, 2018).
- V. Romeo, L. Locatelli, A. Cazzaniga, **R. Scrimieri**, S. Zecchini and S. Castiglioni. "Trpm7 and Magt1 as novel players in the osteogenic differentiation of human BMSC" – SIPMeT "Pathology and Laboratory Medicine 4.0" (October, 23rd-25th, 2018).
- Romeo V., Locatelli L., Cazzaniga A., **Scrimieri R.**, Castiglioni S. "Magnesium and stress in human bone mesenchymal stem cells: the impact on osteogenic differentiation" – ABCD meeting: "From stress response to tissue development and regeneration". (September, 28th-29th, 2018, Pavia, Italy).
- Cazzaniga A., Locatelli L., **Scrimieri R.**, Castiglioni S. "*The dynamic adaptive response of endothelial cells to simulated microgravity*" – ESA-ESTEC "The Netherlands". (June, 18th -22nd, 2018).